

UC Irvine

UC Irvine Electronic Theses and Dissertations

Title

Intramolecular Diels-Alder Reactions in Organic Synthesis

Permalink

<https://escholarship.org/uc/item/9r20m5s6>

Author

Sizemore, Nicholas Blandford Luke

Publication Date

2014

Peer reviewed|Thesis/dissertation

UNIVERSITY OF CALIFORNIA,
IRVINE

Intramolecular Diels–Alder Reactions in Organic Synthesis

DISSERTATION

submitted in partial satisfaction of the requirements
for the degree of

DOCTOR OF PHILOSOPHY

in Chemistry

by

Nicholas Blandford Luke Sizemore

Dissertation Committee:
Professor Scott D. Rychnovsky, Chair
Professor Larry E. Overman
Professor Christopher D. Vanderwal

2014

Chapter 3 Reproduced in part with permission from Sizemore, N.; Rychnovsky, S. D. *Org. Lett.* **2014**, *16*, 688–691. © 2014 American Chemical Society.
Chapter 4 Reproduced with permission from Cleary, L.; Mak, V. W.; Rychnovsky, S. D.; Shea, K. J.; Sizemore, N. *J. Org. Chem.* **2013**, *78*, 4090–4098. © 2013 American Chemical Society.
All other materials © 2014 Nicholas Blandford Luke Sizemore

DEDICATION

To

Anne Szklarski, Dennis and JoAnn Sizemore,
family and friends

in recognition of their values

on life and love

TO WHOM IT MAY CONCERN:
It is springtime. It is late afternoon.

Kurt Vonnegut
Slapstick or Lonesome No More!: A Novel

and work

Some people see things that are and ask, Why?
Some people dream of things that never were and ask, Why not?
Some people have to go to work and don't have time for all that...

George Carlin
Brain Droppings

TABLE OF CONTENTS

	Page
LIST OF FIGURES	v
LIST OF TABLES	vi
LIST OF SCHEMES	vii
ACKNOWLEDGMENTS	ix
CURRICULUM VITAE	x
ABSTRACT OF THE DISSERTATION	xii
CHAPTER 1: Intramolecular Diels–Alder Reactions in Organic Synthesis	
Abstract	1
Introduction	1
Class 1: All-carbon Type 1 Intramolecular Diels–Alder Reactions	4
Class 2: Type 2 Intramolecular Diels–Alder Reactions	8
Class 3: Intramolecular Aza-Diels–Alder Reactions	9
Conclusions	12
References	13
CHAPTER 2: Studies Toward the Total Synthesis of Maoecrystal Z: An Intramolecular Diels–Alder Approach	
Abstract	18
Introduction	18
Results and Discussion	22
Conclusions	32
General Experimental Details	32
Experimental Procedures	33
References	44
CHAPTER 3: Studies Toward the Synthesis of Palhinine Lycopodium Alkaloids: A Morita–Baylis–Hillman/Intramolecular Diels–Alder Approach	
Abstract	48
Introduction	48
Results and Discussion	52
Conclusions and Future Directions	61
General Experimental Details	62
Experimental Procedures	63
References	83

CHAPTER 4: Origins of Regio- and Stereochemistry in Type 2 Intramolecular *N*-Acynitroso Diels–Alder Reactions: A Computational Study of Tether Length and Substituent Effects

Abstract	88
Introduction	88
Background	91
Results	95
Discussion	101
Conclusion	107
Calculated Geometries and Energies	107
References	148

CHAPTER 5: Investigation of Intramolecular Cyano-azadiene Diels–Alder Reactions: Indolizidine and Quinolizidine Synthesis

Abstract	153
Introduction	153
Background	154
Results and Discussion	156
Conclusions and Future Directions	162
General Experimental Details	163
Experimental Procedures	164
NMR Tables for 5.32a , 5.32c , and 5.32e	185
Key NOESY correlation diagrams for 5.32a , 5.32c , and 5.32e	187
References	188

LIST OF FIGURES

	Page
Figure 2.1. Maoecrystal Z and <i>ent</i> -kaurane skeleton.	19
Figure 2.2. Transition state comparison for the IMDA reaction.	21
Figure 2.3. Comparison of IMDA products and maoecrystal Z.	22
Figure 2.4. Precedent and rationale for enone formation.	25
Figure 3.1. Lycopodium natural products isopalhinine A and fawcettimine.	49
Figure 3.2. Representative isotwistane containing natural products.	49
Figure 4.1. Regioselectivity of the type 2 IMDA reaction.	89
Figure 4.2. Regioselectivity of the <i>N</i> -acylnitroso type 2 IMDA reaction.	91
Figure 4.3. Free energy (FE) diagrams and (TS) transition state structures for acyclic dienes of carbon tether lengths 4-6.	96
Figure 4.4. FE diagrams and TS structures for the stereoselectivity of acyclic diene substrates with α -methyl or α -ethereal substituted tethers.	98
Figure 4.5. FE diagrams/TS structures for regioselectivity of unsubstituted cyclic diene and stereoselectivity of substituted cyclic diene substrates	100
Figure 4.6. A visual description of Dunitz's model of olefin strain, where τ describes the torsional strain between the π orbitals and χ_C is a measure of the pyramidalization of the sp^2 center.	102
Figure 4.7. Comparison of external and internal transition structures for α -methyl substituted tether, the analogous unsubstituted transition structures, and the internal α -ethereal substituted tethers.	104
Figure 5.1. Examples of indolizidine and quinolizidine containing natural products.	154
Figure 5.2. Diels–Alder substrates.	157

LIST OF TABLES

	Page
Table 3.1. Optimization of oxidation to aldehyde 3.47 .	58
Table 4.1. Acyclic diene <i>N</i> -acylnitroso type 2 IMDA reactions.	92
Table 4.2. α -Substituted acyclic diene <i>N</i> -acylnitroso type 2 IMDA reactions.	93
Table 4.3. Cyclic diene <i>N</i> -acylnitroso type 2 IMDA reactions.	93
Table 4.4. Computational angles and deviation from experimental angles (Δ) of acyclic diene cycloadducts.	103
Table 4.5. Comparison of dihedral angles from <i>cis</i> and <i>trans</i> approaches in substituted cyclic diene substrates.	105
Table 4.6. Summary of computed substrate selectivities in terms of $\Delta\Delta G^\ddagger$ and product distributions.	106
Table 5.1. Tabulated NMR data for 5.32a .	185
Table 5.2. Tabulated NMR data for 5.32c .	186
Table 5.3. Tabulated NMR data for 5.32e .	186

LIST OF SCHEMES

	Page
Scheme 1.1. The canonical intermolecular Diels–Alder reaction and <i>endo/exo</i> selectivity.	2
Scheme 1.2. The canonical intramolecular Diels–Alder reaction.	3
Scheme 1.3. Type 1 and type 2 intramolecular Diels–Alder reactions.	3
Scheme 1.4. Intramolecular Diels–Alder reactions leading to vicinal quaternary centers.	5
Scheme 1.5. Deslongchamps and co-workers synthesis of (–)-maritamol A.	6
Scheme 1.6. Rychnovsky and Kim’s synthesis of (–)-columbiasin A.	7
Scheme 1.7. Baran’s IMDA strategy toward (±)-maoecrystal V.	8
Scheme 1.8. Shea’s type 2 IMDA approach to welwitindolinone natural products.	9
Scheme 1.9. Intramolecular aza-Diels–Alder reaction classes.	10
Scheme 1.10. Grieco and Carroll’s imine aza-IMDA synthesis of (–)-pseudotabersonine.	11
Scheme 1.11. Heathcock and Stafford’s 2-azadiene IMDA strategy for (–)-secodaphniphylline.	12
Scheme 2.1. Retrosynthetic analysis of maoecrystal Z.	20
Scheme 2.2. Synthesis of coupling partners.	23
Scheme 2.4. Synthesis of reduced derivatives.	25
Scheme 2.5. Synthesis of (<i>S</i>)- <i>t</i> -Bu-PHOX.	26
Scheme 2.6. Revised synthetic route to ketone 2.37 .	27
Scheme 2.7. Planned synthetic operation to tricycle 2.4 .	28
Scheme 2.8. Reisman’s synthesis of spiro lactone 2.48 .	29
Scheme 2.9. Reisman’s synthesis of alkyl iodide 2.52 .	30
Scheme 2.10. Reisman’s total synthesis of (–)-maoecrystal Z.	31

Scheme 3.1.	Landmark syntheses of isotwistane containing (\pm)-9-isocyanopupukeanane.	50
Scheme 3.2.	Reported approaches to palhinine A.	51
Scheme 3.3.	Retrosynthetic analysis of palhinine natural products.	52
Scheme 3.4.	Attempted synthesis of enone 3.30 .	53
Scheme 3.5.	Malonate Michael approach to aldehyde 3.23 .	54
Scheme 3.6.	Trauner and Wilson's synthesis of (+)-SCH 642305.	56
Scheme 3.7.	Mukaiyama–Michael approach to Morita–Baylis–Hillman precursor.	57
Scheme 3.8.	Synthesis of key enone for intramolecular Diels–Alder reaction.	59
Scheme 3.9.	Regioselectivity in the intramolecular Diels–Alder reaction.	60
Scheme 3.10.	Fan and co-worker's strategy toward palhinine A.	61
Scheme 4.1.	Application of the type 2 IMDA reaction to complex products.	90
Scheme 4.2.	Retrosynthetic analysis of stenine.	94
Scheme 5.1.	Previous syntheses of indolizidines and quinolizidine containing cyanoenamines.	155
Scheme 5.2.	Synthetic strategies toward indolizidine alkaloid 261C.	156
Scheme 5.3.	Synthesis of unsubstituted dienophile amine precursors.	158
Scheme 5.4.	Synthesis of substituted dienophile amine precursors.	159
Scheme 5.5.	Synthesis of the Diels–Alder precursors.	160
Scheme 5.6.	Aza-Diels–Alder cyclizations.	161

ACKNOWLEDGMENTS

I would like to express my deepest appreciation to my advisor, Professor Scott Rychnovsky, who gave me a nurturing environment to grow as a scientist. His support has been phenomenal and the freedom that he allowed me during my Ph.D. studies was greatly appreciated. Scott let me explore bad ideas, has given me good ones and showed me the wisdom to discern between them. Without his guidance, mentorship and help, this dissertation would not have been possible.

I would like to thank my committee members, Professor Larry Overman and Professor Christopher Vanderwal, who guided me through the oral examinations. Their feedback has always been constructive and helpful.

My industrial mentors Drs. David Aldous, David Borcharding, James Pribish and Michael Fennie were instrumental in my early scientific development, as was my undergraduate advisor Professor Philip Garner. I never would have considered returning to graduate school if not for their encouragement and support.

I owe a debt of gratitude to Professors Richard Chamberlin, Stephen Hanessian and Andrej Luptak for accepting me into the Medicinal Chemistry and Pharmacology program. In addition, a thank you to David Van Vranken, who demonstrated the proper way to teach Organic Chemistry and whose enthusiasm for education has had lasting effect.

I thank the American Chemical Society for permission to include copyrighted materials as part of my thesis/dissertation. I also thank Organic Syntheses, Professor Rick L. Danheiser, Springer Verlag, and Professor Janine Cossy for the opportunity to write review articles and a book chapter. Financial support was provided by Vertex Pharmaceuticals, the Allergan Foundation, the University of California, Irvine, the National Science Foundation (CRIF CHE-0840513) and the National Institute of General Medicine (GM-43854).

To the past and present members of the Rychnovsky lab, thank you for providing an interesting and exciting place to do chemistry. To the inhabitants of Reines Hall 3004, especially Richard Hill, thank you for putting up with my musical tastes. Renzo Samame: Mi hermano peruano. Dr. Maureen Reilly: Roommate and friend. Gidget Tay: Group organizer, carrier of the torch and friend. Dr. Matt Perry: Life in lab was not the same when you left. I will never forget all the good times we had.

I have to thank my friends, Dr. Evan and Alison Horn: Surrogate parents for a lost and wandering manboy. Dr. Leah Cleary: An amazing chemist and an even better friend. David Jackson: The one who understands where I come from. Dr. Peter Mai: Life coach and motivational force. Joseph Carlson: Inventor of space pizza. Dr. Theo Michels: The dude. Samuel Tartakoff: Role model. Michael and Natalie Turrin: My family and home away from home.

To my family, Dennis and JoAnn Sizemore: I would not be living without you. Obviously you have made everything I do possible. I could not ask for a better set of parents, nor would I. Jennifer Yanke: We have always been on the same page and you are my favorite sister. Stephen Sizemore: Brudder, it's one of these things where you helped me tremendously in the home stretch and moved me across the country, twice. Words cannot express how I feel about all of you and there is no way that "thank you" will ever suffice.

To Anne Szklarski: The love of my life. The only reason I did not quit. The best person I have ever known. What you have given me is beyond compare. Thank you.

CURRICULUM VITAE

Nicholas Blandford Luke Sizemore

- 2005 B.S. in Chemistry, Case Western Reserve University, Cleveland, Ohio
- 2005-08 Assistant Scientist: Exploratory Internal Medicine – Chemistry
Sanofi-Aventis, Bridgewater, New Jersey
- 2009 Associate Scientist: Exploratory Internal Medicine – Chemistry
Sanofi-Aventis, Bridgewater, New Jersey
- 2014 Ph.D. in Organic Chemistry, University of California, Irvine

FIELD OF STUDY

Synthetic Organic Chemistry: Intramolecular Diels–Alder Reactions

HONORS AND AWARDS

- 2013 University of California Regents Dissertation Fellowship
- 2013 Allergan Graduate Fellowship in Synthetic Organic Chemistry
- 2012 ACS Publications Graduate Student/Postdoc Summer Institute
- 2012 Jad and Suad Jaber Research Award
- 2012 ACS Graduate Student Symposium Planning Committee Member
- 2011 NSF: Graduate Research Fellowship Program Honorable Mention
- 2010 Vertex Pharmaceutical Scholar
- 2009 Vertex Pharmaceutical Fellow
- 2004 HHMI: Summer Program for Undergraduate Research Fellow

PUBLICATIONS

5. N. Sizemore; S. D. Rychnovsky. “Studies Toward the Synthesis of Palhinine Lycopodium Alkaloids: A Morita–Baylis–Hillman/Intramolecular Diels–Alder Approach” *Organic Letters* **2014**, *16*, 688–691.

4. L. Cleary; V. W. Mak; S. D. Rychnovsky; K. J. Shea; N. Sizemore. "Origins of Regio- and Stereochemistry in Type 2 Intramolecular *N*-Acylnitroso Diels–Alder Reactions: A Computational Study of Tether Length and Substituent Effects" *Journal of Organic Chemistry* **2013**, *78*, 4090–4098.
3. Medicinal chemistry program toward small molecule inhibitors of arthritis. Sanofi-Aventis. Patent in preparation.
2. N. Sizemore; S. D. Rychnovsky. "Discussion Addendum: Preparation of α -Acetoxy Ethers by the Reductive Acetylation of Esters: *endo*-1-Bornyloxyethyl Acetate" *Organic Syntheses* **2012**, *89*, 143–158.
1. R. C. Smith; C. R. Bodner; M. J. Earl; N. C. Sears; N. E. Hill, L. M. Bishop; N. Sizemore; D. T. Hehemann; J. J. Bohn; J. D. Protasiewicz. "Suzuki and Heck coupling reactions mediated by palladium complexes bearing trans-spanning diphosphines" *Journal of Organometallic Chemistry* **2005**, *690*, 477–481.

BOOK CHAPTERS

1. M. A. Perry; S. D. Rychnovsky; N. Sizemore. "Synthesis of Saturated Tetrahydropyrans" In *Topics in Heterocyclic Chemistry* (Ed. Janine Cossy) Springer, New York, **2014**, *35*, 45–93.

PRESENTATIONS

5. April 2013 245th ACS National Meeting and Exposition, New Orleans, LA N. Sizemore; S. D. Rychnovsky. "Progress toward the Total Synthesis of Palhinine A" ORGN-209.
4. Aug. 2012 244th ACS National Meeting and Exposition, Philadelphia, PA N. Sizemore; L. Cleary; V. W. Mak; S. D. Rychnovsky; K. J. Shea. "Type 2 intramolecular Diels–Alder reactions: A computational method for predicting product distributions" ORGN-379.
3. July 2012 Gaussian Workshop, Ohio Supercomputer Center, Columbus, OH N. Sizemore; L. Cleary; V. W. Mak; K. J. Shea; S. D. Rychnovsky. "Computational Studies of the *N*-Acylnitroso Type 2 Intramolecular Diels–Alder Reaction".
2. Oct. 2011 Vertex Scholar Symposium, University of California, Irvine, CA N. Sizemore; L. Cleary; V. W. Mak; K. J. Shea; S. D. Rychnovsky. "Computational Studies of the Type 2 Intramolecular Diels–Alder Reaction".
1. Aug. 2004 HHMI:SPUR, Case Western Reserve University, Cleveland, OH N. Sizemore; P. P. Garner. "Developing Cost-Effective Peptide Coupling Reagents".

ABSTRACT OF THE DISSERTATION

Intramolecular Diels–Alder Reactions in Organic Synthesis

By

Nicholas Blandford Luke Sizemore

Doctor of Philosophy in Chemistry

University of California, Irvine, 2014

Professor Scott D. Rychnovsky, Chair

Intramolecular Diels–Alder (IMDA) reactions are an important class of reactions in synthetic organic chemistry for the rapid construction of polycyclic frameworks. Three classes of IMDA reactions were investigated synthetically and computationally: 1) all-carbon type 1 IMDA reactions, 2) *N*-acylnitroso type 2 IMDA reactions, and 3) cyano-azadiene IMDA reactions. The first class was implemented in research toward the total synthesis of maoecrystal *Z* and isopalhinine *A*. The second class was studied computationally to understand the origins of regio- and stereochemistry in these reactions. The third class was investigated in the context of indolizine and quinolizidine synthesis.

Chapter 1

Intramolecular Diels–Alder Reactions in Organic Synthesis

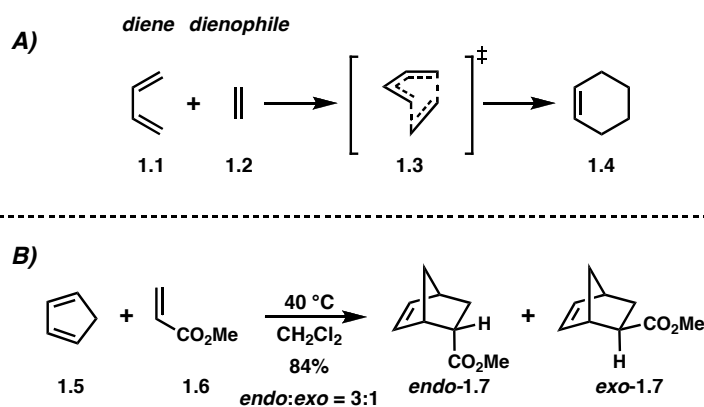
Abstract: Intramolecular Diels–Alder (IMDA) reactions are an important class of reactions in synthetic organic chemistry for the rapid construction of polycyclic frameworks. A brief overview of three classes of IMDA reactions is described in the context of select total syntheses. First, approaches to the installation of vicinal quaternary centers are examined for all-carbon type 1 IMDA reactions. Then, the synthesis of bicyclic bridgehead alkene containing molecules is described by a discussion of the type 2 intramolecular Diels–Alder reaction. Finally, the stereoelectronic features of hetero-Diels–Alder reactions are discussed in the context of nitrogen-containing heterocycles.

Introduction

Since the discovery of the $[4\pi_s + 2\pi_s]$ cycloaddition reaction in 1928 by Professors Otto Diels and Kurt Alder,¹ the Diels–Alder reaction has proven to be a powerful method for the construction of complex molecules.^{2,3} The general reaction requires the union of a 4π electron-component (diene **1.1**) with a 2π -component (dienophile **1.2**) (Scheme 1.1).⁴ When in close proximity, these components undergo a concerted, thermally allowed, suprafacial cycloaddition to afford a cyclohexene derivative (**1.4**).^{5–7} The reactions are typically exothermic and are driven by the formation of 2 new C–C σ bonds (162 kcal/mol) at the expense of 2 C–C π bonds (128 kcal/mol). Frontier molecular orbital (FMO) theory dictates the highest occupied molecular orbital (HOMO) of the electron-rich diene interacts with the lowest occupied molecular orbital (LUMO) of the electron-deficient dienophile.^{8,9} Regiochemistry in these normal-demand Diels–

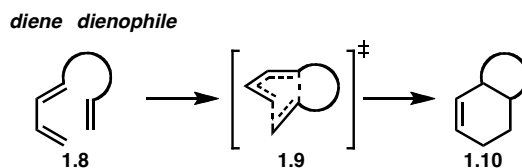
Alder reactions is largely determined by the electronics of the separate components. The predominant product results from the most nucleophilic atom of the diene reacting with the most electrophilic atom of the dienophile. The reaction has the capability of setting up to 4 contiguous stereocenters and the stereochemistry is dictated by the alkene geometry of both components.¹⁰ The formation of *endo* products (**endo-1.7**) is preferred in the intermolecular DA reaction (Scheme 1.1B).¹¹ While the intermolecular variant of this reaction remains a useful tool for synthetic organic chemists,¹² an in-depth discussion of its features and applications are outside the scope of this work.

Scheme 1.1. The canonical intermolecular Diels–Alder reaction and *endo/exo* selectivity.¹¹



The intramolecular Diels–Alder (IMDA) reaction tethers the dienophile and diene fragments together (Scheme 1.2).¹³ These reactions lead to an increase in molecular complexity by forming products that contain at least two new rings. Tethering the two fragments offers two benefits: 1) the overall energy required to bring the reactive fragments together is reduced, and 2) the geometric constraints of the tether dictate the regio- and stereochemistry of the products. The placement of the tether on the diene determines the type of cycloaddition (type 1 vs. type 2), while the introduction of nitrogen atoms on the diene or dienophile allow for the synthesis of heterocycles (hetero-IMDA).

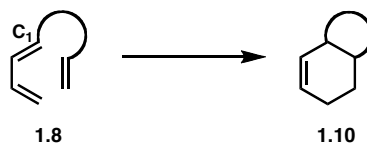
Scheme 1.2. The canonical intramolecular Diels–Alder reaction.



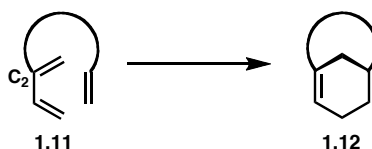
Intramolecular Diels–Alder reactions are divided into two types (Scheme 1.3). The type 1 IMDA reaction is the most common and is defined by tether attachment at the terminus (C1 position) of the diene (Scheme 1.3A, **1.8**).¹⁴ These reactions lead to fused bicyclic products, which are a common structural motif in terpene natural products. The type 2 IMDA reaction has the tether attached at the C2 position of the diene and leads to bridged bicyclic products bearing a bridgehead alkene (Scheme 1.3B, **1.12**).¹⁵ These intriguing frameworks are also found in a number of natural products. Both classes of IMDA reactions have been extensively studied and general reviews of their application to the total synthesis of natural products have been well documented.^{16–18} The examples described below are meant to highlight specific features of the reaction and the differences between and within the classes covered in this dissertation.

Scheme 1.3. Type 1 and type 2 intramolecular Diels–Alder reactions.

A) type 1 IMDA reaction



B) type 2 IMDA reaction



Hetero-Diels–Alder (HDA) reactions have found extensive utility in the construction of oxygen and nitrogen-containing heterocycles.^{19,20} The HDA reactions contain a heteroatom in

either the diene or dienophile fragment. The introduction of a heteroatom has dramatic consequences on the electronics of the reaction and the stereochemistry of the products.²¹ Specifically, a heteroatom situated at the terminus of the diene fragment renders the diene electron-deficient and cyclization occurs with electron-rich dienophiles.²² This case describes an inverse demand Diels–Alder reaction wherein the LUMO of the diene reacts with the HOMO of the dienophile. This reaction has been an effective method for the construction of both tetrahydropyran and piperidine derivatives.^{23–25}

While the general features of Diels–Alder reactions has been thoroughly investigated in empirical laboratory experiments, the recent advent of computational modeling has offered unprecedented insight into the factors controlling regioselective and diastereoselective outcomes.^{26–31} As a result, accurate energy values for cycloaddition pathways and competing ionic or radical mechanisms can be determined.³² The placement of substituents on the diene, the dienophile, and/or the tether can dramatically affect cyclization stereoselectivity.^{33,34} As such, the computational study of these variables is an active area of research. Developments in this field have not only allowed practitioners of organic synthesis to test hypothetical constructions *in silico*, but have also provided mechanistic information to rationalize experimental outcomes that fall outside the generally accepted “rules” of Diels–Alder reactions.

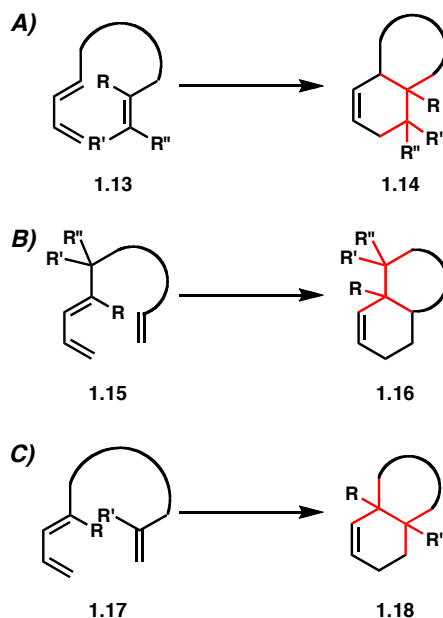
Class 1: All-carbon Type 1 Intramolecular Diels–Alder Reactions

Vicinal quaternary centers are a challenging structural motif present in a number of biologically interesting compounds.³⁵ The steric demand of these congested centers requires a robust and reliable procedure for their installation. Intramolecular Diels–Alder reactions are one of the few methods for building these difficult architectures. The power of IMDA reactions to

construct carbocyclic frameworks is best highlighted in the total synthesis of complex natural products bearing vicinal quaternary centers.

There are three modes of IMDA cyclization that lead to vicinal quaternary centers (Scheme 1.4). The most prevalent method uses a fully substituted dienophile to install the quaternary centers adjacent to the bicyclic fusion on the ring that bears the newly formed alkene (Scheme 1.4 A, **1.14**). The second mode of cyclization installs a single quaternary center next to an existing quaternary center (Scheme 1.4 B). This method sets a vicinal quaternary centers adjacent to the bicyclic fusion on the ring that results from the tether (**1.16**). The least exploited method of vicinal quaternary IMDA cyclization employs a diene and dienophile that have fully substituted termini to create vicinal quaternary centers at the bicyclic fusion (Scheme 1.4 C, **1.18**). This method is the subject of Chapter 3.³⁶

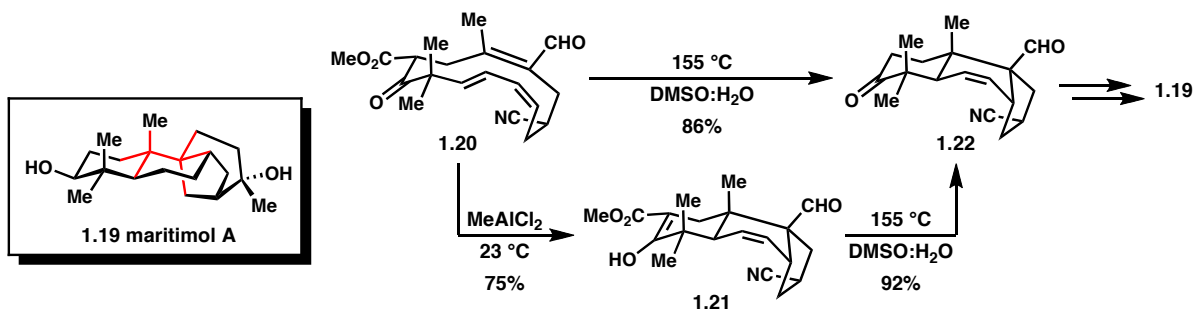
Scheme 1.4. Intramolecular Diels–Alder reactions leading to vicinal quaternary centers.



Mode A: Synthesis of (+)-Maritimol A

An impressive use of a fully substituted dienophile in an IMDA reaction is seen in Deslongchamps and co-workers synthesis of maritimol A (Scheme 1.5).^{37,38} Macrocycle **1.20** was treated with methylaluminum dichloride to effect a transannular Diels–Alder reaction in 75% yield. Resultant tricyclic enol **1.21** underwent Krapcho decarboxylation³⁹ to provide tricyclic ketone **1.22** in 92% yield. Alternatively, promotion of the intramolecular Diels–Alder reaction by heating in aqueous dimethyl sulfoxide led to cyclization with concomitant decarboxylation to afford ketone **1.22** directly. Interestingly, both the Lewis acid promoted and the thermal cyclization reactions proceed with complete stereocontrol to provide the *endo* product as a single diastereomer. This example demonstrates how fully substituted dienes can form quaternary centers and the power of transannular Diels–Alder reactions to construct polycyclic frameworks from a single macrocycle.⁴⁰

Scheme 1.5. Deslongchamps and co-workers synthesis of (–)-maritimol A.^{37,38}

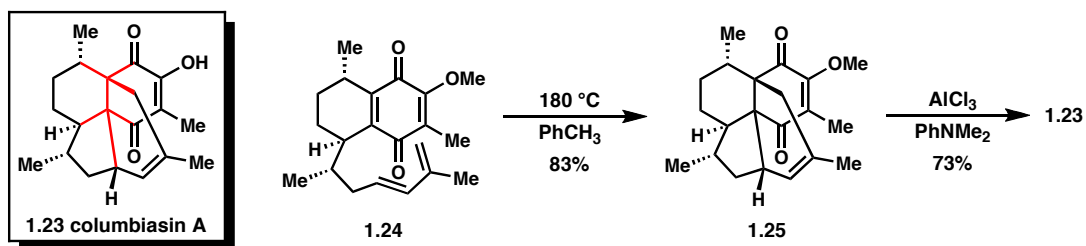


Mode A: Synthesis of (–)-Columbiasin A

Rychnovsky and Kim utilized a late-stage IMDA reaction to synthesize the diterpene natural product columbiasin A (Scheme 1.6).⁴¹ Similar to the transannular work of Deslongchamps, Rychnovsky and Kim's synthetic strategy utilizes a fully substituted dienophile to install the vicinal quaternary centers of columbiasin A. Bicyclic Diels–Alder precursor **1.24** was synthesized in 16 steps from Myer's pseudoephedrine auxiliary.⁴² Upon heating to 180 °C,

precursor **1.24** underwent an IMDA reaction to afford tetracyclic methyl ether **1.25** in 83% yield. While *E/Z* isomerization of the diene was observed under the reaction conditions (*E:Z* = 3:1), cyclization of the *E*-diene was substantially faster. In this case, the stereochemistry of the tether provided ample control of facial selectivity to give *endo* cyclization exclusively. Subsequent methyl ether cleavage of tetracycle **1.25** using aluminum trichloride in the presence of dimethylaniline proceeded in good yield to provide columbiasin A (**1.23**). This example demonstrates utility of IMDA reactions to form vicinal quaternary centers late in a synthetic sequence.

Scheme 1.6. Rychnovsky and Kim's synthesis of (–)-columbiasin A.⁴¹

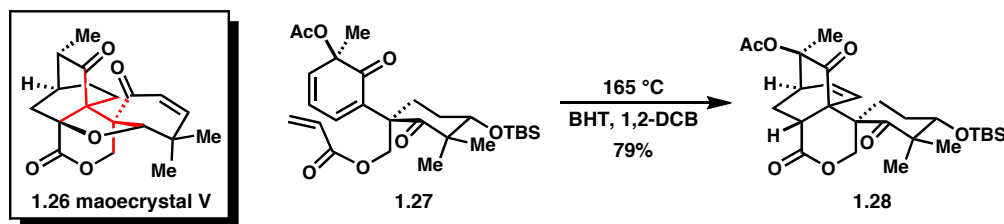


Mode B: Carbon Skeleton Synthesis of (±)-Maoecrystal V

While fully substituted dienophiles are competent cyclization partners, the structure of the target molecule can preclude their use as an effective strategy in synthesis. Baran and co-workers utilized an IMDA reaction toward a racemic synthesis of diterpene natural product maoecrystal V (Scheme 1.7),⁴³ where the vicinal quaternary centers are not suitable for direct installation by mode A. Therefore, Baran's strategy used an IMDA reaction to install a quaternary center adjacent to an existing quaternary center (Scheme 1.4B). When acrylate derivative **1.27** was heated to $165\text{ }^\circ\text{C}$ with radical inhibitor butylhydroxytoluene (BHT), diketone **1.28** was obtained in 79% yield. The major product of the reaction is the result of an electronically disfavored cyclization *via* an *endo* transition state. The constraints of the tether also ensured the regiospecific formation of the desired tetracycle. This example demonstrates the

power of the IMDA reaction to install vicinal quaternary centers despite inherent electronic preferences.

Scheme 1.7. Baran's IMDA strategy toward (\pm)-maoecrystal V.⁴³



Class 2: Type 2 Intramolecular Diels–Alder Reactions

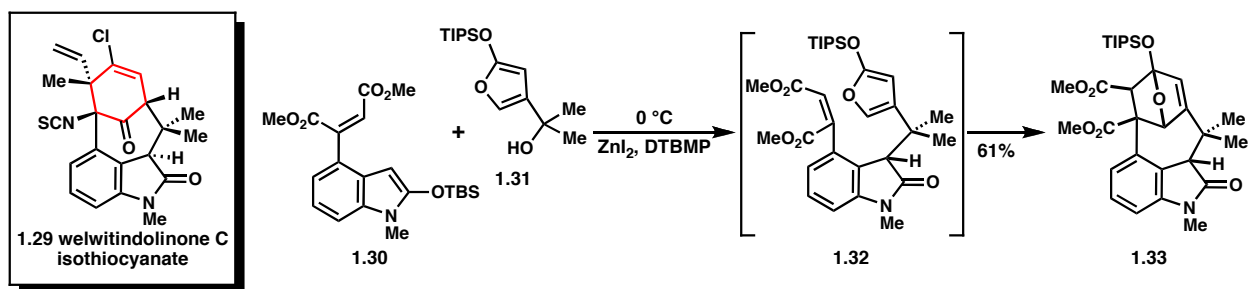
Shea and co-workers pioneered the development of IMDA reactions containing C2 tethered dienes to synthesize bicyclic bridgehead products.^{15,18,44} In order to overcome the strain imparted by the formation of a bridgehead alkene at least one of the following criteria must be met: 1) the dienophile must be activated (highly electron deficient); 2) Lewis-acid must be added; or 3) the reaction must be run at high temperatures. In type 2 IMDA reactions, stereochemical outcomes are dictated by both the nature of the tether and the diene. The regiochemistry of these cyclizations are largely driven by the length and geometric constraints of the tether. Diastereochemical outcomes are dictated by substituents on either the tether or the diene. The stereoselection of the type 2 IMDA reaction is highly substrate dependent and predicting the stereochemical outcome *a priori* is challenging.

Synthesis of Welwitindolinone Intermediates

The potential for highly diastereoselective type 2 IMDA reactions is exemplified by Shea and Cleary's synthetic strategy toward the welwitindolinone family of natural products (Scheme 1.8).⁴⁵ Efficient construction of the highly substituted cyclohexane core present in this family poses a great challenge for organic chemists. Shea's approach employs a type 2 IMDA to install

the cyclohexane ring containing a number of functional groups for further elaboration. The alkylation of silyl ketene aminal **1.30** with alcohol **1.31** in the presence of zinc diiodide and 2,6-di-*tert*-butyl-4-methylpyridine forms furan **1.32**, which undergoes a spontaneous *exo* cyclization (with respect to the activating esters) with the dienophile fragment. The resultant bridgehead alkene **1.33** was obtained in 61% yield as a single diastereomer.

Scheme 1.8. Shea's type 2 IMDA approach to welwitindolinone natural products.⁴⁵



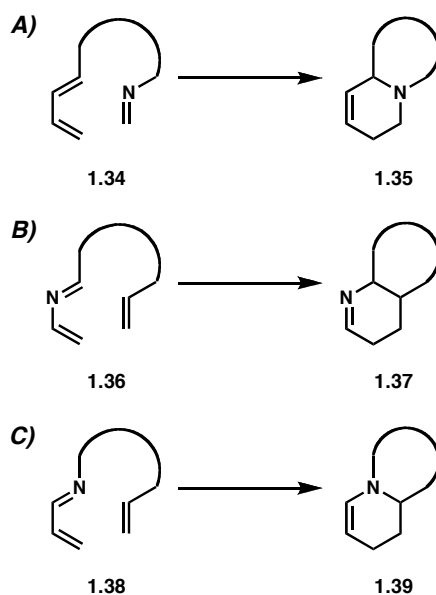
The synthesis of welwitindolinone intermediate **1.33** demonstrates that type 2 IMDA reactions can take place with high levels of regio- and diastereoselectivity. However, the factors governing stereochemical outcomes of *N*-acylnitroso type 2 IMDA reactions are not well understood.⁴⁶ Many recent computational studies of intramolecular Diels–Alder reactions have been limited to type 1 IMDA reactions. As a result, a computational method for these type 2 IMDA reactions was investigated and is discussed in Chapter 4.⁴⁷

Class 3: Intramolecular Aza-Diels–Alder Reactions

Nitrogen containing heterocycles are ubiquitous architectures in natural products and pharmaceuticals. The intramolecular aza-Diels–Alder reaction is a useful method for constructing such heterocycles. Retrosynthetically, aza-IMDA reactions can be divided into two categories: A) aza-IMDA reactions with nitrogen containing dienophiles (imines)^{48,49} and B) aza-IMDA reactions with nitrogen containing dienes^{50,51} (Scheme 1.9). Imine aza-Diels–Alder

reactions have been widely used due to their ease of preparation and high reactivity. Imine dienophiles typically undergo normal electron demand Diels–Alder reactions, whereas azadienes prefer to react in an inverse electron demand manner. In both cases, *endo/exo* selectivity is largely dependent on several factors including tether length, substituents, catalysts and reaction conditions. This selectivity is further obfuscated by the configurational instability of the nitrogen atom (*E/Z* imine isomerization and sp^3 -nitrogen inversion) and typically a convention is assigned with respect to substituents.

Scheme 1.9. Intramolecular aza-Diels–Alder reaction classes.

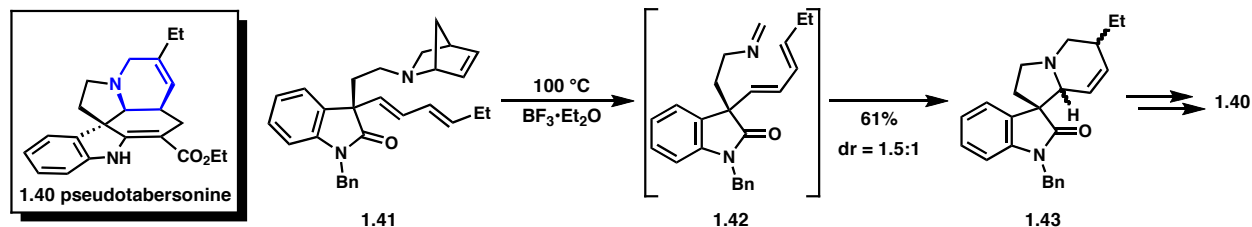


Imine Aza-IMDA Reactions: Synthesis of (–)-Pseudotabersonine

The facility of tethered imine dienophiles to undergo intramolecular aza-Diels–Alder reactions is exemplified by Grieco and Carroll’s synthesis of pseudotabersonine (Scheme 1.10).⁵² Under thermal conditions, azanorbornene **1.41** fragmented in a retro-Diels–Alder reaction to reveal the intermediate imine **1.42**. In the presence of boron trifluoride etherate, imine **1.42** underwent an aza-IMDA reaction to afford spirocyclic indolizidine **1.43** in 61% yield. The product was obtained as a 1.5:1 mixture of diastereomers favoring the *endo* product with respect

to the tether. The diastereomeric mixture was of no consequence since both isomers were converted to a common intermediate *en route* to pseudotabersonine. Though the imine aza-IMDA reaction is a common way to synthesize indolizidine ring systems, 1-azadiene IMDA reactions can also be implemented for such motifs and is discussed in Chapter 5.

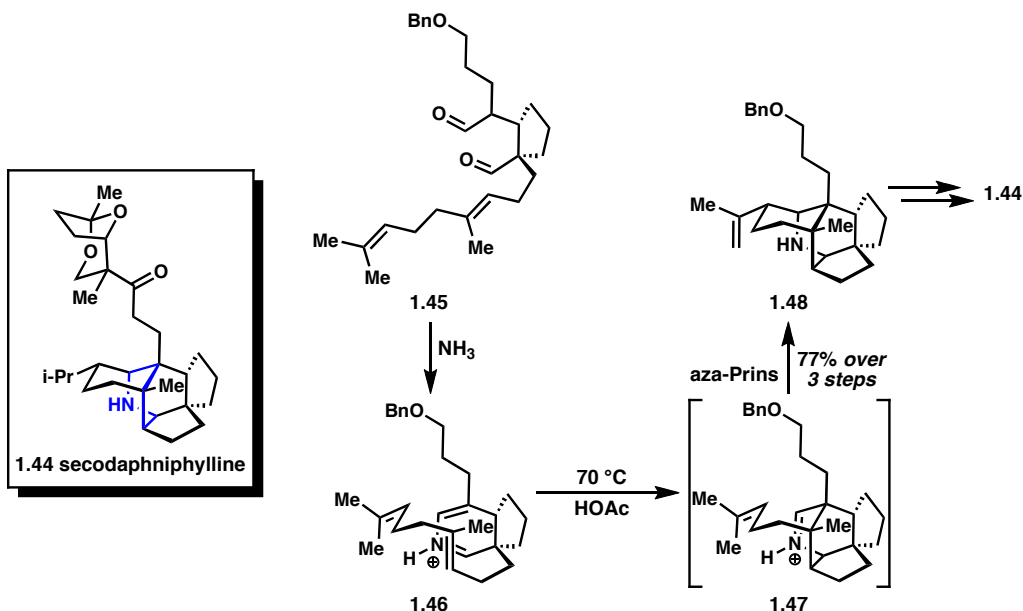
Scheme 1.10. Grieco and Carroll's imine aza-IMDA synthesis of (–)-pseudotabersonine.



2-Azadiene IMDA Reactions: Synthesis of (–)-Secodaphniphylline

Of the limited examples of azadiene IMDA reactions, Heathcock and Stafford's use in the synthesis of (–)-secodaphniphylline clearly demonstrates the utility of 2-azadienes as synthetic intermediates (Scheme 1.11).⁵³ The inverse electron demand nature of the 1- and 2-azadiene cyclization permits the use of normally unreactive (i.e. electron-rich) alkenes. In Heathcock's case, condensation of dialdehyde **1.45** with ammonia provided IMDA substrate **1.46**, which underwent spontaneous cyclization to iminium **1.47** upon treatment with acetic acid at 70 °C. The *exo* cyclization with respect to the tether was dictated by the short tether length and existing stereochemistry. Iminium **1.47** underwent a subsequent aza-Prins cyclization to form tetracycle **1.48**. Subsequent elaboration provided (–)-secodaphniphylline (**1.44**). The effectiveness of 2-azadienes as IMDA substrates is highlighted by the construction of congested centers without the need for dienophile activation and the ability of the IMDA product to engage in a subsequent cyclization.

Scheme 1.11. Heathcock and Stafford's 2-azadiene IMDA strategy for (-)-secodaphniphylline.⁵³



Conclusions

This introduction is meant to provide a brief overview of the general features of IMDA reactions and provide sufficient background for the four projects described in the following chapters. Chapter 2 describes research toward the total synthesis of maocystal Z utilizing a type 1 IMDA reaction to construct the congested core of the diterpene natural product. Chapter 3 describes the synthesis of the isotwistane core of the palhinine family of products by a Morita–Baylis–Hillman/type 1 IMDA approach. This method installs vicinal quaternary centers in the cyclization step. Computational studies on the regio- and stereochemistry of the type 2 intramolecular *N*-acylnitroso Diels–Alder reaction is discussed in Chapter 4. Finally, Chapter 5 presents preliminary results on the scope and diastereoselectivity of aza-IMDA reactions using cyano-1-azadienes in the synthesis of indolizidine and quinolizidine heterocycles.

References

- ¹ Seminal publication: Diels, O.; Alder, K. *Justus Liebigs Ann. Chem.* **1928**, *460*, 98–122.
- ² Evans, D. A.; Johnson, J. S. Chapter 33.1 Diels–Alder Reactions in *Comprehensive Asymmetric Catalysis*; Jacobsen, E. N.; Pfaltz, A.; Yamamoto, H., Eds.; Springer–Verlag: Berlin, Germany, 1999; pp. 1178–1235.
- ³ For industrial applications of the Diels–Alder reaction: Funel, J.-A.; Abele, S. *Angew. Chem., Int. Ed.* **2013**, *52*, 3822–3863.
- ⁴ Early review of preparative aspects of the Diels–Alder reaction: Sauer, J. *Angew. Chem., Int. Ed.* **1966**, *5*, 211–230.
- ⁵ Early mechanistic study of the Diels–Alder reaction: Woodward, R. B.; Katz, T. J. *Tetrahedron* **1959**, *5*, 70–89.
- ⁶ Early review of the mechanism of the Diels–Alder reaction: Sauer, J. *Angew. Chem., Int. Ed.* **1967**, *6*, 16–33.
- ⁷ Critical survey of the Diels–Alder reaction mechanism: Sauer, J.; Sustmann, R. *Angew. Chem., Int. Ed.* **1980**, *19*, 779–807.
- ⁸ Frontier molecular orbital theory of cycloaddition reactions: Houk, K. N. *Acc. Chem. Res.* **1975**, *8*, 361–369.
- ⁹ Fleming, I. *Frontier Orbitals and Organic Chemical Reactions.*; Wiley, 1976; p. 249 pp.
- ¹⁰ Review of catalytic enantioselective Diels–Alder reactions: Corey, E. J. *Angew. Chem., Int. Ed.* **2002**, *41*, 1650–1667.
- ¹¹ Cope, A. C.; Ciganek, E.; LeBel, N. A. *J. Am. Chem. Soc.* **1959**, *81*, 2799–2804.

- ¹² Oppolzer, W. 4.1 - Intermolecular Diels–Alder Reactions in *Comprehensive Organic Synthesis*; Trost, B. M.; Fleming, I. B. T.-C. O. S., Eds.; Pergamon: Oxford, 1991; pp. 315–399.
- ¹³ Roush, W. R. 4.4 - Intramolecular Diels–Alder Reactions in *Comprehensive Organic Synthesis*; Trost, B. M.; Fleming, I. B. T.-C. O. S., Eds.; Pergamon: Oxford, 1991; pp. 513–550.
- ¹⁴ Early study of the type 1 intramolecular Diels–Alder reaction: House, H. O.; Cronin, T. H. *J. Org. Chem.* **1965**, *30*, 1061–1070.
- ¹⁵ Seminal publication of the type 2 intramolecular Diels–Alder reaction: Shea, K. J.; Wise, S. J. *Am. Chem. Soc.* **1978**, *100*, 6519–6521.
- ¹⁶ Review of the Diels–Alder reaction in total synthesis: Nicolaou, K. C.; Snyder, S. A.; Montagnon, T.; Vassilikogiannakis, G. *Angew. Chem., Int. Ed.* **2002**, *41*, 1668–1698.
- ¹⁷ Review of the intramolecular Diels–Alder reaction in natural product synthesis: Takao, K.; Munakata, R.; Tadano, K. *Chem. Rev.* **2005**, *105*, 4779–4807.
- ¹⁸ Review of the type 2 intramolecular Diels–Alder reaction: Bear, B. R.; Sparks, S. M.; Shea, K. *J. Angew. Chem. Int. Ed.* **2001**, *40*, 820–849.
- ¹⁹ Review of the hetero-Diels–Alder reaction: Tietze, L. E.; Ketschau, G. *Top. Curr. Chem.* **1997**, *189*, 1–120.
- ²⁰ Review of the catalytic asymmetric hetero-Diels–Alder reaction: Jorgensen, K. A. *Angew. Chem., Int. Ed.* **2000**, *39*, 3558–3588.
- ²¹ Review of the catalytic enantioselective aza-Diels–Alder reaction: Masson, G.; Lalli, C.; Benohoud, M.; Dagousset, G. *Chem. Soc. Rev.* **2013**, *42*, 902–923.

- ²² Early example of an inverse demand Diels–Alder reaction: Carboni, R. A.; Lindsey Jr., R. V. *J. Am. Chem. Soc.* **1959**, *81*, 4342–4346.
- ²³ Review of the synthesis of tetrahydropyrans: Perry, M. A.; Rychnovsky, S. D.; Sizemore, N. In *Topics in Heterocyclic Chemistry*; Cossy, J., Ed.; Springer: New York, 2014; pp. 43–95.
- ²⁴ Review of the synthesis of piperidones and piperidines: Weintraub, P. M.; Sabol, J. S.; Kane, J. M.; Borcherding, D. R. *Tetrahedron* **2003**, *59*, 2953–2989.
- ²⁵ Review of the synthesis of piperidines: Buffat, M. G. P. *Tetrahedron* **2004**, *60*, 1701–1729.
- ²⁶ Computer-assisted evaluation of six-electron cycloadditions: Schmidt, J. A.; Jorgensen, W. L. *J. Org. Chem.* **1983**, *48*, 3923–3941.
- ²⁷ Review of Density Functional Theory (DFT): Geerlings, P.; De Proft, F.; Langenaeker, W. *Chem. Rev.* **2003**, *103*, 1793–1874.
- ²⁸ Quantum mechanical methods and pericyclic reaction mechanisms: Wiest, O.; Montiel, D. C.; Houk, K. N. *J. Phys. Chem. A* **1997**, *101*, 8378–8388.
- ²⁹ Quantum mechanical methods and pericyclic transition structures: Houk, K. N.; Beno, B. R.; Nendel, M.; Black, K.; Yoo, H. Y.; Wilsey, S.; Lee, J. *J. Mol. Struct. THEOCHEM* **1997**, *398-399*, 169–179.
- ³⁰ Standards for benchmarking computational methods: Guner, V.; Khuong, K. S.; Leach, A. G.; Lee, P. S.; Bartberger, M. D.; Houk, K. N. *J. Phys. Chem. A* **2003**, *107*, 11445–11459.
- ³¹ Sources of error in DFT computations: Pieniazek, S. N.; Clemente, F. R.; Houk, K. N. *Angew. Chem. Int. Ed.* **2008**, *47*, 7746–7749.
- ³² Dynamics of bond formation in Diels–Alder reactions: Black, K.; Liu, P.; Xu, L.; Doubleday, C.; Houk, K. N. *PNAS* **2012**, *109*, 12860–12865.

- ³³ Computational study of stereoselectivity in intramolecular Diels–Alder reactions: Tantillo, D. J.; Houk, K. N.; Jung, M. E. *J. Org. Chem.* **2001**, *66*, 1938–1940.
- ³⁴ Computational study of stereoselectivity in intramolecular Diels–Alder reactions: Paddon-Row, M. N.; Moran, D.; Jones, G. A.; Sherburn, M. S. *J. Org. Chem.* **2005**, *70*, 10841–10853.
- ³⁵ Review of vicinal quaternary centers: Peterson, E. A.; Overman, L. E. *P. Natl. Acad. Sci. USA* **2004**, *101*, 11943–11948.
- ³⁶ See also: Sizemore, N.; Rychnovsky, S. D. *Org. Lett.* **2014**, *16*, 688–691.
- ³⁷ Toro, A.; Lemelin, C.-A.; Preville, P.; Belanger, G.; Deslongchamps, P. *Tetrahedron* **1999**, *55*, 4655–4684.
- ³⁸ Toro, A.; Nowak, P.; Deslongchamps, P. *J. Am. Chem. Soc.* **2000**, *122*, 4526–4527.
- ³⁹ Krapcho, A. P.; Glynn, G. A.; Grenon, B. J. *Tetrahedron Lett.* **1967**, 215–217.
- ⁴⁰ Review of the transannular Diels–Alder reaction in total synthesis: Marsault, E.; Toro, A.; Nowak, P.; Deslongchamps, P. *Tetrahedron* **2001**, *57*, 4243–4260.
- ⁴¹ Kim, A. I.; Rychnovsky, S. D. *Angew. Chem., Int. Ed.* **2003**, *42*, 1267–1270.
- ⁴² Myers, A. G.; Yang, B. H.; Chen, H.; McKinstry, L.; Kopecky, D. J.; Gleason, J. L. *J. Am. Chem. Soc.* **1997**, *119*, 6496–6511.
- ⁴³ Krawczuk, P. J.; Schone, N.; Baran, P. S. *Org. Lett.* **2009**, *11*, 4774–4776.
- ⁴⁴ Shea, K. J.; Wise, S. *Tetrahedron Lett.* **1979**, 1011–1014.
- ⁴⁵ Cleary, L. Ph.D. Dissertation, University of California, Irvine, 2013, pp. 1–559.
- ⁴⁶ *N*-acyl nitroso type 2 intramolecular Diels–Alder reaction: Sparks, S. M.; Chow, C. P.; Zhu, L.; Shea, K. J. *J. Org. Chem.* **2004**, *69*, 3025–3035.

- ⁴⁷ See also: Cleary, L.; Mak, V. W.; Rychnovsky, S. D.; Shea, K. J.; Sizemore, N. *J. Org. Chem.* **2013**, *78*, 4090–4098.
- ⁴⁸ Review of imino aza-Diels–Alder reactions: Buonora, P.; Olsen, J.-C.; Oh, T. *Tetrahedron* **2001**, *57*, 6099–6138.
- ⁴⁹ Review of iminium aza-Diels–Alder reactions: Memeo, M. G.; Quadrelli, P. *Chem. Eur. J.* **2012**, *18*, 12554–12582.
- ⁵⁰ Review of azadiene Diels–Alder reactions: Boger, D. L. *Tetrahedron* **1983**, *39*, 2869–2939.
- ⁵¹ Review of 1-azadiene Diels–Alder reactions: Behforouz, M.; Ahmadian, M. *Tetrahedron* **2000**, *56*, 5259–5288.
- ⁵² Carroll, W. A.; Grieco, P. A. *J. Am. Chem. Soc.* **1993**, *115*, 1164–1165.
- ⁵³ Heathcock, C. H.; Stafford, J. A. *J. Org. Chem.* **1992**, *57*, 2566–2574.

Chapter 2

Studies Toward the Total Synthesis of Maoecrystal Z: An Intramolecular Diels–Alder Approach

Abstract

Maoecrystal Z is an anticancer diterpene natural product with a unique architecture. Examination of a synthetic route to the intramolecular Diels–Alder (IMDA) precursor of maoecrystal Z and computational studies of the proposed IMDA is described herein. Two approaches featuring a palladium-catalyzed cross-coupling reaction and an enantioselective Tsuji–Trost allylation were investigated. A total synthesis of maoecrystal Z by Reisman and co-workers ultimately led to the discontinuation of this research.

Introduction

The total synthesis of biologically active natural products has provided a wealth of information for the discovery and development of pharmaceutical agents.¹ Natural products, obtained in trace quantities from living organisms, often exhibit interesting biological activity *via* modulation of cellular processes. However, biological studies of these products are often hampered by their limited supply. Chemical synthesis not only provides a solution to supply problems, but also access to useful derivatives. A recent review has shown that between 1981 and 2006, 34 of the 100 New Chemical Entities (NCEs) with an anticancer indication were either natural products or synthetic derivatives thereof.² This study also concluded that 11 purely synthetic anticancer NCEs had pharmacophores that are found in natural products. Therefore, natural products remain a valuable starting point for medicinal chemistry programs.

One such intriguing biologically active natural product, maoecrystal Z (**2.1**), was isolated in 2006 by Xu *et al.* from *Isodon eriocalyx*.³ Plants of the *Isodon* genus have been used in Chinese folk medicine to treat a variety of ailments including inflammation and cancer.⁴ Many of the active constituents are diterpenoids of the structurally related *ent*-kaurane class (Figure 2.1), however the unprecedented tetracyclic core and densely functionalized structure of **2.1** present a formidable synthetic challenge. Maoecrystal Z was also shown to be cytotoxic to leukemia, breast and ovarian tumor cell lines, but the low isolation yield (8 mg, 0.0073%) has prohibited further investigation of this activity.³ This project aimed to synthesize **2.1** in order to provide the quantities necessary for comprehensive screening against cancer cell lines, as well as to probe the mechanism of action for the observed cytotoxicity. The construction of a functionalized carbon core will offer the opportunity to synthesize derivatives of maoecrystal Z in order to investigate structure activity relationships (SAR).

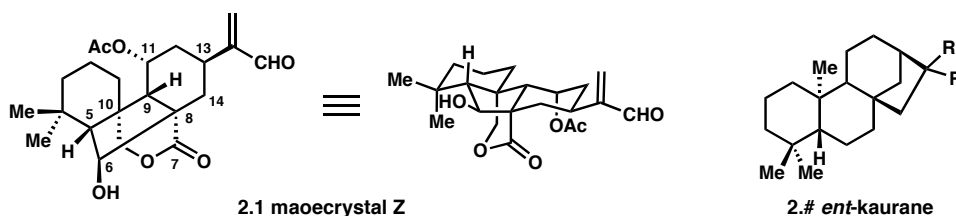


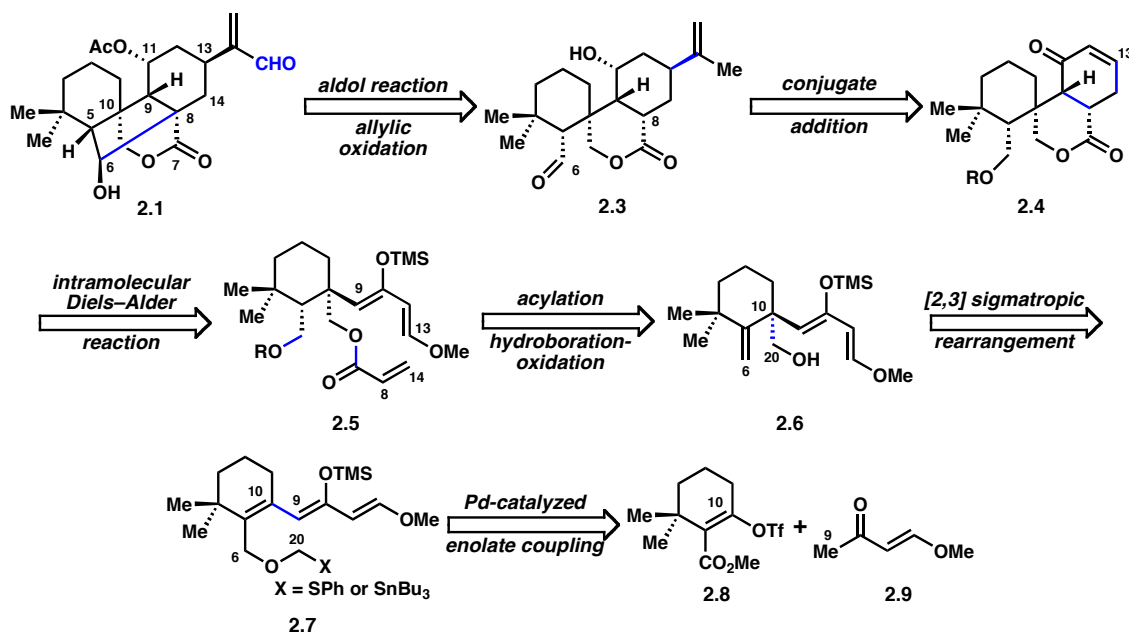
Figure 2.1. Maoecrystal Z and *ent*-kaurane skeleton.

Retrosynthetic Analysis of Maoecrystal Z

The retrosynthetic analysis for maoecrystal Z is outlined in Scheme 2.1. It was envisioned that the C6–C8 bond would be forged *via* an intramolecular aldol reaction of aldehyde **2.3**. The isoprene side chain would be introduced through a conjugate addition onto enone **2.4**, which could be synthetically accessible from an intramolecular Diels–Alder (IMDA) reaction. This reaction would install the C8–C9 and C13–C14 bonds to afford the skeletal core with the necessary functionality to synthesize **2.1**. The IMDA precursor **2.5** would result from

acylation and hydroboration-oxidation of homoallylic alcohol **2.6**. Alcohol **2.6** would arise through the anionic [2,3]-sigmatropic rearrangement of allylic ether **2.7**. The triene moiety of **2.7** could be constructed by a palladium-catalyzed enolate coupling of vinyl triflate **2.8** and enone **2.9**. Both **2.8** and **2.9** are reported compounds that are accessible from inexpensive starting materials.

Scheme 2.1. Retrosynthetic analysis of maoecrystal Z.



Molecular Modeling of the IMDA Reaction

Intramolecular Diels-Alder reactions are often employed in the synthesis of complex natural products because of their ability to rapidly construct six-membered rings with high selectivities.⁵ When predicting the stereochemical outcomes of IMDAs, it is important to consider the different transition states available to the starting substrate.⁶ Both the approach of the dienophile (*endo* vs. *exo*) and the orientation of the diene determine the composition of the products. Density functional theory (DFT) calculations have proven to be a useful tool in determining the outcome of such reactions *in silico*.⁷⁻⁹ Since the selectivity of the proposed

IMDA is not obvious, computational modeling was utilized to investigate its viability as a synthetic strategy.

Our investigation began by selecting a model system (Figure 2.2, **2.10**), and performing a conformational analysis using the MMFF force field in Spartan 08.¹⁰ The conformations with relative energies less than 5.00 kcal/mol and a distance between C13 and C14 of less than 4.00 Å were selected. The data suggested that there were five distinct conformations that could give rise to IMDA products. These conformations were then subjected to distance constraints of 2.51 Å for (C8–C9) and 2.07 Å for the (C13–C14). A DFT geometry optimization using the most relevant basis set (B3LYP/6-31+G(d))⁷ was performed. Transition states were identified and confirmed with frequency calculations. The results are summarized in Figure 2.2.

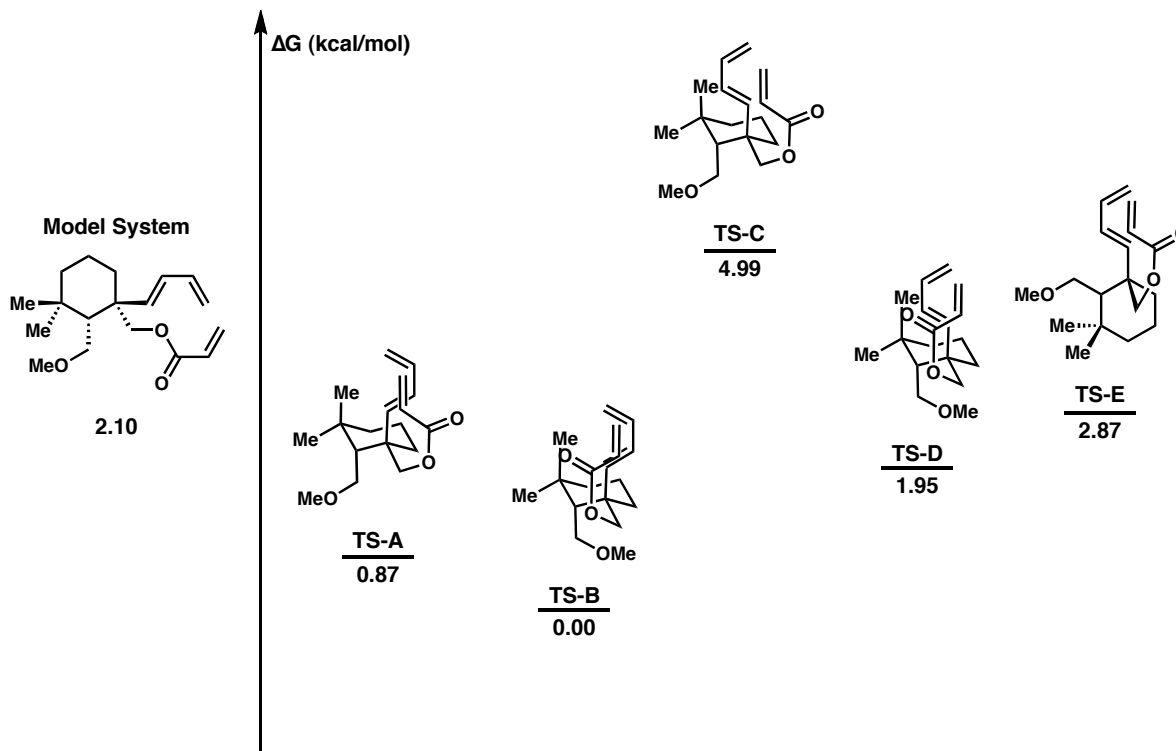


Figure 2.2. Transition state comparison for the IMDA reaction.

As calculated, the desired diene orientation is present in the low energy transition states (TS-A and TS-B), whereas the higher energy transition states (TS-C, TS-D, and TS-E) have the

undesired diene orientation. In the low energy regime, the dienophile shows a slight preference for an *exo* orientation (**TS-B**). While transition state B leads to an undesired diastereomer (**PDT-B**, Figure 2.3), the stereocenter at C8 is alpha to the lactone and should therefore be epimerizable. Since enolate formation is required at C8 for the aldol ring closure, both **PDT-A** and **PDT-B** should be useful products (Figure 2.3). These calculations lead us to believe that the proposed IMDA is a reasonable synthetic strategy.

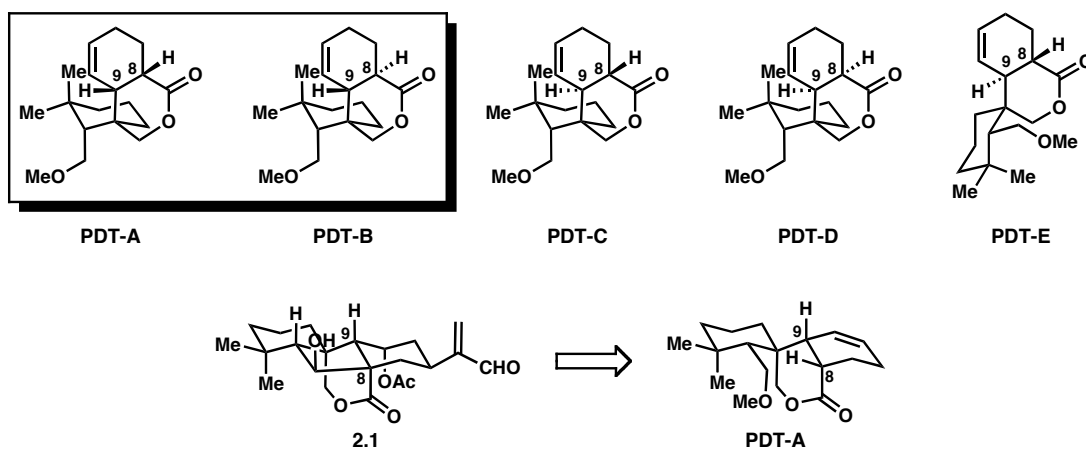


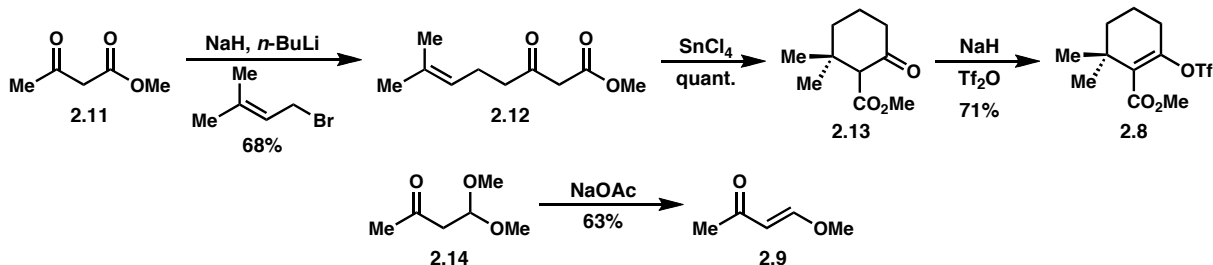
Figure 2.3. Comparison of IMDA products and maoecrystal Z.

Results and Discussion

Synthetic Studies of a Cross-Coupling Strategy to IMDA Precursor 2.5

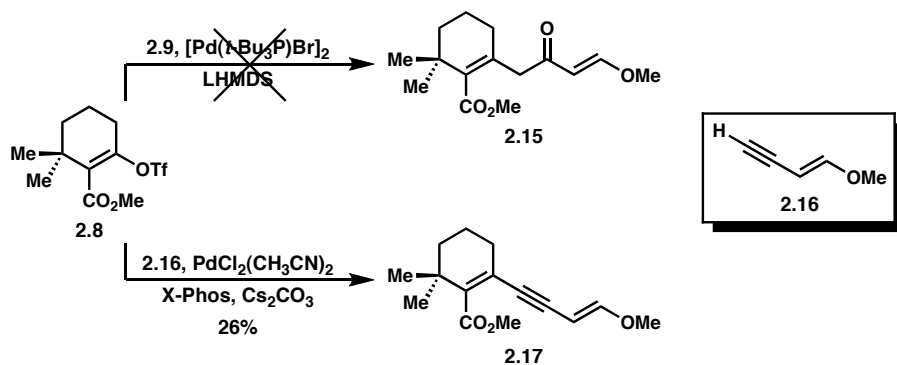
The synthesis began with the preparation of the enol triflate **2.8** as shown in Scheme 2.2. Sequential deprotonation of methyl acetoacetate (**2.11**), followed by treatment with 3,3-dimethylallyl bromide resulted in alkylation of the δ -position to furnish β -keto ester **2.12**.^{11,12} Treatment of β -keto ester **2.12** with tin(IV) chloride resulted in quantitative conversion to cyclic β -keto ester **2.13**. Deprotonation of **2.13** with sodium hydride, followed by trapping with triflic anhydride afforded vinyl triflate **2.8** in good yield.¹³ Enone **2.9** was easily obtained by a base-catalyzed elimination of methanol from 4,4-dimethoxy-2-butanone (**2.14**).¹⁴

Scheme 2.2. Synthesis of coupling partners.



Efforts toward the palladium-catalyzed enolate coupling of **2.8** and **2.9** followed the method developed by Huang *et al.*¹⁵ The transformation requires the exotic $[\text{Pd}(t\text{-Bu}_3\text{P})\text{Br}]_2$ catalyst and provides diminished yield when the enol triflate bears an electron withdrawing group. Using this method for enolate coupling with our system resulted in a complex mixture that was spectroscopically inconsistent with desired enone **2.15** (Scheme 2.3). Additional concerns about the sensitivity of enone **2.15** to the strongly basic conditions led us to abandon the enolate coupling strategy in favor of the more established Sonogashira reaction with known alkyne **2.16**.¹⁶

Scheme 2.3. Strategies for cross-coupling.



Under standard copper-mediated Sonogashira coupling conditions,¹⁷ the primary product obtained was not desired dienyne **2.17**, but the result of undesired alkyne homocoupling. This suggested that oxidative addition of palladium into vinyl triflate **2.8** was a slow process. To increase the rate of oxidative addition, attempts were made to convert the cyclic β -keto ester **2.13**

to a vinyl bromide. Despite investigating a variety of conditions,¹⁸⁻²² a method to carry out this transformation was not identified. Copper-free Sonogashira conditions developed by Buchwald and Gelman²³ were reported to suppress homocoupling of alkynyl partners. Upon subjecting vinyl triflate **2.8** and alkyne **2.16** to these conditions, conversion to **2.17**, was observed by GC/MS. Unfortunately, **2.17** proved to be unstable to purification conditions, storage and further synthetic operations as a crude mixture.

Suspecting the high level of conjugation was responsible for the observed instability, reduced derivatives of vinyl triflate **2.8** were investigated (Scheme 2.4). A DIBAL-H reduction of ester **2.8** afforded alcohol **2.18**, which was subsequently protected to provide silyl ether **2.19**. However, subjecting either alcohol **2.18** or TMS-ether **2.19** to the copper-free Sonogashira conditions, gave complex mixtures that were inconsistent with product formation. The instability of reduced derivatives **2.18** and **2.19** to the reaction conditions led us to attempt alkylations of alcohol **2.18**; the rationale being that the resultant ether moiety would provide enhanced stability and the necessary functionality for the [2,3]-sigmatropic rearrangement. Applying conditions for installing either stannylmethylene²⁴⁻²⁶ or thiophenylmethylene ether²⁷ to alcohol **2.18**, only resulted in rapid decomposition (Scheme 2.4). NMR analysis, in conjunction with a recent report by Knochel *et al.*,²⁸ suggests that the alcohol **2.18** decomposes to the enone **2.25** upon treatment with base (Figure 2.4). At this point, synthetic efforts on this route were halted due to an inability to identify substrates that would provide isolable products.

Scheme 2.4. Synthesis of reduced derivatives.

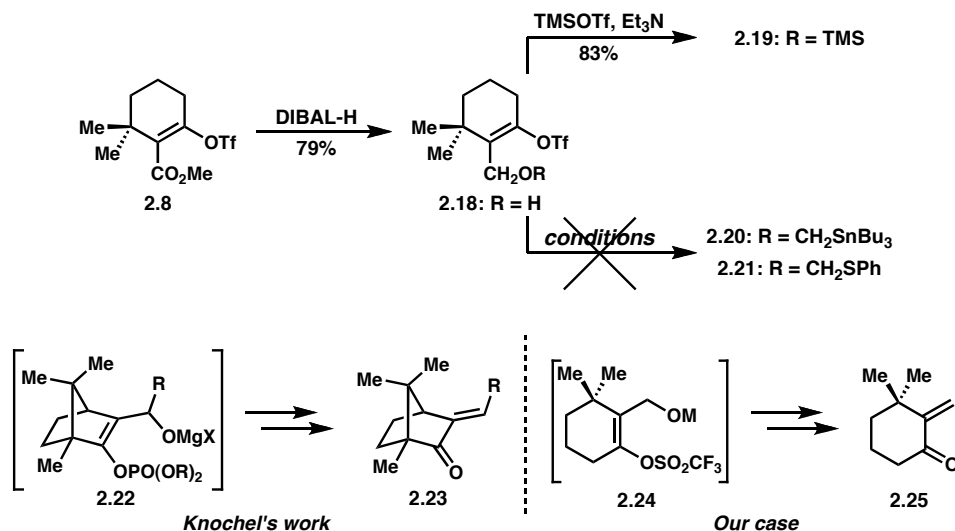
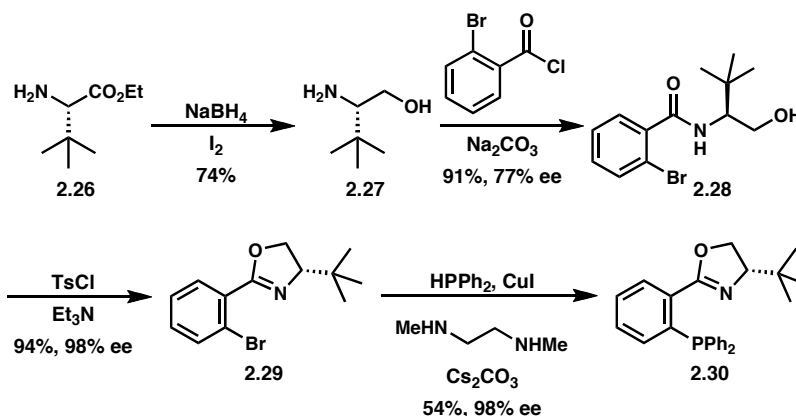


Figure 2.4. Precedent²⁸ and rationale for enone formation.

An Enantioselective Tsuji–Trost Allylation Approach to Tricycle 2.4

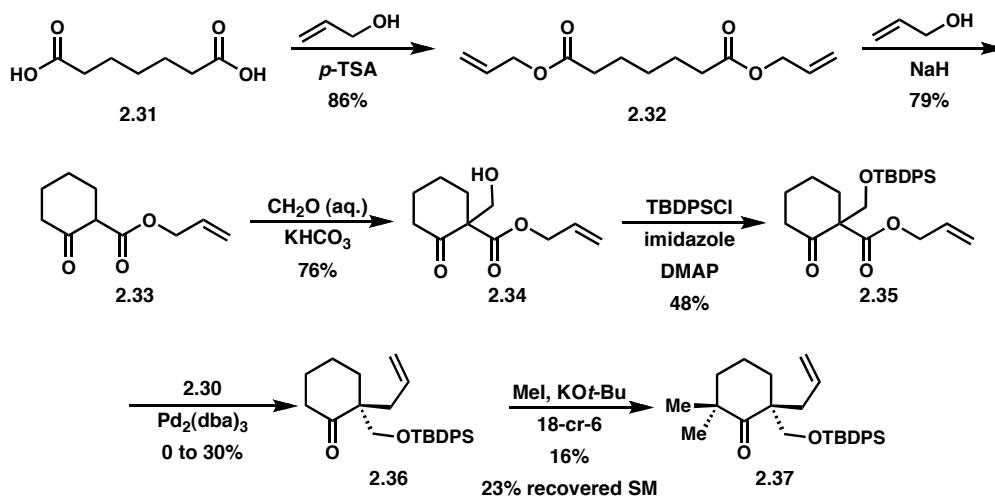
The inability to effectively introduce either a diene precursor or the rearrangement fragment on the cyclohexane core led us to devise a new strategy to access tricycle **2.4**. The revised route (Scheme 2.6-7) is inspired by Stoltz's work on enantioselective Tsuji–Trost allylations.^{29–31} This method requires the use of (*S*)-*t*-Bu-PHOX as the phosphine ligand for maximum enantioselectivity. The synthesis of (*S*)-*t*-Bu-PHOX is outlined in Scheme 2.5. Treatment of ethyl (*S*)-2-amino-3,3-dimethylbutyrate **2.26** with NaBH₄ and I₂ afforded the alcohol **2.27**.³² Alcohol **2.27** was subjected to biphasic conditions with 2-bromobenzoyl chloride and Na₂CO₃ to provide amide **2.28**. Tosylation of the alcohol moiety of **2.28**, followed by heating, led to the formation of the phenyloxazoline **2.29**. Treatment of phenyloxazoline **2.29** with diphenylphosphine in the presence of CuI and *N,N'*-dimethylethylenediamine afforded (*S*)-*t*-Bu-PHOX (**2.30**), as described by Stoltz and Behenna.³⁰

Scheme 2.5. Synthesis of (*S*)-*t*-Bu-PHOX.



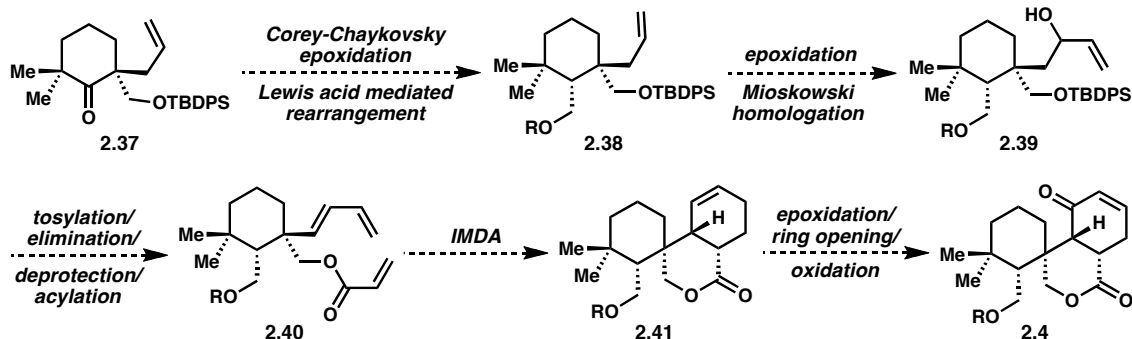
With ligand **2.30** in hand, the synthesis of fully substituted ketone **2.37** was investigated (Scheme 2.6). Commercially available pimelic acid (**2.31**) was esterified with allylic alcohol and catalytic *p*-toluenesulfonic acid to afford the diester **2.32**. A Dieckmann condensation^{33,34} of diester **2.32** was achieved by treatment with NaH in the presence of allylic alcohol to afford the cyclic β -keto ester **2.33**. Subjecting cyclic β -keto ester **2.33** to aqueous formaldehyde and KHCO_3 provided aldol product **2.34** in 76% yield. The alcohol moiety of **2.34** was subsequently protected as the silyl ether **2.35** using TBDPSCI, imidazole and DMAP. Applying the reported enantioselective Tsuji–Trost allylation of silyl ether **2.35** with (*S*)-*t*-Bu-PHOX (**2.30**) and $\text{Pd}_2(\text{dba})_3$ afforded the ketone **2.36** proceeded, albeit in variable low yields.³⁰ This reaction appeared to be extremely sensitive to the presence of oxygen³⁵ and all attempts to fully deoxygenate were unsuccessful in improving the yield. A small-scale permethylation of ketone **2.36** provided the fully substituted ketone **2.37** in low yields, though starting material was recovered. Attempts to improve the yield and reproducibility of the enantioselective allylation, as well as identifying optimal conditions for the permethylation, were met with limited success.

Scheme 2.6. Revised synthetic route to ketone **2.37**.



From the fully-substituted ketone **2.37**, the planned synthetic operations to obtain advanced intermediate **2.4** are outlined in Scheme 2.7. A Corey–Chaykovsky epoxidation³⁶ of ketone **2.37** would install the C5–C6 bond, and a Lewis acid mediated arrangement to the aldehyde,³⁷ followed by reduction and protection of the resultant alcohol would afford the allyl derivative **2.38**. The terminal olefin could be epoxidized and homologated to provide allylic alcohol **2.39** under Mitsunobu conditions.³⁸ Tosylation of the free alcohol, followed by base-promoted elimination, would afford the necessary diene moiety. Next, silyl deprotection of the primary alcohol followed by acylation would afford the IMDA precursor **2.40**. This IMDA precursor would afford the desired tricycle **2.41**, which could be epoxidized, ring opened and oxidized to afford the enone **2.4**.

Scheme 2.7. Planned synthetic operation to tricycle **2.4**.



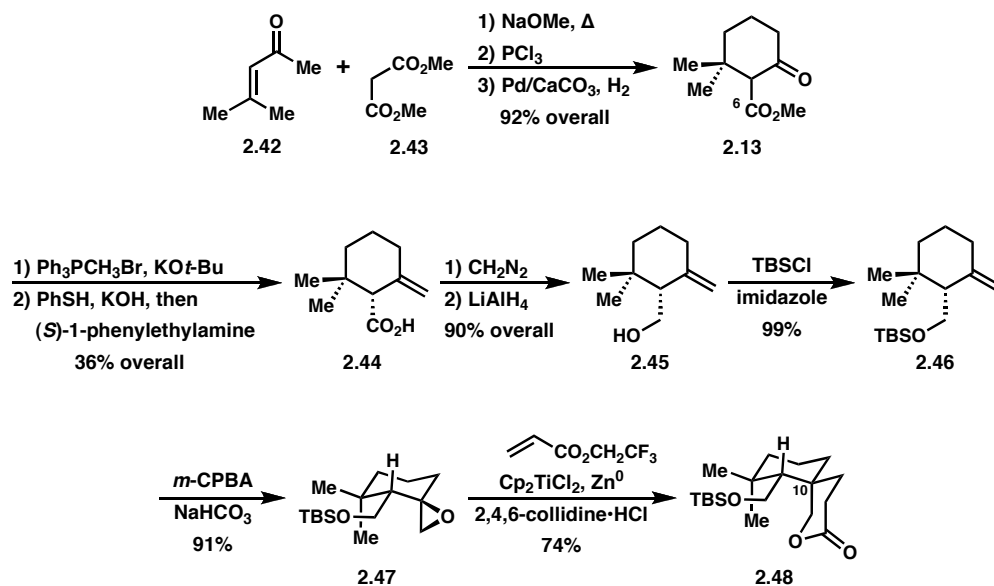
Reisman and Co-workers Total Synthesis of (-)-Maoecrystal Z

During the course of these studies, Reisman and co-workers reported the total synthesis of (-)-maoecrystal Z (Scheme 2.8-10).³⁹ This concise approach features a diastereoselective Ti(III)-mediated reductive epoxide coupling^{40,41} to rapidly access spiro lactone **2.48**. Further elaboration of spiro lactone **2.48** allowed for the Sm(II)-mediated reductive cyclization cascade⁴² to tetracycle **2.56**, which was carried forward to the natural product.

The synthesis of spiro lactone **2.48** began with base-mediated cyclization of 4-methyl-3-penten-2-one (**2.42**) and dimethyl malonate (**2.43**) to afford an intermediate diketone, which was monochlorinated with phosphorus trichloride and reduced with Lindlar's catalyst⁴³ to provide racemic β -keto ester **2.13** in 92% yield over three steps (Scheme 2.8).⁴⁴ Olefination of ketone **2.13** using methylene triphenylphosphorane in the presence of potassium *tert*-butoxide, followed by kinetic resolution afforded 36% yield of carboxylic acid **2.44**. A two-step esterification/reduction sequence provided (-)- γ -cyclogeraniol (**2.45**).⁴⁵ Silyl protection of alcohol **2.45** was achieved using TBSCl and imidazole to afford silyl ether **2.46**. Diastereoselective epoxidation of **2.46** using *m*-chloroperoxybenzoic acid in the presence of sodium bicarbonate led to the formation of epoxide **2.47** in 91% yield. Reductive coupling of epoxide **2.47** with 2,2,2-trifluoroethyl acrylate was achieved using titanocene dichloride in the

presence of zinc metal and 2,4,6-collidine to provide spirolactone **2.48** in 74% yield as a single diastereomer.

Scheme 2.8. Reisman's synthesis of spirolactone **2.48**.^{39,44,45}

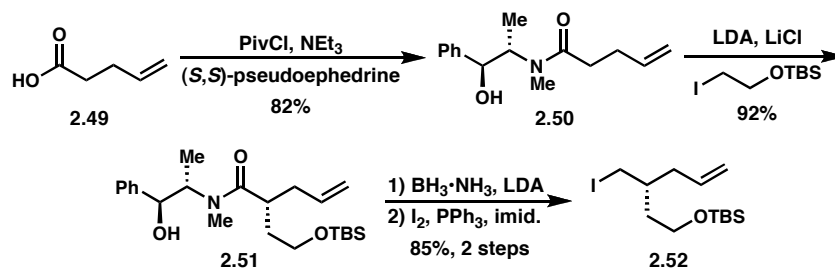


This strategy for constructing the AB fragment of maoecrystal Z provided several advantages over our approach. First, the cyclization of enone **2.42** and diester **2.43** installed the geminal methyl groups in a single step and eliminated the issues associated with their sequential installation. This cyclization also provided the C6 carbon at the ester oxidation state, which allowed for an early-stage kinetic resolution to give enantioenriched material. Finally, the reductive cyclization to spirolactone **2.48**, thought to proceed through a radical pathway, provided the C10 quaternary center required for the synthesis of maoecrystal Z (**2.1**). Reisman's efficient construction of the highly congested AB fragment is remarkable and leaves little room for improvement.

In order to install the remaining two rings of maoecrystal Z, Reisman's strategy required an enolate alkylation of spirolactone **2.48** with the appropriately functionalized electrophile. The synthesis of electrophile **2.52** is shown in Scheme 2.9. Treatment of pent-4-enoic acid (**2.49**)

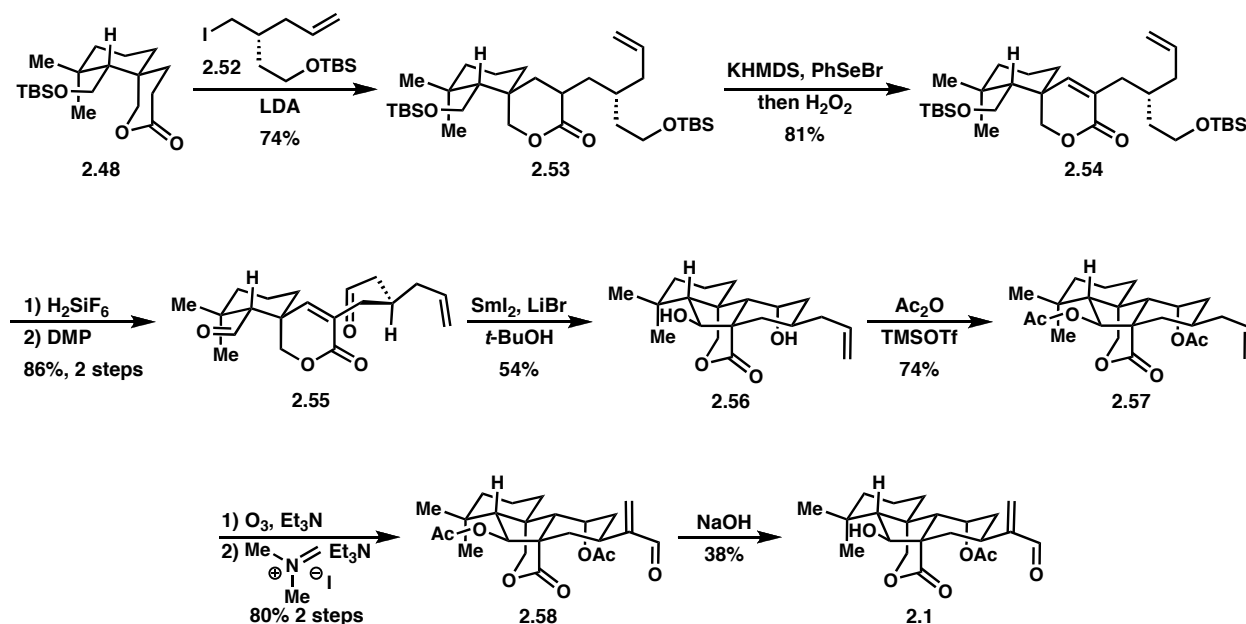
with pivaloyl chloride and triethylamine followed by (*S,S*)-pseudoephedrine led to the formation of amide **2.50**. Stereoselective enolate alkylation using the Myers' protocol⁴⁶ afforded amide **2.51**, which underwent reductive cleavage of the auxiliary and displacement to give iodide **2.52**.

Scheme 2.9. Reisman's synthesis of alkyl iodide **2.52**.³⁹



With spirolactone **2.48** in hand, generation of the enolate using lithium diisopropylamide, followed by alkylation with iodide **2.52**, provided ester **2.53** as an inconsequential mixture of diastereomers (Scheme 2.10). Formation of the α,β -unsaturated ester **2.54** was achieved by oxidation of the intermediate organoselenide. Removal of the silyl protecting groups using fluorosilicic acid, followed by subsequent oxidation to dialdehyde **2.55**, proceeded in 86% yield over two steps. Upon treatment with samarium diiodide in the presence of lithium bromide, dialdehyde **2.55** is believed to undergo ketyl radical formation at the more accessible C11 position. Addition of this ketyl radical into the α,β -unsaturated moiety forged the D ring, leaving a radical alpha to the ester. Subsequent oxidation of the radical to the enolate followed by aldol addition into the pendant aldehyde, generated the C ring. This Sm^{II}-mediate reductive cyclization cascade resulted in the formation of 2 new rings, 4 new stereocenters, and afforded tetracycle **2.56** in 45% yield as a single diastereomer.

Scheme 2.10. Reisman's total synthesis of (-)-maoecrystal Z.³⁹



With the tetracyclic skeleton in place, Reisman and co-workers needed only minor functional group interconversions of **2.56** to access maoecrystal Z. Diol **2.56** was peracetylated by treatment with acetic anhydride and TMSOTf to provide alkene **2.57**. Ozonolysis of alkene **2.57** and alkenylation of the resultant aldehyde with Eshenmoser's salt⁴⁷ led to enal **2.58**. Base mediated monohydrolysis of enal **2.58** proceeded in 38% yield of (-)-maoecrystal Z (**2.1**). The remarkably concise nature of this reported synthesis (19 steps from 4-methyl-3-penten-2-one, 12 steps from known (-)- γ -cyclogeraniol⁴⁵) demonstrates the utility of single-electron reaction pathways in constructing highly congested molecular architectures. As a result of this work, the Reisman group has also recently published syntheses of the related terpene natural products (-)-trichorabdal A and (-)-longikaurin E.^{48,49}

Conclusions

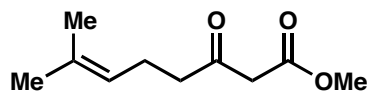
Research on the total synthesis of maoecrystal Z has been discontinued. Computational studies support the IMDA approach to the carbon core of maoecrystal Z as a viable strategy, but the synthetic challenges associated with constructing the IMDA precursor were unable to be overcome. The initial cross-coupling approach was thoroughly investigated, however the inability to identify substrates that would provide isolable intermediates led us to abandon this strategy. The enantioselective Tsuji–Troost allylation strategy suffered from low yields, problems with reproducibility and a high number of synthetic operations to access the IMDA precursor (minimum of 14 steps). In contrast, Reisman and co-workers synthesis of maoecrystal Z is flexible, concise and efficient.³⁹ This elegant approach, coupled with lack of progress toward the Diels–Alder precursor, led us to abandon further studies toward the total synthesis of maoecrystal Z (2.1).

General Experimental Details:

Unless otherwise stated, reactions were carried out using standard procedures for the rigorous exclusion of air and moisture. This included the use of oven-dried glassware, as well as carrying reactions out under an atmosphere of Ar. TLC was carried out using Whatman Partisil[®] K6F TLC plates coated with a 250 μm layer of 60 \AA silica gel. TLC plates were visualized with a UV lamp at 254 nm, or by staining with KMnO_4 , PMA, or vanillin. Organic solutions were concentrated using a Buchi rotary evaporator equipped with a water aspirator. Flash column chromatography was performed using SiliCycle SiliaFlash[®] P60 silica gel. All reagents were purchased from Acros, Alfa Aesar, Sigma-Aldrich, Strem, TCI, or VWR and used without further purification unless otherwise noted. Et_3N and *i*- Pr_2EtN were freshly distilled over CaH prior to

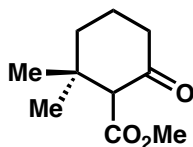
use. Solvents, such as DCM, Et₂O, THF, MeCN and toluene were purchased as HPLC-grade and passed through a solvent purification system equipped with activated alumina columns. Melting points were recorded on an Electrothermal[®] melting point apparatus. Infrared spectra were recorded on a MIDAC Prospect FT-IR spectrometer. GC/MS was carried out using a Finnigan Trace MS equipped for electron ionization. Nuclear magnetic resonance (NMR) spectroscopy was performed using a Bruker Advance 500 spectrometer. Chemical shifts in ¹H NMR spectra are referenced from residual CHCl₃ (δ = 7.26) and reported in parts per million (ppm) with respect to tetramethylsilane. Chemical shifts in ¹³C NMR spectra are referenced from CDCl₃ (δ = 77.07) and reported in ppm with respect to tetramethylsilane. Coupling constants are reported as *J* values and are given in Hertz (Hz). High resolution mass spectrometry was performed by the Mass Spectrometry Laboratory at University of California – Irvine.

Experimental Procedures:

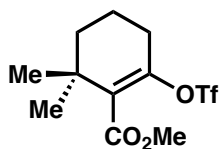


Methyl 7-methyl-3-oxooct-6-enoate (2.12). To a suspension of NaH in THF (1.03 g, 43.0 mmol, 100 mL) at 0 °C was added methyl acetoacetate (4.26 mL, 39.3 mmol) over a period of 25 min, during which the reaction mixture became a clear pale yellow. After addition was complete, the reaction mixture was stirred for 10 min, and *n*-BuLi was added (2.30 M in hexanes, 18.9 mL, 41.3 mmol) over 20 min. The resulting clear orange solution was stirred for 10 min, then warmed to 25 °C and treated with 4-bromo-2-methylbut-2-ene (5.0 mL, 43 mmol). The clear yellow reaction mixture was stirred at 25 °C for an additional 10 min, cooled to 0 °C and quenched with 3.4 M HCl (28 mL). The mixture was diluted with Et₂O (60 mL) and the aqueous extracted with of Et₂O (2 x 40 mL). The combined organics were washed with H₂O (5

x 20 mL), dried over MgSO₄, filtered and concentrated *in vacuo* to a yellow oil (8.1 g). Vacuum distillation afforded the title compound as a clear oil (4.96 g, 68%): bp 88 °C (1.2 torr). Spectral data matched those reported in the literature.^{12,50}

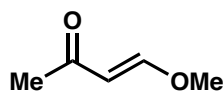


Methyl 2,2-dimethyl-6-oxocyclohexanecarboxylate (2.13). To a solution of **2.12** in DCM (3.44 g, 18.6 mmol, 40 mL) at 0 °C was added SnCl₄ (1.0 M in DCM, 20.0 mL, 20.0 mmol, 1.0 M) dropwise over 20 min. The resulting light yellow reaction mixture was allowed to warm to 25 °C and stir for 14 h. The reaction mixture was quenched into ice water (120 mL), diluted with Et₂O (120 mL) and the aqueous layer extracted with Et₂O (2 x 30 mL). The combined organics were washed with brine (20 mL), dried over MgSO₄, filtered and concentrated *in vacuo* to give the title compound as a brown oil (3.50 g, quantitative). Spectral data matched those reported in the literature.⁵¹ Carried on without further purification.

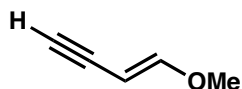


Methyl 6,6-dimethyl-2-(((trifluoromethyl)sulfonyl)oxy)cyclohex-1-enecarboxylate (2.8). To a suspension of NaH in Et₂O (0.537 g, 22.3 mmol, 25 mL) at 0 °C was added a solution of **2.13** in Et₂O (3.50 g, 18.6 mmol, 15 mL) dropwise over 15 min. The reaction mixture was stirred an additional 10 min, Tf₂O (3.80 mL, 22.6 mmol) was added dropwise over 15 min, the mixture was brought to 25 °C and stirred for 18 h. The reaction mixture was then cooled to 0 °C, quenched slowly with H₂O (50 mL), and diluted with Et₂O (100 mL). The aqueous portion was extracted with of Et₂O (2 x 100 mL). The combined organics were washed with of brine (20

mL), dried over MgSO₄, filtered and concentrated *in vacuo* to a tan oil. Flash chromatography was performed using 80 g of SiO₂ (0:100 – 10:90 EtOAc:hexanes) to afford the title compound as a clear yellow oil (4.18 g, 71%): ¹H NMR (500 MHz, CDCl₃) δ 3.80 (s, 3H), 2.38 (t, *J* = 6.5, 2H), 1.86–1.81 (m, 2H), 1.51 (m, 1H), 1.19 (s, 6H); ¹³C (125 MHz, CDCl₃) δ 165.8, 147.3, 52.1, 37.2, 35.2, 27.8, 27.3, 18.7; IR (neat) 2957, 1732, 1419, 1254, 903, 606 cm⁻¹; HRMS (ESI/MeOH) *m/z* calcd for C₁₁H₁₅F₃O₅SNa (M + Na)⁺ 339.0490, found 339.0487.

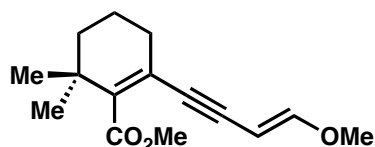


(E)-4-Methoxybut-3-en-2-one (2.9). A mixture of 4,4-dimethoxy-2-butanone (9.85 mL, 74.2 mmol) and NaOAc (271 mg, 3.30 mmol) was heated to 130 °C for 5 h. The MeOH was removed by ambient distillation of the resulting brown mixture. Vacuum distillation afforded the product as a clear oil (4.69 g, 63%): bp 33 °C (1.6 torr). Spectral data matched those reported in the literature.^{14,52}



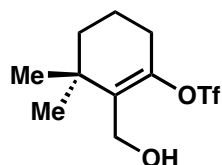
(E)-1-Methoxybut-1-en-3-yne (2.16). A flask containing liquid ammonia (75 mL) was charged with sodium metal (0.1 g, 4.3 mmol) and the resulting deep blue solution was treated with Fe(NO₂)₃·H₂O (50 mg, 0.12 mmol). To the silver-brown mixture was added sodium metal (2.50 g, 109 mmol) in ~0.1 g portions over 1 h. 1,4-Dimethoxybut-2-yne (4.95 g, 44.4 mmol) was then added over a period of 25 min then stirred for 1 h and the ammonia was allowed to evaporate. Solid NH₄Cl (3 x 2.5 g) was added, followed by cold saturated aqueous NH₄Cl (100 mL) and Et₂O (50 mL). The biphasic mixture was filtered and the aqueous extracted with Et₂O (5 x 20 mL). The combined organics were then dried over MgSO₄ and filtered. Et₂O was removed by ambient distillation of the resulting clear tan mixture. Vacuum distillation afforded

the product as a light yellow oil (1.61 g, 45%): bp 35 °C (37 torr). Spectral data matched those reported in the literature.¹⁶



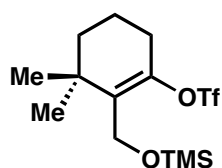
(E)-Methyl 2-(4-methoxybut-3-en-1-yn-1-yl)-6,6-dimethylcyclohex-1-enecarboxylate (2.17).

To a vial containing 2-dicyclohexylphosphino-2',4',6'-triisopropylbiphenyl (3.6 mg, 7.5 μ mol), PdCl₂(MeCN)₂ (0.6 mg, 2.5 μ mol) and Cs₂CO₃ (211 mg, 0.647 mmol), was added 200 μ L of MeCN. The light yellow heterogeneous reaction mixture was treated a solution of **2.8** in MeCN (71 mg, 0.25 mmol, 200 μ L) and stirred at 25 °C for 25 min. The vial was charged with a solution of **2.16** in MeCN (27 mg, 0.33 mmol, 200 μ L) and heated at reflux for 18 h. The resulting brown reaction mixture was cooled to 25 °C, suspended between Et₂O (10 mL) and H₂O (10 mL) and filtered through a plug of Celite[®]. The aqueous was extracted with Et₂O (4 x 5 mL), and the combined organics were dried over MgSO₄, filtered and concentrated *in vacuo* to a brown residue (80 mg). Flash chromatography was performed using 8.0 g of SiO₂ (10:90 – 100:0 DCM:hexanes) to afford the title compound as a clear oil (16 mg, 26%): ¹H NMR (500 MHz, CDCl₃) δ 6.83 (d, *J* = 12.8, 1H), 4.96 (d, *J* = 12.8, 1H), 3.78 (s, 3H), 3.60 (s, 3H), 2.21 (t, *J* = 6.4, 2H), 1.70–1.65 (m, 2H), 1.49–1.46 (m, 2H), 1.13 (s, 6H); ¹³C (125 MHz, CDCl₃) δ 169.8, 158.5, 144.0, 121.6, 89.3, 86.9, 85.1, 56.7, 51.4, 37.9, 33.6, 30.3, 28.2, 18.5.



2-(Hydroxymethyl)-3,3-dimethylcyclohex-1-en-1-yl trifluoromethanesulfonate (2.18). To a solution of **2.8** in Et₂O (200 mg, 0.632 mmol, 5 mL) at 0 °C was added DIBAL-H (1.0 M in

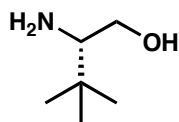
hexanes, 3.1 mL, 3.1 mmol,) dropwise over 15 min. The reaction mixture was warmed to 25 °C, stirred for 4 h and diluted with EtOAc (10 mL). The organics were washed with 1 M HCl (10 mL), and the aqueous extracted with EtOAc (10 mL). The combined organics were washed with brine (10 mL), dried over MgSO₄, filtered and concentrated *in vacuo* to a clear oil. Flash chromatography was performed using 16 g of SiO₂ (0:100 – 10:90 EtOAc:hexanes) to afford the title compound as a clear oil (114 mg, 79%): ¹H NMR (500 MHz, CDCl₃) δ 4.22 (d, *J* = 6.1, 2H), 2.36 (t, *J* = 6.3, 2H), 1.81–1.77 (m, 2H), 1.68 (t, *J* = 6.3, 1H), 1.51–1.49 (m, 2H), 1.17 (s, 6H); ¹³C (125 MHz, CDCl₃) δ 147.0, 136.9, 118.4 (q, *J* = 318), 56.4, 37.9, 35.5, 28.2, 27.8, 19.0; IR (neat) 3413, 2962, 1412, 1211, 1146, 899 cm⁻¹; HRMS (ESI/MeOH) *m/z* calcd for C₁₀H₁₅F₃O₄SNa (M + Na)⁺ 311.0541, found 311.0540.



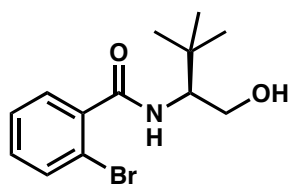
3,3-Dimethyl-2-(((trimethylsilyl)oxy)methyl)cyclohex-1-en-1-yl trifluoromethanesulfonate

(2.19). To a solution of **2.18** in THF (50 mg, 0.17 mmol, 2.0 mL) was added Et₃N (29 μL, 0.21 mmol). The resulting clear solution was cooled to 0 °C and Me₃SiOTf (38 μL, 0.21 mmol) was added dropwise over 2 min. The reaction mixture was stirred for 15 min at 0 °C, then warmed to 25 °C for 3 hours. The reaction mixture was diluted with EtOAc (10 mL), washed with saturated aqueous NH₄Cl (5 mL) and brine (5 mL). The organics were dried over MgSO₄, filtered and concentrated *in vacuo* to a clear oil. Flash chromatography was performed using 4.0 g of SiO₂ (1:99 – 5:95 EtOAc:hexanes) to afford the title compound as a clear oil (52.6 mg, 83%): ¹H NMR (500 MHz, CDCl₃) δ 4.21 (s, 2H), 2.35 (t, *J* = 6.5, 2H), 1.79–1.77 (m, 2H), 1.68 (t, *J* = 6.3, 1H), 1.48–1.46 (m, 2H), 1.15 (s, 6H), 0.13 (s, 9H); ¹³C (125 MHz, CDCl₃) δ 146.2, 135.8, 118.4

(q, $J = 318$), 56.3, 38.3, 35.5, 29.8, 27.9, 18.9, -0.7 ; IR (neat) 2927, 1415, 1250, 1142, 860, 825 cm^{-1} ; HRMS (ESI/MeOH) m/z calcd for $\text{C}_{13}\text{H}_{23}\text{F}_3\text{O}_4\text{SSiNa}$ ($\text{M} + \text{Na}$) $^+$ 383.0936, found 383.0948.

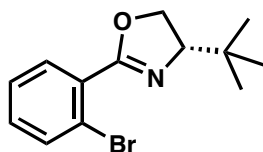


(S)-2-amino-3,3-dimethylbutan-1-ol (2.27). To a suspension of NaBH_4 in THF (3.46 g, 91.5 mmol, 100 mL) was added (*S*)-ethyl 2-amino-3,3-dimethylbutanoate (5.00 g, 38.1 mmol). The resulting white suspension was charged with a solution of I_2 in THF (9.65 g, 38.0 mmol, 25 mL) dropwise over 40 minutes at $0\text{ }^\circ\text{C}$. When gas evolution subsided, the reaction mixture was heated to reflux for 14 hours. The reaction mixture was then cooled to $25\text{ }^\circ\text{C}$ and quenched by the cautious addition of MeOH (50 mL) and the resulting clear solution was stirred 30 minutes at $25\text{ }^\circ\text{C}$, then reduced *in vacuo* to give a white semi-solid. This semi-solid was then dissolved in 20% wt. aqueous KOH (75 mL) and stirred 4 hours. The solution was then extracted with DCM (3 x 75 mL) and the organics were dried over Na_2SO_4 , filtered and concentrated *in vacuo* to give a yellow oil. Vacuum distillation afforded the title compound as a clear oil (3.31 g, 74%): bp $92\text{ }^\circ\text{C}$ (1.6 torr), which solidified to a white solid on standing at $0\text{ }^\circ\text{C}$. Spectral data matched those reported in the literature.^{32,35}

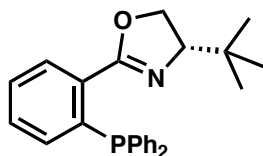


(S)-2-bromo-N-(1-hydroxy-3,3-dimethylbutan-2-yl)benzamide (2.28). To a solution of **2.27** in DCM (3.30 g, 28.2 mmol, 100 mL) was added an aqueous solution of Na_2CO_3 (8.96 g, 84.5 mmol, 75 mL) at $25\text{ }^\circ\text{C}$. To the vigorously stirring bi-phasic mixture was added 2-bromobenzoyl chloride (4.25 mL, 32.4 mmol) dropwise over 10 minutes. After 36 hours, the layers were

separated and the aqueous extracted with DCM (2 x 50 mL). The combined organics were treated with 1M methanolic KOH (15 mL), stirred 15 minutes and neutralized with 3M aqueous HCl. The organics were washed with H₂O (50 mL), and the aqueous was extracted with DCM (2 x 50 mL). The combined organics were dried over Na₂SO₄, filtered and concentrated *in vacuo* to give a white solid. Flash chromatography was performed using 120 g of SiO₂ (25:75 – 35:65 acetone:hexanes) to afford the title compound as a white solid (7.68 g, 91%). Spectral data matched those reported in the literature.²⁹

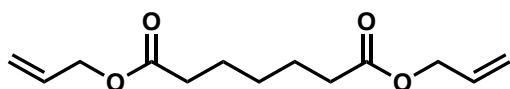


(S)-2-(2-bromophenyl)-4-(tert-butyl)-4,5-dihydrooxazole (2.29). To a solution of **2.28** (7.66 g, 25.5 mmol) and TsCl (6.66 g, 34.9 mmol) in DCM (200 mL) at 25 °C was added Et₃N (18.7 mL, 134 mmol) and the resulting clear beige solution was heated to reflux. After 22 hours, H₂O (75 mL) was added and the temperature increased to 75 °C for 2 hours. The aqueous was extracted with DCM (2 x 25 mL) and the combined organics were dried over Na₂SO₄, filtered and concentrated *in vacuo* to give a semi-solid. Flash chromatography was performed using 120 g of SiO₂ (5:95 EtOAc:hexanes) to afford the title compound as a clear oil (6.75 g, 94%). Spectral data matched those reported in the literature.²⁹

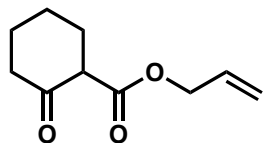


(S)-4-(tert-butyl)-2-(2-(diphenylphosphino)phenyl)-4,5-dihydrooxazole/(S)-tBu-PHOX (2.30). A solution of CuI (169 mg, 0.877 mmol), diphenylphosphine (2.42 mL, 13.9 mmol), *N,N'*-dimethylethylenediamine (0.66 mL, 6.13 mmol) in toluene (20 mL) was stirred at 25°C for 20

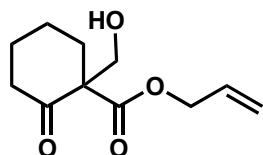
minutes. The reaction mixture was then charged with Cs_2CO_3 (8.70 g, 26.7 mmol) and a solution of **2.29** in toluene (1.95 g, 6.91 mmol, 30 mL). The yellow solution was heated to reflux for 6 hours. The resulting brown-red reaction mixture was filtered through a plug of Celite[®], washed with DCM (2 x 100 mL) and concentrated *in vacuo* to give a yellow oil. Flash chromatography was performed using 120 g of SiO_2 (3:97 – 10:90 Et_2O :hexanes) to afford the title compound as a white solid (1.54 g, 54%). Spectral data matched those reported in the literature.²⁹



Diallyl heptanedioate (2.32). To a solution of pimelic acid in benzene (20.0 g, 125 mmol, 80 mL) was added allyl alcohol (18.8 mL, 276 mmol) and *p*-TSA· H_2O (250 mg, 1.31 mmol). The resulting suspension was then heated to reflux with a Dean–Stark apparatus for 20 hours. The reaction mixture was cooled to 25 °C, concentrated *in vacuo* and partitioned between Et_2O (200 mL) and saturated aqueous NaHCO_3 (100 mL). The organics were then washed with H_2O (2 x 50 mL), then brine (50 mL), dried over MgSO_4 , filtered and concentrated *in vacuo* to give a yellow oil. Vacuum distillation afforded the title compound as a clear oil (25.8 g, 86%): bp 141 °C (1.6 torr). ^1H NMR (500 MHz, CDCl_3) δ 5.90 (dddd, $J = 17.2, 10.4, 5.7, 5.6, 4\text{H}$), 5.30 (dd, $J = 17.2, 1.6, 2\text{H}$), 5.22 (dd, $J = 10.4, 1.2, 2\text{H}$), 4.56 (dd, $J = 5.8, 1.1, 4\text{H}$), 2.33 (t, $J = 7.6, 4\text{H}$), 1.65 (p, $J = 7.6, 4\text{H}$), 1.39–1.32 (m, 2H); ^{13}C (125 MHz, CDCl_3) δ 173.3, 132.3, 118.2, 65.0, 34.0, 28.6, 24.6; IR (neat) 3089, 2943, 2866, 1739, 1651, 1176 cm^{-1} ; HRMS (ESI/MeOH) m/z calcd for $\text{C}_{13}\text{H}_{20}\text{O}_4\text{Na}$ ($\text{M} + \text{Na}$)⁺ 263.1259, found 263.1264.

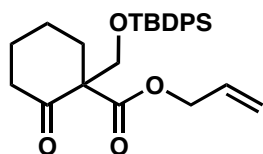


Allyl 2-oxocyclohexanecarboxylate (2.33). To a suspension of NaH in 2:1 toluene:hexanes (499 mg, 20.8 mmol, 15 mL) at 0 °C was added allyl alcohol (396 μ L, 5.83 mmol) over 5 minutes. To the stirring suspension was added **2.32** (4.95 g, 20.6 mmol) in 1 mL over 50 minutes. The reaction mixture was then heated to 95 °C for 1 hour with addition of toluene (20 mL) to maintain efficient stirring. The reaction mixture was cooled to 25 °C, concentrated *in vacuo*, and partitioned between Et₂O (100 mL) and 10% wt. aqueous HCl (35 mL). The organics were washed with H₂O (20 mL), brine (20 mL), dried over MgSO₄, filtered and concentrated *in vacuo* to give a yellow oil. Vacuum distillation afforded the title compound as a clear oil (2.95 g, 79%): bp 91 °C (1.6 torr). Spectral data matched those reported in the literature.³⁰

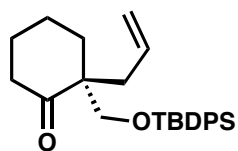


Allyl 1-(hydroxymethyl)-2-oxocyclohexanecarboxylate (2.34). To a solution of **2.33** in THF (1.55 g, 8.50 mmol, 15.5 mL) at 0 °C was added KHCO₃ (2.55 g, 25.5 mmol) and aqueous formaldehyde (37% wt. 4.40 mL, 59.1 mmol) dropwise over 5 minutes. The reaction mixture was stirred at 0 °C for 30 minutes then warmed to 25 °C for 90 minutes. The reaction mixture was then partitioned between DCM (100 mL) and H₂O (100 mL). The aqueous was extracted with DCM (4 x 30 mL) and the combined organics dried over MgSO₄, filtered, and concentrated *in vacuo*. The resulting residue was diluted in THF (20 mL), treated with 2M HCl (3 drops), stirred at 25 °C for 1 hour and concentrated *in vacuo*. Flash chromatography was performed

using 60 g of SiO₂ (10:90 – 45:55 EtOAc:hexanes) to afford the title compound as a clear oil (1.36 g, 76%). Spectral data matched those reported in the literature.³⁰

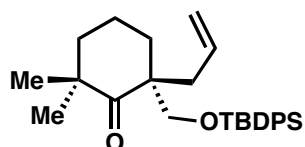


Allyl 1-(((*tert*-butyldiphenylsilyl)oxy)methyl)-2-oxocyclohexanecarboxylate (2.35). To a solution of **2.34** in DMF (1.30 g, 6.13 mmol, 20 mL) was added imidazole (646 mg, 9.49 mmol), DMAP (1.15 g, 9.41 mmol) and TBDPSCl (1.90 mL, 7.31 mmol) at 0 °C. The resulting off-white suspension was warmed to 25 °C and stirred 20 hours. The reaction mixture was partitioned between 2:1 DCM:hexanes (150 mL) and H₂O (75 mL). The aqueous was extracted with 2:1 DCM:hexanes (4 x 30 mL), and the combined organics dried over MgSO₄, filtered, and concentrated *in vacuo* to give a clear oil. Flash chromatography was performed using 120 g of SiO₂ (0:100 – 4:96 EtOAc:hexanes) to afford the title compound as a white solid (1.33 g, 46%). Spectral data matched those reported in the literature.³⁰



(*R*)-2-allyl-2-(((*tert*-butyldiphenylsilyl)oxy)methyl)cyclohexanone (2.36). A flamed-dried, Ar-flushed flask was charged with Pd₂(dba)₃·CHCl₃ (7.8 mg, 7.5 μmol), **2.30** (7.3 mg, 19 μmol), evacuated for 15 minutes and back-filled with Ar. The flask was then charged with THF (freeze-pump-thaw, 20 mL). The resulting purple solution was stirred at 25 °C for 30 minutes. The resulting orange solution was then charged with a solution of **2.35** in THF (136 mg, 301 μmol, 10 mL) and stirred at 25 °C for 18 hours. The reaction mixture was concentrated *in vacuo* to give a green-black residue. Flash chromatography was performed using 12 g of SiO₂ (1:99 – 2.5:97.5

EtOAc:hexanes) to afford the title compound as a clear oil (36 mg, 30%). Spectral data matched those reported in the literature.³⁰



(R)-2-allyl-2-(((tert-butyl-diphenylsilyl)oxy)methyl)-6,6-dimethylcyclohexanone (2.37). To a solution of **22** in toluene (36 mg, 89 μmol , 500 μL) was added $\text{KO}t\text{Bu}$ (39.7 mg, 354 μmol) and 18-crown-6 (single crystal). The resulting yellow solution was charged with MeI (50 μL , 800 μmol) and heated to 70 $^{\circ}\text{C}$ for 3 hours. Additional MeI (50 μL , 800 μmol) was added and the reaction mixture was held at 70 $^{\circ}\text{C}$ for 18 hours. The reaction mixture was partitioned between Et_2O (1 mL) and H_2O (1 mL). The aqueous was extracted with Et_2O (4 x 1 mL), and the combined organics dried over MgSO_4 , filtered, and concentrated *in vacuo* to give a yellow oil. Flash chromatography was performed using 3.5 g of SiO_2 (0:100 – 10:90 EtOAc:hexanes) to afford the title compound as a clear oil (6 mg, 16%, impurities present): $R_f = 0.43$ 5% EtOAc in hexanes); ^1H NMR (500 MHz, CDCl_3) δ 7.69–7.58 (m, 4H), 7.44–7.37 (m, 6H), 5.63–5.42 (m, 1H), 5.05–4.97 (m, 2H), 3.85–3.82 (m, 1 H), 3.63–3.61 (m, 0.5H), 3.43–3.39 (m, 0.5H), 2.54–2.50 (m, 1H), 2.43–2.35 (m, 1H), 2.24–2.20 (m, 1H), 2.06–2.03 (m, 1H), 1.81–1.66 (m, 4H), 1.06–1.01 (m, 15H); MS (ESI/MeOH) m/z calcd for $\text{C}_{13}\text{H}_{20}\text{O}_4$ ($\text{M} - t\text{Bu} - \text{Ph}$)⁺ 303.4, found 303.3.

References

- ¹ Total synthesis of biologically active natural products: Roush, W. R. *J. Am. Chem. Soc.* **2008**, *130*, 6654–6656.
- ² Natural products as sources of new drugs: Newman, D. J.; Cragg, G. M. *J. Nat. Prod.* **2007**, *70*, 461–477.
- ³ Isolation of maocrystal Z: Han, Q.-B.; Cheung, S.; Tai, J.; Qiao, C.-F.; Song, J.-Z.; Tso, T.-F.; Sun, H.-D.; Xu, H.-X. *Org. Lett.* **2006**, *8*, 4727–4730.
- ⁴ Review of biologically active *Isodon* dieterpene natural products: Sun, H.-D.; Huang, S.-X.; Han, Q.-B. *Nat. Prod. Rep.* **2006**, *23*, 673–698.
- ⁵ Review of the intramolecular Diels–Alder reaction in natural product synthesis: Takao, K.; Munakata, R.; Tadano, K. *Chem. Rev.* **2005**, *105*, 4779–4807.
- ⁶ Evans, D. A.; Johnson, J. S. 33.1 Diels–Alder Reactions in *Comprehensive Asymmetric Catalysis*; Jacobsen, E. N.; Pfaltz, A.; Yamamoto, H., Eds.; Springer–Verlag: Berlin, Germany, 1999; pp. 1178–1235.
- ⁷ Computational study of stereoselectivity in type 1 intramolecular Diels–Alder reactions: Tantillo, D. J.; Houk, K. N.; Jung, M. E. *J. Org. Chem.* **2001**, *66*, 1938–1940.
- ⁸ Computational study of stereoselectivity in type 1 intramolecular Diels–Alder reactions: Paddon-Row, M. N.; Moran, D.; Jones, G. A.; Sherburn, M. S. *J. Org. Chem.* **2005**, *70*, 10841–10853.
- ⁹ DFT study of intramolecular Diels–Alder cycloadditions: Khuong, K. S.; Beaudry, C. M.; Trauner, D.; Houk, K. N. *J. Am. Chem. Soc.* **2005**, *127*, 3688–3689.
- ¹⁰ Spartan'08; Wavefunction, Inc. Irvine, CA, 2008.

- ¹¹ Huckin, S. N.; Weiler, L. *J. Am. Chem. Soc.* **1974**, *96*, 1082–1087.
- ¹² Sum, F.-W.; Weiler, L. *Can. J. Chem.* **1979**, *57*, 1431–1441.
- ¹³ Piers, E.; Tse, H. L. A. *Can. J. Chem.* **1993**, *71*, 983–994.
- ¹⁴ Lienhard, U.; Fahrni, H. P.; Neuenschwander, M. *Helv. Chim. Act.* **1978**, *61*, 1609–1621.
- ¹⁵ Huang, J.; Bunel, E.; Faul, M. M. *Org. Lett.* **2007**, *9*, 4343–4346.
- ¹⁶ Adams, H.; Anderson, J. C.; Bell, R.; Neville Jones, D.; Peel, M. R.; Tomkinson, N. C. O. *J. Chem. Soc., Perkin Trans. 1* **1998**, 3967–3974.
- ¹⁷ Li, H.; Yang, H.; Petersen, J. L.; Wang, K. K. *J. Org. Chem.* **2004**, *69*, 4500–4508.
- ¹⁸ Appel, R. *Angew. Chem., Int. Ed.* **1975**, *14*, 801–811.
- ¹⁹ Gruber, L.; Tomoskozi, I.; Radics, L. *Synthesis* **1975**, 708.
- ²⁰ Buchi, G.; Weinreb, S. M. *J. Am. Chem. Soc.* **1971**, *93*, 746–752.
- ²¹ Paquette, L. A.; Heidelbaugh, T. M. *Synthesis* **1998**, 495–508.
- ²² Masters, K.-S.; Flynn, B. L. *J. Org. Chem.* **2008**, *73*, 8081–8084.
- ²³ Gelman, D.; Buchwald, S. L. *Angew. Chem., Int. Ed.* **2003**, *42*, 5993–5996.
- ²⁴ Keck, G. E.; Giles, R. L.; Cee, V. J.; Wager, C. A.; Yu, T.; Kraft, M. B. *J. Org. Chem.* **2008**, *73*, 9675–9691.
- ²⁵ Peng, F.; Yu, M.; Danishefsky, S. J. *Tetrahedron Lett.* **2009**, *50*, 6586–6587.
- ²⁶ Buchwald, S. L.; Nielsen, R. B.; Dewan, J. C. *Organometallics* **1989**, *8*, 1593–1598.
- ²⁷ Matsumoto, K.; Fujie, S.; Ueoka, K.; Suga, S.; Yoshida, J. *Angew. Chem., Int. Ed.* **2008**, *47*, 2506–2508.
- ²⁸ Piller, F. M.; Bresser, T.; Fischer, M. K. R.; Knochel, P. *J. Org. Chem.* **2010**, *75*, 4365–4375.
- ²⁹ Behenna, D. C.; Stoltz, B. M. *J. Am. Chem. Soc.* **2004**, *126*, 15044–15045.

- ³⁰ Mohr, J. T.; Behenna, D. C.; Harned, A. M.; Stoltz, B. M. *Angew. Chem., Int. Ed.* **2005**, *44*, 6924–6927.
- ³¹ McFadden, R. M.; Stoltz, B. M. *J. Am. Chem. Soc.* **2006**, *128*, 7738–7739.
- ³² McKennon, M. J.; Meyers, A. I.; Drauz, K.; Schwarm, M. *J. Org. Chem.* **1993**, *58*, 3568–3571.
- ³³ Seminal publication of Dieckmann condensation: Dieckmann, W. *Ber. Dtsch. Chem. Ges.* **1894**, *27*, 102–103.
- ³⁴ Review of Dieckmann condensation: Schaefer, J. P.; Bloomfield, J. J. *Org. React.* **1967**, *15*, 1–203.
- ³⁵ Detailed procedure on a similar substrate outlining the rigorous exclusion of oxygen: Mohr, J. T.; Krout, M. R.; Stoltz, B. M. *Org. Synth.* **2009**, *86*, 194–211.
- ³⁶ Carita, A.; Burtoloso, A. C. B. *Tetrahedron Lett.* **2010**, *51*, 686–688.
- ³⁷ Liao, X.; Stanley, L. M.; Hartwig, J. F. *J. Am. Chem. Soc.* **2011**, *133*, 2088–2091.
- ³⁸ Alcaraz, L.; Harnett, J. J.; Mioskowski, C.; Martel, J. P.; Le Gall, T.; Shin, D.-S.; Falck, J. R. *Tetrahedron Lett.* **1994**, *35*, 5449–5452.
- ³⁹ Total synthesis of (–)-maoecrysal Z: Cha, J. Y.; Yeoman, J. T. S.; Reisman, S. E. *J. Am. Chem. Soc.* **2011**, *133*, 14964–14967 and references therein.
- ⁴⁰ Seminal publication on Ti(III)-reductive epoxide opening: RajanBabu, T. V.; Nugent, W. A. *J. Am. Chem. Soc.* **1989**, *111*, 4525–4527.
- ⁴¹ Seminal publication on Ti(III)-reductive epoxide opening: RajanBabu, T. V.; Nugent, W. A. *J. Am. Chem. Soc.* **1994**, *116*, 986–997.
- ⁴² Review of Sm(II)-mediated coupling reactions: Szostak, M.; Fazakerley, N. J.; Parmar, D.; Procter, D. J. *Chem. Rev.* **2014**, Ahead of Print.

- ⁴³ Lindlar, H.; Dubuis, R. *Org. Synth.* **1966**, *46*.
- ⁴⁴ Synthesis of methyl 2,2-dimethyl-6-oxocyclohexanecarboxylate: Steiner, U.; Willhalm, B. *Helv. Chim. Act.* **1952**, *35*, 1752–1756.
- ⁴⁵ Synthesis of (–)- γ -cyclogeraniol: Tanimoto, H.; Oritani, T. *Tetrahedron* **1997**, *53*, 3527–3536.
- ⁴⁶ Myers, A. G.; Yang, B. H.; Chen, H.; McKinstry, L.; Kopecky, D. J.; Gleason, J. L. *J. Am. Chem. Soc.* **1997**, *119*, 6496–6511.
- ⁴⁷ Schreiber, J.; Maag, H.; Hashimoto, N.; Eschenmoser, A. *Angew. Chem., Int. Ed.* **1971**, *10*, 330–331.
- ⁴⁸ Total synthesis of (–)-trichorabdal A and (–)-longikaurin E: Yeoman, J. T. S.; Mak, V. W.; Reisman, S. E. *J. Am. Chem. Soc.* **2013**, *135*, 11764–11767.
- ⁴⁹ Unified strategy for the synthesis of (–)-maoecrystal Z, (–)-trichorabdal A, and (–)-longikaurin E: Yeoman, J. T. S.; Cha, J. Y.; Mak, V. W.; Reisman, S. E. *Tetrahedron* **2014**, Ahead of Print.
- ⁵⁰ Resek, J. E. *J. Org. Chem.* **2008**, *73*, 9792–9794.
- ⁵¹ White, J. D.; Skeeane, R. W.; Trammell, G. L. *J. Org. Chem.* **1985**, *50*, 1939–1948.
- ⁵² Konkol, M.; Schmidt, H.; Steinborn, D. *J. Mol. Catal. A Chem.* **2007**, *269*, 119–124.

Chapter 3

Studies Toward the Synthesis of Palhinine Lycopodium Alkaloids: A Morita–Baylis–Hillman/Intramolecular Diels–Alder Approach

Abstract

A synthetic route to the isotwistane core of palhinine lycopodium alkaloids is described. A Morita–Baylis–Hillman/intramolecular Diels–Alder (IMDA) strategy used in this study sets the vicinal all-carbon quaternary centers present in this family of natural products in a single step. The regioselectivity of the IMDA reaction is dictated by the conditions employed for silyl enol ether formation, with one set of conditions providing the core of cardionine and alternate conditions generating the desired isotwistane core of isopalhinine A.

Introduction

Isopalhinine A (**3.1**) is a lycopodium alkaloid recently isolated from the nodding club-moss *Palhinhaea cernua* (Figure 3.1).¹ It contains an unprecedented pentacyclic architecture and is the most complex member of the palhinine family of natural products. This family is closely related to the fawcettimine class of lycopodium alkaloids,^{2–5} however the palhinine subclass contains a C4–C16 linkage that gives a tricyclo[4.3.1.0^{3,7}]decane (isotwistane) core.⁶ The densely functionalized core of the palhinine family of natural products, including the vicinal quaternary relationship of C4–C12, led us to embark on a total synthesis of **3.1** using a route that would allow us access to the entire family.

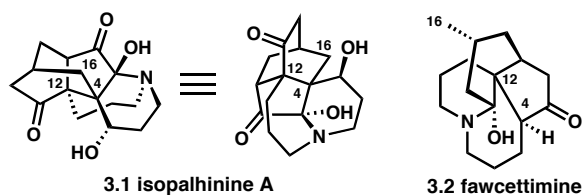


Figure 3.1. Lycopodium natural products isopalhinine A and fawcettimine.

The isotwistane motif is found in a variety of natural products including palhinine and cardionine (Figure 3.2).^{7,8} This unusual architecture has drawn significant interest from synthetic organic chemists. Several recent synthetic methods have been applied to isotwistane installation, including Rhodium carbenoid C–H insertion⁹ and radical cyclization.¹⁰ The primary modes for isotwistane construction are exemplified by the seminal publications of Corey¹¹ and Yamamoto¹² in their syntheses of (±)-9-isocyanopupukeanane (Scheme 3.1, **3.7**), an allomone sesquiterpene used by the nudibranch *Phyllidia varicosa* as a defensive secretion.¹³

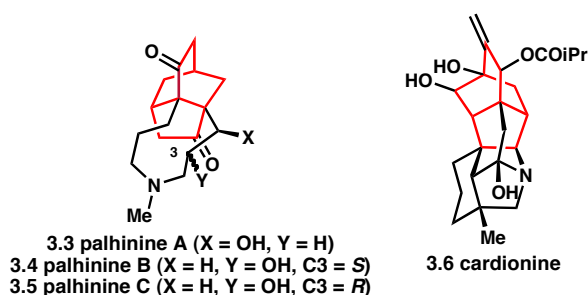


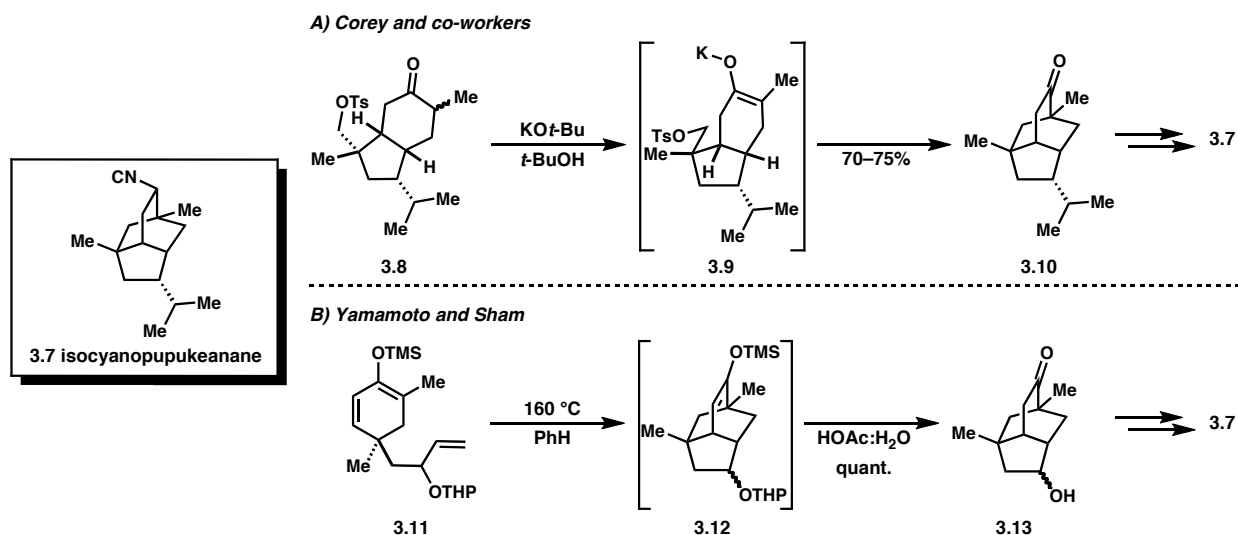
Figure 3.2. Representative isotwistane (in red) containing natural products.

Methods of Isotwistane Construction: (±)-9-isocyanopupukeanane

Two distinct modes of isotwistane construction were described in the syntheses of (±)-9-isocyanopupukeanane by Corey and Yamamoto (Scheme 3.1). Corey's strategy generated the tricyclic system through an intermolecular enolate alkylation of bicyclic *cis*-hydrindane **3.8**.¹¹ Indeed, treatment of keto tosylate **3.8** with potassium *tert*-butoxide in anhydrous *tert*-butanol facilitated the formation of potassium enolate **3.9**. Subsequent alkylation furnished tricyclic

ketone **3.10**, which was further elaborated to the natural product (**3.7**). This approach capitalizes on the conformational constraints of the existing bicyclic hydrindane to control regio- and stereochemistry of cyclization. In contrast, Yamamoto employs an IMDA reaction of cyclohexanone derivative **3.11** to simultaneously install the [2.2.2]- and cyclopentyl fragments of the isotwistane (Scheme 3.1 B).¹² At 160 °C in benzene, siloxydiene **3.11** underwent cycloaddition to give intermediate silyl enol ether **3.12**. Acid hydrolysis of the silyl enol ether and pyranyl moieties afforded tricyclic keto alcohol **3.13** in quantitative yield. This strategy rapidly increases molecular complexity with excellent facial selectivity in the cyclization, which is dictated by the short tether. Despite the utility of these methods neither strategy was proven effective for the installation of vicinal quaternary centers.

Scheme 3.1. Landmark syntheses of isotwistane containing (\pm)-9-isocyanopupukeanane.^{11,12}

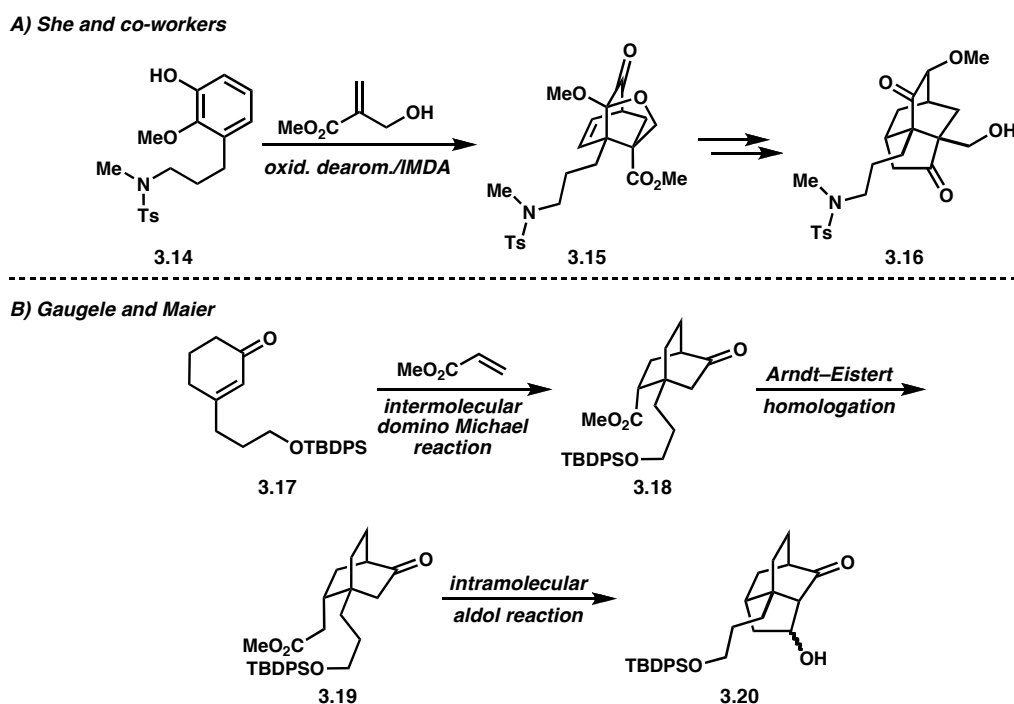


Reported Synthetic Approaches to Palhinine A Isotwistane Intermediates

During the course of this research, three approaches to palhinine A were disclosed.¹⁴⁻¹⁶ The first report by She and co-workers utilizes an oxidative dearomatization/intramolecular Diels–Alder (IMDA) sequence for construction of the [2.2.2]-bicycle, which was subsequently

elaborated to a functionalized isotwistane (Scheme 3.2 A, **3.16**).¹⁴ Gaugele and Maier described an approach to the isotwistane core employing a domino Michael, Arndt–Eistert homologation, intramolecular aldol sequence (Scheme 3.2 B, **3.20**).¹⁵ The third and most closely related report by Fan and co-workers¹⁶ is presented in the discussion section (Scheme 3.10) for direct comparison to our synthetic strategy.

Scheme 3.2. Reported approaches to palhinine A.^{14,15}

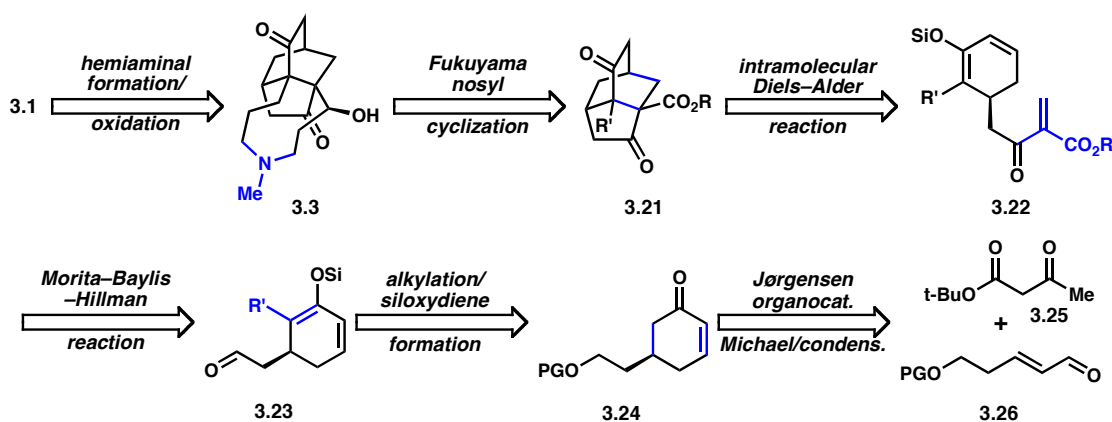


Retrosynthetic Analysis of Palhinine Natural Products

A retrosynthetic analysis is shown in Scheme 3.3. We rationalized that a late-stage installation of the azanone ring using Fukuyama’s nosyl cyclization strategy^{17–21} and further functionalization to the natural products could lead back to differentially functionalized isotwistane **3.21**. Isotwistane **3.21** could arise from an intramolecular Diels–Alder reaction²² that simultaneously sets the required vicinal quaternary centers.²³ This strategy offered synthetic flexibility to access the entire family by providing three oxygen-bearing carbons at distinct

oxidation states. A Morita–Baylis–Hillman reaction^{24–27} could be used to install the dieneophile fragment of siloxydiene **3.22**. Standard enolate manipulations would lead back to aldehyde **3.23**, which could be accessible from cyclohexenone **3.24**. It was envisioned that enone **3.24** could be constructed enantioselectively in a single step from *tert*-butyl acetoacetate **3.25** and enal **3.26** using an organocatalytic Michael addition/condensation/decarboxylation cascade protocol developed by Jørgensen and co-workers.²⁸

Scheme 3.3. Retrosynthetic analysis of palhinine natural products.

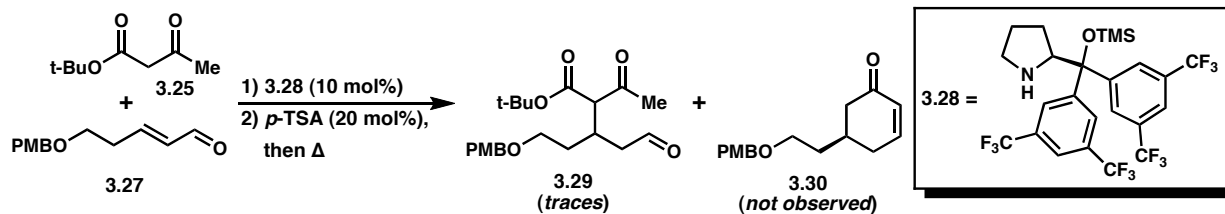


Results and Discussion

Initial Synthetic Approaches to Aldehyde 3.23

Synthetic efforts to access functionalized enone **3.24** were met with limited success (Scheme 3.4). Treatment of known enal **3.27**²⁹ with pyrrolidine catalyst **3.28**³⁰ in the presence of *tert*-butyl acetoacetate led to incomplete conversion to the Michael adduct. Traces of intermediate β -ketoester **3.29** were observed by TLC (confirmed by MS), but significant quantities of both starting materials remained. Subsequent heating of the reaction mixture with *p*-toluenesulfonic acid resulted in significant decomposition and the desired enone **3.30** was never observed.

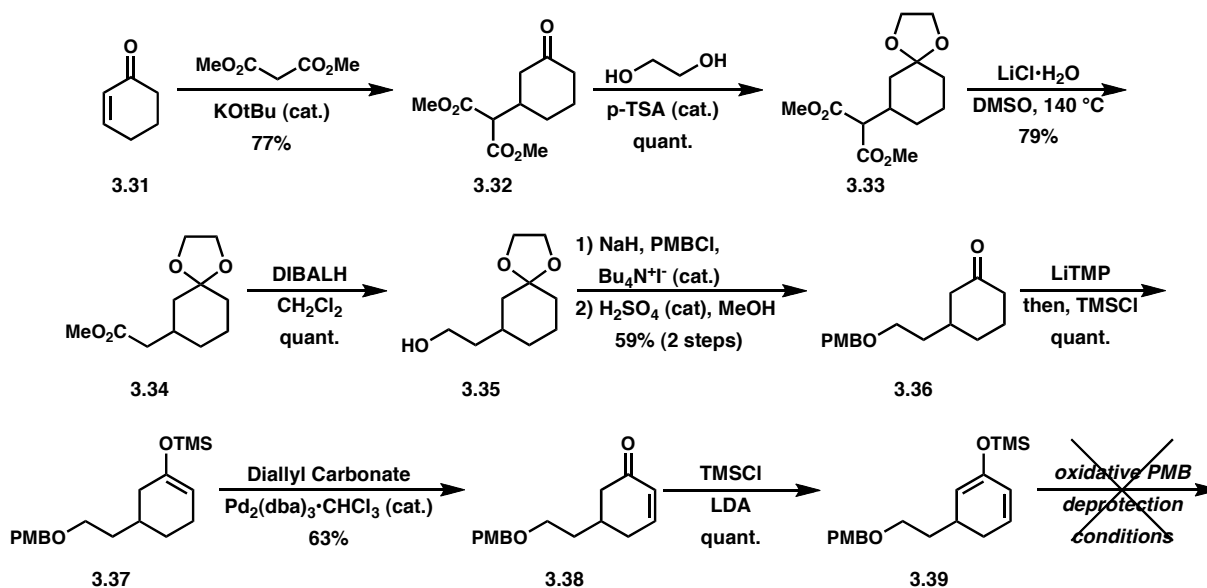
Scheme 3.4. Attempted synthesis of enone **3.30**.



Further examination of the Jørgensen method revealed that this cascade sequence is highly sensitive to the purity of catalyst **3.28**.³⁰ Catalyst sensitivity was problematic due to the extreme lability of the trimethylsilyl moiety. Difficulties in obtaining pure catalyst were responsible for the low conversion to β -ketoester **3.29**. In addition, it is known that the aldol condensation/decarboxylation sequence can be problematic, often requiring extensive screening of reaction times, Brønsted acids and catalyst loading.³¹ Since the setbacks of this protocol outweighed the utility of the reaction, particularly so early in a synthetic sequence, other methods to access aldehyde **3.23** were explored.

The malonate Michael reaction of cyclohexenone has proven to be a robust, reliable method for the introduction of ethoxy substituents beta to the ketone.³²⁻³⁴ As such, a racemic malonate Michael sequence to aldehyde **3.23** was investigated (Scheme 3.5). The sequence began with the potassium *tert*-butoxide catalyzed addition of dimethyl malonate to cyclohexenone **3.31**. The resulting ketone **3.32** was then protected as the acetal by treatment with ethylene glycol in the presence of *p*-toluenesulfonic acid to afford diester **3.33** quantitatively. Subsequent removal of a single ester moiety under Krapcho decarboxylation conditions³⁵ provided acetal **3.34**. The remaining ester was then reduced to alcohol **3.35** using diisobutylaluminium hydride.

Scheme 3.5. Malonate Michael approach to aldehyde **3.23**.



Protection of the resultant alcohol moiety was required for further functionalization of cyclohexyl ring, as well as to prevent acetal formation upon revealing the masked ketone. As a result, alcohol **3.35** was protected as the *p*-methoxybenzyl ether before acid-catalyzed hydrolysis of the acetal. The desired ketone **3.36** was obtained in 59% yield over 2 steps. Hard enolization of ketone **3.36** using lithium tetramethylpiperidide (LiTMP), followed by trapping with trimethylsilyl chloride (TMSCl) resulted in quantitative formation of silyl enol ether **3.37**. The regioselectivity of this transformation is rationalized by a preferential deprotonation on the less hindered side of ketone **3.36** with the sterically demanding LiTMP base. A Tsuji-modified Saegusa oxidation^{36,37} of silyl enol ether **3.37** proceeded without complication to provide enone **3.38**. Since α -alkylation of enone **3.38** proved difficult, presumably due to undesired oligomerization, efforts to install the siloxydiene moiety were undertaken. Dropwise addition of lithium diisopropylamide to a pre-mixed solution of enone **3.38** and TMSCl resulted in quantitative formation of siloxydiene **3.39**. This *in situ* quenching protocol was key to preventing undesired oligomerization.

With siloxydiene **3.39** in hand, conditions to remove the *p*-methoxybenzyl protecting group were examined. The presence of alkenes precluded the use of hydrogenolysis, however oxidative methods proved unfruitful as well.³⁸ When either ceric ammonium nitrate (CAN)³⁹ or 2,3-dichloro-5,6-dicyano-1,4-benzoquinone (DDQ)⁴⁰ were employed as the oxidant, significant decomposition was observed. Examination of ¹H NMR spectra of the crude reaction mixtures suggested that aromatization of the cyclohexyl moiety was responsible for the undesired products. While a change in protecting group strategy could circumvent this issue, the synthetic sequence required to access enone **3.38** severely limited the types of protecting groups that could be employed.

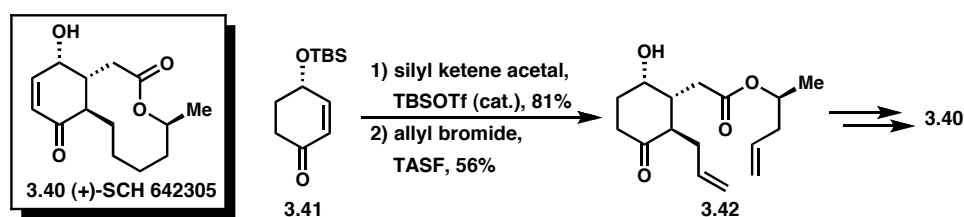
The inflexibility in suitable protecting groups coupled with the high number of functional group interconversions led us to abandon the malonate Michael approach to aldehyde **3.23**, but a number of key insights were gleaned from this strategy. First, early installation of the α -side chain is necessary to prevent the oligomerization of enones like **3.38**. Introduction of this side chain is crucial for the installation of the vicinal quaternary centers in isotwistane **3.21** and would also simplify the regioselectivity of silyl enol ether formation. Second, a more direct method to install the ethoxy side chain would reduce the number of steps required to access aldehydes like **3.23** and increase the number of viable protecting groups. Finally, this route led to the realization that late-stage installation of the siloxydiene moiety is required to prevent undesired aromatization.

Mukaiyama–Michael Approach to Aldehyde 3.47

With the lessons of the initial synthetic studies to aldehyde **3.23** in mind, identification of a streamlined approach to a suitable aldehyde became a priority. Inspiration for a concise synthetic strategy came from Trauner and Wilson's synthesis of (+)-SCH 642305 (Scheme 3.6,

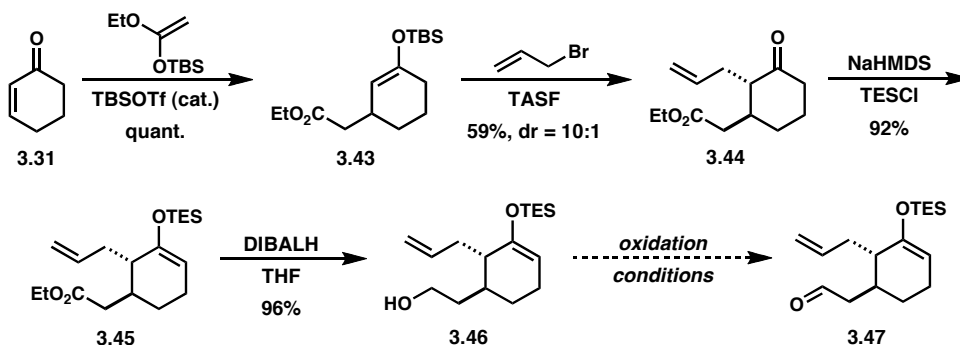
3.40).⁴¹ Their approach to this macrolide natural product employs a Mukaiyama–Michael reaction^{42–45}/allylation sequence to rapidly install the *trans*- α,β -substituted cyclohexyl motif. Enantiopure enone **3.41** underwent facile *tert*-butyldimethylsilyl trifluoromethanesulfonate (TBSOTf) catalyzed conjugate addition with an elaborate silyl ketene acetal, followed by tris-(dimethylamino)-sulfonium difluorotrimethylsilicate (TASF)^{46,47} mediated allylation to provide ketone **3.42**. This example provided the basis for a revised approach to aldehyde **3.47**.

Scheme 3.6. Trauner and Wilson’s synthesis of (+)-SCH 642305.⁴¹

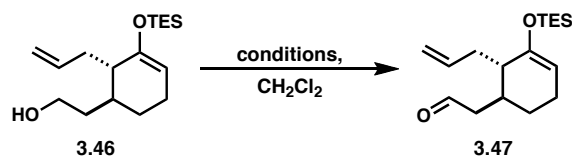


Our Mukaiyama–Michael strategy to aldehyde **3.47** is outlined in Scheme 3.7. Treatment of cyclohexenone with the silyl ketene acetal of ethyl acetate in the presence TBSOTf resulted in conjugate addition and silyl transfer to afford silyl enol ether **3.43** in high yield. One advantage of this approach is that the regioselective generation of silyl enol ether **3.43** provides a natural point of introduction for the required allyl side chain. This transformation was achieved by the use of allyl bromide and TASF to afford ketone **3.44**.⁴⁸ This tandem vicinal difunctionalization⁴⁹ simplifies the synthetic sequence to aldehyde **3.47** by differentiating the α and α' positions of ketone **3.44**. Kinetic deprotonation of ketone **3.44** under hard enolization conditions and trapping as TES enol ether **3.45** served two roles: first, to mask the ketone functionality and second, to serve as the handle for oxidation to the enone. Ester **3.45** was converted to alcohol **3.46** by reduction with DIBAL-H. With alcohol **3.46** in hand, identification of suitable oxidation conditions to key aldehyde **3.47** began.

Scheme 3.7. Mukaiyama–Michael approach to Morita–Baylis–Hillman precursor.



The optimization of the oxidation of alcohol **3.46** to aldehyde **3.47** is shown in Table 3.1. While the transformation seemed straightforward, a number of side reactions were encountered, specifically hydrolysis of the silyl enol ether moiety or isomerization to the thermodynamically favored, fully substituted silyl enol ether. Chromium-based oxidants, like pyridinium chlorochromate (PCC),⁵⁰ resulted in rapid decomposition (entry 1). Swern oxidation conditions⁵¹ caused significant silyl deprotection before the oxidation was complete, while the related Parikh–Doering oxidation⁵² proved sluggish (entries 2-5). Dess–Martin periodinane⁵³ (DMP) alone proved to acidic and led to silyl deprotection (entry 6). Acetate and carbonate buffers also proved ineffective (entries 7 and 8). The addition of triethylamine suppressed the desilylation reaction, but it also promoted the undesired isomerization (entry 11). By employing aromatic nitrogen bases the isomerization was minimized, though conversion to product remained low (entries 12-15). The cleanest reaction profiles were achieved using 2,6-lutidine, though extended reaction times increased the propensity for the aforementioned side reactions (entries 16-18). Finally, treatment of alcohol **3.46** with DMP in the presence of a large excess of 2,6-lutidine at 0 °C for 45 minutes provided high yields of the desired aldehyde **3.47**, with no side products. This protocol scaled well to afford 74% yield on gram-scale.

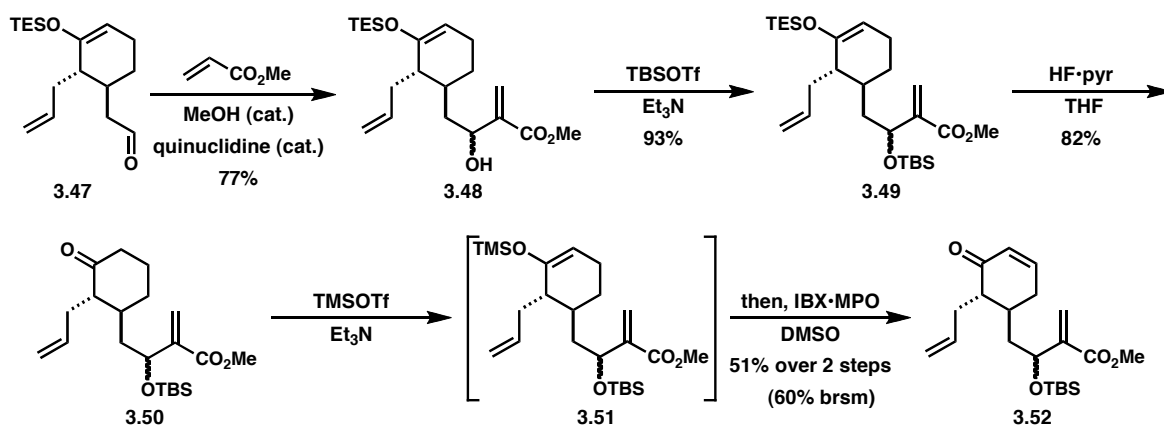
Table 3.1. Optimization of oxidation to aldehyde **3.47**.

Entry	Oxidant (equiv)	Base/Additive (equiv)	Time (min)	Temp. (°C)	Result
1	PCC (1.5)	4Å MS	15	-78	Decomposition
2	COCl ₂ :DMSO (1.2:2.0)	Et ₃ N (4.0)	60	-78	Incomplete conversion and silyl deprotection
3	SO ₃ :pyr (4.0)	Et ₃ N (5.0)	60	-40	No reaction
4	SO ₃ :pyr (4.0)	Et ₃ N (5.0)	60	0	No reaction
5	SO ₃ :pyr (4.0)	Et ₃ N (5.0)	60	25	Incomplete conversion
6	DMP (1.5)	N/A	20	0	Silyl deprotection
7	DMP (1.5)	NaOAc (5.0)	20	0	Silyl deprotection
8	DMP (1.5)	NaHCO ₃ (15)	30	0	Silyl deprotection
9	DMP (1.5)	Et ₃ N (5.0)	30	-78	No reaction
10	DMP (1.5)	Et ₃ N (5.0)	30	-40	No reaction
11	DMP (1.5)	Et ₃ N (5.0)	30	0	Silyl isomerization
12	DMP (1.5)	Pyridine (5.0)	20	0	No reaction
13	DMP (1.5)	Pyridine (5.0)	40	25	Incomplete conversion
14	DMP (1.5)	<i>N</i> -methyl imidazole (5.0)	20	0	No Reaction
15	DMP (1.5)	<i>N</i> -methyl imidazole (5.0)	40	25	Incomplete conversion
16	DMP (1.5)	2,6-lutidine (5.0)	20	0	Incomplete conversion
17	DMP (1.5)	2,6-lutidine (5.0)	20	0	Incomplete conversion
18	DMP (3.0)	2,6-lutidine (5.0)	180	25	Silyl isomerization, silyl deprotection, and desired product
19	DMP (3.0)	2,6-lutidine (15)	45	0	Desired product (74%)

With functionalized aldehyde **3.47** in hand, methods to forge the C4–C5 bond and elaborate the cyclohexyl ring were investigated (Scheme 3.8). Treatment of aldehyde **3.47** with methyl acrylate in the presence of catalytic amounts of methanol and quinuclidine provided excellent yields of allylic alcohol **3.48** as an inconsequential 1:1 mixture of diastereomers.⁵⁴ Allylic alcohol **3.48** was protected as TBS ether **3.49** to prevent mixed ketal formation upon hydrolysis of the enol ether moiety. Unfortunately, attempts at direct oxidation of TES enol ether **3.49** proved challenging primarily due to low reactivity. Both the Tsuji-modification of Saegusa–Ito oxidation,^{36,37} and Nicolaou’s IBX·MPO protocol⁵⁵ primarily led to mixtures containing mostly recovered starting material with traces of ketone **3.50**, suggesting that insertion into the

O–Si bond is not efficient and the resultant enolate is more easily protonated than oxidized. To circumvent this issue, TES enol ether **3.49** was selectively hydrolyzed upon treatment with HF·pyridine to afford ketone **3.50**. Soft enolization of ketone **3.50** using TMSOTf and triethylamine afforded the TMS enol ether **3.51**, which could be directly oxidized to desired enone **3.52** in moderate yields using IBX·MPO.

Scheme 3.8. Synthesis of key enone for intramolecular Diels–Alder reaction.

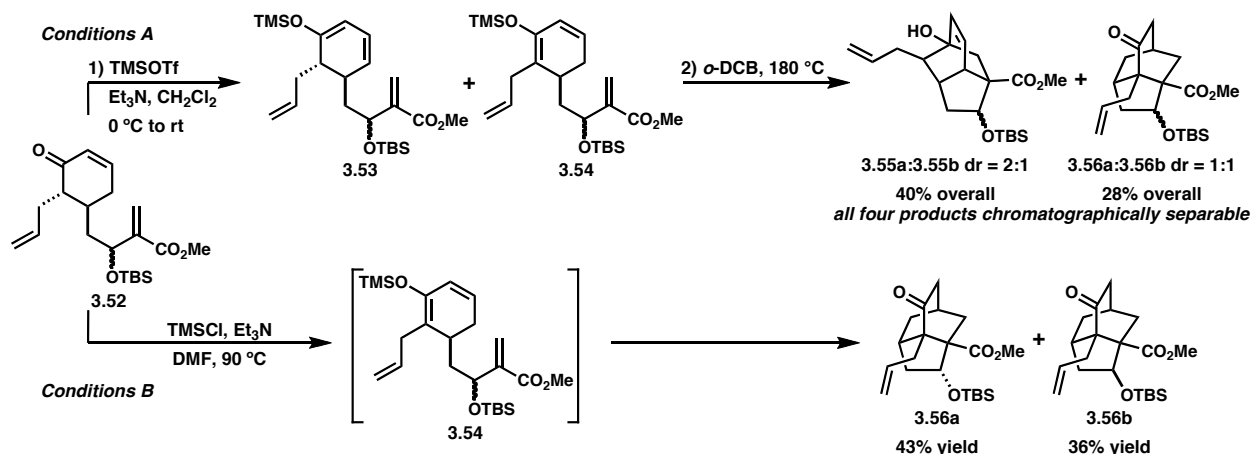


Initial attempts to perform the intramolecular Diels–Alder reaction of enone **3.52** using the soft enolization conditions (conditions A: TMSOTf, Et₃N), followed by heating in *o*-dichlorobenzene (DCB) led to a mixture of regioisomers (Scheme 3.9). In this case, the major products were the isotwistanes arising from γ -deprotonation of enone (linear-conjugated siloxydiene **3.53**), as opposed to α -deprotonation (cross-conjugated siloxydiene **3.54**). The product distribution is believed to be the result of modest regioselectivity of siloxydiene formation, based on NMR spectroscopic analysis, rather than a reversible 1,5-hydride shift occurring during the IMDA reaction.

The major products of this IMDA reaction were isotwistanes **3.55a** and **3.55b**. While these products are not useful for the synthesis of pahlinine lycopodiums, they contain the core of delphinium alkaloid cardionine **3.6**.⁷ Interestingly, the mismatched electronic activation of the

diene and dienophile did not derail the cyclization; decalin products resulting from Michael addition of the silyl enol ether moiety into the acrylate fragment were not observed.

Scheme 3.9. Regioselectivity in the intramolecular Diels–Alder reaction.



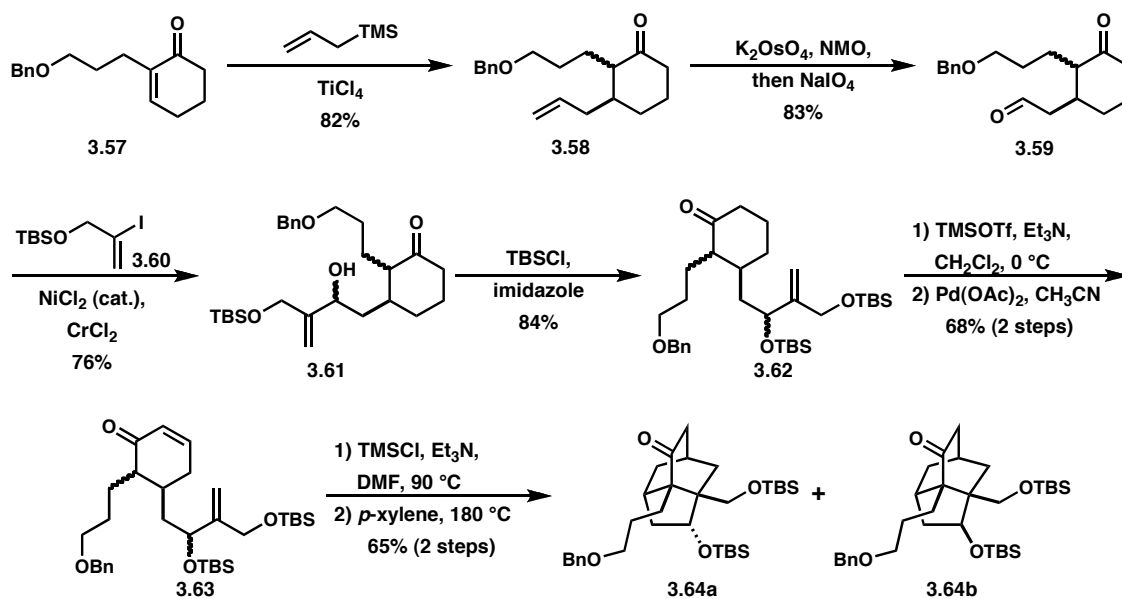
Using conditions previously described for cross-conjugated siloxydiene formation,¹⁶ selective formation of the desired Diels–Alder precursor **3.54** was anticipated. Treatment with TMSOTf and Et₃N in CH₂Cl₂ at 0 °C to room temperature (conditions A) unexpectedly led to the IMDA products directly. These conditions afforded diastereomeric isotwistanes **3.55a** and **3.55b** in 40% yield as the only isolated products. This surprising result suggests that despite mismatched electronics and a demanding steric environment, this IMDA reaction is particularly facile. Computational studies to better understand the energetics of both cyclizations are currently underway.

Fan and Co-worker's Approach to Isotwistane Intermediates 3.64a and 3.64b

During the course of this research, a dramatically similar approach to the isotwistane core of palhinine A was disclosed by Fan and co-workers (Scheme 3.10).¹⁶ Known enone **3.57**⁵⁶ (available in 4 steps from cyclohexanone), was subjected to Sakurai allylation conditions^{57,58} to afford a diastereomeric mixture of ketone **3.58** (dr ≈ 1:1). The alkene moiety of **3.58** was dihydroxylated using potassium osmate in the presence of *N*-methylmorpholine *N*-oxide. Oxidative cleavage of the resultant diol with sodium periodate led to aldehyde **3.59**, which

underwent Nozaki–Hiyama–Kishi alkenylation^{59–61} to provide keto alcohol **3.61**. This reaction showed no selectivity resulting in a mixture of four diastereomers (*dr* \cong 1:1:1:1). Silylation of alcohol **3.61** afforded ketone **3.62** and a two-step oxidation of ketone **3.62** to enone **3.63** proceeded uneventfully. The conditions used to generate the silyoxydiene IMDA precursor, the disclosure of which coincided with our unselective silyoxydiene formation protocol, proceeded quantitatively and upon heating to 180 °C in *p*-xylene afforded a 1:1 diastereomeric mixture of isotwistanes **3.64a** and **3.64b**.

Scheme 3.10. Fan and co-worker's strategy toward palhinine A.¹⁶



Conclusions and Future Directions

In summary, a synthetic route to differentially functionalized isotwistanes **3.56a** and **3.56b** has been developed (10 steps, 12% overall yield from cyclohexenone). The key feature of this approach is the use of a Mukaiyama–Michael/allylation sequence to rapidly access aldehyde **3.47**, which efficiently undergoes a Morita–Baylis–Hillman reaction to install the dienophile fragment. The regiochemical outcome of the IMDA reaction depends on the conditions

employed for silyl enol ether formation and the desired isotwistanes **3.56a** and **3.56b** were accessed under surprisingly mild conditions.

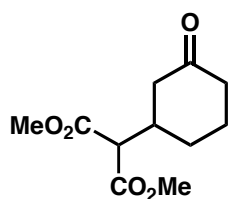
There are remarkable similarities between the developed route and Fan *et al.*'s approach. Both syntheses utilize a highly functionalized aldehyde to forge the C4–C5 bond and install the dienophile fragment. The IMDA reactions used to install the vicinal quaternary centers of the palhinine family differ only in the oxidation state of the dienophile (ester vs. silyl ether). While the developed route offers easier analysis of the intermediates due to a reduction in the number of diastereomers, Fan's strategy provides additional functionalization at the bridgehead side chain. Given the closely related nature of isotwistane intermediates **3.56** and **3.64**, and the convergence of synthetic sequences needed to access palhinine A and isopalhinine A, studies toward the completion of this family was halted.

General Experimental Details:

Unless otherwise stated, reactions were carried out using standard procedures for the rigorous exclusion of air and moisture. This included the use of oven-dried glassware, as well as carrying reactions out under an atmosphere of Ar. When specified, glassware was washed with 0.5 M ethanolic HCl, then 0.5 M ethanolic KOH and oven-dried for a minimum of 4 h prior to use. Thin layer chromatography (TLC) was carried out using glass plates coated with a 250 μm layer of 60 Å silica gel. TLC plates were visualized with a UV lamp at 254 nm, or by staining with KMnO_4 , PMA, or vanillin. Organic solutions were concentrated using a rotary evaporator equipped with a water aspirator. Flash column chromatography was performed using 40-63 μm silica gel. Silica gel was deactivated by preparation of a slurry (1:99 Et_3N :hexanes) prior to chromatography. All reagents were purchased from Acros, Alfa Aesar, Sigma-Aldrich, Strem,

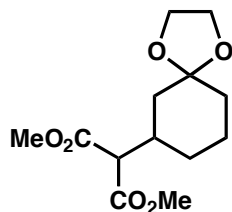
TCI, or VWR and used without further purification unless otherwise noted. Et₃N and *i*-Pr₂EtN were freshly distilled over CaH₂ prior to use. Solvents, such as CH₂Cl₂, Et₂O, THF, MeCN and toluene were purchased as HPLC-grade and passed through a solvent purification system equipped with activated alumina columns. Infrared spectra were recorded on a FT-IR spectrometer. Nuclear magnetic resonance (NMR) spectroscopy was performed using a 500 MHz spectrometer. Chemical shifts in ¹H NMR spectra are referenced from residual CHCl₃ or C₆D₅H (δ = 7.26 or 7.16, respectively) and reported in parts per million (ppm) with respect to tetramethylsilane. Chemical shifts in ¹³C NMR spectra are referenced from CDCl₃ or C₆D₆ (δ = 77.07 or 128.06, respectively) and reported in ppm with respect to tetramethylsilane. Coupling constants are reported as *J* values and are given in Hertz (Hz). High resolution mass spectrometry (ESI-MS) was performed by the Mass Spectrometry Laboratory at University of California – Irvine.

Experimental Procedures:

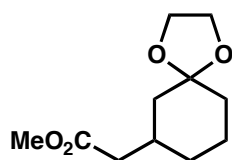


Dimethyl 2-(3-oxocyclohexyl)malonate (3.32). To a solution of cyclohexenone (2.92 mL, 30.0 mmol, 1.00 equiv) in THF (20 mL) at 0 °C was added dimethyl malonate (3.81 mL, 33.0 mmol, 1.10 equiv) over a period of 5 min. The resulting yellow solution was treated with KO^{*t*}Bu (330 mg, 3.00 mmol, 0.10 equiv), stirred for 5 min, then warmed to 25 °C. After 2 h, TLC showed consumption of starting material. The yellow heterogeneous reaction mixture was quenched with H₂O (5.0 mL) and partitioned between EtOAc (50 mL) and H₂O (200 mL). The

aqueous portion was extracted with EtOAc (4 x 20 mL) and the combined organics were dried over MgSO₄, filtered and concentrated *in vacuo* to give a yellow oil. Flash chromatography was performed using 200 g of SiO₂ (10:90 – 30:70 EtOAc:hexanes) to afford the title compound as a clear oil (5.30 g, 77%): R_f = 0.35 (30:70 EtOAc:hexanes). Spectral data matched those reported in the literature.³⁴

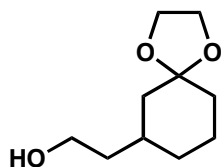


Dimethyl 2-(1,4-dioxaspiro[4.5]decan-7-yl)malonate (3.32). To a solution of diester **3.32** (1.00 g, 4.38 mmol, 1.00 equiv) in benzene (20 mL) was added p-TSA·H₂O (42 mg, 0.22 mmol, 0.05 equiv) and ethylene glycol (0.49 mL, 8.76 mmol, 2.00 equiv). The reaction mixture was heated to 95 °C with a Dean–Stark apparatus. After 2 h, TLC showed consumption of starting material. The yellow heterogeneous reaction mixture was quenched with NaCHO₃ (sat. aq.) (20 mL) and diluted with EtOAc (20 mL). The aqueous portion was extracted with EtOAc (20 mL) and the combined organics were dried over MgSO₄, filtered and concentrated *in vacuo* to afford the title compound as a crude yellow oil (1.21 g, quant.) carried on without further purification: R_f = 0.53 (40:60 EtOAc:hexanes). Spectral data matched those reported in the literature.⁶²

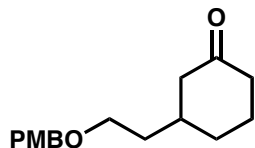


Methyl 2-(1,4-dioxaspiro[4.5]decan-7-yl)acetate (3.34). To a solution of acetal **3.33** (1.21 g, 4.38 mmol, 1.00 equiv) in DMSO (8.9 mL) was added LiCl (390 mg, 9.20 mmol, 2.10 equiv) and H₂O (90.0 μL, 4.80 mmol, 1.10 equiv). The resulting yellow solution was heated to 140 °C.

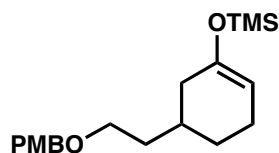
After 18 h, TLC showed consumption of starting material. The yellow heterogeneous reaction mixture was cooled to 25 °C, quenched with H₂O (50 mL) and extracted with EtOAc (2 x 50 mL). The combined organics were washed with 1 M HCl (50 mL), NaHCO₃ (sat. aq.) (50 mL) and brine (25 mL), then dried over MgSO₄, filtered and concentrated *in vacuo* to give a crude yellow oil (0.95 g). Flash chromatography was performed using 40 g of SiO₂ (10:90 – 20:80 EtOAc:hexanes) to afford the title compound as a clear oil (0.73 g, 79%): R_f = 0.49 (20:80 EtOAc:hexanes). Spectral data matched those reported in the literature.³³



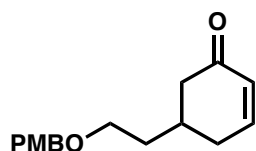
2-(1,4-Dioxaspiro[4.5]decan-7-yl)ethanol (3.35). To a solution of monoester **3.34** (700 mg, 3.27 mmol, 1.00 equiv) in CH₂Cl₂ (16 mL) at -78 °C was added DIBAL-H (1.0 M in hexanes, 9.80 mL, 9.80 mmol, 3.00 equiv) dropwise over 10 min. After 1 h at -78 °C, TLC showed consumption of starting material. The reaction mixture was quenched by addition of NH₄Cl (sat. aq.) (20 mL) and warmed to 0 °C, then 1 M HCl (20 mL) was added. The resulting heterogeneous mixture was extracted with CH₂Cl₂ (4 x 20 mL) and combined organics were vigorously stirred with 1 M potassium sodium tartrate (100 mL) for 1 h. The organics were dried over Na₂SO₄, filtered and concentrated *in vacuo* to afford the title compound as a crude clear oil (610 mg, quant.) carried on without further purification: R_f = 0.17 (40:60 EtOAc:hexanes). Spectral data matched those reported in the literature.⁶³



3-(2-((4-Methoxybenzyl)oxy)ethyl)cyclohexanone (3.36). To a suspension of NaH (90 mg, 3.75 mmol, 1.20 equiv) in THF (10 mL) at 0 °C was added a solution of alcohol **3.35** (580 mg, 3.11 mmol, 1.00 equiv) over a period of 5 min. After addition was complete, the reaction mixture was charged with tetrabutylammonium iodide (57 mg, 0.16 mmol, 0.05 equiv) and *p*-methoxybenzyl chloride (0.50 mL, 3.75 mmol, 1.20 equiv). The resulting white/yellow suspension was then warmed to 25 °C. After 18 h, TLC showed consumption of starting material. The reaction mixture was quenched by addition of NH₄Cl (sat. aq.) (20 mL) and extracted with Et₂O (2 x 20 mL). The combined organics were dried over MgSO₄, filtered and concentrated *in vacuo* to a yellow oil (1.1 g) containing a mixture of PMB acetal and PMB ketone by ¹H NMR. Flash chromatography was performed using 60 g of SiO₂ (10:90 – 20:80 EtOAc:hexanes). A solution of the isolated acetal (308 mg) in MeOH (20 mL) was treated with aqueous H₂SO₄ (0.8% v/v, 20 mL) for 1 h at 25 °C. The reaction mixture was then partitioned between NaHCO₃ (sat. aq.) (25 mL) and Et₂O (25 mL). The aqueous was extracted with Et₂O (2 x 25 mL) and combined organics dried over MgSO₄, filtered and concentrated *in vacuo* to give a crude yellow oil. Flash chromatography was performed using 40 g of SiO₂ (10:90 – 20:80 EtOAc:hexanes) to afford the title compound as a clear oil (480 mg combined, 59% overall): R_f = 0.29 (20:80 EtOAc:hexanes); ¹H NMR (500 MHz, CDCl₃) δ 7.24 (d, *J* = 8.6 Hz, 2H), 6.87 (d, *J* = 8.6 Hz, 2H), 4.41 (s, 2H), 3.80 (s, 3H), 3.46 (td, *J* = 6.5, 2.2 Hz, 2H), 2.43 (dq, *J* = 12.7, 2.6, 2.2 Hz, 1H), 2.39–2.32 (m, 1H), 2.24 (td, *J* = 13.4, 6.2 Hz, 1H), 2.07–1.92 (m, 3H), 1.92–1.85 (m, 1H), 1.71–1.62 (m, 2H), 1.62–1.54 (m, 1H), 1.40–1.29 (m, 1H); ¹³C NMR (126 MHz, CDCl₃) δ 211.8, 159.3, 130.5, 129.4, 113.9, 72.8, 67.4, 55.4, 48.1, 41.6, 36.5, 36.2, 31.4, 25.3.

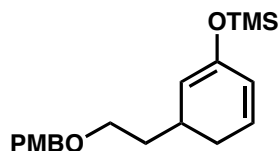


((5-(2-((4-Methoxybenzyl)oxy)ethyl)cyclohex-1-en-1-yl)oxy)trimethylsilane (3.37). To a solution of 2,2,6,6-tetramethylpiperidine (220 μL , 1.31 mmol, 1.50 equiv) in THF (6.0 mL) at 0 $^{\circ}\text{C}$ was added *n*-BuLi (2.2 M in hexanes, 550 μL , 1.21 mmol, 1.40 equiv) dropwise over 2 min. The resulting yellow solution was stirred for 1 h, then cooled to -78°C . The reaction mixture was charged with TMSCl (170 μL , 1.21 mmol, 1.40 equiv), followed by dropwise addition of a solution of ketone **3.36** (228 mg, 0.871 mmol, 1.00 equiv) in THF (6.0 mL) over 5 min. After 2 h at -78°C , TLC showed consumption of starting material. The reaction mixture was quenched with NaHCO_3 (sat. aq.) (4 mL), warmed to 25 $^{\circ}\text{C}$ and partitioned between Et_2O (10 mL) and NaHCO_3 (sat. aq.) (10 mL). The aqueous portion was extracted with Et_2O (2 x 25 mL) and the combined organics were dried over Na_2SO_4 , filtered and concentrated *in vacuo* to afford the title compound as a crude yellow oil (310 mg, quant.) carried on without further purification: $R_f = 0.55$ (10:90 EtOAc:hexanes); ^1H NMR (500 MHz, CDCl_3) δ 7.26 (d, $J = 8.5$ Hz, 2H), 6.88 (d, $J = 8.5$ Hz, 2H), 4.85 (br s, 1H), 4.43 (s, 2H), 3.80 (s, 3H), 3.49 (t, $J = 6.7$ Hz, 2H), 2.09–1.99 (m, 2H), 1.87–1.76 (m, 1H), 1.76–1.52 (m, 4H), 1.44–1.37 (m, 1H), 1.19–1.08 (m, 1H), 0.17 (s, 9H); ^{13}C NMR (126 MHz, CDCl_3) δ 159.2, 149.7, 130.8, 129.4, 113.9, 103.9, 72.8, 68.1, 55.4, 36.5, 36.1, 31.4, 28.7, 23.3, 0.5.



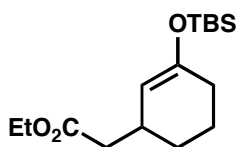
5-(2-((4-Methoxybenzyl)oxy)ethyl)cyclohex-2-enone (3.38). A solution of silyl enol ether **3.37** (310 mg, 0.871 mmol, 1.00 equiv) in MeCN (5 mL) was added diallyl carbonate (170 μL , 1.20

mmol, 1.40 equiv) and Pd₂dba₃·CHCl₃ (61 mg, 0.059 mmol, 0.068 equiv). The reaction mixture was sparged with Ar for 5 minutes and stirred at 25 °C. After 16 h, TLC showed consumption of starting material. The resultant green-yellow reaction mixture was quenched with NH₄Cl (sat. aq.) (10 mL) and diluted with CH₂Cl₂ (20 mL). The aqueous portion was extracted with CH₂Cl₂ (2 x 10 mL) and the combined organics were dried over MgSO₄, filtered and concentrated *in vacuo* to afford a crude oil (320 mg). Flash chromatography was performed using 24 g of SiO₂ (2:98 – 50:50 EtOAc:hexanes) to afford the title compound as a clear yellow oil (143 mg, 63%): R_f = 0.53 (40:60 EtOAc:hexanes); ¹H NMR (500 MHz, CDCl₃) δ 7.24 (d, *J* = 8.6 Hz, 2H), 6.95 (ddd, *J* = 9.9, 5.6, 2.6 Hz, 1H), 6.88 (d, *J* = 8.5 Hz, 2H), 6.02 (d, *J* = 10.5 Hz, 1H), 4.42 (s, 2H), 3.81 (s, 3H), 3.49 (td, *J* = 6.4, 2.2 Hz, 2H), 2.53 (dd, *J* = 16.0, 3.8 Hz, 1H), 2.44 (dt, *J* = 18.5, 5.2 Hz, 1H), 2.30 (td, *J* = 12.3, 6.2 Hz, 1H), 2.14 (dd, *J* = 16.0, 12.6 Hz, 1H), 2.07 (ddt, *J* = 18.5, 10.0, 2.2 Hz, 1H), 1.73–1.64 (m, 2H); ¹³C NMR (126 MHz, CDCl₃) δ 199.9, 159.3, 150.0, 130.5, 129.9, 129.4, 114.0, 72.9, 67.2, 55.4, 44.4, 35.6, 32.5, 32.3.



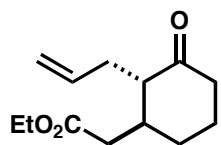
((3-(2-((4-Methoxybenzyl)oxy)ethyl)cyclohexa-1,5-dien-1-yl)oxy)trimethylsilane (3.39). To a vial containing a single crystal of 1,10-phenanthroline was added a solution of enone **3.38** (10 mg, 0.038 mmol, 1.00 equiv) in THF (100 μL) and a solution of TMSCl (5.8 mg, 0.054 mmol, 1.40 equiv) in THF (100 μL). The resulting mixture was cooled to -78 °C and a solution of LDA (0.161 mmol, 4.20 equiv) in THF (300 μL) was added dropwise over 2 minutes. The resulting brown solution was stirred at -78 °C for 1 h, at which time TLC indicated consumption of starting material. The reaction mixture was quenched with aqueous phosphate buffer (0.5 mL; pH = 7), diluted with hexanes (1 mL) and warmed to 25 °C. The reaction mixture was partitioned

between hexanes (5 mL) and aqueous buffer (5 mL). The aqueous was extracted with hexanes (5 mL). Combined organics were dried over MgSO_4 , filtered and concentrated *in vacuo* to afford the title compound as a clear yellow oil (14 mg, quant) carried on without further purification: $R_f = 0.59$ (10:90 EtOAc:hexanes); ^1H NMR (500 MHz, CDCl_3) δ 7.26 (d, $J = 8.4$ Hz, 2H), 6.87 (d, $J = 8.4$ Hz, 2H), 5.79 (dt, $J = 9.2, 4.3$ Hz, 1H), 5.66 (dt, $J = 9.9, 1.9$ Hz, 1H), 4.80 (dd, $J = 4.6, 2.1$ Hz, 1H), 4.42 (d, $J = 2.1$ Hz, 2H), 3.80 (s, 3H), 3.47 (td, $J = 6.6, 3.4$ Hz, 2H), 2.58–2.48 (m, 1H), 2.29–2.20 (m, 1H), 1.98–1.89 (m, 1H), 1.71 (dt, $J = 13.5, 6.8$ Hz, 1H), 1.62 (dq, $J = 13.5, 6.8$ Hz, 1H), 0.17 (s, 9H); ^{13}C NMR (126 MHz, CDCl_3) δ 159.2, 148.0, 130.8, 129.4, 128.1, 126.1, 113.9, 107.4, 72.8, 67.9, 55.4, 34.9, 29.9, 29.0, 0.3.



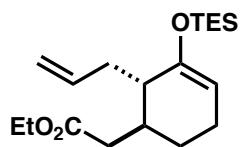
Ethyl 2-(3-((*tert*-butyldimethylsilyl)oxy)cyclohex-2-en-1-yl)acetate (3.43). To a solution of cyclohexenone (2.8 mL, 29 mmol, 1.0 equiv) in CH_2Cl_2 (60 mL) at 0 °C was added TBSOTf (340 μL , 1.5 mmol, 0.05 equiv) dropwise over a period of 2 min. The reaction mixture was stirred for 5 min, and a solution of silyl ketene acetal (8.7 g, 43 mmol, 1.5 equiv) in CH_2Cl_2 (20 mL) was added in a steady stream over 2 min. After 15 min, TLC showed consumption of starting material. The reaction mixture was concentrated *in vacuo* to a yellow oil. Flash chromatography was performed using 120 g of SiO_2 (1:1.5:97.5 Et_3N :EtOAc:hexanes) to afford the title compound as a clear yellow oil (9.1 g, quant.): $R_f = 0.38$ (5:95 EtOAc:hexanes); ^1H NMR (500 MHz, C_6D_6) δ 4.86 (br s, 1H), 3.96 (q, $J = 7.1$, 2H), 2.68 (m, 1H), 2.13 (app d, 2H), 1.87 (m, 2H) 1.60 (m, 1H), 1.53 (m, 1H), 1.40 (m, 1H), 1.05 (m, 1H), 1.00 (t, $J = 7.1$, 3H) 0.96 (s, 9H), 0.10 (s, 6H); ^{13}C (126 MHz, C_6D_6) δ 171.9, 151.9, 107.7, 59.9, 41.8, 32.2, 30.2, 29.0,

26.0, 21.6, 18.3, 14.5, -4.2, -4.3.; IR (neat) 2930, 1734, 1663, 1251, 837, 779 cm^{-1} ; HRMS (ESI/MeOH) m/z calcd for $\text{C}_{16}\text{H}_{31}\text{O}_3\text{Si}$ ($\text{M} + \text{H}$)⁺ 299.2043, found 299.2044.

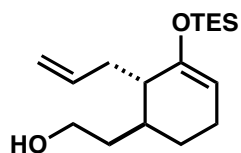


rac-Ethyl 2-((1S,2S)-2-allyl-3-oxocyclohexyl)acetate (3.44). A solution of **3.43** (4.75 g, 15.9 mmol, 1.0 equiv) and allyl bromide (4.75 mL, 54.2 mmol, 3.4 equiv) in THF (110 mL) was stirred with 4 Å molecular sieves at 25 °C for 1 h, then cooled to -40 °C and treated with a solution of tris(dimethylamino)sulfonium difluorotrimethylsilicate (4.97 g, 18.0 mmol, 1.1 equiv) in DMF (10 mL) over 10 min. The tan opaque reaction mixture was stirred for 30 min, then warmed to 25 °C. TLC showed consumption of starting material. The reaction mixture was filtered and partitioned between Et_2O (100 mL) and H_2O (100 mL). The aqueous was extracted with Et_2O (2 x 50 mL) and the combined organics were concentrated *in vacuo*. The resulting yellow oil was partitioned between pentane (150 mL) and washed with H_2O (2 x 50 mL). The aqueous was extracted with pentane (50 mL) and the combined organics were dried over MgSO_4 , filtered and concentrated to a crude yellow oil. Flash chromatography was performed using 120 g of SiO_2 (5:95 – 20:80 Et_2O :pentane) to afford the title compound as a pale yellow oil (2.10 g, dr = 92:8, 59%); R_f = 0.30 (10:90 EtOAc :hexanes); ^1H NMR (500 MHz, C_6D_6) δ 5.90 (dddd, J = 17.2, 10.5, 7.6, 6.3 Hz, 1H), 5.01 (dq, J = 17.2, 1.5 Hz, 1H), 4.98 (ddt, J = 10.4, 2.2, 1.2 Hz, 1H), 3.93 (q, J = 7.1 Hz, 2H), 2.40–2.35 (m, 1H), 2.32–2.24 (m, 2H), 2.15 (dtd, J = 13.5, 4.3, 1.4 Hz, 1H), 2.01–1.95 (m, 3H), 1.83–1.76 (m, 1H), 1.66–1.62 (m, 1H), 1.50–1.44 (m, 1H), 1.26–1.12 (m, 2H), 0.95 (t, J = 7.1 Hz, 3H); ^{13}C NMR (126 MHz, C_6D_6) δ 208.9, 171.7, 136.7, 116.4, 60.2, 54.1, 41.2, 39.3, 38.5, 31.5, 30.2, 24.9, 14.3; IR (neat) 2937, 1732, 1714, 1174,

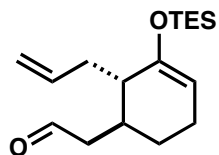
1155, 1034, 916 cm^{-1} ; HRMS (ESI/MeOH) m/z calcd for $\text{C}_{13}\text{H}_{21}\text{O}_3$ ($\text{M} + \text{H}$)⁺ 225.1491, found 225.1493.



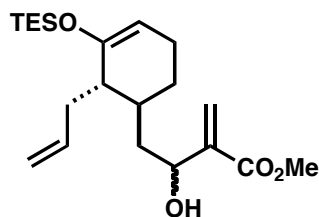
***rac*-Ethyl 2-((1*S*,2*S*)-2-allyl-3-((triethylsilyl)oxy)cyclohex-3-en-1-yl)acetate (3.45).** To a solution of triethylsilyl chloride (5.80 mL, 34.8 mmol, 3.8 equiv) in THF (100 mL) was added a solution of sodium hexamethyldisilazide (1.0 M in THF, 36 mL, 36 mmol) at 25 °C. The resulting mixture was cooled to -78 °C for 10 min and a solution of **3.44** in THF (2.08 g, 9.27 mmol, 10 mL) was added dropwise over 10 min. The reaction mixture was stirred an additional 50 min at which time TLC showed consumption of starting material. The reaction mixture was then warmed to 25 °C, quenched with H_2O (50 mL) and diluted with pentane (150 mL). The organic portion was washed with brine (50 mL), dried over MgSO_4 , filtered and concentrated *in vacuo* to give a crude yellow oil (10 g). Flash chromatography was performed using 120 g of deactivated SiO_2 (0:1:99 – 2:1:97 $\text{Et}_2\text{O}:\text{Et}_3\text{N}:\text{pentane}$) to afford the title compound as a clear pale yellow oil (2.89 g, 92%): $R_f = 0.38$ (2.5:97.5 $\text{EtOAc}:\text{hexanes}$); ^1H NMR (500 MHz, C_6D_6) δ 5.92 (dddd, $J = 17.1, 10.2, 7.5, 6.5$ Hz, 1H), 5.09 (ddd, $J = 17.1, 3.7, 1.6$ Hz, 1H), 5.06–5.03 (m, 1H), 4.84 (t, $J = 3.8$ Hz, 1H), 3.95 (dq, $J = 7.1, 1.2$ Hz, 2H), 2.63–2.57 (m, 1H), 2.41–2.27 (m, 3H), 2.22–2.18 (app q, 1H), 2.04–2.02 (m, 1H), 1.94 (dddd, $J = 9.2, 5.5, 3.3, 1.7$ Hz, 1H), 1.89 (dtd, $J = 7.2, 5.8, 1.6$ Hz, 1H), 1.68–1.62 (m, 1H), 1.32 (dq, $J = 18.5, 5.1$ Hz, 1H), 0.99 (t, $J = 8.0$ Hz, 9H), 0.97 (t, $J = 7.1$ Hz, 3H), 0.67–0.62 (m, 6H); ^{13}C NMR (126 MHz, C_6D_6) δ 172.4, 151.8, 137.5, 116.3, 102.5, 60.0, 44.1, 38.2, 36.8, 32.9, 23.5, 21.1, 14.4, 7.1, 5.5; IR (neat) 2957, 1734, 1184, 1055, 1031, 1016, 744 cm^{-1} ; HRMS (ESI/MeOH) m/z calcd for $\text{C}_{19}\text{H}_{35}\text{O}_3\text{Si}$ ($\text{M} + \text{H}$)⁺ 339.2355, found 339.2347.



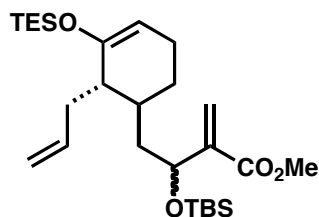
***rac*-2-((1*S*,2*S*)-2-Allyl-3-((triethylsilyloxy)cyclohex-3-en-1-yl)ethanol (3.46).** To a solution of **3.45** (2.48 g, 8.39 mmol) in THF (100 mL) at $-78\text{ }^{\circ}\text{C}$ was added DIBAL-H (7.50 mL, 42.1 mmol, 5.0 equiv) dropwise over 10 min. The reaction mixture was stirred at $-78\text{ }^{\circ}\text{C}$ for an additional 10 min then warmed to $0\text{ }^{\circ}\text{C}$ for 1 h. TLC showed consumption of starting material. The reaction mixture was quenched by slow addition of aqueous potassium sodium tartrate (35 g in 120 mL) and stirred for 2 h. The hazy reaction mixture was extracted with pentane (4 x 100 mL). The combined organic extracts were washed with H_2O (50 mL) and brine (50 mL), dried over MgSO_4 , filtered and concentrated *in vacuo* to crude oil (3.5 g). Flash chromatography was performed using 80 g of deactivated SiO_2 (4:1:95 – 14:1:85 EtOAc:Et₃N:hexanes) to afford the title compound as a clear oil (2.40 g, 96%): $R_f = 0.30$ (15:85 EtOAc:hexanes); ^1H NMR (500 MHz, C_6D_6) δ 5.89 (dddd, $J = 17.1, 10.0, 7.2, 6.9$ Hz, 1H), 5.09 (ddd, $J = 17.1, 2.2, 1.5$ Hz, 1H), 5.04 (ddt, $J = 10.0, 2.2, 1.1$ Hz, 1H), 4.88 (t, $J = 3.7$ Hz, 1H), 3.49–3.42 (m, 2H), 2.63–2.57 (m, 1H), 2.39–2.28 (m, 1H), 2.02–1.92 (m, 2H), 1.92–1.82 (m, 2H), 1.65–1.52 (m, 2H), 1.43 (ddt, $J = 14.1, 7.8, 6.5$ Hz, 1H), 1.24 (dq, $J = 13.4, 5.5$ Hz, 1H), 1.18 (br s, 1H), 1.01 (t, $J = 7.8$ Hz, 9H), 0.69–0.64 (m, 6H); ^{13}C NMR (126 MHz, C_6D_6) δ 152.2, 137.9, 116.1, 102.6, 60.9, 44.7, 36.7, 36.3, 32.4, 23.7, 21.4, 7.1, 5.6; IR (neat) 3350, 2953, 2914, 2876, 1662, 1174, 727 cm^{-1} ; HRMS (ESI/MeOH) m/z calcd for $\text{C}_{17}\text{H}_{33}\text{O}_2\text{Si}$ ($\text{M} + \text{H}$)⁺ 297.2250, found 297.2255.



***rac*-2-((1*S*,2*S*)-2-Allyl-3-((triethylsilyl)oxy)cyclohex-3-en-1-yl)acetaldehyde (3.47).** To a solution of **3.46** (1.40 g, 4.72 mmol) and 2,6-lutidine (8.26 mL, 71.3 mmol, 15.1 equiv) in wet CH₂Cl₂ (100 mL) at 0 °C was added 3 portions of Dess–Martin periodinane (5.88 g, 13.9 mmol, 2.94 equiv) over 10 min. The reaction mixture was stirred at 0 °C for an additional 45 min. TLC showed consumption of starting material. The reaction mixture was diluted with Et₂O (200 mL) and quenched with a solution of H₂O:Na₂SO₃ (sat. aq.):NaHCO₃ (sat. aq.) (8:1:1; 200 mL). The resulting heterogeneous mixture was filtered through a pad of Celite and the aqueous portion extracted with Et₂O (2 x 50 mL). Combined organics were washed with brine (50 mL), dried over MgSO₄, filtered and concentrated *in vacuo* to crude yellow semi-solid (8 g). Flash chromatography was performed using 200 g of deactivated SiO₂ (1:1:98 – 5:1:94 Et₂O:Et₃N:pentane) to afford the title compound as a clear oil (1.03 g, 74%): R_f = 0.59 (10:90 EtOAc:hexanes); ¹H NMR (500 MHz, CDCl₃) δ 9.79–9.74 (m, 1H), 5.79 (dddd, *J* = 17.6, 10.8, 7.6, 6.6 Hz, 1H), 5.06–5.01 (m, 2H), 4.82 (t, *J* = 3.8 Hz, 1H), 2.49–2.41 (m, 2H), 2.38–2.30 (m, 2H), 2.19 (dtd, *J* = 15.5, 8.3, 1.1, 1H), 2.01–1.96 (m, 2H), 1.83–1.78 (m, 1H), 1.70–1.63 (m, 1H), 1.37–1.31 (m, 1H), 0.97 (t, *J* = 7.9 Hz, 9H), 0.66 (q, *J* = 7.9 Hz, 6H); ¹³C NMR (126 MHz, CDCl₃) δ 202.8, 151.1, 137.2, 116.5, 102.7, 47.4, 44.0, 36.3, 30.1, 23.3, 20.8, 6.9, 5.2; IR (neat) 2954, 2876, 1726, 1664, 1193, 1178, 744, 729 cm⁻¹; HRMS (ESI/MeOH) *m/z* calcd for C₁₇H₃₁O₂Si (M + H)⁺ 295.2093, found 295.2097.

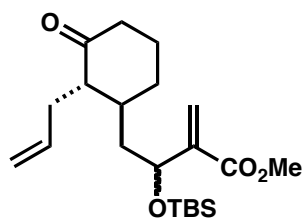


rac-Methyl 4-((1S,2S)-2-allyl-3-((triethylsilyloxy)cyclohex-3-en-1-yl)-3-hydroxy-2-methylenebutanoate (3.48). To a microwave vial containing **3.47** (1.03 g, 3.05 mmol) was added methyl acrylate (370 μ L, 3.96 mmol, 1.30 equiv), quinuclidine (96 mg, 0.86 mmol, 0.25 equiv), and MeOH (103 μ L, 2.55 mmol, 0.75 equiv). The vial was capped and the reaction mixture stirred at 25 $^{\circ}$ C for 40 h. TLC showed consumption of starting material. The crude reaction mixture was purified by flash column chromatography directly using 120 g of deactivated SiO₂ (5:1:94 – 10:1:89 EtOAc:Et₃N:hexanes) to afford the title compound as a clear oil (1.01 g, 77%; ~1:1 mixture of diastereomers): R_f = 0.21 (10:90 EtOAc:hexanes); ¹H NMR (500 MHz, C₆D₆) δ 6.14–6.11 (m, 1H), 6.11–6.08 (m, 1H), 6.00–5.88 (m, 2H), 5.63 (t, J = 1.3 Hz, 1H), 5.57 (t, J = 1.3 Hz, 1H), 5.17–5.13 (m, 1H), 5.13–5.09 (m, 1H), 5.09–5.06 (m, 1H), 5.06–5.03 (m, 1H), 4.92 (t, J = 3.7 Hz, 1H), 4.89 (t, J = 3.8 Hz, 1H), 4.57–4.50 (m, 2H), 3.32 (s, 3H), 3.31 (s, 3H), 2.66 (dddd, J = 14.0, 6.8, 5.2, 3.7 Hz, 2H), 2.37 (ddd, J = 22.8, 15.8, 8.0 Hz, 2H), 2.22–1.81 (m, 11H), 1.80–1.68 (m, 3H), 1.67–1.55 (m, 2H), 1.48–1.40 (m, 1H), 1.36–1.27 (m, 1H), 1.02 (dd, J = 16.7, 8.0 Hz, 18H), 0.73–0.63 (m, 12H); ¹³C NMR (126 MHz, C₆D₆) δ 166.79, 166.76, 152.3, 152.1, 144.5, 144.1, 138.0, 137.9, 124.1, 123.7, 116.2, 116.1, 102.8, 102.7, 70.3, 69.4, 51.29, 51.26, 45.4, 44.0, 40.6 (2), 36.8, 36.7, 32.8, 32.5, 24.7, 22.9, 21.4, 21.3, 7.13, 7.12, 5.56, 5.55; IR (neat) 3478, 2953, 1720, 1665, 1439, 1192, 744 cm^{-1} ; HRMS (ESI/MeOH) m/z calcd for C₂₁H₃₆O₄SiNa (M + Na)⁺ 403.2281, found 403.2283.



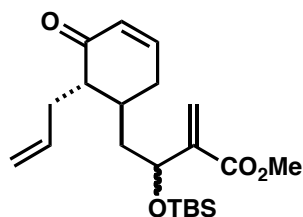
rac-Methyl 4-((1S,2S)-2-allyl-3-((triethylsilyl)oxy)cyclohex-3-en-1-yl)-3-((tert-butyl)dimethylsilyl)oxy)-2-methylenebutanoate (3.49). To a solution of **3.48** (1.00 g, 2.63 mmol) in CH₂Cl₂ (30 mL) was added Et₃N (1.32 mL, 9.47 mmol, 3.60 equiv), the mixture was cooled to -78 °C and treated with TBSOTf (1.07 mL, 4.65 mmol, 1.78 equiv) dropwise over 2 min. The solution was held at -78 °C for 5 min then slowly warmed to 25 °C over 40 min at which time TLC analysis showed consumption of starting material. The crude reaction mixture was diluted in Et₂O (100 mL), and quenched with aqueous phosphate buffer (100 mL; pH = 7). The aqueous portion was extracted with Et₂O (3 x 25 mL), combined organics were washed with brine (50 mL), dried over MgSO₄, filtered and concentrated *in vacuo*. Chromatography was performed using 60 g of deactivated SiO₂ (2.5:1:96.5 EtOAc:Et₃N:hexanes) to afford the title compound as a clear oil (1.26 g, 97%; ~1:1 mixture of diastereomers): R_f = 0.72 (10:90 EtOAc:hexanes); ¹H NMR (500 MHz, C₆D₆) δ 6.31–6.25 (m, 2H), 6.07–5.89 (m, 4H), 5.16 (td, *J* = 17.9, 2.0 Hz, 2H), 5.09 (dd, *J* = 10.1, 1.0 Hz, 2H), 4.98–4.90 (m, 3H), 4.88 (t, *J* = 3.8 Hz, 1H), 3.39 (s, 3H), 3.36 (s, 3H), 2.71–2.59 (m, 2H), 2.42 (dq, *J* = 14.3, 7.8 Hz, 2H), 2.35–2.25 (m, 1H), 2.24–2.11 (m, 2H), 2.09–1.77 (m, 9H), 1.68 (ddd, *J* = 14.0, 6.9, 5.5 Hz, 1H), 1.65–1.58 (m, 1H), 1.54 (td, *J* = 11.2, 5.4 Hz, 1H), 1.35 (dt, *J* = 11.0, 5.9 Hz, 1H), 1.07–0.94 (m, 36H), 0.74–0.60 (m, 12H), 0.11 (s, 3H), 0.08 (s, 3H), 0.02 (s, 3H), 0.00 (s, 3H); ¹³C NMR (126 MHz, C₆D₆) δ 166.5, 166.4, 152.39, 152.35, 145.6, 145.2, 138.1, 137.8, 124.5, 124.1, 116.24, 116.19, 102.8, 102.4, 70.5, 69.1, 51.31, 51.27, 45.9, 45.0, 42.8, 42.7, 37.0, 36.7, 32.9, 32.1, 26.2, 25.4, 22.7, 21.6, 21.3, 18.4, 18.3, 7.2, 7.2, 7.1, 5.57, 5.55, -4.3, -4.4, -4.7, -4.8.; IR (neat) 2942, 2877, 1720,

1665, 1192, 1089, 832 cm^{-1} ; HRMS (ESI/MeOH) m/z calcd for $\text{C}_{27}\text{H}_{50}\text{O}_4\text{Si}_2\text{Na}$ ($\text{M} + \text{Na}$)⁺ 517.3145, found 517.3136.



rac-Methyl 4-((1S,2S)-2-allyl-3-oxocyclohexyl)-3-((tert-butyldimethylsilyl)oxy)-2-methylenebutanoate (3.50). To a Nalgene bottle containing a solution of HF·pyr (70 %wt HF, 6.30 g, 315 mmol, 125 equiv) in THF (50 mL) was added Et_3N (1.32 mL, 9.47 mmol, 3.60 equiv) at 0 °C, followed by a solution of **3.49** (1.25 g, 2.53 mmol) in THF (50 mL) over 10 min. The solution was held at 0 °C for 5 min then slowly warmed to 25 °C over 30 min at which time TLC analysis showed consumption of starting material. The crude reaction mixture was diluted in Et_2O (100 mL), and quenched by slow addition of NaHCO_3 (sat. aq.) (250 mL) in small portions with vigorous stirring. The resulting aqueous was extracted with Et_2O (2 x 50 mL). Combined organics were washed with NaHCO_3 (sat. aq.) (50 mL), H_2O (50 mL) and brine (50 mL), then dried over MgSO_4 , filtered and concentrated *in vacuo*. Chromatography was performed using 80 g of deactivated SiO_2 (2.5:1:96.5 – 5:1:94 $\text{EtOAc}:\text{Et}_3\text{N}:\text{hexanes}$) to afford the title compound as a hazy oil (0.79 g, 82% (88% based on recovered **3.#**); ~1:1 mixture of diastereomers): $R_f = 0.40$ (10:90 $\text{EtOAc}:\text{hexanes}$); ^1H NMR (500 MHz, C_6D_6) δ 6.26 (s, 2H), 6.03–5.86 (m, 4H), 5.18 (d, $J = 17.1$ Hz, 1H), 5.11 (d, $J = 17.2$ Hz, 1H), 5.04 (d, $J = 10.3$ Hz, 2H), 4.84 (d, $J = 8.3$ Hz, 2H), 3.39 (s, 3H), 3.38 (s, 3H), 2.57–2.42 (m, 3H), 2.42–2.32 (m, 1H), 2.28–2.14 (m, 2H), 2.10 (td, $J = 7.6, 3.9$ Hz, 1H), 2.02–1.83 (m, 7H), 1.83–1.72 (m, 2H), 1.72–1.64 (m, 1H), 1.58–1.29 (m, 5H), 1.27–1.16 (m, 1H), 1.16–1.05 (m, 1H), 0.95 (s, 9H), 0.93 (s, 9H), 0.04 (s, 3H), -0.02 (s, 6H), -0.06 (s, 3H); ^{13}C NMR (126 MHz, C_6D_6) δ 209.9, 209.7, 166.4,

166.3, 145.09, 145.06, 137.1, 136.8, 124.7, 124.3, 116.48, 116.45, 70.1, 68.6, 55.6, 55.4, 51.5, 51.4, 43.5, 43.1, 41.2, 40.8, 39.3, 38.7, 32.7, 31.7, 31.1, 29.2, 26.1, 26.0, 24.82, 24.80, 18.3, 18.2, -4.41, -4.42, -4.8, -5.0; IR (neat) 2954, 2852, 1712, 1634, 1090, 834, 775 cm^{-1} ; HRMS (ESI/MeOH) m/z calcd for $\text{C}_{21}\text{H}_{36}\text{O}_4\text{SiNa}$ ($\text{M} + \text{Na}$)⁺ 403.2281, found 403.2280.



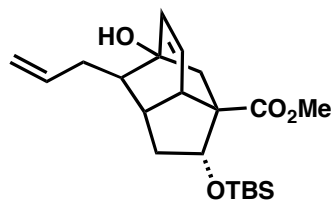
rac-Methyl 4-((1S,6S)-6-allyl-5-oxocyclohex-3-en-1-yl)-3-((tert-butyldimethylsilyl)oxy)-2-methylenebutanoate (3.52). To a solution of **3.50** (252 mg, 0.662 mmol, 1.00 equiv) in CH_2Cl_2 (35 mL) at 0 °C was added Et_3N (440 μL , 3.15 mmol, 4.77 equiv), followed by dropwise addition of TMSOTf (390 μL , 2.15 mmol, 3.25 equiv) over 5 min. TLC analysis after 30 min at 0 °C showed consumption of starting material. The crude reaction mixture was diluted in Et_2O (50 mL), and quenched with aqueous phosphate buffer (50 mL; pH = 7). The resulting aqueous was extracted with Et_2O (2 x 10 mL). Combined organics were dried over MgSO_4 , filtered and concentrated *in vacuo* to give the crude TMS enol ether as a pale yellow oil (300 mg, quant.: R_f = 0.69 (10:90 EtOAc:hexanes)). To a separate vial containing 2-iodoxybenzoic acid (IBX) (550 mg, 2.65 mmol, 4.00 equiv) and 4-methoxypyridine *N*-oxide (332 mg, 2.65 mmol, 4.00 equiv) was added DMSO (4 mL). The heterogeneous mixture was stirred for 30 min until dissolution occurred. The resultant pale yellow solution was added to a vial containing the crude silyl enol ether which was capped under an atmosphere of air and stirred vigorously at 25 °C for 16 h at which time TLC analysis indicated consumption of silyl enol ether. The crude reaction mixture was partitioned between Et_2O (40 mL), and aqueous NaHCO_3 (5% wt, 40 mL) and filtered through a pad of Celite. The white precipitate was washed with Et_2O (3 x 20 mL) and the

aqueous extracted with the washings. Combined organics were washed with NaHCO₃ (sat. aq.) (30 mL), H₂O (30 mL) and brine (30 mL), then dried over MgSO₄, filtered and concentrated *in vacuo* to give a crude yellow oil (212 mg). Chromatography performed using 48 g of deactivated SiO₂ (2.5:1:96.5 – 7.5:1:91.5 EtOAc:Et₃N:hexanes) to afford the title compound as a clear oil (131 mg, 52% (60% based on recovered **3.#**); ~1:1 mixture of diastereomers): R_f = 0.30 (10:90 EtOAc:hexanes); ¹H NMR (500 MHz, C₆D₆) δ 6.32–6.20 (m, 3H), 6.20–6.12 (m, 1H), 5.98–5.72 (m, 6H), 5.05 (d, *J* = 17.0 Hz, 2H), 5.00 (d, *J* = 10.1 Hz, 2H), 4.84–4.73 (m, 2H), 3.40 (s, 3H), 3.36 (s, 3H), 2.55 (dt, *J* = 13.9, 6.9 Hz, 1H), 2.48–2.21 (m, 7H), 2.15 (dd, *J* = 10.9, 5.6 Hz, 1H), 2.07 (dd, *J* = 12.3, 6.6 Hz, 1H), 2.00–1.87 (m, 2H), 1.75–1.67 (m, 1H), 1.61 (pd, *J* = 14.1, 2.9 Hz, 2H), 1.51–1.42 (m, 1H), 0.94 (s, 9H), 0.92 (s, 9H), 0.02 (s, 3H), -0.03 (s, 3H), -0.04 (s, 3H), -0.06 (s, 3H); ¹³C NMR (126 MHz, C₆D₆) δ 199.0, 198.9, 166.2, 166.2, 146.6, 146.4, 144.9, 144.6, 136.3, 136.0, 129.4, 129.1, 124.7, 124.4, 117.1, 116.9, 69.6, 68.7, 52.3, 51.5, 51.42, 51.40, 42.7, 42.3, 34.1, 33.9, 33.4, 32.7, 30.3, 28.6, 26.1, 26.0, 18.3, 18.2, -4.38, -4.44, -4.8, -5.0; IR (neat) 2953, 2929, 1718, 1676, 1256, 1090, 837, 776 cm⁻¹; HRMS (ESI/MeOH) *m/z* calcd for C₂₁H₃₄O₄SiNa (M + Na)⁺ 401.2124, found 401.2121.

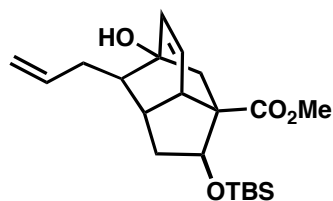
Divergent siloxydiene formation/Diels–Alder cyclization protocol: To a vial containing **3.52** (68.5 mg, 181 μmol, 1.00 equiv) was added CH₂Cl₂ (7.0 mL) and Et₃N (177 μL, 1.27 mmol, 7.00 equiv). The reaction mixture was cooled to 0 °C and TMSOTf (150 μL, 832 μmol, 4.60 equiv) was added dropwise over 2 min. After 1 h at 0 °C, TLC analysis indicated consumption of starting material. The crude reaction mixture was diluted with Et₂O (50 mL), and quenched with aqueous phosphate buffer (25 mL; pH = 7) and the aqueous was extracted with Et₂O (2 x 25 mL). The combined organics were washed with brine (25 mL), dried over MgSO₄, filtered and

concentrated *in vacuo* to give a crude yellow oil (90.0 mg, quant.) consistent with a mixture of siloxydienes. A solution of siloxydienes in benzene (42.0 mg, 93.0 μmol , 1.00 equiv) was transferred to an acid/base treated microwave vial and benzene was added and removed under vacuum to dry the sample, to a yellow residue. The vial was then charged with 1,2-dichlorobenzene (2.0 mL), degassed by sparging with Argon for 10 min, and heated to 180 °C for 40 h. The brown reaction mixture was chromatographed directly using 12.0 g of SiO_2 (0:100 – 20:80 EtOAc:hexanes) to afford **3.55a** (4.7 mg, 14%), **3.55b** (9.0 mg, 26%), **3.56a** (4.8 mg, 14%) and **3.56b** (4.8 mg, 14%) as clear oils.

Selective siloxydiene formation/Diels–Alder cyclization protocol: To an acid/base treated microwave vial was added a solution of **3.52** (20.0 mg, 52.8 μmol , 1.00 equiv) in benzene (2.00 mL). The solution was dried by azeotropic distillation with benzene and the resulting yellow residue was dissolved in DMF (1 mL). The clear yellow reaction mixture was charged with Et_3N (45.0 μL , 317 μmol , 6.00 equiv) and TMSCl (40.0 μL , 317 μmol , 6.00 equiv). The reaction mixture was capped and heated to 90 °C for 96 h. The crude brown reaction mixture was diluted with EtOAc (5 mL), and quenched with aqueous phosphate buffer (5 mL; pH = 7) and the aqueous was extracted with EtOAc (3 x 5 mL). The combined organics were washed with NaHCO_3 (sat. aq.) (5 mL) and brine (5 mL), then dried over MgSO_4 , filtered and concentrated *in vacuo* to give a crude brown oil. Chromatography performed using 8.0 g of deactivated SiO_2 (0:1:99 – 20:1:79 EtOAc: Et_3N :hexanes) to afford **3.56a** (8.6 mg, 43%) and **3.56b** (7.1 mg, 36%) as clear oils.

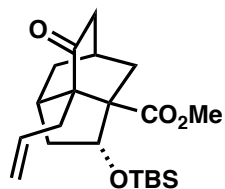


***rac*-(2*R*)-Methyl 4-allyl-2-((*tert*-butyldimethylsilyl)oxy)-5-hydroxy-2,3,3*a*,4,5,7*a*-hexahydro-1*H*-1,5-methanoindene-1-carboxylate (3.55a).** $R_f = 0.31$ (10:90 EtOAc:hexanes); ^1H NMR (500 MHz, C_6D_6) δ 6.17 (d, $J = 8.5$ Hz, 1H), 5.84 (dd, $J = 8.5, 6.4$ Hz, 1H), 5.69 (dddd, $J = 16.3, 10.2, 7.7, 5.8$ Hz, 1H), 5.02–4.92 (m, 2H), 4.54 (dd, $J = 10.1, 4.6$ Hz, 1H), 3.36 (s, 3H), 2.84–2.77 (m, 1H), 2.51–2.44 (m, 1H), 2.32–2.20 (m, 3H), 1.57–1.47 (m, 2H), 1.40 (s, 1H), 1.34 (dd, $J = 10.9, 3.3$ Hz, 1H), 1.27 (dd, $J = 13.7, 4.7$ Hz, 1H), 0.96 (s, 9H), 0.03 (s, 3H), 0.02 (s, 3H); ^{13}C NMR (126 MHz, C_6D_6) δ 175.5, 140.2, 137.9, 125.9, 115.9, 77.5, 74.6, 59.3, 57.2, 51.6, 44.6, 44.1, 40.9, 37.2, 36.4, 26.0, 18.3, -4.7, -4.9; IR (neat) 3472, 2952, 2930, 2856, 1725, 1258, 1107, 838 cm^{-1} ; HRMS (ESI/MeOH) m/z calcd for $\text{C}_{21}\text{H}_{34}\text{O}_4\text{SiNa}$ ($\text{M} + \text{Na}$) $^+$ 401.2124, found 401.2122.

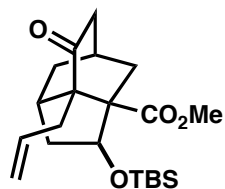


***rac*-(2*S*)-Methyl 4-allyl-2-((*tert*-butyldimethylsilyl)oxy)-5-hydroxy-2,3,3*a*,4,5,7*a*-hexahydro-1*H*-1,5-methanoindene-1-carboxylate (3.55b).** $R_f = 0.09$ (10:90 EtOAc:hexanes); ^1H NMR (500 MHz, C_6D_6) δ 6.22 (dd, $J = 8.5, 6.4$ Hz, 1H), 5.98 (d, $J = 8.3$ Hz, 1H), 5.71 (dddd, $J = 16.9, 10.4, 7.7, 6.2$ Hz, 1H), 5.05–4.92 (m, 2H), 4.10 (dd, $J = 6.2, 2.5$ Hz, 1H), 3.39 (s, 3H), 3.36 (dd, $J = 6.1, 4.9$ Hz, 1H), 2.45–2.36 (m, 1H), 1.90 (d, $J = 13.1$ Hz, 1H), 1.80–1.67 (m, 2H), 1.63–1.58 (m, 1H), 1.57–1.48 (m, 1H), 1.39–1.32 (m, 1H), 1.28 (d, $J = 13.2$ Hz, 1H), 1.00 (dd, $J = 9.9, 3.4$ Hz, 1H), 0.95 (s, 9H), 0.05 (s, 3H), 0.02 (s, 3H); ^{13}C NMR (126 MHz, C_6D_6) δ 173.7, 137.8,

136.8, 128.7, 116.0, 80.6, 74.9, 61.0, 56.0, 51.1, 46.2, 45.4, 40.7, 39.9, 36.4, 25.9, 18.1, -4.4, -5.1; IR (neat) 3454, 2952, 2930, 2857, 1728, 1253, 1089, 835 cm^{-1} ; HRMS (ESI/MeOH) m/z calcd for $\text{C}_{21}\text{H}_{34}\text{O}_4\text{SiNa}$ ($\text{M} + \text{Na}$) $^+$ 401.2124, found 401.2126.



***rac*-(2*R*)-Methyl 7a-allyl-2-((*tert*-butyldimethylsilyl)oxy)-7-oxooctahydro-1*H*-1,5-methanoindene-1-carboxylate (3.56a).** $R_f = 0.44$ (10:90 EtOAc:hexanes); ^1H NMR (500 MHz, C_6D_6) δ 6.08 (dtdd, $J = 17.0, 9.9, 5.1, 0.8$ Hz, 1H), 5.01 (dd, $J = 9.9, 4.0$ Hz, 1H), 4.98–4.90 (m, 2H), 3.19 (s, 3H), 2.80–2.74 (m, 1H), 2.67 (dd, $J = 13.8, 5.0$ Hz, 1H), 2.35 (ddd, $J = 13.8, 9.7, 7.2$ Hz, 1H), 2.23 (dt, $J = 18.6, 2.9$ Hz, 1H), 1.94–1.84 (m, 3H), 1.70 (ddd, $J = 9.8, 5.0, 2.3$ Hz, 2H), 1.48–1.40 (m, 1H), 1.32–1.26 (m, 1H), 1.12 (dd, $J = 13.8, 4.1$ Hz, 1H), 1.00 (s, 9H), 0.20 (s, 3H), 0.17 (s, 3H); ^{13}C NMR (126 MHz, C_6D_6) δ 210.9, 173.9, 135.9, 117.0, 74.0, 59.2, 58.0, 51.4, 45.5, 43.0, 37.8, 36.9, 33.4, 29.7, 26.1, 25.0, 18.4, -4.5, -4.6; IR (neat) 2951, 2929, 2855, 1730, 1256, 835 cm^{-1} ; HRMS (ESI/MeOH) m/z calcd for $\text{C}_{21}\text{H}_{34}\text{O}_4\text{SiNa}$ ($\text{M} + \text{Na}$) $^+$ 401.2124, found 401.2132.



***rac*-(2*S*)-Methyl 7a-allyl-2-((*tert*-butyldimethylsilyl)oxy)-7-oxooctahydro-1*H*-1,5-methanoindene-1-carboxylate (3.56b).** $R_f = 0.25$ (10:90 EtOAc:hexanes); ^1H NMR (500 MHz, C_6D_6) δ 6.05–5.93 (m, 1H), 5.06–4.92 (m, 2H), 4.25 (t, $J = 7.4$ Hz, 1H), 3.39 (s, 3H), 2.44 (dd, $J = 13.8, 6.8$ Hz, 1H), 2.36–2.24 (m, 2H), 2.14–2.02 (m, 2H), 1.96 (d, $J = 14.1$ Hz, 1H), 1.77 (dd, $J = 16.8, 3.8$ Hz, 1H), 1.59 (ddd, $J = 12.8, 8.2, 4.5$ Hz, 1H), 1.45 (dd, $J = 12.7, 6.3$ Hz, 1H), 1.36–

1.29 (m, 1H), 1.16 (ddd, $J = 12.7, 6.1, 3.1$ Hz, 1H), 0.93 (s, 9H), 0.71 (dd, $J = 13.6, 5.2$ Hz, 1H), 0.05 (s, 3H), 0.04 (s, 3H); ^{13}C NMR (126 MHz, C_6D_6) δ 212.7, 174.8, 135.1, 117.6, 70.4, 51.4, 49.6, 49.2, 42.4, 36.3, 34.6, 34.1, 33.9, 31.3, 27.1, 25.9, 18.1, -4.1, -5.0; IR (neat) 2952, 2930, 2857, 1728, 1256, 837 cm^{-1} ; HRMS (ESI/MeOH) m/z calcd for $\text{C}_{21}\text{H}_{34}\text{O}_4\text{SiNa}$ ($\text{M} + \text{Na}$) $^+$ 401.2124, found 401.2119.

References

- ¹ Isolation of isopalhinine A, palhinine B and palhinine C: Dong, L.-B.; Gao, X.; Liu, F.; He, J.; Wu, X.-D.; Li, Y.; Zhao, Q.-S. *Org. Lett.* **2013**, *15*, 3570–3573.
- ² Review on lycopodium alkaloids: Ma, X.; Gang, D. R. *Nat. Prod. Rep.* **2004**, *21*, 752–772.
- ³ Review on lycopodium alkaloids: Hirasawa, Y.; Kobayashi, J.; Morita, H. *Heterocycles* **2009**, *77*, 679–729.
- ⁴ Isolation of fawcettimine: Burnell, R. H. *J. Chem. Soc.* **1959**, 3091–3093.
- ⁵ Review of synthetic approaches to fawcettimine alkaloids: Wang, X.; Li, H.; Lei, X. *Synlett* **2013**, *24*, 1032–1043.
- ⁶ Isolation of palhinine A: Zhao, F.-W.; Sun, Q.-Y.; Yang, F.-M.; Hu, G.-W.; Luo, J.-F.; Tang, G.-H.; Wang, Y.-H.; Long, C.-L. *Org. Lett.* **2010**, *12*, 3922–3925.
- ⁷ Isolation of cardionine: De Gabriel, la F.; Gavin, J. A.; Reina, M.; Acosta, R. D. *J. Org. Chem.* **1990**, *55*, 342–344.
- ⁸ Review of hetisane alkaloids: Bessonova, I. A.; Saidkhodzhaeva, S. A. *Chem. Nat. Compd.* **2000**, *36*, 419–477.
- ⁹ Srikrishna, A.; Ravi P., K.; Gharpure, S. J. *Tetrahedron Lett.* **2001**, *42*, 3929–3931.
- ¹⁰ Njardarson, J. T.; McDonald, I. M.; Spiegel, D. A.; Inoue, M.; Wood, J. L. *Org. Lett.* **2001**, *3*, 2435–2438.
- ¹¹ Corey, E. J.; Behforouz, M.; Ishiguro, M. *J. Am. Chem. Soc.* **1979**, *101*, 1608–1609.
- ¹² Yamamoto, H.; Sham, H. L. *J. Am. Chem. Soc.* **1979**, *101*, 1609–1611.
- ¹³ Isolation of 9-isocyanopupukeanane: Burreson, B. J.; Scheuer, P. J.; Finer, J.; Clardy, J. *J. Am. Chem. Soc.* **1975**, *97*, 4763–4764.
- ¹⁴ Zhao, C.; Zheng, H.; Jing, P.; Fang, B.; Xie, X.; She, X. *Org. Lett.* **2012**, *14*, 2293–2295.

- ¹⁵ Gaugele, D.; Maier, M. E. *Synlett* **2013**, *24*, 955–958.
- ¹⁶ Zhang, G.-B.; Wang, F.-X.; Du, J.-Y.; Qu, H.; Ma, X.-Y.; Wei, M.-X.; Wang, C.-T.; Li, Q.; Fan, C.-A. *Org. Lett.* **2012**, *14*, 3696–3699 and references therein.
- ¹⁷ Seminal publication on nosyl cyclization: Fukuyama, T.; Jow, C.-K.; Cheung, M. *Tetrahedron Lett.* **1995**, *36*, 6373–6374.
- ¹⁸ Seminal publication on nosyl cyclization: Kan, T.; Fujiwara, A.; Kobayashi, H.; Fukuyama, T. *Tetrahedron* **2002**, *58*, 6267–6276.
- ¹⁹ Seminal publication on nosyl cyclization: Kan, T.; Kobayashi, H.; Fukuyama, T. *Synlett* **2002**, 697–699.
- ²⁰ Nosyl cyclization in fawcettimine synthesis: Pan, G.; Williams, R. M. *J. Org. Chem.* **2012**, *77*, 4801–4811.
- ²¹ Review of nosyl cyclization strategies: Kan, T.; Fukuyama, T. *Chem. Commun.* **2004**, *0*, 353–359.
- ²² Review of the intramolecular Diels–Alder reaction in natural product synthesis: Takao, K.; Munakata, R.; Tadano, K. *Chem. Rev.* **2005**, *105*, 4779–4807.
- ²³ Review of vicinal quaternary centers: Peterson, E. A.; Overman, L. E. *P. Natl. Acad. Sci. USA* **2004**, *101*, 11943–11948.
- ²⁴ Seminal publication Morita–Baylis–Hillman reaction: Morita, K. Japanese patent 43003364, 1968; Chem. Abstr. **1968**, *69*, 58828s.
- ²⁵ Seminal publication Morita–Baylis–Hillman reaction: Morita, K.; Suzuki, Z.; Hirose, H. *Bull. Chem. Soc. Jpn.* **1968**, *41*, 2815.
- ²⁶ Seminal publication Morita–Baylis–Hillman reaction: Baylis, A. B.; Hillman, M. E. D. German patent 2155113, 1972; Chem. Abstr. **1972**, *77*, 34174q.

- ²⁷ Review of Morita–Baylis–Hillman reaction: Basavaiah, D.; Reddy, B. S.; Badsara, S. S. *Chem. Rev.* **2010**, *110*, 5447–5674.
- ²⁸ Jørgensen organocatalytic enone synthesis: Carlone, A.; Marigo, M.; North, C.; Landa, A.; Jørgensen, K. A. *Chem. Commun.* **2006**, *0*, 4928–4930.
- ²⁹ Barbazanges, M.; Meyer, C.; Cossy, J. *Org. Lett.* **2008**, *10*, 4489–4492.
- ³⁰ Synthesis of organocatalyst: Halland, N.; Jørgensen, K. A.; Marigo, M.; Braunton, A.; Bachmann, S.; Fielenbach, D. WO 2005080298, Sep 01, 2005.
- ³¹ Discussion of reaction optimization: Bolze, P.; Dickmeiss, G.; Jørgensen, K. A. *Org. Lett.* **2008**, *10*, 3753–3756.
- ³² Asymmetric malonate Michael strategy: Ohshima, T.; Xu, Y.; Takita, R.; Shimizu, S.; Zhong, D.; Shibasaki, M. *J. Am. Chem. Soc.* **2002**, *124*, 14546–14547.
- ³³ Asymmetric malonate Michael strategy: Ohshima, T.; Xu, Y.; Takita, R.; Shibasaki, M. *Tetrahedron* **2004**, *60*, 9569–9588.
- ³⁴ Malonate Michael strategy: Seo, J. W.; Comninos, J. S.; Chi, D. Y.; Kim, D. W.; Carlson, K. E.; Katzenellenbogen, J. A. *J. Med. Chem.* **2006**, *49*, 2496–2511.
- ³⁵ Krapcho decarboxylation: Krapcho, A. P.; Glynn, G. A.; Grenon, B. J. *Tetrahedron Lett.* **1967**, 215–217.
- ³⁶ Saegusa–Ito oxidation: Ito, Y.; Hirao, T.; Saegusa, T. *J. Org. Chem.* **1978**, *43*, 1011–1013.
- ³⁷ Tsuji-modification of Saegusa–Ito oxidation: Minami, I.; Takahashi, K.; Shimizu, I.; Kimura, T.; Tsuji, J. *Tetrahedron* **1986**, *42*, 2971–2977.
- ³⁸ Wuts, P. G. M.; Greene, T. W. Protection for the Hydroxyl Group, Including 1,2- and 1,3-Diols in *Greene’s Protective Groups in Organic Synthesis*; John Wiley & Sons, Inc., 2006; pp. 16–366.

- ³⁹ CAN-mediated cleavage of PMB-ether: Johansson, R.; Samuelsson, B. *J. Chem. Soc., Perkin Trans. I* **1984**, 2371–2374.
- ⁴⁰ DDQ-mediated cleavage of PMB-ether: Horita, K.; Yoshioka, T.; Tanaka, T.; Oikawa, Y.; Yonemitsu, O. *Tetrahedron* **1986**, *42*, 3021–3028.
- ⁴¹ Wilson, E. M.; Trauner, D. *Org. Lett.* **2007**, *9*, 1327–1329.
- ⁴² Seminal publication of Mukaiyama–Michael reaction: Narasaka, K.; Soai, K.; Mukaiyama, T. *Chem. Lett.* **1974**, 1223–1224.
- ⁴³ Seminal publication of Mukaiyama–Michael reaction: Kita, Y.; Segawa, J.; Haruta, J.; Fujii, T.; Tamura, Y. *Tetrahedron Lett.* **1980**, *21*, 3779–3782.
- ⁴⁴ Seminal publication of Mukaiyama–Michael reaction: Kita, Y.; Segawa, J.; Haruta, J.; Yasuda, H.; Tamura, Y. *J. Chem. Soc., Perkin Trans. I* **1982**, 1099–1104.
- ⁴⁵ Enantioselective variant of Mukaiyama–Michael reaction: Kobayashi, S.; Suda, S.; Yamada, M.; Mukaiyama, T. *Chem. Lett.* **1994**, 97–100.
- ⁴⁶ Seminal publication of TASF-mediated alkylation: Noyori, R.; Nishida, I.; Sakata, J.; Nishizawa, M. *J. Am. Chem. Soc.* **1980**, *102*, 1223–1225.
- ⁴⁷ Seminal publication of TASF-mediated alkylation: Noyori, R.; Nishida, I.; Sakata, J. *Tetrahedron Lett.* **1980**, *21*, 2085–2088.
- ⁴⁸ The diastereomeric ratio of the TASF-mediated allylation was determined by ¹H NMR integration of the major and minor vinyl peaks ($\delta = 5.90$ and 5.68 ppm, respectively).
- ⁴⁹ Review of tandem vicinal difunctionalization: Chapdelaine, M. J.; Hulce, M. *Org. React.* **1990**, *38*, 277–653.
- ⁵⁰ PCC oxidation: Corey, E. J.; Suggs, J. W. *Tetrahedron Lett.* **1975**, *16*, 2647–2650.
- ⁵¹ Swern oxidation: Omura, K.; Swern, D. *Tetrahedron* **1978**, *34*, 1651–1660.

- ⁵² Parikh–Doering oxidation: Parikh, J. R.; Doering, W. v. E. *J. Am. Chem. Soc.* **1967**, *89*, 5505–5507.
- ⁵³ Martin–Dess oxidation: Dess, D. B.; Martin, J. C. *J. Org. Chem.* **1983**, *48*, 4155–4156.
- ⁵⁴ Quinuclidine-mediated Morita–Baylis–Hillman reactions: Aggarwal, V. K.; Emme, I.; Fulford, S. Y. *J. Org. Chem.* **2003**, *68*, 692–700.
- ⁵⁵ IBX·MPO oxidation: Nicolaou, K. C.; Gray, D. L. F.; Montagnon, T.; Harrison, S. T. *Angew. Chem., Int. Ed.* **2002**, *41*, 996–1000.
- ⁵⁶ Taber, D. F.; Sheth, R. B. *J. Org. Chem.* **2008**, *73*, 8030–8032.
- ⁵⁷ Seminal publication of Sakurai reaction: Hosomi, A.; Sakurai, H. *J. Am. Chem. Soc.* **1977**, *99*, 1673–1675.
- ⁵⁸ Review of Sakurai reaction: Hosomi, A. *Acc. Chem. Res.* **1988**, *21*, 200–206.
- ⁵⁹ Seminal publication of Nozaki–Hiyama–Kishi reaction: Okude, Y.; Hirano, S.; Hiyama, T.; Nozaki, H. *J. Am. Chem. Soc.* **1977**, *99*, 3179–3181.
- ⁶⁰ Seminal publication of Nozaki–Hiyama–Kishi reaction: Jin, H.; Uenishi, J.; Christ, W. J.; Kishi, Y. *J. Am. Chem. Soc.* **1986**, *108*, 5644–5646.
- ⁶¹ Review of Nozaki–Hiyama–Kishi reaction: Kishi, Y. *Pure Appl. Chem.* **1992**, *64*, 343–350.
- ⁶² Motokura, K.; Fujita, N.; Mori, K.; Mizugaki, T.; Ebitani, K.; Kaneda, K. *J. Am. Chem. Soc.* **2005**, *127*, 9674–9675.
- ⁶³ Tzvetkov, N. T.; Schmoldt, P.; Neumann, B.; Stammeler, H.-G.; Mattay, J. *Tetrahedron: Asymmetry* **2006**, *17*, 993–998.

Chapter 4

Origins of Regio- and Stereochemistry in Type 2 Intramolecular *N*-Acylnitroso Diels–Alder Reactions: A Computational Study of Tether Length and Substituent Effects

Abstract: Quantum mechanical calculations have been used to investigate type 2 intramolecular *N*-acylnitroso Diels–Alder reactions. Experimentally observed regioselectivities and diastereoselectivities of these reactions have been reproduced using B3LYP/6-31+G(d) DFT calculations. The factors that govern selectivity (i.e. tether length, tether substitution and diene substitution) were systematically investigated. Tethers less than 6 carbon atoms lead to 1,3 regioisomers due to conformational restrictions. Substituents on the tether lead to diastereoselective outcomes dictated by transannular interactions in the transition states. The modest diastereoselectivity of diene-substituted substrates is rationalized as arising from reduction of eclipsing interactions in the flattened diene transition states. This method should prove valuable for planning syntheses involving type 2 intramolecular Diels–Alder reactions.

Introduction

The type 2 intramolecular Diels–Alder (type 2 IMDA) reaction involves the union of a diene and a dienophile that are tethered at the C2 position of the diene (**4.1**) to afford bicyclic bridgehead alkene products (Figure 4.1).^{1–3} This reaction can either afford 1,3- or 1,4-regioisomers as products (**4.2** and **4.3**, respectively), which is largely dependent upon the length or rigidity of the tether. The regiochemical nomenclature is determined by counting along the newly formed ring from the bridgehead alkene to the other end of the tether.

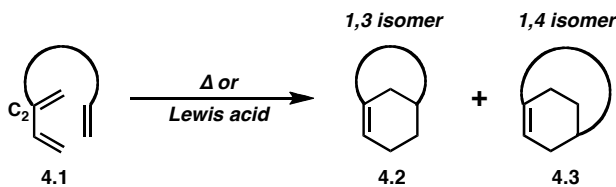


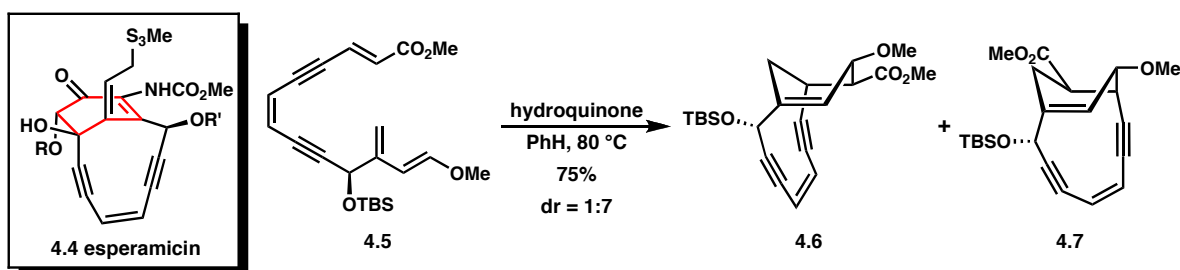
Figure 4.1. Regioselectivity of the type 2 IMDA reaction.

The type 2 IMDA reaction is a powerful method for the construction of polycyclic frameworks that has found utility in the synthesis of challenging bridgehead olefins and complex organic molecules (Scheme 4.1). Schreiber and Kiessling's approach to esperamicin (**4.4**) attempted to employ a type 2 IMDA reaction to access the cyclohexenyl core of the molecule.⁴ Though rigid ene-diyne **4.5** was originally reported to afford the desired 1,3-regioisomer (**4.6**), subsequent synthetic studies and NMR experiments revealed that the major product was in fact the 1,4-regioisomer (**4.7**).⁵ In contrast, Baran and co-workers synthesis of taxadienone (**4.8**)⁶ features a Lewis acid promoted type 2 IMDA reaction to afford the taxane core in a highly diastereoselective manner.^{7,8} More recently, Stoltz and Hong utilized a related IMDA reaction to assemble the tricyclic core of 9 β -presilphiperfolan-1 α -ol (**4.11**), which proceeded in high yield, but afforded the desired diastereomer (**4.14**) as the minor product.⁹

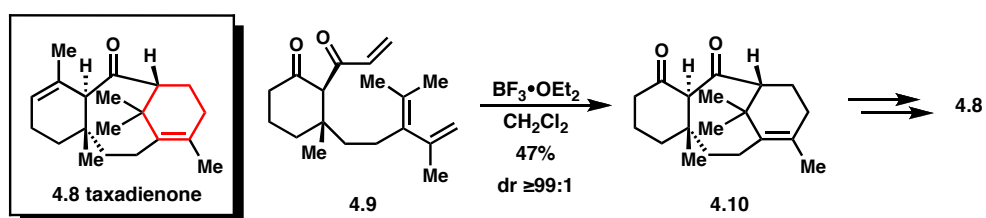
These examples highlight two important facts. First, the type 2 IMDA reaction is a powerful method for the rapid synthesis of complex architectures. Second, the regio- and stereochemical outcomes of these reactions can be challenging to predict. With the second point in mind, we set out to develop a simple computational method for predicting product distributions in type 2 IMDA reactions.

Scheme 4.1. Application of the type 2 IMDA reaction to complex products.^{4-6,9}

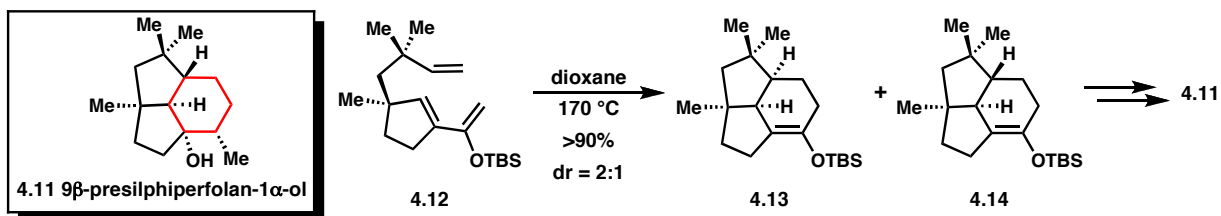
A) Schreiber and Kiessling



B) Baran and co-workers



C) Stoltz and Hong



In this report we provide an analysis of contributing factors to the regio- and stereoselectivity of the type 2 IMDA reaction. The *N*-acylnitroso type 2 IMDA reaction was chosen for this computational study since this reaction has provided a wealth of experimental data concerning both regio- and diastereoselectivities.¹⁰⁻¹² The computational method accurately describes the observed product distributions and identifies contributing factors to regio- and stereochemistry.

Hetero-Diels–Alder reactions of *N*-acylnitroso dienophiles have been useful tools for the synthesis of biologically active molecules.¹³ The *N*-acylnitroso type 2 IMDA reaction has been studied as a method to synthesize medium ring lactams and *cis*-1,4-cyclohexyl aminoalcohols.¹⁰ This reaction is attractive because it employs synthetically tractable precursors (diene esters) to

assemble complex cycloadducts that can be further functionalized (Figure 4.2). The increased reactivity of the *N*-acylnitroso moiety allows these reactions to proceed under ambient or even cryogenic temperatures without the use of Lewis acids; a feature absent from the all-carbon type 2 IMDA reactions.

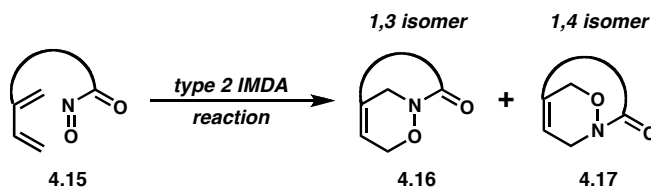


Figure 4.2. Regioselectivity of the *N*-acylnitroso type 2 IMDA reaction.

We have employed density functional theory (DFT) calculations in an effort to understand the observed regio- and stereochemical outcomes of the *N*-acylnitroso type 2 IMDA reaction. In particular, we have sought to understand how subtle changes in tether length and substitution play a dramatic, non-obvious role in determining the stereochemical outcome of these reactions. Tether length was investigated to determine the regiochemical reliability of the method, whereas tether and diene substitution were investigated to determine stereochemical reliability. The method described herein correlates well with experimental data and provides insight into predicting the outcomes of these important reactions.

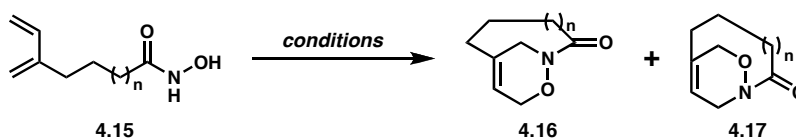
Background

Scope of the N-acylnitroso Type 2 IMDA Reaction

Several factors including tether length and substitution, as well as diene substitution have been shown experimentally to affect product distributions in this reaction. Tether length plays an important role for the regiochemical product distribution of the *N*-acylnitroso type 2 IMDA reaction (Table 4.1).^{10,11} The cycloaddition of dienes and nitroso groups with 4- or 5-carbon

tethers (**4.15a** and **4.15b**) results in exclusive formation of the 1,3-regioisomers (**4.16**). The standard reaction conditions failed to provide products in the 6-carbon tethered case (entry 3), however upon masking the diene as the 9,10-dimethylantracene adduct (**4.15d**), thermolysis led to a 1:1 mixture of 1,3- and 1,4-regioisomers (entry 4). The regiochemical crossover with a tether of 6 or more carbons favors the electronically preferred 1,4-regioisomer (**4.17**) due to increased flexibility of the tether. This change in regiomer preference has also been observed in Lewis acid-catalyzed type 2 IMDA reactions.¹⁴

Table 4.1. Acyclic diene *N*-acylnitroso type 2 IMDA reactions.¹¹



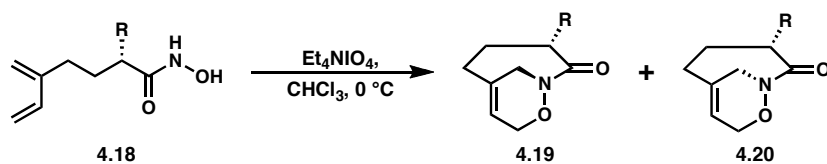
entry	n	conditions	% yield	ratio (4.16 : 4.17)
1	1 (4.15a)	Et ₄ NIO ₄ , CHCl ₃ , 0 °C	75	>95:5
2	2 (4.15b)	Et ₄ NIO ₄ , CHCl ₃ , 0 °C	80	>95:5
3	3 (4.15c)	Et ₄ NIO ₄ , CHCl ₃ , 0 °C	not isolated	N/A
4	3 ^a (4.15d)	PhH, 80 °C	60	50:50

a) Starting material was the dimethylantracene adduct of the acyl nitroso diene.

The stereochemistry of *N*-acylnitroso type 2 IMDA reactions is influenced by substitutions on the tether.¹⁰ Of particular interest was the stereochemical reversal of product distribution in α -carbonyl substituted cases (Table 4.2). Alkyl α -substituents, such as benzyl or allyl groups (**4.18a** and **4.18b**), afforded diastereomer **4.19** exclusively with an *anti* relationship between the substituent and the bridging carbon (entries 1 and 2). In contrast, ethereal α -substituents, such as benzyl or *tert*-butyldiphenylsiloxy ethers (**4.18a** and **4.18b**), provide *syn* diastereomer **4.20** as the predominate product (entries 3 and 4). The preferential formation of the *syn* diastereomer in ethereal cases was originally hypothesized to be a manifestation of a dipole minimization in the transition state. However, ethereal substrates showed negligible changes in

diastereoselectivity across solvents of varying polarity, indicating that the observed selectivity was not correlated to dipole minimization.

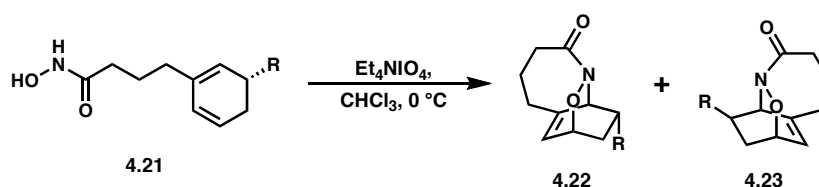
Table 4.2. α -Substituted acyclic diene N-acylnitroso type 2 IMDA reactions.¹⁰



entry	R	% yield	<i>anti:syn</i> (4.19:4.20)
1	Bn (4.18a)	83	>95:5
2	allyl (4.18b)	70	>95:5
3	OBn (4.18c)	62	<5:95
4	OTBDPS (4.18d)	70	16:84

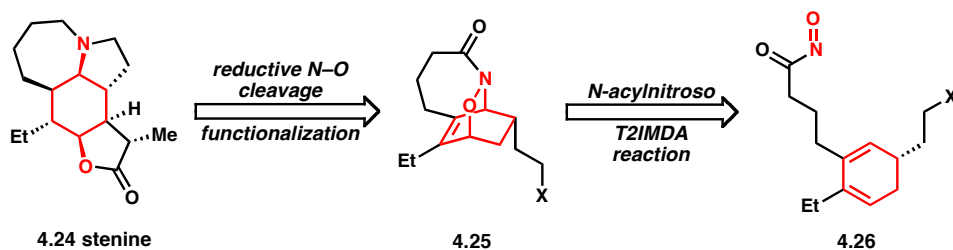
Cyclic diene substrates, both unsubstituted and substituted, have been previously investigated (Table 4.3). In both cases, the 1,3-regioisomer is obtained exclusively, and in the substituted example there is a preference for a *trans* relationship between the substituent and the newly formed bonds (4.22). These substituted dienes are model systems for the synthesis of several members of the stemona alkaloids, including stenine (Scheme 4.2, 4.24).¹²

Table 4.3. Cyclic diene N-acylnitroso type 2 IMDA reactions.¹²



entry	R	% yield	<i>cis:trans</i> (4.22:4.23)
1	H (4.21a)	50	N/A
2	CH ₂ CH ₂ OTBS (4.21b)	50	86:14

Scheme 4.2. Retrosynthetic analysis of stenine.



Previous Theoretical Studies

Comparisons of quantum mechanical methods for studying pericyclic reaction mechanisms, including intermolecular Diels–Alder reactions, have been reported.¹⁵ A subsequent computational study by Leach and Houk describes the transition state and mechanism of intermolecular hetero-Diels–Alder reactions, including *N*-acylnitroso examples.¹⁶ The study concluded that these reactions proceed through a concerted, yet highly asynchronous, *endo* transition state. While type 1 intermolecular Diels–Alder reactions have been extensively studied computationally,^{17–23} there have been no computational studies of either the type 2 IMDA reaction or *N*-acylnitroso type 2 IMDA reaction.

Computational Methods

Conformational analysis of starting materials and products were performed in Spartan '08²⁴ using MMFF.²⁵ Geometry optimization, transition state identification, and vibrational frequency analysis were carried out with Gaussian 09²⁶ using B3LYP/6-31+G(d)^{27,28} as convergent, gas-phase calculations performed at 273 K. Transition states were confirmed by IRC calculations.²⁹ Free energies are reported from the unscaled frequencies. Graphics were generated using the CYLview program.³⁰

Results

Acyclic Dienes and the Role of Tether Lengths in Product Distribution

The calculated energy diagrams and transition states for the acyclic diene *N*-acylnitroso type 2 IMDA reaction for 4-, 5- and 6-carbon tethered substrates are shown in Figure 4.3. The reaction is highly exothermic, with a late transition state, which resembles the products. In the case of 4-carbon tether **SM-A**, the 1,3-regioisomeric **TS-A** is 4.8 kcal mol⁻¹ lower in energy than the 1,4-regioisomeric **TS-A'**. A comparison of C–N distances in the transition states shows less advanced bond formation in the lower energy **TS-A** than in **TS-A'** (2.10 Å vs. 2.01 Å). Both TSs display a high level of asynchronicity, as evident by the large differences between the C–O and C–N bond distances (2.80 Å vs. 2.10 Å for **TS-A**). The 7-membered ring resulting from C–N bond formation **TS-A** adopts a chair geometry, whereas the 8-membered ring of **TS-A'** is a chair-boat conformation. In both cases, these conformations result in the tether β-carbon oriented away from the C1 carbon of the adjacent diene terminus (internal orientation). The free energy of **PDT-A'** is also dramatically higher than **PDT-A** (8.9 kcal mol⁻¹).

Extending the tether length to 5-carbons results in a smaller $\Delta\Delta G^\ddagger$ (1.9 kcal mol⁻¹) between **TS-B** and **TS-B'**, favoring 1,3-regioisomeric **TS-B**, in contrast to $\Delta\Delta G^\ddagger$ of **TS-A** and **TS-A'** (4.8 kcal mol⁻¹). As compared to the chair structure adopted by **TS-A**, **TS-B** tether must adopt a chair-boat conformation where the tether β-carbon is oriented toward the C1 carbon of the adjacent diene terminus (external tether). As a result of this orientation, A^{1,3} strain between the γ-carbon of the tether and C1 of the diene destabilizes **TS-B** compared to **TS-A**. Formation of the C–O bond is more advanced in **TS-B** than **TS-B'** (2.59 Å vs. 2.74 Å) and the difference in free energies of **PDT-B** and **PDT-B'** (5.2 kcal mol⁻¹) is less than in the 4-carbon tether example.

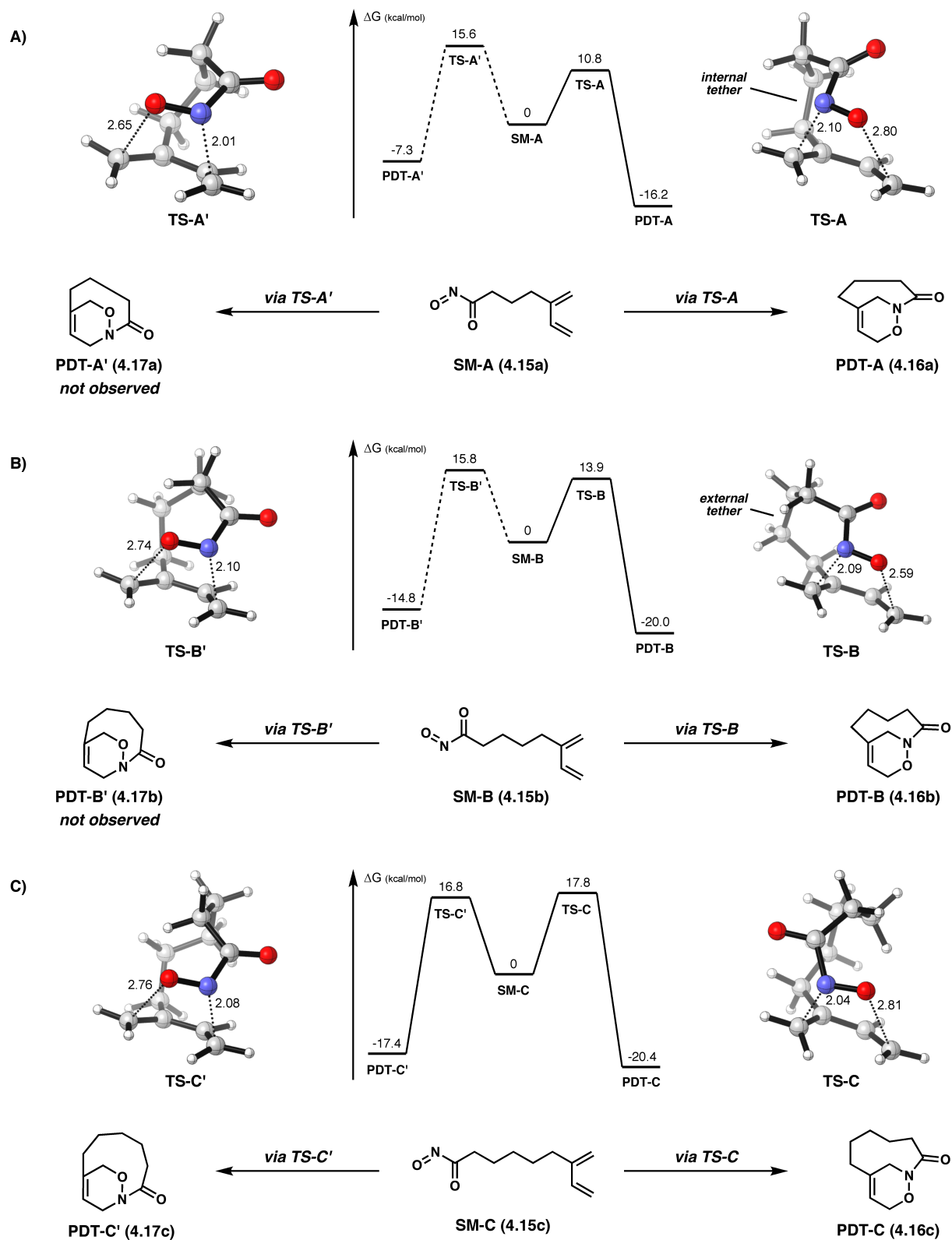


Figure 4.3. Free energy (FE) diagrams and (TS) transition state structures for acyclic dienes of carbon tether lengths 4-6 (A-C).³¹

When the tether length is extended to 6-carbons the 1,4- regioisomeric **TS-C'** is now 1.0 kcal mol⁻¹ lower in energy than the 1,3-regioisomeric **TS-C**. Higher activation energies are required for these pathways compared to the 4- and 5-carbon tether cases (by 2.9-7.0 kcal mol⁻¹). Distances between each pair of atoms undergoing new bond formation are similar in both **TS-C'** and **TS-C**, which also both exhibit asynchronous bond formation. **TS-C'** adopts an internal tether orientation while **TS-C** possesses an external tether orientation; however, there are limited steric interactions in **TS-C** as compared to **TS-B** due to the flexibility of the long tether.

Diastereoselectivity of α -Substituted Tether Substrates

The calculated energy diagrams and transition states for the *N*-acylnitroso type 2 IMDA reaction with α -substituted substrates are shown in Figure 4.4. In the case of substrate **SM-D** (analogous to Table 4.2, entries 1 and 2) with a methyl group α to the acylnitroso, **TS-D** leading to the *anti*-diastereomer is 2.7 kcal mol⁻¹ lower in energy than the *syn*-diastereomeric **TS-D'**. Both TSs display a high level of asynchronicity however, **TS-D** exhibits an internal tether orientation, whereas the tether in **TS-D'** is arranged in an external orientation. This conformation places the γ -hydrogen of **TS-D'** in direct proximity of the terminal olefin, causing a net destabilizing effect. Because the internal tether is favored, the *anti*-diastereomer is predicted, which reflects the experimental results that benzyl substituted **4.19a** or allyl substituted **4.19b** are obtained as single diastereomers.

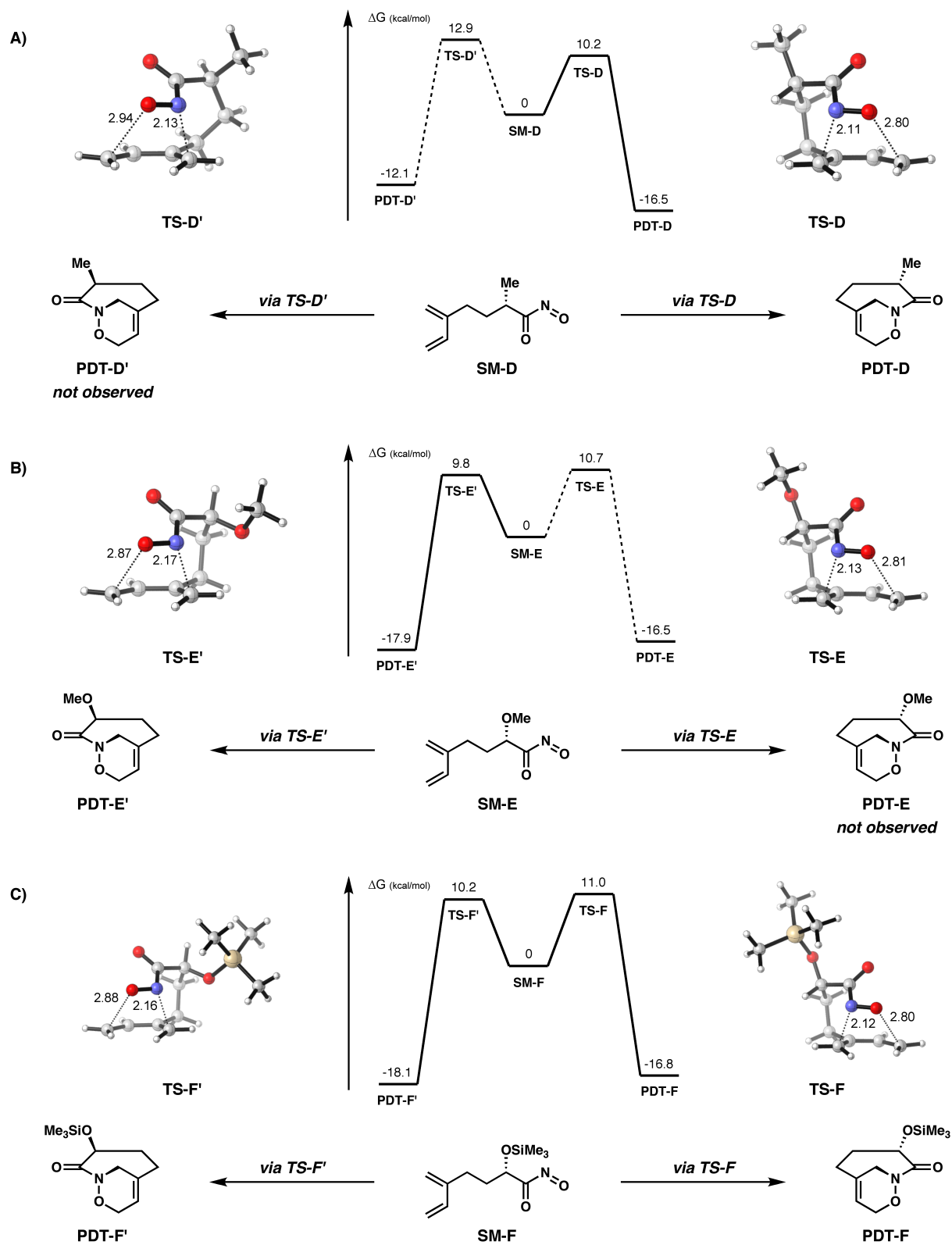


Figure 4.4. FE diagrams and TS structures for the stereoselectivity (*syn* vs. *anti*) of acyclic diene substrates with α -methyl (A) or α -etheral (B-C) substituted tethers.³¹

The models with ethereal α -substituents (**SM-E** and **SM-F**) are similar to each other and are in direct contrast to α -methyl substrate **SM-D**. Both **TS-E'** and **TS-E** adopt internal tether orientations as well as display similar levels of asynchronicity and bond development. For ethereal substrates **SM-E** and **SM-E'** (analogous to Table 4.2, entry 3), $\Delta\Delta G^\ddagger$ has decreased to 0.9 kcal mol⁻¹ and *syn*-diastereomeric pathway through **TS-E'** is now preferred. Similarly, **TS-F'** and **TS-F** (analogous to Table 4.2, entry 4) adopt internal tether orientations with a $\Delta\Delta G^\ddagger$ of 0.8 kcal mol⁻¹ and again the *syn*-diastereomeric pathway through **TS-F'** is preferred. All transition states for the ethereal substrates possess a tether in an internal orientation and there is only a slight energetic preference for the *syn*-diastereomers. Nevertheless, the model accurately predicts the major *syn* products (**4.20**) from the cycloadditions of substrates such as benzyl ether **4.18c** or *tert*-butyldiphenylsiloxy ether **4.18d**.

Cyclic Dienes and Product Distributions

Calculated energy diagrams and transition states for the cyclic diene *N*-acylnitroso type 2 IMDA reactions are shown in Figure 4.5. Similar to the acyclic diene with a 4-carbon tether (**TS-A**), **TS-G** is 3.5 kcal mol⁻¹ lower in energy than the **TS-G'**, favoring the 1,3-regioisomer. Both TSs display a high level of asynchronicity, internal tether orientation, and the free energy of **PDT-G'** is dramatically higher than **PDT-G** ($\Delta G = 9.6$ kcal mol⁻¹).

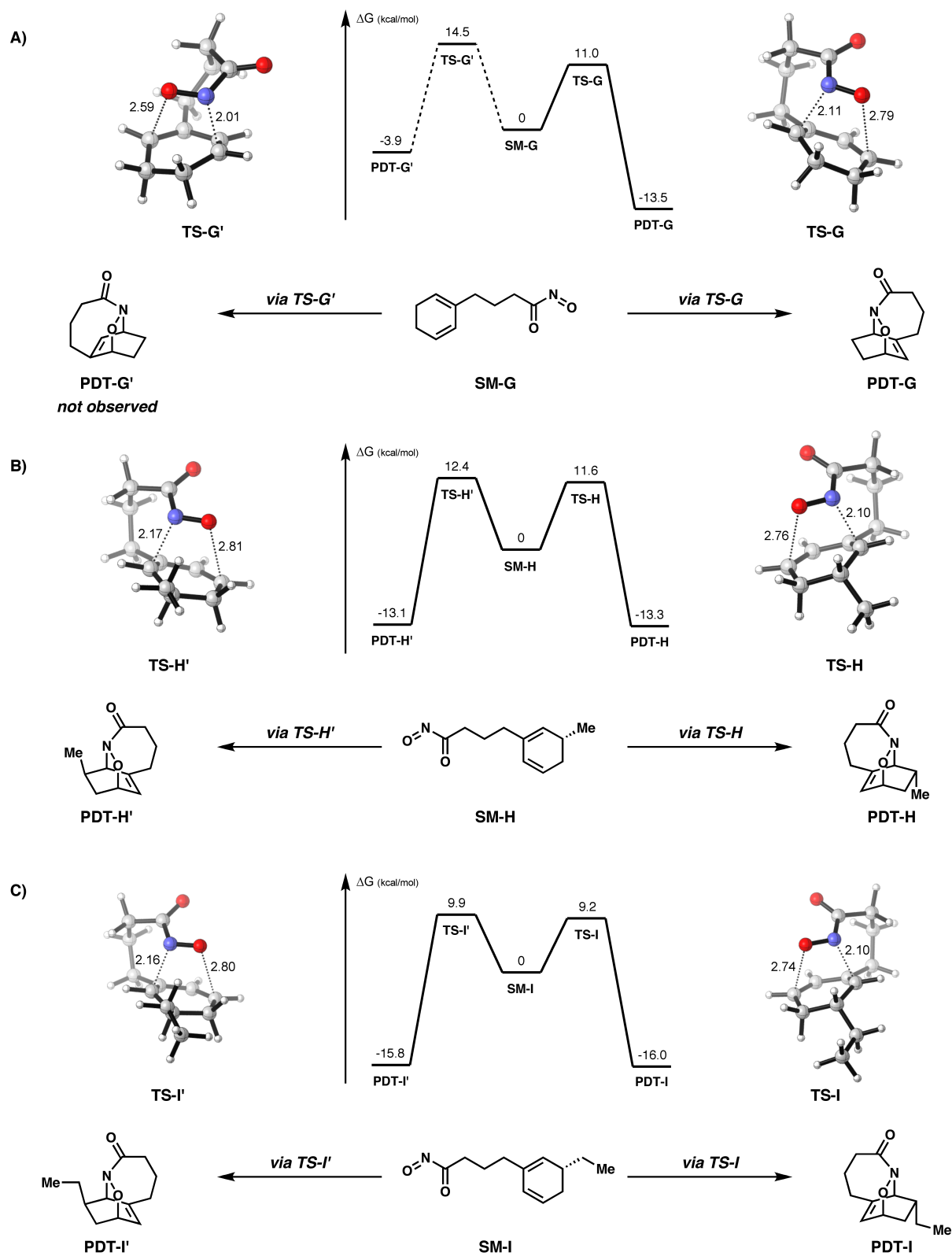


Figure 4.5. FE diagrams/TS structures for regioselectivity (1,3 vs. 1,4) of unsubstituted cyclic diene (A) and stereoselectivity (*cis* vs. *trans*) of substituted cyclic diene substrates (B-C).³¹

Substituted cyclic diene substrates **SM-H** and **SM-I** were examined for diastereoselectivity. Both data sets have very similar characteristics; the $\Delta\Delta G^\ddagger$ between *cis* and *trans* TSs is small (Me = 0.8 kcal mol⁻¹, Et = 0.7 kcal mol⁻¹) favoring the *trans* product. Formation of the C–N bond is slightly more advanced in **TS-H** than **TS-H'** (2.10 Å vs. 2.17 Å), though the inter-atom distances of the developing bonds in the Me and Et cases are similar to **TS-G**. The small magnitude of $\Delta\Delta G^\ddagger$ for **TS-I** and **TS-I'** accurately predicts the 6:1 ratio of diastereomers and thus the stereochemical outcome of the cycloaddition of **4.21b**.

Discussion

Tether Length Dictates Regiochemistry

The regiochemical outcome (1,3 vs. 1,4 product formation) is largely dictated by the nature of the tether, where the increased flexibility afforded by a longer tether lowers the energy of the TS leading to the 1,4 product. For even numbered tethers (i.e. 4- and 6-carbon cases), TSs leading to 1,3 products proceed through an internal tether orientation in order to reduce eclipsing interactions. In contrast, TSs leading to 1,3 products for odd numbered tethers (5-carbon case) adopt an external conformation. While this conformation reduces eclipsing interactions in the tether, it also raises the energy of the TS by introducing an A^{1,3} interaction between the tether and the diene. The calculations comparing cycloadduct precursors with tether lengths of 4 and 5 carbons to a substrate with 6 carbons unequivocally confirm that the strain imparted by the tether causes the reaction to prefer the 1,3 regioisomeric product in the 4 and 5 carbon cases.

Cycloadduct Olefin Strain: Comparison of Calculated and X-ray Geometries

To confirm the accuracy of this computational method, the calculated geometry of the products in the unsubstituted acyclic cases were compared to the X-ray crystallographic data. In

particular, the torsional angles (τ) and pyrimidalization angles (χ) about the bridgehead olefin and the bridgehead amide were calculated as previously described by Winkler and Dunitz (Figure 4.6).³² An unstrained sp^2 alkene, such as ethene, is expected to have each substituent 90° to the π system and thus τ , χ_{C1} , and χ_{C2} all equal to zero. So-called “twist amides”³³ represent extremely strained systems, such as 1-aza-2-adamantanone^{34,35} or 2-quinuclidone,³⁶ where the π orbitals are virtually perpendicular to each other ($\tau \approx 90^\circ$). An accurate computational method would describe the molecules so that the difference in the angles between the computational and X-ray data (Δ) would be zero.

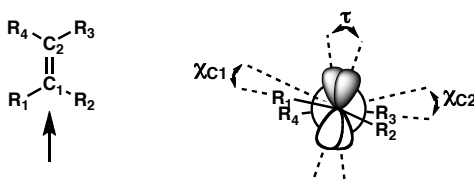
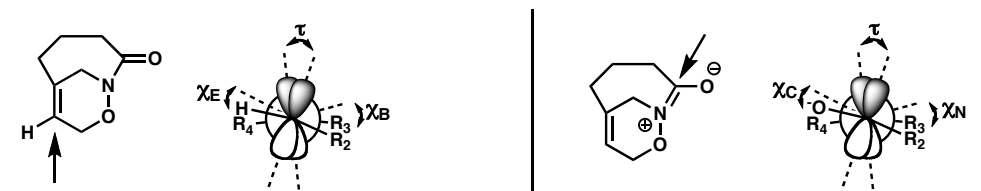


Figure 4.6. A visual description of Dunitz’s model of olefin strain, where τ describes the torsional strain between the π orbitals and χ_C is a measure of the pyrimidalization of the sp^2 center.

The computed angles describing the olefin and amide for each of the 1,3 cycloadducts, as well as the deviation from experimental angles are shown in Table 4.4. In all cases, the difference between the computational and experimental angles is small ($\Delta \leq 4.4^\circ$), supporting the validity of the computational method. This data also shows that as tether length is increased the olefin adopts a more sp^2 -like geometry as indicated by the decrease in the torsional angle of the olefin. The computational angles for the 6-carbon tethered 1,4 regioisomeric product (**4.17c**) show a much greater torsional strain about both the olefin and the amide than the 1,3 products (**4.16a-c**). These angles represent the physical limit of allowed strain in these systems as synthesized by the type 2 IMDA because the 1,4 products for the 4- and 5-carbon tethers are not observed experimentally.

Table 4.4. Computational angles and deviation from experimental angles (Δ) of acyclic diene cycloadducts.



		Computational angle		Δ	Computational angle		Δ
4.16a	χ_B	23.4°		3.1°	χ_N	54.5°	-0.3°
	χ_E	11.3°		2.3°	χ_C	0.4°	0.0°
	τ_{olefin}	6.95°		0.1°	τ_{amide}	3.20°	-0.3°
4.16b	χ_B	14.1°		0.6°	χ_N	53.2°	0.6°
	χ_E	8.4°		4.4°	χ_C	1.1°	-0.4°
	τ_{olefin}	3.7°		0.1°	τ_{amide}	10.70°	0.4°
4.16c	χ_B	9.3°		-1.9°	χ_N	47.5°	-1.5°
	χ_E	4.8°		-1.6°	χ_C	2.8°	-1.3°
	τ_{olefin}	2.25°		-0.9°	τ_{amide}	15.35°	-1.1°
4.17c	τ_{olefin}	11.3°		N/A	τ_{amide}	19.7°	N/A

Transannular Interactions Drive Syn/anti Diastereoselectivity

Our model indicates the diastereoselectivity of tether-substituted substrates is controlled through steric interactions in the transition state. Substrates with alkyl substitution α to the acyl-nitroso group preferentially form the *anti* cycloadducts, whereas ether substitution favors *syn* products. The rest of the tether is not an innocent bystander and must be in the internal conformation to avoid steric interactions with the diene. Further tether substitution and substituents such as alkenes and alkynes will likely cause an impact on the diastereoselectivity, and will be the topic of future studies.

A comparison of α -substituted TSs leading to *syn* products is shown in Figure 4.7. The α -Me substrate prefers to adopt an external orientation of the tether (**TS-D'**) in order to avoid a steric interaction (2.12 Å) between the terminal diene hydrogen and the methyl hydrogen present in the internal tether orientation (**TS-D''**). This close contact interaction is analogous to a *syn*

pentane interaction, and is more energetically disfavored than the allylic-type close contact interaction (2.08 Å) present in **TS-D'** which is 1.0 kcal mol⁻¹ lower in energy than **TS-D''**. Interestingly, the externally oriented **TS-A''** also was identified in the unsubstituted 4-carbon tether and was 2.2 kcal mol⁻¹ higher in energy than the internally oriented **TS-A**. In contrast, the ether **TS-E'** and silyl ether **TS-F'** are able to accommodate an internal orientation due to the reduced steric demand of ether substitution as opposed to alkyl substituted **TS-D''**.

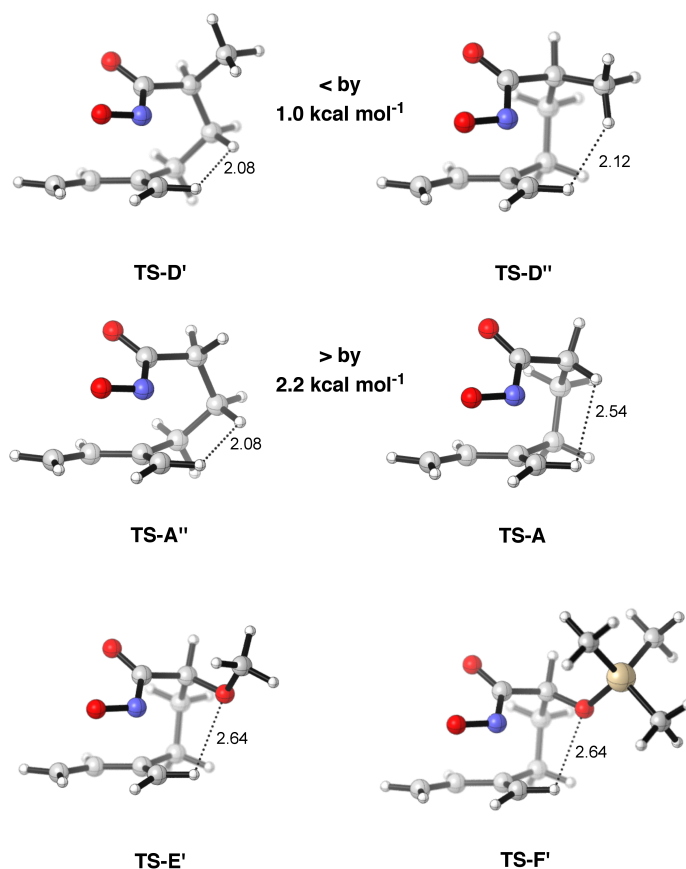
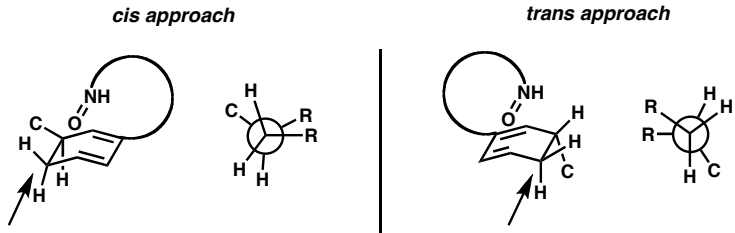


Figure 4.7. Comparison of external (left) and internal (right) transition structures for α -methyl substituted tether (TS-Ds), the analogous unsubstituted transition structures (TS-As), and the internal α -ethereal substituted tethers (TS-E and TS-F). Interatomic distances relevant to close contact interactions are given in Å and depicted as dotted lines.

Diene Substitution Has Modest Effects on Cis/trans Diastereoselectivity

While there is a clear preference for the formation of 1,3-regioisomeric products in the case of cyclic dienes (Figure 4.5 A), substituted dienes show only a modest preference for *trans* products (Figure 4.5 B and C). The less than expected magnitude of $\Delta\Delta G^\ddagger$ as well as the calculated and experimental diastereoselectivities resulting from diene substitution may be rationalized by examining various physical parameters influencing the transition states. The concerted, highly asynchronous, nature of the transition states result in C–N bond formation preceding C–O bond formation. Conformational restrictions of the cyclic diene also limit the torsional freedom of substituents on the diene. As a result, *trans* approach TSs (Table 4.5, entries 1 and 3), while sterically less demanding, are required to adopt a more eclipsed conformation than *cis* approach TSs (entries 2 and 4). This eclipsed conformation flattens the diene and effectively raises the free energy of the *trans* approach pathway.

Table 4.5. Comparison of dihedral angles from *cis* and *trans* approaches in substituted cyclic diene substrates.



entry	structure/approach	R-R	C-H	dihedrals H-H	average
1	TS-H/ <i>trans</i>	2.6°	5.5°	8.0°	5.4°
2	TS-H'/ <i>cis</i>	14.1°	21.9°	23.1°	19.7°
3	TS-I/ <i>trans</i>	6.0°	10.1°	12.2°	9.4°
4	TS-I'/ <i>cis</i>	13.5°	21.5°	22.5°	19.2°

Experimental studies have shown that the regio- and stereochemical outcomes of *N*-acylnitroso type 2 IMDA reactions are attributable to tether length and substituent effect,

respectively. This study has identified a computational method that accurately describes the observed product distributions (Table 4.6). Tether length studies show the appropriate regiochemical crossover (at tether length = 6-carbon) and the computational products are in good agreement with the X-ray crystallographic data. Studies of substrates with α -substitution also agree with the experimental results that carbon-linked substituents lead to *anti*-products, while oxygen-linked substituents afford *syn*-products. Perhaps more importantly, these studies revealed that tether-diene steric interactions, not dipole minimization, give rise to the observed stereoselectivity. Studies of cyclic diene systems have also recapitulated experimental results with regard to regio- and stereoselectivity. These studies suggest the modest stereoselectivity is a result of the required eclipse conformation that the less hindered *trans* product must adopt in the transition state.

Table 4.6. Summary of computed substrate selectivities in terms of $\Delta\Delta G^\ddagger$ (in kcal mol⁻¹) and product distributions (experimental values in parentheses).

entry	substrate	selectivity	$\Delta\Delta G^\ddagger$ DFT (expt.)	distr. DFT (expt.)
1	4.15a	1,3:1,4	4.8 (>1.6)	>99:1 (>95:5)
2	4.15b	1,3:1,4	1.9 (>1.6)	>97:3 (>95:5)
3	4.15c	1,3:1,4	-1.0 (0)	20:80 (50:50)
4	4.21a	1,3:1,4	3.5 (>1.6)	>99:1 (>95:5)
5	4.18a	<i>anti:syn</i>	2.7 (>1.6)	>99:1 (>95:5)
6	4.18b	<i>anti:syn</i>	2.7 (>1.6)	>99:1 (>95:5)
7	4.18c	<i>anti:syn</i>	-0.9 (<-1.6)	19:81 (<5:95)
8	4.18d	<i>anti:syn</i>	-0.8 (-0.9)	22:78 (16:84)
9	4.21b (SM-H)	<i>trans:cis</i>	0.8 (0.97)	78:22 (86:14)
10	4.21b (SM-I)	<i>trans:cis</i>	0.9 (0.97)	73:25 (86:14)

Conclusion

These computational studies have demonstrated that the type 2 IMDA reaction can be effectively modeled using density functional theory. As a result, current efforts to model other classes of type 2 IMDA reactions and additional tether substitution patterns are underway. We believe this computational study will provide a simple method to predict complex *N*-acylnitroso, and other type 2 IMDA reactions, which will lead to a broader applicability of these synthetically useful reactions.

Calculated geometries and energies:

The B3LYP/6-31+G(d) optimized geometry of each species is given below, as well as the following energies at that geometry:

1. B3LYP electronic energy (E)
2. B3LYP zero-point energy (ZPE)
3. B3LYP free energy at 273 K (G)

All energies are reported in Hartree.

SM-A

C	-3.667451	-0.884879	-0.631708	H	-0.692650	2.335259	0.865745
C	-1.913662	0.705980	0.230506	C	-1.158495	-0.351562	1.012823
C	-3.083812	0.323944	-0.576268	H	-1.869634	-0.982082	1.562132
C	-1.530891	1.998745	0.260755	H	-0.533676	0.134070	1.769428
H	-4.545779	-1.051485	-1.248820	C	-0.272798	-1.277238	0.143102
H	-3.516353	1.131440	-1.167952	H	0.145401	-2.061363	0.784889

H	-0.889363	-1.775630	-0.612613	N	3.083314	0.698588	-0.358650
C	0.871577	-0.561380	-0.584565	O	3.674450	0.051559	-1.195501
H	0.507678	0.317459	-1.137003	O	2.130340	-0.279541	1.496745
H	1.330525	-1.211383	-1.344002	H	-2.058967	2.762854	-0.305658
C	1.990580	-0.107792	0.311991	H	-3.308990	-1.740308	-0.065358

0 imaginary frequencies

E = -516.557866

ZPE = 0.177230

G = -516.416532

TS-A

H	-0.083239	-0.837481	2.353041	H	-1.596839	-2.108944	1.042123
C	0.607249	-0.792415	1.516520	H	-1.216599	-2.624859	-0.599402
C	1.139528	-1.314295	-0.849771	C	-2.114913	-0.654472	-0.472490
C	2.399811	-0.819828	-0.867174	H	-3.159313	-0.976637	-0.381749
C	0.240897	-1.311826	0.286101	H	-1.923867	-0.493102	-1.540697
H	2.963186	-0.781858	-1.794726	C	-1.919885	0.686570	0.270069
H	1.642293	-0.618797	1.784763	C	-0.604556	1.316317	-0.133184
H	0.718738	-1.677694	-1.787213	O	-0.441458	1.973497	-1.131201
H	2.913361	-0.468910	0.020749	O	1.614268	1.538183	0.424142
N	0.528503	1.214335	0.889545	H	-1.963301	0.539889	1.355323
C	-1.191833	-1.764860	0.082507	H	-2.714214	1.383468	-0.018016

1 imaginary frequency

E = -516.547151

ZPE = 0.179185

G = -516.399305

TS-A'

H -2.604763 -0.665734 1.464590

C -1.980940 -1.064920 0.669826

C -0.533082 -0.721825 -1.274753

C 0.262161 -1.850061 -1.109633

C -1.513629 -0.265245 -0.324186

H 1.047625 -2.056927 -1.829526

H -1.817313 -2.136802 0.683983

H -0.242649 -0.026429 -2.059567

H -0.044264 -2.694455 -0.502506

C -1.768117 1.233078 -0.293670

H -2.431948 1.458202 0.549139

H -2.297909 1.552702 -1.202161

C -0.466744 2.071013 -0.163846

H -0.740014 3.072492 0.188828

H -0.002172 2.213552 -1.147328

C 0.601698 1.492614 0.805152

C 1.437777 0.420767 0.125891

O 2.356752 0.642305 -0.625601

H 0.134265 1.096413 1.710119

H 1.294511 2.292076 1.087437

O 0.530162 -1.215690 1.510191

N 1.196367 -1.058648 0.481654

1 imaginary frequency

E = -516.540434

ZPE = 0.179503

G = -516.391689

TS-A''

H -0.334022 -1.061760 2.154515

C 0.462431 -0.924306 1.432987

C	1.386117	-1.157227	-0.852762	H	-1.103984	-1.619436	-1.483989
C	2.621326	-0.668776	-0.603213	C	-2.192355	-0.803484	0.208695
C	0.302183	-1.273643	0.107318	H	-2.222601	-0.932148	1.295380
H	3.332784	-0.534716	-1.412448	H	-3.165371	-1.149515	-0.159768
H	1.441125	-0.746957	1.862393	C	-2.036923	0.693554	-0.145952
H	1.134071	-1.408565	-1.882248	C	-0.620648	1.228081	-0.289915
H	2.967176	-0.398750	0.388710	O	-0.242354	1.873845	-1.233881
N	0.283136	1.149430	0.972948	O	1.395396	1.606125	0.763998
C	-1.075908	-1.680303	-0.388619	H	-2.544553	1.305503	0.612644
H	-1.270963	-2.732025	-0.132600	H	-2.517289	0.909220	-1.105394

1 imaginary frequency

E = -516.542670

ZPE = 0.178717

G = -516.395828

PDT-A

H	-0.528587	-0.498914	2.083677	H	0.617185	-1.698364	-1.856649
C	0.288196	-0.612887	1.369493	H	2.864919	-1.271663	-0.063162
C	0.835611	-1.364443	-0.843774	N	0.719563	0.706602	0.860899
C	2.129676	-0.649538	-0.589047	C	-1.579258	-1.556995	-0.099138
C	-0.101456	-1.373136	0.121341	H	-2.054542	-1.946988	0.811243
H	2.575944	-0.295141	-1.522181	H	-1.783753	-2.271914	-0.904940
H	1.141628	-1.037441	1.905610	C	-2.206835	-0.179505	-0.478981

H	-3.296922	-0.235803	-0.365808	O	0.120806	2.103409	-0.876168
H	-2.006078	0.006039	-1.541098	O	1.988218	0.561587	0.274761
C	-1.697489	1.060237	0.311927	H	-1.895392	0.952413	1.384426
C	-0.217549	1.358500	0.023208	H	-2.248907	1.938189	-0.036327

0 imaginary frequencies

E = -516.597837

ZPE = 0.185129

G = -516.442388

PDT-A'

H	0.686767	-1.890989	-1.573800	H	2.424273	-0.923072	1.494469
C	-0.065338	-1.718472	-0.799203	C	2.002672	0.700154	0.101786
C	-0.373497	-0.823124	1.414684	H	2.986383	0.927819	-0.327082
C	-1.736351	-0.429975	0.865691	H	1.906917	1.302566	1.012745
C	0.520498	-1.261874	0.505544	C	0.919194	1.220125	-0.902091
H	-2.245323	0.282697	1.515562	C	-0.459764	1.309002	-0.240581
H	-0.655066	-2.633546	-0.672440	O	-0.756866	2.237781	0.490808
H	-0.051876	-0.393658	2.361854	H	0.898069	0.625014	-1.817355
H	-2.424100	-1.248572	0.630765	H	1.191827	2.246187	-1.167516
C	1.962508	-0.814861	0.506036	O	-0.990370	-0.706318	-1.364214
H	2.557284	-1.412326	-0.195178	N	-1.416686	0.254333	-0.426568

0 imaginary frequencies

E = -516.583336

ZPE = 0.184809

G = -516.428194

SM-B

C	2.797910	0.409408	-0.033016	C	-2.791976	0.564497	-0.163064
C	1.644753	-0.397400	0.497432	C	-3.434682	-0.524488	-0.915785
H	1.929357	-0.744799	1.503879	H	-3.792421	-0.246118	-1.907625
H	1.577462	-1.309793	-0.112872	C	-3.634497	-1.787055	-0.501871
C	0.318437	0.367888	0.525562	H	-4.139571	-2.508411	-1.138017
H	0.447763	1.294773	1.099912	H	-3.317540	-2.145773	0.473804
H	0.058285	0.674581	-0.493658	C	-2.769071	1.803750	-0.692600
C	-0.815989	-0.467405	1.133532	H	-3.201669	2.014437	-1.668260
H	-0.543071	-0.756164	2.158864	H	-2.322638	2.644072	-0.167283
H	-0.929442	-1.400304	0.566574	N	4.139520	-0.298109	-0.086204
C	-2.171036	0.276781	1.190767	O	4.102813	-1.284444	-0.788908
H	-2.869962	-0.316789	1.794688	O	2.808838	1.557881	-0.395982
H	-2.029498	1.223698	1.726805				

0 imaginary frequencies

E = -555.872656

ZPE = 0.205506

G = -555.705457

TS-B

C	-1.561642	1.304343	-0.710555	C	0.886037	1.798493	-0.361416
H	-1.350326	1.615807	-1.732545	H	0.885097	2.885603	-0.182048
C	-0.432009	1.267058	0.185041	H	0.882789	1.684491	-1.453746
C	-0.554806	0.730361	1.458668	C	2.207284	1.227349	0.184245
H	-1.519860	0.643007	1.942743	H	2.234892	1.292289	1.280935
H	0.294048	0.696401	2.132283	H	3.008686	1.889837	-0.168218
C	-2.810795	0.852157	-0.434189	C	2.555961	-0.203119	-0.261450
H	-3.142378	0.577530	0.559761	H	3.593143	-0.408643	0.032031
H	-3.560523	0.802965	-1.218301	H	2.523056	-0.269243	-1.357073
N	-0.802937	-1.248126	0.820084	C	1.675718	-1.320730	0.333022
O	-1.941747	-1.440013	0.391272	H	1.622842	-1.235166	1.423740
C	0.276175	-1.376779	-0.246657	H	2.136111	-2.290361	0.102879
O	0.011927	-1.662792	-1.389183				

1 imaginary frequency

E = -555.859081

ZPE = 0.208082

G = -555.683277

TS-B'

C	0.326381	-1.161703	-1.175992	C	-0.582892	-2.131398	0.887517
H	0.086932	-0.553785	-2.046300	H	0.346532	-2.627824	1.140814
C	-0.762059	-1.441999	-0.269451	H	-1.398033	-2.253270	1.596627

C	1.658902	-1.447014	-0.961995	H	-1.214712	1.819788	-1.173897
H	1.990198	-2.181749	-0.236823	H	-1.995601	2.639497	0.158393
H	2.399712	-1.136420	-1.690611	C	-0.121063	1.757033	0.721267
C	-2.100637	-0.790306	-0.584504	H	0.116893	2.797934	0.971812
H	-2.909513	-1.488731	-0.336062	H	-0.237212	1.205978	1.657039
H	-2.170159	-0.611203	-1.665883	C	1.086425	1.243664	-0.033478
C	-2.385177	0.536085	0.158321	O	1.590929	1.789342	-0.985553
H	-2.422596	0.340959	1.239127	N	1.838593	0.022602	0.531176
H	-3.399829	0.845120	-0.128983	O	1.392469	-0.379783	1.606045
C	-1.441538	1.730474	-0.102922				

1 imaginary frequency

E = -555.855612

ZPE = 0.207854

G = -555.680246

PDT-B

C	0.742417	-1.497375	-0.857514	H	2.891320	-1.683192	-0.558871
H	0.510272	-1.898300	-1.843693	H	2.372096	-0.314652	-1.572761
C	-0.210024	-1.389995	0.081623	N	1.039116	0.466446	0.935314
C	0.178579	-0.651367	1.349415	O	2.263176	-0.083339	0.499720
H	0.762371	-1.257709	2.048011	C	0.482810	1.408893	0.054852
H	-0.684325	-0.268649	1.895524	O	1.137644	1.935740	-0.829666
C	2.119450	-0.915466	-0.689695	C	-1.670120	-1.658799	-0.161139

H	-2.052225	-2.435732	0.518012	H	-2.881520	1.596378	-0.704481
H	-1.797541	-2.043277	-1.180976	H	-1.598619	0.774129	-1.568796
C	-2.543510	-0.384429	0.029074	C	-0.988813	1.767675	0.275969
H	-2.753041	-0.233158	1.097152	H	-1.262164	1.739892	1.337451
H	-3.518740	-0.595239	-0.428630	H	-1.058304	2.810767	-0.046436
C	-2.012447	0.941599	-0.565774				

0 imaginary frequencies

E = -555.921100

ZPE = 0.214605

G = -555.737298

PDT-B'

C	0.553319	-1.153215	-1.272158	H	-2.025649	-0.930304	-1.790377
H	0.372884	-0.912514	-2.317620	C	-2.399218	0.162090	0.061864
C	-0.456177	-1.377751	-0.412872	H	-2.467010	-0.072744	1.133171
C	-0.050085	-1.625885	1.014118	H	-3.432616	0.343554	-0.263210
H	0.427423	-2.608018	1.120338	C	-1.610353	1.483006	-0.111201
H	-0.885380	-1.572584	1.717263	H	-1.351686	1.640810	-1.166318
C	1.906636	-0.841220	-0.660214	H	-2.302347	2.292742	0.150516
H	2.448339	-1.700742	-0.250757	C	-0.331904	1.711669	0.763474
H	2.559880	-0.310172	-1.352087	H	-0.216058	2.791717	0.901954
C	-1.902017	-1.092862	-0.712129	H	-0.445543	1.253575	1.748304
H	-2.551660	-1.936975	-0.437933	C	0.941559	1.259340	0.063542

O 1.416675 1.896892 -0.865247

O 0.931824 -0.636022 1.500594

N 1.595839 0.069094 0.473919

0 imaginary frequencies

E = -555.911860

ZPE = 0.213881

G = -555.729018

SM-C

C 3.572143 2.130656 -0.014234

H -0.348492 -1.525104 -0.576152

C 3.687314 -0.366995 -0.321164

H -0.458571 0.232965 -0.647136

C 4.219032 0.954769 0.045731

H 5.539788 -1.355656 0.038193

C 4.502015 -1.439865 -0.276835

H 2.541265 2.220410 -0.346242

H 4.068414 3.054866 0.268125

C -1.189713 -0.624319 1.202338

H 5.255151 0.953439 0.386078

H -0.949655 -1.470781 1.859076

H 4.157683 -2.432347 -0.557097

H -1.059054 0.286014 1.801047

C 2.234355 -0.507114 -0.732167

C -2.662102 -0.748408 0.788698

H 2.109749 -1.447481 -1.283707

H -3.297674 -0.986730 1.656619

H 1.963885 0.297563 -1.429717

H -2.820585 -1.571565 0.078044

C 1.251423 -0.495829 0.458054

C -3.239470 0.500930 0.179006

H 1.500818 -1.329924 1.129081

N -4.656345 0.392518 -0.358907

H 1.387643 0.422318 1.043574

O -4.749341 -0.456196 -1.218096

C -0.213826 -0.607131 0.016275

O -2.746031 1.596724 0.095390

0 imaginary frequencies

E = -595.187654

ZPE = 0.234264

G = -594.993189

TS-C

C	-1.580431	1.426606	-0.572311	H	0.750104	1.124750	1.948382
H	-1.137753	2.287082	-1.070886	H	-0.006857	2.663007	1.591547
C	-0.965955	1.017060	0.670653	C	1.354282	-1.540940	-0.881533
C	-1.534452	0.012470	1.443315	H	2.335682	-1.981982	-0.679916
H	-2.576004	-0.262070	1.321157	C	1.401456	2.047291	0.095746
H	-1.085913	-0.264774	2.390706	H	2.091092	2.743991	0.591337
C	-2.592333	0.789001	-1.210341	H	0.971021	2.611627	-0.742883
H	-3.100116	-0.078497	-0.806809	C	1.519666	-0.097441	-1.421836
H	-2.942737	1.147722	-2.174421	H	2.083979	-0.178912	-2.358595
N	-0.922458	-1.611581	0.370277	H	0.532874	0.287140	-1.698887
O	-1.405987	-1.720195	-0.767524	C	2.243405	0.878822	-0.456491
C	0.588599	-1.549683	0.417467	H	3.097477	1.322775	-0.983948
O	1.093166	-1.589125	1.518765	H	2.672342	0.322677	0.387254
C	0.306118	1.709582	1.134018	H	0.832467	-2.145523	-1.628020

1 imaginary frequency

E = -595.168046

ZPE = 0.236809

G = -594.964895

TS-C'

C	-0.801498	1.089990	-1.166922	C	0.440463	-1.614851	0.942006
H	-0.213476	0.711073	-1.999595	H	0.354745	-0.750979	1.606201
C	-0.080558	1.805219	-0.137932	H	0.258374	-2.496296	1.574441
C	-0.688348	2.217558	1.007084	C	-0.683117	-1.563975	-0.069095
H	-1.756670	2.143051	1.170036	O	-0.750976	-2.207037	-1.089404
H	-0.115266	2.687697	1.802776	N	-1.922303	-0.743804	0.314123
C	-2.135930	0.736305	-1.138365	O	-1.853261	-0.251251	1.442941
H	-2.852789	1.225970	-0.488456	H	3.346892	1.218000	0.220064
H	-2.558272	0.173455	-1.963437	C	2.245186	-0.495601	-0.543730
C	1.420914	1.994119	-0.321283	H	3.228608	-0.709600	-0.981247
H	1.716423	2.924123	0.179245	H	1.564113	-0.412485	-1.398156
H	1.642058	2.135754	-1.388235	C	1.833143	-1.718793	0.297339
C	2.312551	0.851114	0.228044	H	2.564040	-1.866227	1.104190
H	2.061705	0.697374	1.285896	H	1.872700	-2.614492	-0.333757

1 imaginary frequency

E = -595.169969

ZPE = 0.236927

G = -594.966490

PDT-C

C	1.048267	-1.524758	-0.859864	H	-1.335589	-2.856917	0.962977
H	0.808301	-2.038210	-1.790759	H	-1.278022	-2.748468	-0.797112
C	0.199838	-1.553679	0.178091	C	-0.905629	1.812828	0.678537
C	0.559560	-0.690817	1.375353	H	-1.107274	1.344022	1.644584
H	1.271577	-1.178912	2.048939	C	-2.296539	-1.077089	0.168932
H	-0.314795	-0.426535	1.968859	H	-2.346923	-0.651658	1.179896
C	2.285166	-0.669339	-0.881742	H	-3.255735	-1.590090	0.027400
H	3.205729	-1.264315	-0.908236	C	-2.032953	1.497814	-0.337296
H	2.268988	-0.016538	-1.764868	H	-2.981772	1.775581	0.142721
N	1.214301	0.527483	0.879607	H	-1.908718	2.170357	-1.194247
O	2.445508	0.148010	0.307621	C	-2.136966	0.055630	-0.881292
C	0.496859	1.491411	0.162166	H	-1.256992	-0.143843	-1.504510
O	0.979364	2.091869	-0.786236	H	-2.993455	0.036210	-1.567222
C	-1.178347	-2.161526	0.125109	H	-0.909938	2.895052	0.855281

0 imaginary frequencies

E = -595.237164

ZPE = 0.243532

G = -595.025634

PDT-C'

C	0.848191	-1.258576	-1.215370	C	0.040324	-1.620492	-0.206114
H	0.525725	-1.339562	-2.251516	C	0.555780	-1.485251	1.203479

H	1.095553	-2.392418	1.503919	H	-0.109906	2.657555	1.440213
H	-0.257186	-1.329195	1.921496	C	0.822624	1.420146	-0.015107
C	2.100577	-0.465387	-0.893690	O	0.945173	2.075402	-1.042236
H	2.967001	-1.069489	-0.602544	N	1.750632	0.395075	0.251790
H	2.388608	0.180730	-1.723696	O	1.516255	-0.392285	1.395631
C	-1.418534	-1.961912	-0.371055	H	-3.370262	-1.119850	-0.027654
H	-1.684987	-2.866041	0.195385	C	-2.107722	0.560887	-0.617824
H	-1.625352	-2.174290	-1.427572	H	-3.042441	0.853769	-1.112897
C	-2.331590	-0.793412	0.108298	H	-1.376424	0.436580	-1.425683
H	-2.208858	-0.664655	1.192014	C	-1.676966	1.763150	0.253890
C	-0.304940	1.683590	0.972671	H	-2.438289	1.941884	1.026156
H	-0.309072	0.948216	1.777315	H	-1.666424	2.649845	-0.389701

0 imaginary frequencies

E = -595.231755

ZPE = 0.242971

G = -595.020834

SM-D

C	-3.361291	-1.454475	-0.771519	H	-4.264902	0.701571	0.366978
H	-4.433598	-1.449644	-0.589294	C	-2.568740	1.921333	0.522098
H	-2.952666	-2.342982	-1.246711	H	-3.123445	2.745852	0.961521
C	-2.582663	-0.408351	-0.431388	H	-1.503946	2.081147	0.374674
C	-3.192306	0.779497	0.186230	C	-1.084919	-0.443617	-0.670012

H -0.861246 -1.218890 -1.413600
H -0.757271 0.510450 -1.100556
C -0.277430 -0.736184 0.612675
H -0.586310 -1.711796 1.009308
H -0.511420 0.004993 1.384917
C 1.242927 -0.776489 0.391211
H 1.481414 -1.429263 -0.460528
C 1.998846 -1.317557 1.632061

H 1.662002 -2.337313 1.845391
H 1.795118 -0.697431 2.512216
H 3.083017 -1.347156 1.476370
C 1.806157 0.585995 0.061333
N 3.203838 0.629074 -0.545903
O 3.267431 -0.022217 -1.564928
O 1.315431 1.670471 0.252991

0 imaginary frequencies

E = -555.872743

ZPE = 0.205636

G = -555.704069

TS-D

H -0.578862 0.874716 2.354865
C -1.195729 0.572728 1.514253
C -1.853182 0.837810 -0.863086
C -2.850932 -0.076995 -0.879431
C -1.027818 1.174448 0.278618
H -3.350604 -0.330136 -1.809712
H -2.097523 0.033104 1.776656
H -1.578005 1.313186 -1.804418
H -3.216495 -0.574245 0.011926

N -0.380516 -1.271758 0.901872
C 0.145967 2.114035 0.078523
H 0.385745 2.592122 1.036185
H -0.136245 2.917192 -0.614675
C 1.417565 1.412278 -0.453708
H 2.269330 2.097300 -0.355675
H 1.315279 1.186639 -1.523108
C 1.732384 0.095075 0.298049
C 0.709190 -0.946809 -0.126406

O	0.778348	-1.603807	-1.135236	H	3.891406	0.349015	0.318844
O	-1.270334	-1.973186	0.437137	H	3.287821	-0.576201	-1.075706
H	1.626440	0.265535	1.377090	H	3.372504	-1.335975	0.520310
C	3.157339	-0.398237	-0.003626				

1 imaginary frequency

E = -555.862128

ZPE = 0.207103

G = -555.687847

TS-D'

H	-0.157925	1.083431	2.163232	C	1.501049	1.524150	0.061546
C	-0.922515	0.712952	1.490756	H	1.593424	1.561818	1.153182
C	-2.072990	0.724984	-0.702980	H	2.269623	2.205442	-0.325060
C	-3.047927	-0.162954	-0.406822	C	1.824305	0.100629	-0.444216
C	-1.007574	1.154844	0.186100	H	2.112252	0.171218	-1.500291
H	-3.744820	-0.489288	-1.172880	C	0.652239	-0.877285	-0.471106
H	-1.741708	0.193038	1.972623	O	0.419851	-1.600118	-1.406884
H	-2.013488	1.096845	-1.725166	C	3.003700	-0.522504	0.333792
H	-3.191281	-0.583481	0.582739	H	3.877033	0.138168	0.276957
N	-0.093690	-1.145236	0.871477	H	3.285718	-1.493824	-0.086264
C	0.109594	2.024508	-0.366867	H	2.750598	-0.664264	1.390330
H	-0.020375	3.061639	-0.024520	O	-1.001137	-1.948839	0.728847
H	0.047770	2.051626	-1.462145				

1 imaginary frequency

E = -555.857171

ZPE = 0.206907

G = -555.683481

PDT-D

H	-0.110875	0.800606	2.089540	C	1.560089	1.260633	-0.460160
C	-0.872082	0.505041	1.366413	H	2.491276	1.830411	-0.344993
C	-1.685497	0.884900	-0.859913	H	1.485391	0.984711	-1.519726
C	-2.493093	-0.351268	-0.597402	C	1.706250	-0.066093	0.351023
C	-0.870879	1.342864	0.107813	C	0.517890	-1.004919	0.037894
H	-2.713078	-0.884432	-1.526243	O	0.556675	-1.814424	-0.868344
H	-1.833052	0.477296	1.887574	O	-1.802134	-1.343217	0.281535
H	-1.635937	1.267737	-1.877859	H	1.723524	0.165833	1.422787
H	-3.438013	-0.143541	-0.079627	C	3.025882	-0.763896	-0.007254
N	-0.619094	-0.866204	0.871856	H	3.874166	-0.113012	0.234337
C	0.354392	2.188327	-0.110902	H	3.061851	-1.008749	-1.072821
H	0.581450	2.770392	0.792674	H	3.140446	-1.698860	0.551477
H	0.212462	2.902629	-0.930714				

0 imaginary frequencies

E = -555.912166

ZPE = 0.213157

G = -555.730409

PDT-D'

H	0.525721	0.452535	1.950064	C	1.657735	0.946584	-0.908066
C	-0.413189	0.408374	1.402483	H	2.694479	1.299300	-0.996375
C	-1.566463	1.236402	-0.531715	H	1.255668	0.889752	-1.926711
C	-2.548023	0.143971	-0.217987	C	1.700281	-0.517396	-0.360239
C	-0.494087	1.397371	0.264298	H	2.180299	-1.096428	-1.156327
H	-3.031629	-0.219129	-1.129378	C	0.284887	-1.153859	-0.352633
H	-1.225164	0.492831	2.130110	O	-0.072580	-1.847674	-1.286942
H	-1.648319	1.743263	-1.491805	C	2.581287	-0.712108	0.890748
H	-3.325338	0.456213	0.490496	H	3.628815	-0.542445	0.614395
N	-0.572676	-0.904225	0.746607	H	2.501772	-1.735809	1.273162
C	0.816046	2.016897	-0.142773	H	2.357582	-0.028701	1.714358
H	1.359852	2.377212	0.740259	O	-1.933486	-1.056576	0.424938
H	0.672679	2.877566	-0.807160				

0 imaginary frequencies

E = -555.904629

ZPE = 0.213139

G = -555.723313

SM-E

C	3.348080	-1.759922	-0.650823	H	2.851940	-2.433803	-1.344986
H	4.311113	-2.083585	-0.262618	C	2.803327	-0.580471	-0.292895

C	3.527329	0.303332	0.633786	C	-1.031663	0.194052	-0.314754
H	4.468390	-0.098876	1.009956	H	-1.262726	-0.259093	-1.295040
C	3.150944	1.529032	1.035145	C	-2.143200	-0.227703	0.644657
H	3.770308	2.104965	1.716955	N	-2.468382	-1.706813	0.680512
H	2.229345	2.001680	0.705467	O	-2.854730	-2.099255	-0.400448
C	1.450149	-0.153426	-0.827288	O	-2.775569	0.466274	1.396026
H	1.476167	0.900167	-1.126230	O	-0.936265	1.591021	-0.420280
H	1.219360	-0.734971	-1.728645	C	-1.974115	2.213171	-1.174717
C	0.314491	-0.353761	0.197400	H	-1.724093	3.275110	-1.218827
H	0.549161	0.151208	1.140844	H	-2.951163	2.092605	-0.691646
H	0.213548	-1.423374	0.421397	H	-2.012206	1.805522	-2.195650

0 imaginary frequencies

E = -631.074770

ZPE = 0.209855

G = -630.903760

TS-E

H	-0.881361	0.713920	2.391523	H	-2.243290	-0.387760	1.857358
C	-1.488443	0.335656	1.574687	H	-2.231422	1.124393	-1.670673
C	-2.346771	0.565281	-0.742316	H	-3.357639	-1.116089	0.134194
C	-3.155457	-0.519849	-0.748546	N	-0.368443	-1.301621	0.803751
C	-1.522488	1.005513	0.365933	C	-0.563969	2.160939	0.143830
H	-3.663956	-0.822249	-1.659140	H	-0.345696	2.634226	1.108809

H	-1.042749	2.924307	-0.482567	O	-1.141164	-2.136338	0.350669
C	0.765219	1.739053	-0.516076	H	1.355329	0.597269	1.250352
H	1.491996	2.555972	-0.445808	O	2.726186	0.425584	-0.287270
H	0.626662	1.520701	-1.581705	C	3.495856	-0.608598	0.313817
C	1.386236	0.499130	0.152127	H	3.482042	-0.523347	1.411510
C	0.580962	-0.743849	-0.256067	H	4.519273	-0.476915	-0.044211
O	0.768117	-1.367899	-1.268344	H	3.137933	-1.603521	0.019320

1 imaginary frequency

E = -631.06359

ZPE = 0.211445

G = -630.886696

TS-E'

H	-0.127648	0.507793	-2.247161	C	0.136034	2.120488	-0.114955
C	0.772375	0.289170	-1.684453	H	-0.475285	2.452836	-0.958847
C	2.306063	0.814025	0.196446	H	0.693390	2.995148	0.245673
C	3.201271	-0.179381	-0.002355	C	-0.802399	1.642855	1.017175
C	1.107381	1.056269	-0.588332	H	-1.585700	2.392439	1.180366
H	4.023038	-0.327722	0.691931	H	-0.251927	1.534218	1.959169
H	1.481248	-0.379711	-2.157851	C	-1.472156	0.292938	0.709261
H	2.440974	1.458188	1.065433	C	-0.418239	-0.821624	0.807620
H	3.161580	-0.854076	-0.850600	O	-0.112747	-1.312968	1.865329
N	0.146941	-1.407003	-0.492842	O	1.114681	-2.125011	-0.275812

H -2.197858 0.074529 1.509058

O -2.137738 0.389353 -0.534300

C -3.040281 -0.678224 -0.802003

1 imaginary frequency

E = -631.065285

ZPE = 0.211443

G = -630.888118

H -3.546651 -0.430157 -1.737693

H -3.787053 -0.771567 0.000423

H -2.510565 -1.632982 -0.922164

PDT-E

H -0.420354 0.706254 2.094381

C -1.149878 0.276058 1.405889

C -2.210117 0.573006 -0.727172

C -2.673902 -0.836213 -0.508145

C -1.453989 1.159818 0.217751

H -2.833229 -1.352199 -1.458737

H -2.027923 -0.012319 1.990500

H -2.339079 1.015551 -1.713280

H -3.596216 -0.896906 0.083088

N -0.620439 -0.962726 0.796171

C -0.489477 2.291482 -0.012253

H -0.345038 2.863885 0.913966

H -0.859197 2.990056 -0.771605

0 imaginary frequencies

C 0.874688 1.714255 -0.498449

H 1.658664 2.472256 -0.390109

H 0.800183 1.476891 -1.565909

C 1.394443 0.430065 0.201075

C 0.452279 -0.778529 -0.107533

O 0.641565 -1.507683 -1.057700

O -1.696884 -1.679295 0.245751

H 1.471997 0.582052 1.290050

O 2.682611 0.211669 -0.323970

C 3.414397 -0.832931 0.305977

H 3.507295 -0.649997 1.388276

H 4.409066 -0.825391 -0.145405

H 2.947885 -1.810632 0.136101

E = -631.11459

ZPE = 0.217526

G = -630.930041

PDT-E'

H	-0.459041	0.327662	-1.821910	C	-0.951681	1.609082	0.931742
C	0.526555	0.116863	-1.410654	H	-1.836225	2.249113	1.036636
C	2.167400	0.894234	0.162016	H	-0.455629	1.573736	1.908964
C	2.767052	-0.462325	-0.060401	C	-1.456560	0.173994	0.649741
C	1.049168	1.216152	-0.513460	C	-0.275896	-0.850121	0.681128
H	3.349207	-0.789958	0.804820	O	-0.010346	-1.415781	1.725156
H	1.201943	-0.158430	-2.225546	O	1.750913	-1.537652	-0.281679
H	2.541115	1.503198	0.983440	H	-2.077775	-0.127449	1.505206
H	3.407208	-0.504491	-0.950620	O	-2.250924	0.179734	-0.526792
N	0.449570	-1.054438	-0.508369	C	-3.028875	-1.000730	-0.703173
C	0.035071	2.247131	-0.094745	H	-3.636425	-0.842728	-1.597191
H	-0.521238	2.612569	-0.966285	H	-3.688586	-1.166670	0.160942
H	0.510808	3.113593	0.380019	H	-2.392900	-1.885160	-0.846530

0 imaginary frequencies

E = -631.116967

ZPE = 0.217773

G = -630.932226

SM-F

C	-3.235049	-2.494935	0.864445	N	1.123007	2.526503	0.419203
H	-4.152958	-3.072231	0.778675	O	0.825119	2.984162	1.495519
H	-2.382389	-2.999694	1.311879	O	-0.928259	2.639298	-0.702024
C	-3.163179	-1.216168	0.444843	O	1.086251	-0.083011	0.238211
C	-4.356475	-0.574057	-0.127891	Si	2.548758	-0.889649	-0.077114
H	-5.227733	-1.223998	-0.216294	C	3.310781	-1.125697	1.621622
C	-4.472925	0.704886	-0.522895	H	3.499950	-0.160308	2.105706
H	-5.413230	1.078830	-0.918509	H	4.265594	-1.662762	1.555790
H	-3.657379	1.420818	-0.466048	H	2.645934	-1.702840	2.275421
C	-1.867442	-0.435290	0.553374	C	3.633737	0.171313	-1.197657
H	-2.073719	0.567142	0.950625	H	3.800430	1.164741	-0.764989
H	-1.206341	-0.928600	1.272415	H	3.198307	0.308614	-2.195809
C	-1.130414	-0.315952	-0.796741	H	4.613822	-0.303296	-1.338929
H	-1.765120	0.175173	-1.542178	C	2.182724	-2.543790	-0.910632
H	-0.903973	-1.319313	-1.176603	H	1.685146	-2.415357	-1.880595
C	0.192310	0.461236	-0.714864	H	1.537697	-3.172707	-0.284844
H	0.641760	0.479817	-1.722965	H	3.111741	-3.099539	-1.094465
C	-0.031749	1.920366	-0.339729				

0 imaginary frequencies

E = -1000.489969

ZPE = 0.283353

G = -1000.253087

TS-F

H	1.900300	-0.746798	2.364370	O	0.375699	1.227602	-1.397090
C	2.526748	-0.303194	1.596533	O	2.056449	2.146493	0.384798
C	3.558248	-0.421993	-0.657525	H	-0.249738	-0.797403	1.066216
C	4.266470	0.729751	-0.597943	O	-1.522839	-0.683639	-0.570953
C	2.702168	-0.948745	0.386165	Si	-2.903778	0.070593	0.051017
H	4.806088	1.089691	-1.468852	C	-4.233355	-0.321628	-1.216648
H	3.197279	0.474624	1.940975	H	-5.200373	0.109260	-0.927301
H	3.555523	-0.974526	-1.596899	H	-4.366119	-1.404718	-1.326466
H	4.356408	1.327270	0.302342	H	-3.964000	0.083152	-2.199466
N	1.330335	1.238347	0.768990	C	-3.315914	-0.687205	1.734652
C	1.865879	-2.179515	0.088881	H	-3.461195	-1.772179	1.659399
H	1.629785	-2.685428	1.033075	H	-4.242207	-0.255361	2.136355
H	2.451071	-2.887858	-0.511345	H	-2.528647	-0.504297	2.477680
C	0.548791	-1.867858	-0.651661	C	-2.649648	1.930329	0.236577
H	-0.108566	-2.744032	-0.624762	H	-1.894008	2.177943	0.993037
H	0.730716	-1.634745	-1.707866	H	-3.587096	2.410846	0.547835
C	-0.222620	-0.685443	-0.028744	H	-2.334230	2.385721	-0.709211
C	0.515748	0.616911	-0.370340				

1 imaginary frequency

E = -1000.478126

ZPE = 0.284825

G = -1000.235523

TS-F'

H	-0.607099	0.493576	2.125353	O	-1.144687	-1.178464	-2.009648
C	-1.566772	0.216257	1.705622	O	-1.918901	-2.170112	0.256786
C	-3.429312	0.673326	0.128670	H	0.818650	0.395758	-1.949495
C	-4.193221	-0.404532	0.415506	O	1.090444	0.592394	0.106629
C	-2.140171	0.991381	0.719801	Si	2.640433	-0.084748	0.218758
H	-5.106425	-0.596801	-0.139878	C	3.161746	0.260442	1.991077
H	-2.131674	-0.529386	2.252305	H	4.182592	-0.096049	2.179434
H	-3.761908	1.338915	-0.668109	H	2.496678	-0.242079	2.703769
H	-3.952535	-1.109998	1.203462	H	3.138002	1.335222	2.208528
N	-0.998186	-1.369040	0.352861	C	3.784369	0.779306	-1.011653
C	-1.350884	2.153630	0.149570	H	4.803433	0.376307	-0.942527
H	-0.628007	2.499079	0.893976	H	3.839230	1.857418	-0.816030
H	-2.026741	2.993246	-0.060746	H	3.454451	0.643633	-2.049680
C	-0.591238	1.802510	-1.149140	C	2.585074	-1.934770	-0.142754
H	0.082597	2.627494	-1.410408	H	3.581430	-2.378780	-0.015119
H	-1.288782	1.673077	-1.985811	H	2.266018	-2.149649	-1.170684
C	0.241256	0.511420	-1.020318	H	1.898076	-2.454709	0.535399
C	-0.709446	-0.691813	-0.995801				

1 imaginary frequency

E = -1000.480026

ZPE = 0.284874

G = -1000.236807

PDT-F

H	-1.524913	0.757271	2.051182	O	-0.346294	-1.325298	-1.151924
C	-2.223203	0.222100	1.404960	O	-2.557701	-1.801789	0.284552
C	-3.429937	0.346659	-0.666832	H	0.317218	0.880497	1.140302
C	-3.681648	-1.110455	-0.416832	O	1.478730	0.636799	-0.544569
C	-2.712593	1.042856	0.232974	Si	2.874178	-0.119746	0.038889
H	-3.820740	-1.654504	-1.354940	C	4.113673	0.092101	-1.357100
H	-3.019180	-0.179305	2.038501	H	5.090356	-0.332150	-1.091100
H	-3.672387	0.756240	-1.645805	H	4.260209	1.151950	-1.597938
H	-4.552819	-1.290476	0.225544	H	3.762374	-0.411693	-2.265487
N	-1.561087	-0.937410	0.770690	C	3.443807	0.782162	1.602664
C	-1.927372	2.293883	-0.051623	H	3.634283	1.844529	1.405070
H	-1.815753	2.890027	0.864234	H	4.373457	0.343107	1.988342
H	-2.429376	2.927173	-0.792163	H	2.700758	0.719387	2.408620
C	-0.523614	1.903872	-0.606351	C	2.581020	-1.939928	0.432755
H	0.153096	2.763238	-0.538196	H	1.860717	-2.083423	1.248137
H	-0.617301	1.651157	-1.668918	H	3.522246	-2.414394	0.742434
C	0.213100	0.705656	0.059280	H	2.197777	-2.476895	-0.441909
C	-0.574697	-0.619092	-0.193840				

0 imaginary frequencies

E = -1000.528975

ZPE = 0.290717

G = -1000.279797

PDT-F'

H	-0.428455	0.376327	1.700267	O	-1.071262	-1.184827	-1.897162
C	-1.414735	0.028125	1.400023	O	-2.498435	-1.733940	0.289407
C	-3.359241	0.613864	0.117222	H	0.760815	0.421924	-1.829845
C	-3.695607	-0.836771	0.296592	O	1.160769	0.585198	0.202586
C	-2.224627	1.077444	0.672310	Si	2.686033	-0.160165	0.188059
H	-4.334614	-1.203520	-0.510884	C	3.344938	0.117262	1.927100
H	-1.919619	-0.409761	2.265809	H	4.356993	-0.293723	2.034362
H	-3.934626	1.201017	-0.596573	H	2.707850	-0.368659	2.676066
H	-4.187269	-1.044711	1.255393	H	3.390918	1.186383	2.167641
N	-1.273322	-1.051442	0.397857	C	3.778674	0.688192	-1.097812
C	-1.455119	2.289963	0.219790	H	4.785972	0.251108	-1.099535
H	-0.846933	2.685382	1.042215	H	3.881451	1.760200	-0.888467
H	-2.122960	3.093769	-0.112764	H	3.379218	0.581368	-2.114287
C	-0.534382	1.893707	-0.975381	C	2.513653	-1.994171	-0.211893
H	0.209393	2.682946	-1.141985	H	3.496492	-2.484133	-0.208403
H	-1.152944	1.830659	-1.879248	H	2.069312	-2.160001	-1.201247
C	0.235684	0.551117	-0.874909	H	1.880839	-2.507121	0.522365
C	-0.757843	-0.650149	-0.849264				

0 imaginary frequencies

E = -1000.531482

ZPE = 0.290924

G = -1000.281905

SM-G

C	2.751295	0.070765	0.461796	C	-1.589565	0.627838	-0.585517
C	1.497393	0.114705	-0.363806	C	-2.146530	1.013266	0.725461
H	0.815952	-0.654848	0.031044	H	-1.907829	2.002072	1.114328
H	1.759265	-0.227245	-1.375853	C	-2.914442	0.169799	1.439143
C	0.822800	1.488610	-0.384356	H	-3.292581	0.460023	2.417440
H	0.642176	1.818158	0.645818	C	-2.090276	-0.458644	-1.210025
H	1.510171	2.221505	-0.823370	H	-1.728124	-0.736303	-2.199397
C	-0.499305	1.490448	-1.182329	C	-3.204609	-1.221336	0.925234
H	-0.303982	1.172235	-2.214969	H	-4.153742	-1.595552	1.326794
H	-0.854201	2.530213	-1.238420	H	-2.423252	-1.905868	1.299957
N	3.478049	-1.260530	0.499655	C	-3.228851	-1.254080	-0.612365
O	3.825926	-1.617599	-0.604867	H	-3.205108	-2.291266	-0.967303
O	3.247755	0.944029	1.127415	H	-4.182003	-0.829066	-0.973470

0 imaginary frequencies

E = -593.989406

ZPE = 0.213568

G = -593.813554

TS-G

C	0.749945	-0.840804	1.317339	C	-1.186529	-1.950503	0.028725
H	0.202647	-1.016131	2.241787	H	-1.169733	-2.729345	0.802328
C	0.114387	-1.175778	0.069998	H	-1.253591	-2.467323	-0.937192
C	0.682410	-0.686692	-1.104528	C	-2.456027	-1.086480	0.207201
H	0.199941	-0.925266	-2.049691	H	-2.585522	-0.801211	1.258498
C	2.134294	-0.284036	-1.207623	H	-3.336445	-1.677718	-0.072971
H	2.203419	0.618418	-1.824335	C	-2.388091	0.197128	-0.645982
H	2.639850	-1.079598	-1.772291	H	-2.123877	-0.038852	-1.683277
C	1.947271	-0.202040	1.350832	H	-3.361441	0.699249	-0.640468
H	2.343903	0.135264	2.306282	C	-1.383179	1.148410	-0.034930
C	2.848905	-0.067064	0.153547	O	-1.630068	1.884240	0.892126
H	3.330446	0.915911	0.175259	N	-0.055415	1.252477	-0.746298
H	3.661926	-0.800062	0.272585	O	0.787077	1.876571	-0.099614

1 imaginary frequency

E = -593.979105

ZPE = 0.215900

G = -593.795988

TS-G'

C	0.346293	0.154729	-1.305078	C	0.357278	1.277831	-0.419365
H	-0.442781	0.057501	-2.044834	C	1.374582	1.370666	0.485402

H	1.323930	2.119241	1.273943	H	-0.813428	2.760411	0.576148
C	1.160210	-0.951800	-1.038362	C	-2.200219	1.269285	-0.193111
H	1.040048	-1.843075	-1.647184	H	-2.504020	0.902215	-1.181457
C	2.658513	0.593676	0.346951	H	-3.007600	1.930975	0.143262
H	3.354888	1.198987	-0.254075	C	-2.131388	0.063271	0.782625
H	3.126891	0.483067	1.330144	H	-3.150339	-0.266881	1.008910
C	2.473781	-0.800224	-0.310121	H	-1.638224	0.351681	1.714197
H	3.275293	-0.979410	-1.038348	C	-1.424607	-1.130831	0.157027
H	2.550496	-1.595669	0.439208	O	-1.962989	-1.937911	-0.566717
C	-0.903801	2.112862	-0.304908	N	0.020594	-1.416335	0.544983
H	-1.003238	2.782011	-1.171966	O	0.397998	-0.780028	1.545568

1 imaginary frequency

E = -593.974742

ZPE = 0.216312

G = -593.790406

PDT-G

C	-0.749759	-0.726039	-1.368549	H	-2.162330	0.079264	2.119484
H	-0.530589	-0.963788	-2.407007	H	-2.149149	-1.613491	1.612507
C	-0.047889	-1.194793	-0.319182	C	-1.749888	0.329726	-0.992325
C	-0.435982	-0.481304	0.960764	H	-2.209802	0.825968	-1.847786
H	0.152406	-0.789660	1.825402	C	-2.762052	-0.208238	0.026970
C	-1.938639	-0.590786	1.282814	H	-3.493038	0.572660	0.259947

H	-3.301585	-1.066866	-0.388522	C	2.295168	0.239914	0.721579
C	1.252647	-1.947828	-0.324650	H	2.119042	-0.109943	1.745103
H	1.352108	-2.564648	-1.225894	H	3.227253	0.811948	0.725258
H	1.291414	-2.627199	0.539032	C	1.211670	1.210827	0.233507
C	2.452094	-0.955470	-0.257728	O	1.483986	2.151922	-0.486867
H	2.618136	-0.541426	-1.259572	N	-0.113074	0.945924	0.656141
H	3.359613	-1.510526	0.011598	O	-1.064759	1.450602	-0.273350

0 imaginary frequencies

E = -594.025487

ZPE = 0.221285

G = -593.835079

PDT-G'

C	-0.336316	0.158507	1.408174	C	-2.499322	-0.646455	0.355914
H	0.280853	-0.006159	2.288523	H	-3.122890	-0.665850	1.255500
C	-0.167063	1.201112	0.567596	H	-2.881999	-1.406317	-0.332733
C	-1.035072	1.077959	-0.653798	C	1.119367	1.991149	0.495810
H	-0.925755	1.907531	-1.355813	H	1.334409	2.518689	1.433740
C	-1.057613	-1.003469	0.746526	H	1.049692	2.754868	-0.289018
H	-0.985220	-1.936458	1.303889	C	2.306637	1.018155	0.197977
C	-2.494463	0.757585	-0.306698	H	2.620083	0.554268	1.141163
H	-2.901300	1.525276	0.360935	H	3.160979	1.606470	-0.160669
H	-3.091666	0.756966	-1.224298	C	2.068995	-0.134380	-0.831235

H	3.035952	-0.614765	-1.009555	O	1.586995	-2.145809	0.408935
H	1.695195	0.259058	-1.778537	N	-0.256773	-1.184473	-0.538304
C	1.156667	-1.234303	-0.276655	O	-0.567223	-0.113869	-1.419770

0 imaginary frequencies

E = -594.010059

ZPE = 0.220832

G = -593.819806

SM-H

H	3.994945	0.195443	0.612081	H	3.489219	2.496600	1.430615
C	3.115221	0.727238	0.203183	H	2.526741	2.817962	-0.024006
C	2.500737	-1.086999	-1.446975	C	0.087536	-1.421973	1.466607
C	1.243760	-0.879635	0.655040	H	-0.011801	-0.844250	2.394907
C	1.675381	-1.633926	-0.536538	H	0.313371	-2.456248	1.765807
C	1.909633	0.246582	0.986530	C	-1.264143	-1.434521	0.719757
C	2.987624	0.333372	-1.280776	H	-1.179807	-2.022013	-0.202320
H	2.786295	-1.641030	-2.339021	H	-2.013305	-1.942739	1.338435
H	3.949136	0.477125	-1.788747	C	-1.762108	-0.028123	0.378306
H	1.294491	-2.644781	-0.673565	H	-1.009247	0.527433	-0.202295
H	1.634807	0.798363	1.886307	H	-1.930423	0.576686	1.281422
H	2.273964	1.014264	-1.780447	C	-3.038510	-0.016251	-0.413056
C	3.365603	2.232044	0.373179	N	-3.595510	1.351863	-0.758571
H	4.274253	2.541951	-0.157084	O	-3.848445	2.000969	0.233015

O -3.670113 -0.949051 -0.840969

0 imaginary frequencies

E = -633.305157

ZPE = 0.241534

G = -633.102839

TS-H

C	-0.343239	0.174509	1.686701	H	1.109164	2.493756	1.510292
H	0.326880	0.210287	2.543710	H	0.903071	2.731610	-0.222412
C	-0.018807	0.958150	0.525613	C	2.510267	1.381363	0.282773
C	-0.707315	0.689050	-0.656200	H	2.883785	0.861897	1.173853
H	-0.448368	1.265626	-1.542230	H	3.211654	2.198283	0.073370
C	-1.386149	-0.694970	1.675872	C	2.492486	0.385386	-0.895648
H	-1.539463	-1.353601	2.528337	H	3.518080	0.116623	-1.170469
C	-2.081207	0.050971	-0.695995	H	2.002150	0.826991	-1.770916
H	-2.069933	-0.679543	-1.513070	C	1.791557	-0.883718	-0.463746
C	-2.458241	-0.687147	0.621509	O	2.328745	-1.768540	0.161012
H	-3.345804	-0.209281	1.069354	C	-3.127743	1.128052	-1.051772
H	-2.758578	-1.717110	0.402819	H	-3.176847	1.907231	-0.281249
N	0.387170	-1.076798	-0.984284	H	-4.121960	0.671550	-1.133435
O	-0.199764	-2.011799	-0.436683	H	-2.901479	1.610283	-2.010779
C	1.105993	1.972636	0.543924				

1 imaginary frequency

E = -633.294025

ZPE = 0.243949

G = -633.084332

TS-H'

C	0.250949	-1.263362	1.360418	H	-1.399968	-2.199624	-1.484357
H	-0.444235	-1.622223	2.117232	C	-2.728503	-0.946686	-0.337257
C	-0.181668	-1.246508	-0.015846	H	-3.053688	-0.847878	0.705745
C	0.626920	-0.603134	-0.941690	H	-3.562310	-1.398535	-0.888397
H	0.312204	-0.584410	-1.983530	C	-2.431845	0.461540	-0.895494
C	1.442091	-0.734224	1.738413	H	-3.365323	1.026038	-0.993499
H	1.677147	-0.663487	2.798851	H	-1.957647	0.398512	-1.881576
C	2.114678	-0.415096	-0.721363	C	-1.553876	1.207167	0.082659
C	2.518572	-0.306384	0.777747	O	-1.973636	1.781694	1.059533
H	3.409848	-0.926049	0.955931	H	2.532496	-1.363466	-1.101304
H	2.820180	0.719135	1.020422	C	2.721661	0.707493	-1.575899
N	-0.088394	1.334328	-0.284793	H	2.350697	1.684658	-1.254750
O	0.595907	1.718048	0.661075	H	2.476250	0.574541	-2.637097
C	-1.494928	-1.871650	-0.441239	H	3.814560	0.704965	-1.483854
H	-1.673936	-2.775351	0.156165				

1 imaginary frequency

E = -633.292946

ZPE = 0.243819

G = -633.083159

PDT-H

C	-0.425931	-0.045196	1.663205	H	1.108847	2.279698	1.891523
H	-0.098174	-0.040695	2.700273	H	0.736943	2.790077	0.240798
C	-0.048162	0.863720	0.744437	C	2.388103	1.366347	0.386691
C	-0.458650	0.433125	-0.649991	H	2.818188	0.765914	1.197389
H	-0.113904	1.112197	-1.430881	H	3.072763	2.206621	0.215518
C	-1.186516	-1.200154	1.077103	C	2.366002	0.479705	-0.888616
H	-1.367469	-2.012973	1.781570	H	3.395548	0.217727	-1.148264
C	-1.978399	0.192700	-0.809167	H	1.939403	1.022506	-1.739808
H	-2.101371	-0.350855	-1.753660	C	1.652398	-0.851666	-0.617569
C	-2.451741	-0.713226	0.359968	O	2.265595	-1.832271	-0.241628
H	-3.093346	-0.163272	1.059759	C	-2.751572	1.513276	-0.896270
H	-3.018349	-1.571772	-0.015736	H	-2.619461	2.111682	0.013644
N	0.251293	-0.871460	-0.816403	H	-3.824747	1.320402	-1.012783
O	-0.374195	-1.852215	0.003772	H	-2.427368	2.116895	-1.753720
C	1.011509	1.923362	0.858883				

0 imaginary frequencies

E = -633.34109

ZPE = 0.249234

G = -633.124105

PDT-H'

C	-0.188749	-0.981613	-1.546435	H	1.427040	-2.494889	1.004985
H	0.259852	-1.340962	-2.469692	C	2.694650	-0.878655	0.259980
C	0.278174	-1.263769	-0.315672	H	3.071534	-0.588437	-0.728173
C	-0.401627	-0.410288	0.736421	H	3.531663	-1.344446	0.795374
H	-0.006825	-0.569535	1.740666	C	2.294170	0.423424	1.007108
C	-1.270843	0.060466	-1.544565	H	3.188318	1.040082	1.134345
H	-1.546373	0.411645	-2.539889	H	1.902315	0.200977	2.006183
C	-1.938985	-0.586026	0.754227	C	1.325363	1.262203	0.163292
C	-2.468013	-0.376249	-0.694096	O	1.730414	2.117078	-0.601205
H	-2.919378	-1.288058	-1.102021	H	-2.112104	-1.625378	1.060523
H	-3.225384	0.415263	-0.716038	C	-2.612918	0.339093	1.775672
N	-0.052558	0.978355	0.310704	H	-2.451485	1.390912	1.517382
O	-0.778395	1.302777	-0.868682	H	-2.220040	0.171536	2.786743
C	1.566129	-1.935849	0.068392	H	-3.693534	0.154598	1.802754
H	1.882047	-2.657061	-0.694926				

0 imaginary frequencies

E = -633.340753

ZPE = 0.249352

G = -633.123635

SM-I

H	-2.568167	-1.206258	-0.995113	C	-1.988316	-0.431659	-0.455603
---	-----------	-----------	-----------	---	-----------	-----------	-----------

C	-0.933219	-2.023450	1.206405	H	1.916148	-2.352741	-1.720855
C	0.369288	-1.259125	-0.726022	C	2.893722	-0.819402	-0.565470
C	0.122838	-2.185904	0.388666	H	2.968506	-1.404938	0.359038
C	-0.615641	-0.407094	-1.096164	H	3.824270	-0.983819	-1.122550
C	-1.889213	-0.870705	1.019581	C	2.807626	0.678908	-0.208838
H	-1.078628	-2.689723	2.054434	H	2.655399	1.289509	-1.103483
H	-2.881102	-1.135022	1.402519	H	3.755402	0.994479	0.246651
H	0.835003	-2.991522	0.558330	C	1.728638	0.967946	0.809832
H	-0.467227	0.255196	-1.949583	N	0.635448	1.989090	0.478801
H	-1.535585	-0.022900	1.631527	O	1.014390	2.832854	-0.305579
C	-2.732463	0.905928	-0.638343	O	1.666931	0.514879	1.926902
H	-2.689537	1.180151	-1.702465	C	-4.199772	0.883334	-0.192384
H	-2.189937	1.691049	-0.095208	H	-4.691352	1.834025	-0.430182
C	1.709547	-1.313785	-1.424132	H	-4.299326	0.727674	0.888126
H	1.667575	-0.725219	-2.349912	H	-4.758346	0.084630	-0.698629

0 imaginary frequencies

E = -672.618013

ZPE = 0.271048

G = -672.385701

TS-I

C	0.221253	0.005133	1.787817	C	0.357042	0.893506	0.666648
H	1.000733	-0.000674	2.547416	C	-0.466607	0.678512	-0.438278

H	-0.342798	1.330609	-1.300809	H	3.449604	2.322968	-0.088798
C	-0.782794	-0.907688	1.834616	C	2.686098	0.547692	-1.093702
H	-0.798628	-1.643637	2.635775	H	3.677670	0.349015	-1.514336
C	-1.805419	-0.027551	-0.366568	H	2.069713	1.024076	-1.864687
C	-1.994537	-0.843199	0.945327	C	2.096267	-0.780619	-0.673167
H	-2.801597	-0.392456	1.546989	O	2.742929	-1.678213	-0.184721
H	-2.331629	-1.858813	0.714887	H	-1.841898	-0.721632	-1.215665
N	0.648423	-1.005062	-1.031515	C	-2.941074	1.005833	-0.577913
O	0.169609	-2.002237	-0.487059	H	-2.979213	1.686619	0.284450
C	1.433323	1.958929	0.624890	H	-2.700784	1.626336	-1.452639
H	1.539559	2.406331	1.621911	C	-4.316145	0.360553	-0.795314
H	1.102295	2.761418	-0.046446	H	-4.630908	-0.238510	0.067100
C	2.815160	1.459172	0.144544	H	-4.305374	-0.298865	-1.672378
H	3.321469	0.898149	0.939683	H	-5.082871	1.126458	-0.961002

1 imaginary frequency

E = -672.607635

ZPE = 0.272495

G = -672.370981

TS-I'

C	0.366259	1.523968	1.206132	C	-0.382699	0.531153	-0.873717
H	1.185794	1.936399	1.791855	H	-0.223463	0.316235	-1.928747
C	0.592400	1.243664	-0.190150	C	-0.790817	1.171973	1.821711

H	-0.875345	1.295558	2.899882	C	2.575664	-0.779782	-1.041569
C	-1.833075	0.512254	-0.434534	H	1.970806	-0.841971	-1.953497
C	-2.022930	0.695722	1.100250	H	3.446562	-1.434043	-1.155904
H	-2.830061	1.419105	1.284627	C	1.799234	-1.266997	0.160022
H	-2.357767	-0.241277	1.560629	O	2.316393	-1.701331	1.162405
N	0.292306	-1.323918	0.012684	H	-2.240896	1.415906	-0.922738
O	-0.274335	-1.483837	1.091762	C	-2.623565	-0.681367	-1.007187
C	1.867355	1.670495	-0.889461	H	-2.293538	-1.597763	-0.506269
H	2.189328	2.641661	-0.490892	H	-2.368838	-0.793599	-2.070875
H	1.642548	1.827088	-1.952311	C	-4.143348	-0.524161	-0.872147
C	3.040704	0.669752	-0.787205	H	-4.456044	-0.464306	0.177308
H	3.506634	0.717888	0.204734	H	-4.663809	-1.379205	-1.319092
H	3.812964	0.947696	-1.514864	H	-4.498571	0.383362	-1.378839

1 imaginary frequency

E = -672.606689

ZPE = 0.272385

G = -672.369950

PDT-I

C	0.113981	-0.301811	1.738250	H	-0.098616	1.144216	-1.240323
H	0.554562	-0.335216	2.732116	C	-0.538413	-1.504338	1.118189
C	0.249664	0.728298	0.881799	H	-0.522360	-2.391480	1.752615
C	-0.252806	0.358576	-0.499741	C	-1.731586	-0.095500	-0.531501

C	-1.934202	-1.154973	0.586173	H	3.512324	0.772759	-1.399711
H	-2.557565	-0.767975	1.402002	H	1.899498	1.394408	-1.759987
H	-2.415191	-2.056506	0.193151	C	2.009723	-0.588820	-0.807455
N	0.612148	-0.804250	-0.866379	O	2.794312	-1.493632	-0.595809
O	0.229572	-1.934316	-0.090336	H	-1.878086	-0.575585	-1.507901
C	1.153284	1.923860	0.993726	C	-2.691869	1.101825	-0.432966
H	1.315379	2.203697	2.041685	H	-2.571175	1.585139	0.546939
H	0.689481	2.786955	0.495200	H	-2.411301	1.851306	-1.187547
C	2.532943	1.624153	0.333952	C	-4.162864	0.718421	-0.640056
H	3.132662	1.031000	1.034822	H	-4.505393	-0.001504	0.112687
H	3.067345	2.569890	0.178711	H	-4.317137	0.265681	-1.627777
C	2.492173	0.853047	-1.013847	H	-4.810696	1.600117	-0.572001

0 imaginary frequencies

E = -672.654861

ZPE = 0.277705

G = -672.411164

PDT-I'

C	-0.435835	-0.876702	1.701608	C	0.619006	0.183381	1.841155
H	-1.051276	-1.188498	2.542368	H	0.696740	0.598174	2.847112
C	-0.654742	-1.239840	0.423990	C	1.724025	-0.589160	-0.241400
C	0.210700	-0.438787	-0.528382	C	1.961752	-0.277368	1.264957
H	0.017925	-0.666060	-1.577608	H	2.337836	-1.148833	1.812868

H	2.688047	0.533895	1.384064	H	-3.241120	0.919296	-1.707462
N	-0.222402	0.966335	-0.267182	C	-1.603316	1.235853	-0.410919
O	0.255056	1.373925	1.009604	O	-2.153366	2.131704	0.200996
C	-1.840617	-1.955448	-0.158877	H	1.955288	-1.644889	-0.437969
H	-2.294516	-2.635561	0.571935	C	2.580086	0.268757	-1.190875
H	-1.520476	-2.566279	-1.015374	H	2.409315	1.329308	-0.968617
C	-2.916526	-0.930732	-0.628467	H	2.235303	0.108889	-2.222887
H	-3.475150	-0.585111	0.249695	C	4.078222	-0.052152	-1.114180
H	-3.634467	-1.442603	-1.281675	H	4.481815	0.121336	-0.109317
C	-2.385800	0.327915	-1.368903	H	4.647869	0.575847	-1.809080
H	-1.806206	0.047907	-2.255883	H	4.274654	-1.100481	-1.374934

0 imaginary frequencies

E = -672.654444

ZPE = 0.277638

G = -672.410842

References

- ¹ Seminal publication of the type 2 intramolecular Diels–Alder reaction: Shea, K. J.; Wise, S. J. *Am. Chem. Soc.* **1978**, *100*, 6519–6521.
- ² Seminal publication of the type 2 intramolecular Diels–Alder reaction: Shea, K. J.; Wise, S. *Tetrahedron Lett.* **1979**, 1011–1014.
- ³ Review of the type 2 intramolecular Diels–Alder reaction: Bear, B. R.; Sparks, S. M.; Shea, K. *J. Angew. Chem. Int. Ed.* **2001**, *40*, 820–849.
- ⁴ Type 2 IMDA approach to esperamicin: Schreiber, S. L.; Kiessling, L. L. *J. Am. Chem. Soc.* **1988**, *110*, 631–633.
- ⁵ Structural reassignment of type 2 IMDA product: Schreiber, S. L.; Kiessling, L. L. *Tetrahedron Lett.* **1989**, *30*, 433–436.
- ⁶ Synthesis of taxanes utilizing a type 2 IMDA reaction: Mendoza, A.; Ishihara, Y.; Baran, P. S. *Nat. Chem.* **2012**, *4*, 21–25.
- ⁷ An earlier example of type 2 IMDA approach to taxanes: Jackson, R. W.; Shea, K. J. *Tetrahedron Lett.* **1994**, *35*, 1317–1320.
- ⁸ Example of type 2 IMDA approach to taxanes including discussion of diastereoselectivity: Winkler, J. D.; Kim, H. S.; Kim, S.; Penkett, C. S.; Bhattacharya, S. K.; Ando, K.; Houk, K. N. *J. Org. Chem.* **1997**, *62*, 2957–2962.
- ⁹ Related IMDA approach to 9 β -presilphiperfolan-1 α -ol: Hong, A. Y.; Stoltz, B. M. *Angew. Chem. Int. Ed.* **2012**, *51*, 9674–9678.
- ¹⁰ Seminal publication on the *N*-acylnitroso type 2 IMDA reaction: Sparks, S. M.; Chow, C. P.; Zhu, L.; Shea, K. J. *J. Org. Chem.* **2004**, *69*, 3025–3035.

- ¹¹ Seminal publication on the *N*-acylnitroso type 2 IMDA reaction: Sparks, S. M.; Vargas, J. D.; Shea, K. J. *Org. Lett.* **2000**, *2*, 1473–1475.
- ¹² *N*-acylnitroso type 2 IMDA approach to stenine: Zhu, L.; Lauchli, R.; Loo, M.; Shea, K. J. *Org. Lett.* **2007**, *9*, 2269–2271.
- ¹³ Review of the nitrosocarbonyl Diels–Alder reaction: Bodnar, B. S.; Miller, M. J. *Angew. Chem. Int. Ed.* **2011**, *50*, 5630–5647.
- ¹⁴ Seminal publication of the Lewis acid-catalyzed type 2 IMDA reaction: Shea, K. J.; Gilman, J. W. *Tetrahedron Lett.* **1983**, *24*, 657–660.
- ¹⁵ Quantum mechanical methods and pericyclic reaction mechanisms: Wiest, O.; Montiel, D. C.; Houk, K. N. *J. Phys. Chem. A* **1997**, *101*, 8378–8388.
- ¹⁶ Computational study of hetero-Diels–Alder reaction of nitroso-containing dienophiles: Leach, A. G.; Houk, K. N. *J. Org. Chem.* **2001**, *66*, 5192–5200.
- ¹⁷ Computational study of stereoselectivity in type 1 intramolecular Diels–Alder reactions: Tantillo, D. J.; Houk, K. N.; Jung, M. E. *J. Org. Chem.* **2001**, *66*, 1938–1940.
- ¹⁸ Computational study of hetero-Diels–Alder reaction of imine-containing dienophiles: Iafe, R. G.; Houk, K. N. *J. Org. Chem.* **2008**, *73*, 2679–2686.
- ¹⁹ Computational study of tether composition and selectivity in type 1 intramolecular Diels–Alder reactions: Paddon-Row, M. N.; Longshaw, A. I.; Willis, A. C.; Sherburn, M. S. *Chem. Asian J.* **2009**, *4*, 126–134.
- ²⁰ Computational study of allylic stereocontrol in type 1 intramolecular Diels–Alder reactions: Lilly, M. J.; Miller, N. A.; Edwards, A. J.; Willis, A. C.; Turner, P.; Paddon-Row, M. N.; Sherburn, M. S. *Chem. Eur. J.* **2005**, *11*, 2525–2536.

- ²¹ Computational study of *cis/trans* stereoselectivity in type 1 intramolecular Diels–Alder reactions: Paddon-Row, M. N.; Moran, D.; Jones, G. A.; Sherburn, M. S. *J. Org. Chem.* **2005**, *70*, 10841–10853.
- ²² Computational study of ester-linked type 1 intramolecular Diels–Alder reactions: Cayzer, T. N.; Paddon-Row, M. N.; Moran, D.; Payne, A. D.; Sherburn, M. S.; Turner, P. *J. Org. Chem.* **2005**, *70*, 5561–5570.
- ²³ Computational study of *cis/trans* stereoselectivity in type 1 intramolecular Diels–Alder reactions: Pearson, E. L.; Willis, A. C.; Sherburn, M. S.; Paddon-Row, M. N. *Org. Biomol. Chem.* **2008**, *6*, 513–522.
- ²⁴ Spartan'08 Wavefunction, Inc. Irvine, CA. See also: Shao, Y.; Molnar, L.F.; Jung, L.F.; Kussmann, J.; Ochsenfeld, C.; Brown, S.T.; Gilbert, A.T.B.; Slipchenko, L.V.; Levchenko, S.V.; O'Neill, D.P.; DiStasio Jr., R.A.; Lochan, R.C.; Wang, T.; Beran, G.J.O.; Besley, N.A.; Herbert, J.M.; Lin, C.Y.; Van Voorhis, T.; Chien, S.H.; Sodt, A.; Steele, R.P.; Rassolov, V.A.; Maslen, P.E.; Korambath, P.P.; Adamson, R.D.; Austin, B.; Baker, J.; Byrd, E.F.C.; Dachsel, H.; Doerksen, R.J.; Dreuw, A.; Dunietz, B.D.; Dutoi, A.D.; Furlani, T.R.; Gwaltney, S.R.; Heyden, A.; Hirata, S.; Hsu, C-P.; Kedziora, G.; Khalliulin, R.Z.; Klunzinger, P.; Lee, A.M.; Lee, M.S.; Liang, W.Z.; Lotan, I.; Nair, N.; Peters, B.; Proynov, E.I.; Pieniazek, P.A.; Rhee, Y.M.; Ritchie, J.; Rosta, E.; Sherrill, C.D.; Simmonett, A.C.; Subotnik, J.E.; Woodcock III, H.L.; Zhang, W.; Bell, A.T.; Chakraborty, A.K.; Chipman, D.M.; Keil, F.J.; Warshel, A.; Hehre, W.J.; Schaefer, H.F.; Kong, J.; Krylov, A.I.; Gill P.M.W.; Head-Gordon, M. *Phys. Chem. Chem. Phys.*, **2006**, *8*, 3172–3191.

- ²⁵ Seminal publication of Merck molecular force field: Halgren, T. A. *J. Comput. Chem.* **1996**, *17*, 490–519.
- ²⁶ Gaussian 09, Revision C.01, Frisch, M. J.; Trucks, G. W.; Schlegel, H. B.; Scuseria, G. E.; Robb, M. A.; Cheeseman, J. R.; Scalmani, G.; Barone, V.; Mennucci, B.; Petersson, G. A.; Nakatsuji, H.; Caricato, M.; Li, X.; Hratchian, H. P.; Izmaylov, A. F.; Bloino, J.; Zheng, G.; Sonnenberg, J. L.; Hada, M.; Ehara, M.; Toyota, K.; Fukuda, R.; Hasegawa, J.; Ishida, M.; Nakajima, T.; Honda, Y.; Kitao, O.; Nakai, H.; Vreven, T.; Montgomery, Jr., J. A.; Peralta, J. E.; Ogliaro, F.; Bearpark, M.; Heyd, J. J.; Brothers, E.; Kudin, K. N.; Staroverov, V. N.; Kobayashi, R.; Normand, J.; Raghavachari, K.; Rendell, A.; Burant, J. C.; Iyengar, S. S.; Tomasi, J.; Cossi, M.; Rega, N.; Millam, J. M.; Klene, M.; Knox, J. E.; Cross, J. B.; Bakken, V.; Adamo, C.; Jaramillo, J.; Gomperts, R.; Stratmann, R. E.; Yazyev, O.; Austin, A. J.; Cammi, R.; Pomelli, C.; Ochterski, J. W.; Martin, R. L.; Morokuma, K.; Zakrzewski, V. G.; Voth, G. A.; Salvador, P.; Dannenberg, J. J.; Dapprich, S.; Daniels, A. D.; Farkas, Ö.; Foresman, J. B.; Ortiz, J. V.; Cioslowski, J.; Fox, D. J. Gaussian, Inc., Wallingford CT, 2009.
- ²⁷ Seminal publication of B3LYP density functional: Becke, A. D. *J. Chem. Phys.* **1993**, *98*, 5648.
- ²⁸ Seminal publication of B3LYP density functional: Lee, C.; Yang, W.; Parr, R. G. *Phys. Rev. B Condens. Matter* **1988**, *37*, 785–789.
- ²⁹ Seminal publication of IRC calculations: Gonzalez, C.; Schlegel, H. B. *J. Chem. Phys.* **1989**, *90*, 2154–2161.
- ³⁰ Legault, C. Y.; CYLview, 1.0b; Université de Sherbrooke: Quebec, Canada, 2009; <http://www.cylview.org>.

- ³¹ Structures calculated at the B3LYP/6-31+G(d) level. Forming bonds are shown as dotted lines, interatomic distances given in Å, and free energies given in kcal mol⁻¹. Experimentally unobserved pathways are shown as dashed lines. Nomenclature of tether orientation (internal vs. external) is shown for illustrative purposes.
- ³² Seminal publication on non-planar amides: Winkler, F. K.; Dunitz, J. D. *J. Mol. Biol.* **1971**, *59*, 169–182.
- ³³ On solvolysis of twist amides: Aubé, J. *Angew. Chem. Int. Ed.* **2012**, *51*, 3063–3065.
- ³⁴ The synthesis and reactions of the most twisted amide: Kirby, A. J.; Komarov, I. V; Wothers, P. D.; Feeder, N. *Angew. Chem. Int. Ed.* **1998**, *37*, 785–786.
- ³⁵ The synthesis and reactions of the most twisted amide: Kirby, A. J.; Komarov, I. V; Feeder, N. *J. Chem. Soc., Perkin Trans. 2* **2001**, 522–529.
- ³⁶ Synthesis of 2-quinuclidonium tetrafluoroborate: Tani, K.; Stoltz, B. M. *Nature* **2006**, *441*, 731–734.

Chapter 5

Investigation of Intramolecular Cyano-azadiene Diels–Alder Reactions: Indolizidine and Quinolizidine Synthesis

Abstract: Progress toward understanding the scope and diastereoselectivity of an intermolecular aza-Diels–Alder reaction is described herein. The cyanoenamine products that result from this cyclization have interesting structures and are underutilized intermediates in organic synthesis. Assembly of the Diels–Alder precursors was achieved using an imine condensation/oxidative cyanation protocol. By this method, several indolizidine and quinolizidine structures were constructed.

Introduction

Indolizidine and quinolizidine are important heterocyclic motifs present in many alkaloid natural products (Figure 5.1).^{1,2} These saturated heterocyclic systems and highly substituted derivatives provide an organized template for specific biological binding.^{3,4} While several synthetic methods for the synthesis of quinolizidine and indolizidine have been reported,^{5–9} the Diels–Alder reaction of cyano-azadienes is an underdeveloped strategy for the preparation of such heterocycles.¹⁰ Described herein are the initial studies for the construction of highly substituted cyanoenamine containing indolizidines and quinolizidines via the Diels–Alder reaction.

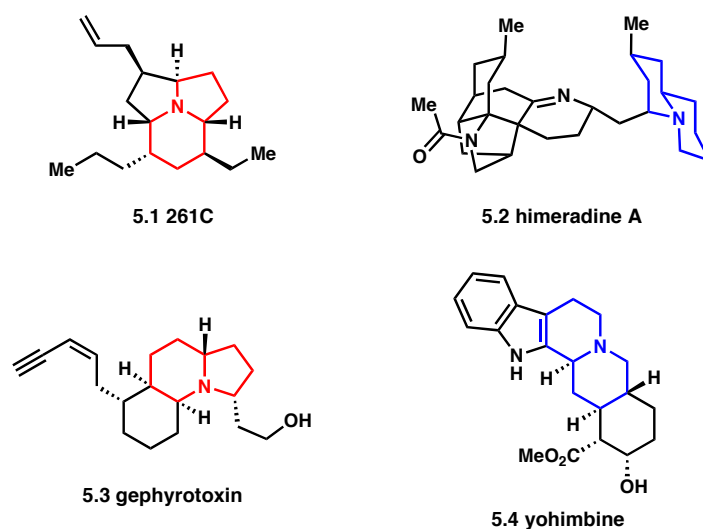


Figure 5.1. Examples of indolizidine (red) and quinolizidine (blue) containing natural products.^{11–14}

Cyanoenamine derivatives provide an intriguing functional handle for divergent synthetic strategies, particularly in the realm of reductive cyanation precursors,^{15,16} though little has been reported on the chemistry of this functional group.^{17–21} Modular syntheses of such heterocyclic systems offer the opportunity for late-stage introduction of sensitive moieties without the use of protecting groups or additional synthetic operations. Furthermore, this type of Diels-Alder cyclization is an underdeveloped transformation in terms of scope and diastereocontrol.¹⁰ With these specific aims in mind, we set out to investigate the synthesis of cyanoenamine containing indolizidines and quinolizidines.

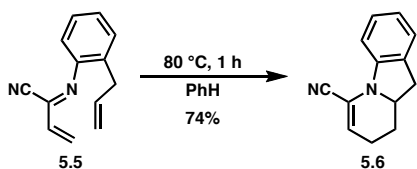
Background

While reports on the synthesis of cyanoenamine containing quinolizidine and indolizidines in the literature are limited, there have been a few key studies.^{22–29} Fowler and Grierson initially reported the rapid cyclization of aniline-derived indolizidines (Scheme 5.1 A).²³ A subsequent report revealed that alkyl-derived substrates are less reactive, requiring

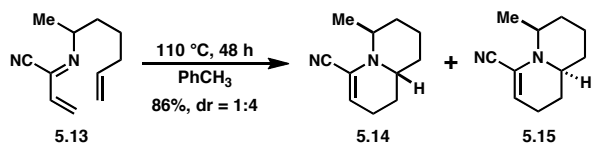
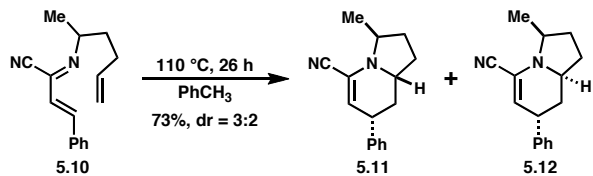
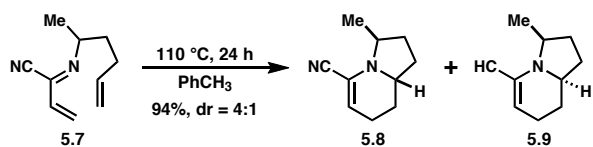
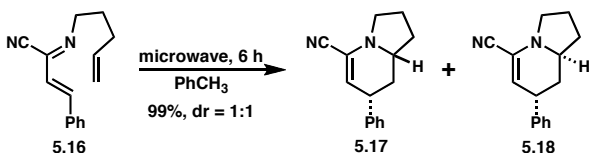
higher temperatures and longer reaction times.²⁴ Despite the high yields (73–92%) of the Diels–Alder reaction, the diastereoselectivity of these transformations was modest (4:1–3:2) and a reversal of the *cis/trans* preference was observed with cyano-azadiene **5.13**. Masson and Zhu described an improved one-pot condensation/oxidative cyanation protocol to access homoallyl-derived substrates.²⁹ In their sole example of an aza-Diels–Alder cyclization, cinnamaldehyde derivative **5.16** underwent smooth cyclization to afford the requisite indolizidines as a 1:1 mixture of diastereomers (Scheme 5.1 B). Despite solid precedent for the desired cyclization, these limited reports lack much information about the diastereoselectivity of this transformation, particularly with respect to dienophile substitution.

Scheme 5.1. Previous syntheses of indolizidines and quinolizidine containing cyanoenamines.^{23,24,29}

A) Grierson and Fowler



B) Masson and Zhu

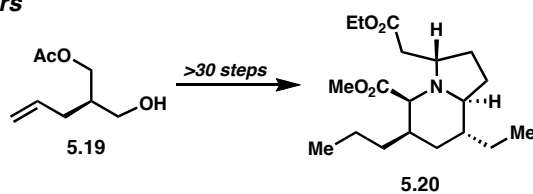


Indolizidine alkaloid 261C (**5.1**, Figure 1), isolated from the skin of the Madagascan frog *Mantella betsileo*, provides a unique opportunity to investigate the subsequent reactivity of cyanoenamines.¹¹ Toyooka and co-workers have reported on synthetic studies toward 261C, starting from known alcohol **5.19** (Scheme 5.2 A).³⁰ However, their strategy requires over 30 synthetic steps to reach advanced intermediate **5.20**. Implementation of an intramolecular

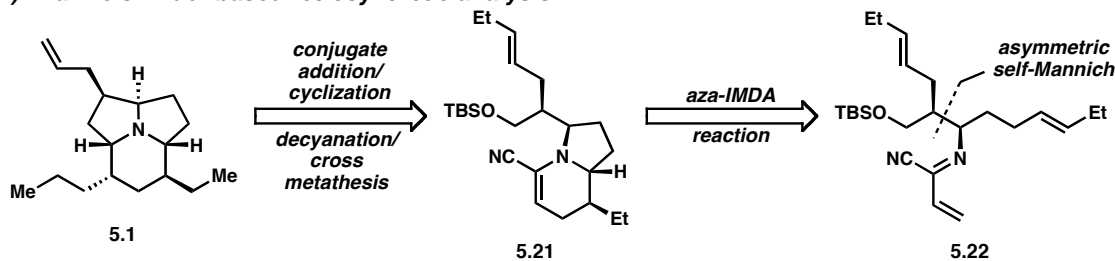
aza-Diels–Alder reaction would dramatically shorten the synthesis of 261 C (**5.1**). The importance of understanding the diastereoselectivity of these cyclizations is highlighted in a retrosynthetic analysis of 261C (Scheme 5.2 B). An aza-Diels–Alder reaction of cyano-iminodiene **5.22**, derived from the asymmetric self-Mannich reaction³¹ of a known aldehyde,³² would set two key stereocenters for the piperidine fragment of 261C and rapidly lead to intermediate **5.21**. This cyanoenamine could undergo a conjugate addition/cyclization cascade to close the final ring, followed by decyanation/cross metathesis, to furnish 261C (**5.1**). With this strategy in mind, we set out to investigate the feasibility diastereoselective aza-Diels–Alder cyclizations.

Scheme 5.2. Synthetic strategies toward indolizidine alkaloid 261C.³⁰

A) Toyooka and co-workers



B) Aza-Diels–Alder based retrosynthetic analysis



Results and Discussion

Substrate Design

A few key design considerations were taken into account when selecting substrates for this study (Figure 5.2). Tether length was varied to access either indolizidines ($n = 1$) or quinolizidines ($n = 2$). To probe reactivity and selectivity, the dienophile substitution (R, R', R''

= Me/H) was varied. In order to reduce the volatility of intermediates in the synthetic sequence, a phenethyl substituent was introduced α to the nitrogen on the tether, which also provided a useful chromophore for reaction monitoring. In addition, the cinnamaldehyde-derived diene fragment was chosen to investigate steric effects and reduce volatility. Preliminary studies using Grierson and Fowler's triflation/cyanation protocol to access the Diels–Alder substrates proved to have varying degrees of reproducibility.²³ These issues led to the identification of Masson and Zhu's one-pot imine condensation/oxidative cyanation protocol as the preferred way to install the nitrile moiety.²⁹

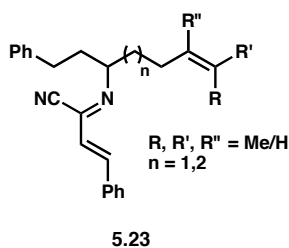


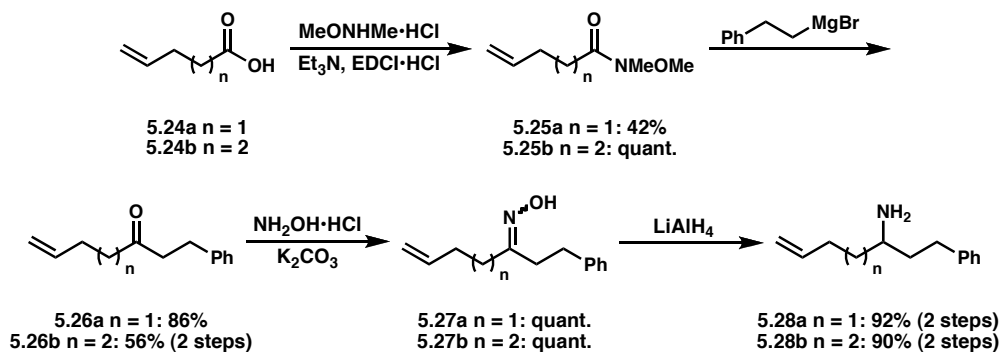
Figure 5.2. Diels–Alder substrates.

Simple Unsubstituted Dienophile Synthesis

Synthesis of the unsubstituted dienophile amine precursors began from commercially available 4-pentenoic acid **5.24a** and 5-hexenoic acid **5.24b** (Scheme 5.3). The acids underwent standard amide coupling with *N,O*-dimethylhydroxylamine hydrochloride, in the presence of triethylamine and *N*-(3-dimethylaminopropyl)-*N'*-ethylcarbodiimide hydrochloride, resulting in usable quantities of amides **5.25a-b**. Using the protocol described by Woerpel and co-workers,³³ Weinreb amides³⁴ **5.25a-b** were treated with freshly prepared phenylethylmagnesium bromide to furnish desired ketones **5.26a-b**. Condensation of ketones **5.26a-b** with hydroxylamine hydrochloride in the presence of potassium carbonate resulted in quantitative conversion to oximes **5.27a-b**, which were isolated as an inconsequential 1:1 mixture of *E:Z* isomers. The oximes were reduced using lithium aluminum hydride to furnish desired amines **5.28a-b** in high

yields. Although the earlier steps were low yielding, due to the volatility of both starting materials and products, this sequence afforded gram quantities of amines **5.28a-b** and provided a useful strategy for the synthesis of substituted dienophile amine precursors.

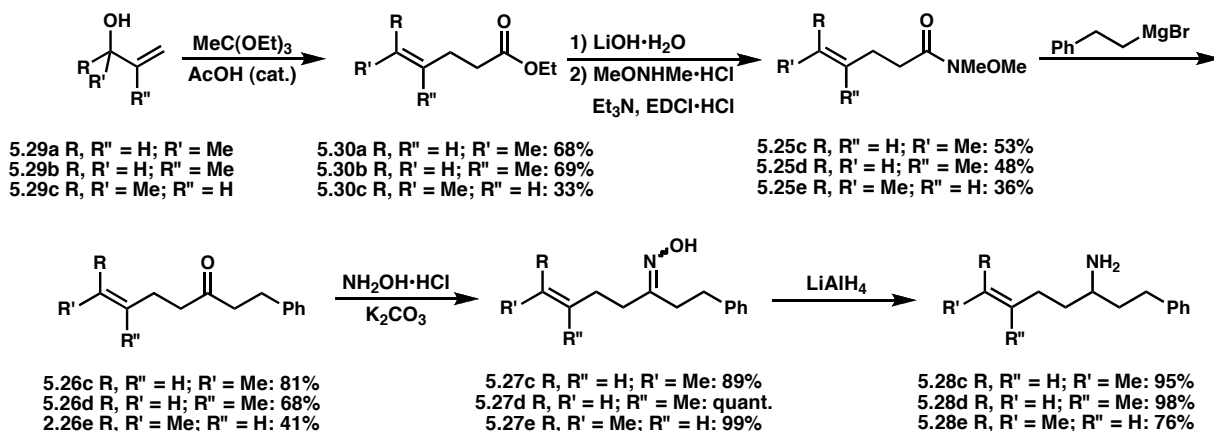
Scheme 5.3. Synthesis of unsubstituted dienophile amine precursors.



Substituted Dienophile Synthesis

The synthesis of substituted dienophile amine precursors began from commercially available allylic alcohol derivatives **5.29a-c** (Scheme 5.4). The alcohols underwent a Johnson orthoester Claisen rearrangement³⁵ with triethylorthoacetate in the presence of acetic acid to afford esters **5.30a-c**. Lithium hydroxide-mediated hydrolysis of the esters proceeded quantitatively and the crude acids were subjected to standard coupling conditions to furnish desired amides **5.25c-e**. As before, Weinreb amides **5.25c-e** were treated with freshly prepared phenylethylmagnesium bromide to access ketones **5.26c-e**. Condensation of the ketones with hydroxylamine hydrochloride in the presence of potassium carbonate led to quantitative conversion to oximes **5.27c-e** (1:1 mixture of *E:Z* isomers), which were reduced using lithium aluminum hydride to furnish desired amines **5.28c-e** in good yields. Yields were consistently lower for most steps in the sequence with the 1,1-disubstituted alkene substrate, but usable quantities were obtained by this method.

Scheme 5.4. Synthesis of substituted dienophile amine precursors.

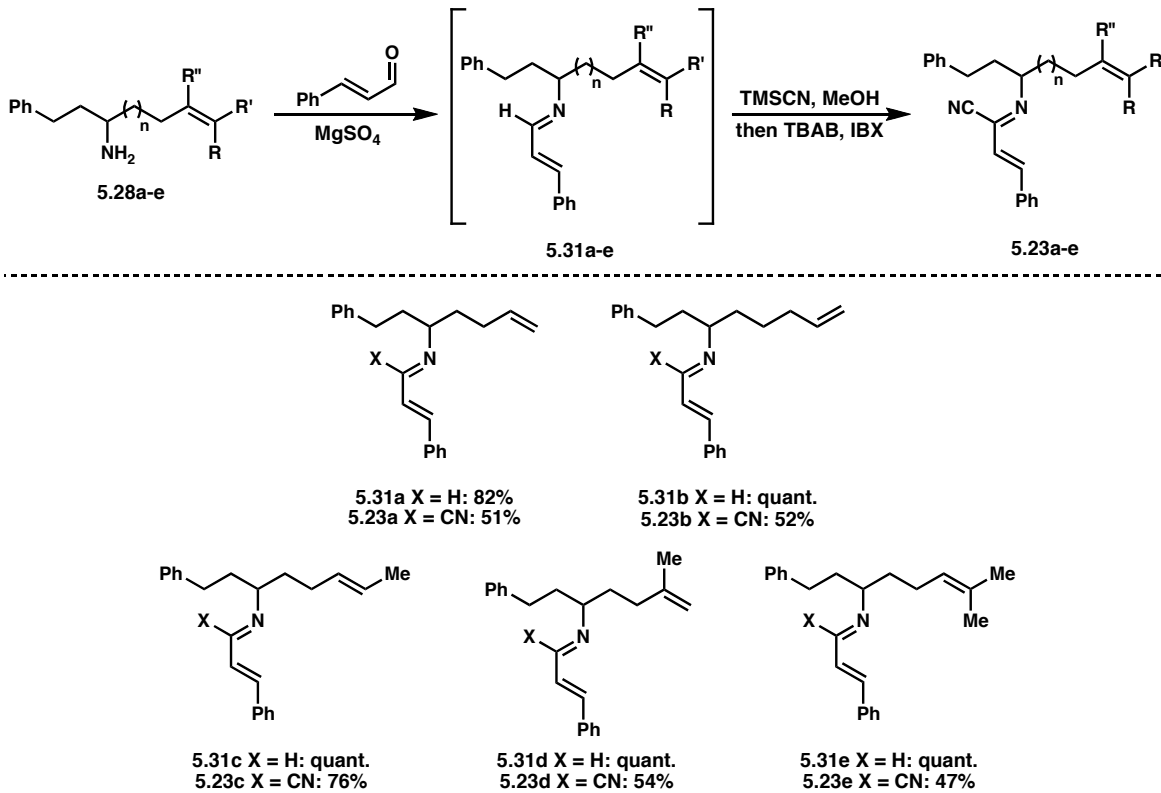


Synthesis of the Cyclization Precursors and Cyanoenamine Products

With amines **5.28a-e** in hand, strategies to access cyano-azadienes **5.23a-e** were investigated. While previous studies suggested Masson and Zhu's imine condensation/oxidative cyanation protocol²⁹ was the preferred method (*vide supra*), initial attempts to perform the reaction as described were met with mixed results. The yields were significantly lower than reported and inconsistent upon subsequent runs. In addition, monitoring the reaction was difficult due to the sensitive nature of the intermediates.

In order to address these issues, a modified procedure to access the Diels–Alder precursors was identified (Scheme 5.5). Treatment of amines **5.28a-e** with *trans*-cinnamaldehyde in the presence of magnesium sulfate for extended periods of time led to high yields of intermediate imines **5.31a-e**, which could be observed by NMR spectroscopy. Imines **5.31a-e** were pretreated with trimethylsilyl cyanide and a stoichiometric amount of methanol to initiate the Strecker reaction,³⁶ followed by addition of tetrabutylammonium bromide and 2-iodoxybenzoic acid to furnish Diels–Alder precursors **5.23a-e** in modest, but reproducible yields.

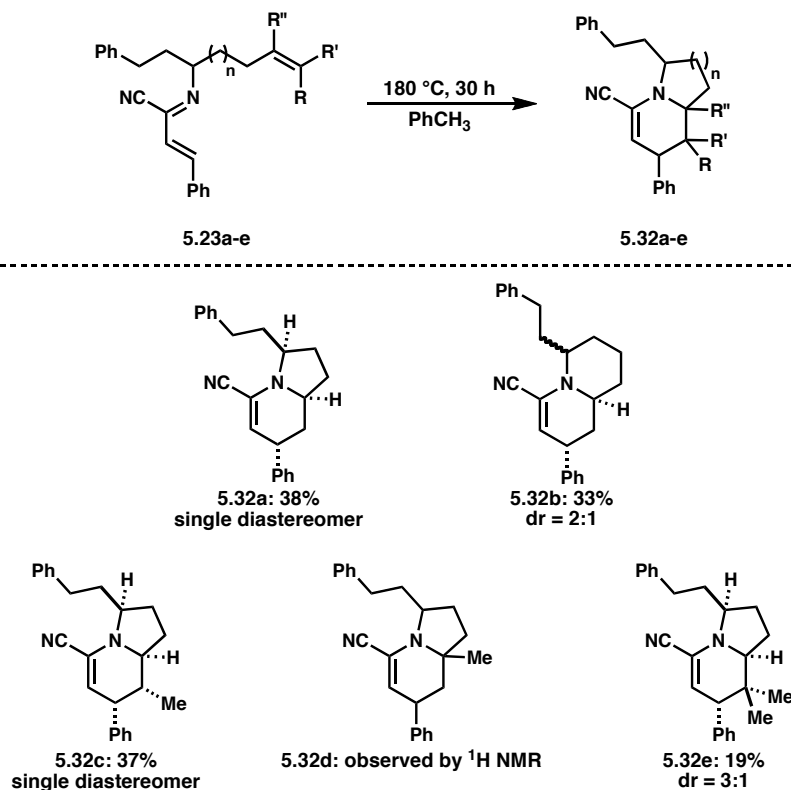
Scheme 5.5. Synthesis of the Diels–Alder precursors.



Diels–Alder Cyclization

The Diels–Alder cycloaddition with cyano-azadienes **5.23a-e** occurred under thermal conditions, to afford indolizidines **5.32a** and **5.32c-e** and quinolizidine **5.32b** (Scheme 5.6). While the yields are not optimal for this transformation, these preliminary results provide some information about the scope and diastereoselectivity of the reaction. Temperatures lower than 180 °C did not provide sufficient conversion to product, however shorter reaction times at 180 °C were not investigated. It may be possible to improve these yields by either reducing reaction times, or using Bronsted or Lewis acids to catalyze the cyclization.

Scheme 5.6. Aza-Diels–Alder cyclizations.



Simple unsubstituted alkene substrates afforded similar yields of indolizidine **5.32a** and quinolizidine **5.32b** (38% and 33%, respectively), but the cyclization of precursor **5.23a** gave indolizidine **5.32a** as a single diastereomer. Quinolizidine **5.32b** was isolated as an inseparable 2:1 mixture of diastereomers, the stereochemistry of which could not be determined, due to significant overlap in the alkyl region of the ^1H NMR spectrum. Tentative assignment of indolizidine **5.32a** by NOESY correlations, suggests a *cis* relationship between the substituents on the pyrrolidine ring. NOESY correlations also clearly indicate an *exo*-oriented cyclization with respect to the tether, resulting in a *trans* relationship between the piperidine phenyl substituent and the tether. This result is in sharp contrast to the virtual lack of selectivity reported by Grierson and Fowler, as well as Masson and Zhu.^{24,29} The preference for *exo*-cyclization was observed in the substituted dienophile substrates as well.

E-alkene **5.23c** underwent cyclization to give indolizidine **5.32c** in 37% yield as a single diastereomer, which was comparable to unsubstituted alkene substrate **5.32a**. The stereochemistry of the dienophile was transferred to the product, suggesting that the cyclization occurs in a concerted fashion rather than through a step-wise ionic or a di-radical pathway. As with simple indolizidine **5.32a**, NOESY correlations, suggest a *cis* relationship between the substituents on the pyrrolidine ring. While this is not the desired relationship for the synthesis of 261C (Scheme 5.2. B), the role that diene substituents have on diastereoselectivity of cyclization is unclear and remains an active area of interest within this research project.

Perhaps most interesting is the finding that 1,1-disubstituted alkene **5.23d** and trisubstituted alkene **5.23e** undergo cyclization to give indolizidines **5.32d** and **5.32e**, respectively. These are the first examples of this type of cyclization where quaternary centers are generated, albeit in reduced yields. Indolizidine **5.32d** was observed by ¹H NMR spectroscopy and HRMS, but an analytically pure sample could not be obtained. The stereochemical outcome of this cyclization could not be determined. Indolizidine **5.32e** was obtained in 19% yield as a 3:1 mixture of diastereomers. The major diastereomer in this cyclization suggests an *exo* mode of cyclization and also appears to exhibit a *cis* relationship between substituents on the pyrrolidine ring, which is the same diastereoselectivity observed in the less substituted cases.

Conclusions and Future Directions

These initial studies provide a solid foundation for further investigation into the synthesis of cyanoenamine containing indolizidines and quinolizidines. The aza-Diels–Alder approach to constructing these molecules has proven a viable synthetic strategy beyond simple, unsubstituted cases. Additionally, interesting diastereoselective outcomes have been observed, several of

which are in direct opposition to literature examples. Future computational studies should provide a better understanding on the origins of the observed diastereoselectivities for this class of Diels–Alder reactions. Once the oxidative Strecker and the cyclization reactions are optimized, a more comprehensive study on the role that substituents play in determining the diastereoselectivity of the cyclization will be initiated.

General Experimental Details:

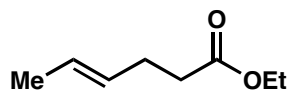
Unless otherwise stated, reactions were carried out using standard procedures for the rigorous exclusion of air and moisture. This included the use of oven-dried glassware, as well as carrying reactions out under an atmosphere of Ar. When specified, glassware was washed with 0.5 M ethanolic HCl, then 0.5 M ethanolic KOH and oven-dried for a minimum of 4 h prior to use. Thin layer chromatography (TLC) was carried out using glass plates coated with a 250 μm layer of 60 Å silica gel. TLC plates were visualized with a UV lamp at 254 nm, or by staining with KMnO_4 , PMA, or vanillin. Organic solutions were concentrated using a rotary evaporator equipped with a water aspirator. Flash column chromatography was performed using 40-63 μm silica gel. Silica gel was deactivated by preparation of a slurry (1:99 Et_3N :hexanes) prior to chromatography. All reagents were purchased from Acros, Alfa Aesar, Sigma-Aldrich, Strem, TCI, or VWR and used without further purification unless otherwise noted. Et_3N and *i*- Pr_2EtN were freshly distilled over CaH_2 prior to use. Solvents, such as CH_2Cl_2 , Et_2O , THF, MeCN and toluene were purchased as HPLC-grade and passed through a solvent purification system equipped with activated alumina columns. Infrared spectra were recorded on a FT-IR spectrometer. Nuclear magnetic resonance (NMR) spectroscopy was performed using a 500 MHz spectrometer. Chemical shifts in ^1H NMR spectra are referenced from residual CHCl_3 or C-

$^6\text{D}_5\text{H}$ ($\delta = 7.26$ or 7.16 , respectively) and reported in parts per million (ppm) with respect to tetramethylsilane. Chemical shifts in ^{13}C NMR spectra are referenced from CDCl_3 or C_6D_6 ($\delta = 77.07$ or 128.06 , respectively) and reported in ppm with respect to tetramethylsilane. Coupling constants are reported as J values and are given in Hertz (Hz). High resolution mass spectrometry (ESI-MS) was performed by the Mass Spectrometry Laboratory at University of California – Irvine.

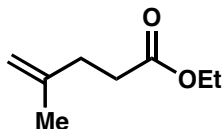
Experimental Procedures:

General procedure for Johnson ortho-ester Claisen rearrangement:

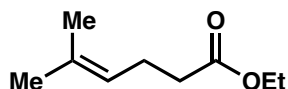
To a dry Ar-flushed microwave vial was added the appropriate alcohol (42.1 mmol, 1.00 equiv), triethylorthoacetate (62.7 mmol, 1.49 equiv) and AcOH (1.25 mmol, 0.03 equiv). The vial was then capped and heated thermally at $140\text{ }^\circ\text{C}$ until starting material was consumed. The reaction mixture was then cooled to $25\text{ }^\circ\text{C}$, partitioned between Et_2O (10 mL) and H_2O (10 mL), and the aqueous was extracted with Et_2O (3×5 mL). The combined organics were stirred with 1 M aq. HCl (10 mL) at $25\text{ }^\circ\text{C}$ for 30 min, washed with brine (10 mL), dried over MgSO_4 , filtered and concentrated *in vacuo*.



(E)-Ethyl hex-4-enoate (5.30a). Clear yellow oil (4.08 g, 68%): $R_f = 0.28$ (5:95 EtOAc:hexanes). Spectral data matched those reported in the literature.³⁷



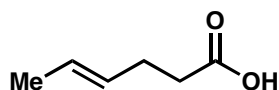
Ethyl 4-methylpent-4-enoate (5.30b). Clear yellow oil (4.16 g, 69%): $R_f = 0.31$ (5:95 EtOAc:hexanes). Spectral data matched those reported in the literature.³⁸



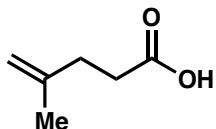
Ethyl 5-methylhex-4-enoate (5.30c). Clear yellow oil (2.18 g, 33%): $R_f = 0.38$ (5:95 EtOAc:hexanes). Spectral data matched those reported in the literature.³⁹

General procedure for ester hydrolysis:

To a solution of ester (1.00 equiv) in THF (20 mL) was added a solution of LiOH (5.00 equiv) in 1:1 H₂O:MeOH (40 mL) and the reaction mixture was heated to 60 °C for 1 h or until starting material was consumed by TLC analysis. The reaction mixture was then cooled to 25 °C, partitioned between Et₂O (20 mL) and 1M aq. NaOH (20 mL). The aqueous layer was extracted with Et₂O (3 x 20 mL) and the combined organic layers were washed with 1 M aq. NaOH (3 x 10 mL). The aqueous washes were acidified to pH = 1 and extracted with Et₂O (4 x 20 mL). Combined organics were washed with brine (10 mL), dried over MgSO₄, filtered and the Et₂O removed by atmospheric distillation. The crude products were carried on directly without further purification.

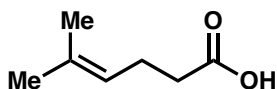


(E)-Hex-4-enoic acid (5.24c). Clear oil (4.10 g, quant.): $R_f = 0.48$ (1:1 EtOAc:hexanes). Spectral data matched those reported in the literature.^{40,41}



4-Methylpent-4-enoic acid (5.24d). Clear oil (4.23 g, quant.): $R_f = 0.50$ (1:1 EtOAc:hexanes).

Spectral data matched those reported in the literature.⁴²

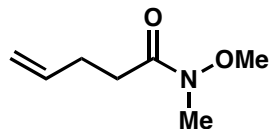


5-Methylhex-4-enoic acid (5.24e). Clear oil (2.37 g, quant.): $R_f = 0.47$ (1:1 EtOAc:hexanes).

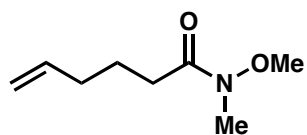
Spectral data matched those reported in the literature.^{43,44}

General procedure for amide coupling:

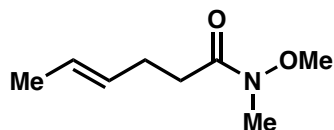
To a solution of carboxylic acid (1.00 equiv) in CH_2Cl_2 (0.35 M) at 0 °C was added Et_3N (3.00 equiv). A single portion of *N,O*-dimethylhydroxylamine hydrochloride (1.00 equiv) was added and the mixture was stirred for 10 min, followed by the addition of *N*-Ethyl-*N'*-(3-dimethylaminopropyl)carbodiimide hydrochloride (1.00 equiv) in 2 equal portions over 5 min. The resulting heterogeneous mixture was then slowly warmed to 25 °C, stirred for 12 h, then quenched by the addition of H_2O (100 mL). The aqueous portion was extracted with CH_2Cl_2 (3 x 30 mL) and the combined organics were washed with 1 M aq. HCl (200 mL), sat. aq. NaHCO_3 (100 mL), and brine (50 mL). The organics were dried over MgSO_4 and filtered. Solvent was removed by atmospheric distillation and the product purified by vacuum distillation.



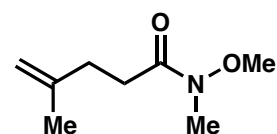
N-Methoxy-*N*-methylpent-4-enamide (**5.25a**). Clear oil (2.15 g, 42%): bp 76 °C (15 torr); $R_f = 0.61$ (1:1 EtOAc:hexanes). Spectral data matched those reported in the literature.⁴⁵



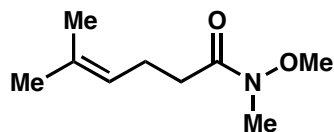
N-Methoxy-*N*-methylhex-5-enamide (**5.25b**). Clear oil (7.00 g, quant. not distilled, carried on directly): $R_f = 0.60$ (1:1 EtOAc:hexanes). Spectral data matched those reported in the literature.⁴⁶



(*E*)-*N*-Methoxy-*N*-methylhex-4-enamide (**5.25c**). Clear oil (3.00 g, 53% over 2 steps): bp 88–91 °C (15 torr); $R_f = 0.60$ (1:1 EtOAc:hexanes). Spectral data matched those reported in the literature.³³



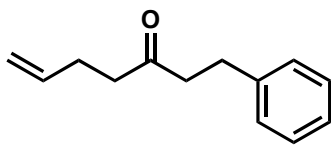
N-Methoxy-*N*,4-dimethylpent-4-enamide (**5.25d**). Clear oil (2.21 g, 48% over 2 steps): bp 82–85 °C (15 torr); $R_f = 0.66$ (1:1 EtOAc:hexanes). Spectral data matched those reported in the literature.⁴⁷



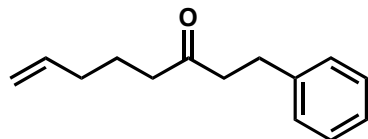
***N*-Methoxy-*N*,5-dimethylhex-4-enamide (5.25e).** Clear oil (0.85 g, 36% over 2 steps): bp 93–97 °C (15 torr); $R_f = 0.59$ (1:1 EtOAc:hexanes). Spectral data matched those reported in the literature.⁴⁸

General procedure for ketone synthesis:

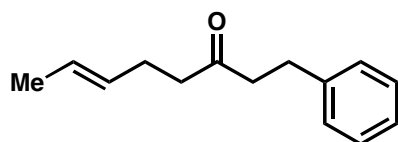
A flame-dried Ar-flushed round bottom flask was charged with freshly ground Mg° turnings (12.3 mmol, 1.49 equiv) and THF (10 mL). A single crystal of I₂ was added, followed by dropwise addition of (2-bromoethyl)benzene (10.2 mmol, 1.25 equiv) while heating to reflux. Stirred for 30 min at reflux then cooled to 25 °C. The resulting clear tan solution was then added to a pre-cooled solution (–10 °C) of amide (1.00 equiv) in THF (20 mL) dropwise over 10 min, then slowly warmed to 25 °C. After 1 h, TLC indicated consumption of starting material. The resulting heterogeneous white slurry was partitioned between Et₂O (20 mL) and sat. aq. NH₄Cl (20 mL). The aqueous was extracted with Et₂O (2 x 10 mL) and the combined organics were washed with brine (10 mL), dried over MgSO₄, filtered and concentrated *in vacuo* to give a crude yellow oil. Chromatography was performed using 40 g SiO₂ (0:100 – 10:90 EtOAc:hexanes).



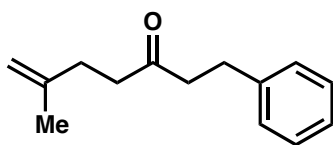
1-Phenylhept-6-en-3-one (5.26a). Clear yellow oil (1.30 g, 83%): $R_f = 0.49$ (1:9 EtOAc:hexanes). Spectral data matched those reported in the literature.^{49,50}



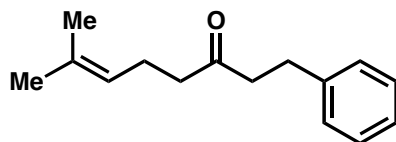
1-Phenylhept-6-en-3-one (5.26b). Clear yellow oil (5.02 g, 56% over 2 steps): $R_f = 0.47$ (1:9 EtOAc:hexanes); $^1\text{H NMR}$ (500 MHz, CDCl_3) δ 7.34–7.23 (m, 2H), 7.22–7.14 (m, 3H), 5.74 (ddt, $J = 17.0, 10.2, 6.7$ Hz, 1H), 5.05–4.91 (m, 2H), 2.89 (t, $J = 7.6$ Hz, 2H), 2.72 (t, $J = 7.6$ Hz, 2H), 2.38 (t, $J = 7.4$ Hz, 2H), 2.03 (q, $J = 7.1$ Hz, 3H), 1.66 (p, $J = 7.4$ Hz, 2H); $^{13}\text{C NMR}$ (126 MHz, CDCl_3) δ 210.0, 141.3, 138.1, 128.6, 128.4, 126.2, 115.3, 44.5, 42.2, 33.2, 29.9, 22.9; IR (neat) 3063, 3027, 2932, 1714, 1453, 913, 699; HRMS (ESI/MeOH) m/z calcd for $\text{C}_{14}\text{H}_{18}\text{ONa}$ ($\text{M} + \text{Na}$) $^+$ 225.1255, found 225.1248.



(E)-1-Phenylhept-6-en-3-one (5.26c). Clear yellow oil (1.35 g, 81%): $R_f = 0.49$ (1:9 EtOAc:hexanes). Spectral data matched those reported in the literature.³³



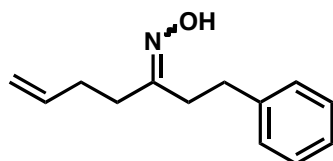
6-Methyl-1-phenylhept-6-en-3-one (5.26d). Clear yellow oil (1.14 g, 68%): $R_f = 0.50$ (1:9 EtOAc:hexanes); $^1\text{H NMR}$ (500 MHz, CDCl_3) δ 7.38–7.31 (m, 2H), 7.29–7.22 (m, 3H), 4.81–4.77 (m, 1H), 4.74–4.69 (m, 1H), 3.02–2.95 (app t, 2H), 2.86–2.79 (app t, 2H), 2.63–2.58 (app t, 2H), 2.34 (t, $J = 7.6$ Hz, 2H), 1.79 (s, 3H); $^{13}\text{C NMR}$ (126 MHz, CDCl_3) δ 209.5, 144.5, 141.2, 128.6, 128.4, 126.2, 110.3, 44.4, 41.3, 31.5, 29.9, 22.7; IR (neat) 3064, 3026, 2931, 1714, 1452, 889. HRMS (ESI/MeOH) m/z calcd for $\text{C}_{14}\text{H}_{18}\text{ONa}$ ($\text{M} + \text{Na}$) $^+$ 225.1255, found 225.1263.



7-Methyl-1-phenyloct-6-en-3-one (5.26e). Clear yellow oil (0.44 g, 41%): $R_f = 0.48$ (1:9 EtOAc:hexanes). Spectral data matched those reported in the literature.⁴⁸

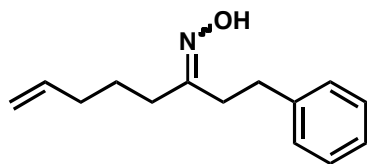
General procedure for oxime formation

To a solution of hydroxylamine hydrochloride (8.00 mmol, 1.25 equiv) in H₂O (6.0 mL) was added K₂CO₃ (8.00 mmol, 1.25 equiv) slowly in small portions, followed by a solution of ketone (6.40 mmol, 1.00 equiv) in EtOH (6.0 mL). The resulting cloudy mixture was brought to reflux for 4 h and cooled to 25 °C. Additional hydroxylamine hydrochloride and K₂CO₃ (1.00 equiv each) were added and the reaction mixture refluxed for 1 h at which time TLC indicated consumption of starting material. The reaction mixture was cooled to 25 °C and partitioned between Et₂O (20 mL) and H₂O (20 mL). The aqueous portion was extracted with Et₂O (20 mL) and the combined organics were washed with brine (10 mL), dried over MgSO₄ and concentrated *in vacuo*. The resulting crude oil was then chromatographed using 40 g of SiO₂ (0:100 – 20:80 EtOAc:hexanes). Products were isolated as a 1:1 mixture of *E:Z* oximes.

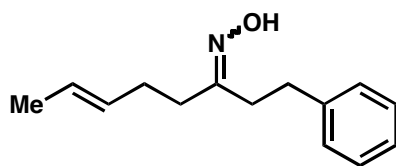


1-Phenylhept-6-en-3-one oxime (5.27a). Clear yellow oil (1.55 g, quant.): $R_f = 0.30$ (1:9 EtOAc:hexanes); ¹H NMR (500 MHz, CDCl₃) δ 8.95 (br s, 2H), 7.33–7.25 (m, 4H), 7.25–7.14 (m, 6H), 5.89–5.74 (m, 2H), 5.12–4.94 (m, 4H), 2.89–2.81 (app q, 4H), 2.69–2.61 (app t, 2H), 2.56–2.45 (m, 4H), 2.34–2.19 (m, 6H); ¹³C NMR (126 MHz, CDCl₃) δ 160.6, 160.5, 141.5,

141.4, 137.6, 137.5, 128.59, 128.57, 128.4 (2), 126.3, 126.2, 115.42, 115.35, 36.3, 34.1, 32.7, 31.7, 30.3, 30.2, 29.7, 27.5; IR (neat) 3241, 3082, 2927, 1641, 1496, 1453, 915; HRMS (ESI/MeOH) m/z calcd for $C_{13}H_{17}NONa$ ($M + Na$)⁺ 226.1208, found 226.1200.

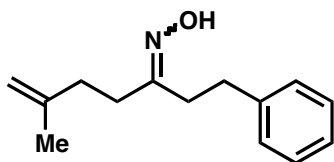


1-Phenyloct-7-en-3-one oxime (5.27b). Clear yellow oil (5.40 g, quant.): $R_f = 0.24$ (1:9 EtOAc:hexanes); ¹H NMR (500 MHz, CDCl₃) δ 8.82 (br s, 2H), 7.28 (t, $J = 7.6$ Hz, 4H), 7.25–7.14 (m, 6H), 5.88–5.71 (m, 2H), 5.08–4.94 (m, 4H), 2.91–2.80 (m, 4H), 2.68–2.61 (m, 2H), 2.55–2.47 (m, 2H), 2.43–2.35 (m, 2H), 2.18–2.01 (m, 6H), 1.68–1.56 (m, 4H); ¹³C NMR (126 MHz, CDCl₃) δ 161.1, 161.0, 141.6, 141.4, 138.20, 138.18, 128.59, 128.56, 128.43, 128.42, 126.23, 126.22, 115.2 (2), 36.2, 34.1, 34.0, 33.4, 32.7, 31.8, 30.1, 27.6, 25.4, 25.0; IR (neat) 3244, 3078, 2928, 1640, 1496, 1454; HRMS (ESI/MeOH) m/z calcd for $C_{14}H_{20}NO$ ($M + H$)⁺ 218.1545, found 218.1545.

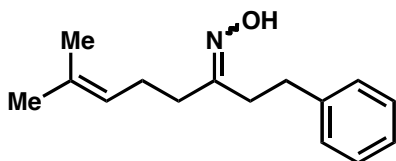


(6E)-1-Phenyloct-6-en-3-one oxime (5.27c). Clear yellow oil (1.24 g, 89%): $R_f = 0.25$ (1:9 EtOAc:hexanes); ¹H NMR (500 MHz, CDCl₃) δ 8.59 (br s, 2H), 7.29 (t, $J = 7.5$ Hz, 4H), 7.26–7.16 (m, 6H), 5.57–5.35 (m, 4H), 2.89–2.80 (app q, 4H), 2.66–2.60 (app t, 2H), 2.53–2.47 (app t, 2H), 2.46–2.40 (app t, 2H), 2.26–2.20 (app q, 2H), 2.18 (s, 4H), 1.64 (t, $J = 5.4$ Hz, 6H); ¹³C NMR (126 MHz, CDCl₃) δ 160.9, 160.8, 141.6, 141.5, 130.2, 130.0, 128.59, 128.57, 128.4 (2), 126.23, 126.21, 126.0, 125.9, 36.4, 34.7, 32.6, 31.7, 30.1, 29.3, 28.7, 28.1, 18.07, 18.05; IR

(neat) 3241, 3026, 2918, 1496, 1452, 965; HRMS (ESI/MeOH) m/z calcd for $C_{14}H_{19}NONa$ ($M + Na$)⁺ 240.1364, found 240.1373.



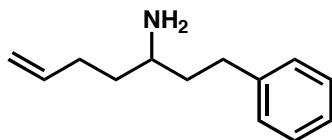
6-Methyl-1-phenylhept-6-en-3-one oxime (5.27d). Clear yellow oil (1.48 g, quant.): $R_f = 0.27$ (1:9 EtOAc:hexanes); 1H NMR (500 MHz, $CDCl_3$) δ 8.89 (br s, 2H), 7.34–7.25 (m, 4H), 7.25–7.13 (m, 6H), 4.79–4.65 (m, 4H), 2.89–2.83 (app q, 4H), 2.67–2.63 (app t, 2H), 2.55–2.49 (app q, 4H), 2.30–2.15 (m, 6H), 1.76 (s, 3H), 1.71 (s, 3H); ^{13}C NMR (126 MHz, $CDCl_3$) δ 160.83, 160.81, 145.0, 144.8, 141.5, 141.4, 128.59, 128.58, 128.4 (2), 126.3, 126.2, 110.6, 110.5, 36.2, 34.2, 33.4, 33.0, 32.7, 31.8, 30.1, 26.5, 22.54, 22.51; IR (neat) 3239, 3083, 2931, 1650, 1496, 1453, 890; HRMS (ESI/MeOH) m/z calcd for $C_{14}H_{19}NONa$ ($M + Na$)⁺ 240.1364, found 240.1355.



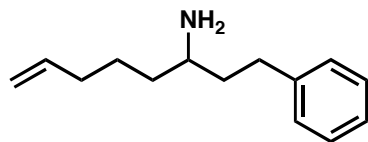
7-Methyl-1-phenyloct-6-en-3-one oxime (5.27e). Clear yellow oil (0.40 g, 99%): $R_f = 0.23$ (1:9 EtOAc:hexanes); 1H NMR (500 MHz, $CDCl_3$) δ 8.32 (br s, 2H), 7.29 (t, $J = 7.5$ Hz, 4H), 7.25–7.15 (m, 6H), 5.14 (t, $J = 7.1$ Hz, 1H), 5.08 (t, $J = 6.4$ Hz, 1H), 2.89–2.82 (app q, 4H), 2.67–2.61 (app t, 2H), 2.54–2.47 (app t, 2H), 2.43–2.36 (app t, 2H), 2.27–2.12 (m, 6H), 1.69 (s, 3H), 1.68 (s, 3H), 1.62 (s, 3H), 1.59 (s, 3H); ^{13}C NMR (126 MHz, $CDCl_3$) δ 161.2, 161.1, 141.6, 141.5, 132.9, 132.7, 128.59, 128.57, 128.4 (2), 126.23, 126.21, 123.4, 123.2, 36.5, 34.8, 32.7, 31.8, 30.1, 28.2, 25.8 (2), 24.9, 24.3, 17.9, 17.8; IR (neat) 3234, 2925, 1496, 1453, 960, 699; HRMS (ESI/MeOH) m/z calcd for $C_{15}H_{21}NONa$ ($M + Na$)⁺ 254.1521, found 254.1509.

General procedure for oxime reduction:

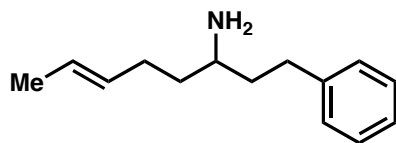
To a stirring suspension of LiAlH₄ (2.00 equiv) in Et₂O (0.5 M) at 0 °C was added a solution of oxime (1.00 equiv) in Et₂O (0.5 M) at an approximate rate of 1 mL/min (gas evolution observed). The heterogeneous grey reaction mixture was warmed to 25 °C, then heated to reflux for 16 h, or until TLC analysis of a quenched aliquot indicated consumption of starting material. The reaction mixture was cooled to 25 °C and treated sequentially with H₂O (1 mL/g of LiAlH₄), 10% w/w aq. NaOH (1 mL/g of LiAlH₄) and H₂O (3 mL/g of LiAlH₄) at a rate sufficient to prevent reflux, then stirred vigorously for 1 h. The resulting white heterogeneous mixture was filtered through a pad of Celite, washed with Et₂O (3 x 20 mL), and concentrated *in vacuo* to give a light yellow oil. Chromatography was performed using Et₃N-deactivated SiO₂ (5-10 g/mmol substrate; 0:1:99 – 99:1:0 EtOAc:Et₃N:hexanes).



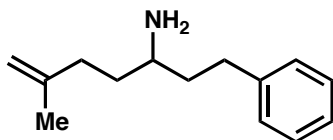
1-Phenylhept-6-en-3-amine (5.28a). Clear oil (1.17 g, 92%): R_f = 0.12 (49:1:50 EtOAc:Et₃N:hexanes); ¹H NMR (500 MHz, CDCl₃) δ 7.34 (dd, *J* = 13.7, 6.0 Hz, 2H), 7.30–7.20 (m, 3H), 5.88 (ddt, *J* = 16.8, 10.0, 6.7 Hz, 1H), 5.09 (d, *J* = 17.1 Hz, 1H), 5.02 (d, *J* = 10.2 Hz, 1H), 2.87–2.77 (m, 2H), 2.75–2.65 (m, 1H), 2.24 (td, *J* = 15.0, 6.4 Hz, 1H), 2.15 (td, *J* = 15.0, 7.0 Hz, 1H), 1.87–1.78 (m, 1H), 1.64 (tdd, *J* = 14.4, 8.8, 6.0 Hz, 2H), 1.51–1.41 (m, 1H), 1.28 (s, 2H); ¹³C NMR (126 MHz, CDCl₃) δ 142.5, 138.7, 128.48, 128.46, 125.9, 114.7, 50.5, 40.0, 37.4, 32.7, 30.6; IR (neat) 3372, 3026, 2924, 1639, 1453, 910; HRMS (ESI/MeOH) *m/z* calcd for C-¹³H₂₀N (M + H)⁺ 190.1596, found 190.1587.



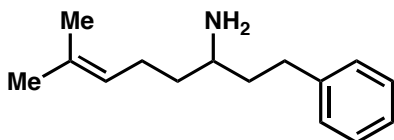
1-Phenyloct-7-en-3-amine (5.28b). Clear oil (4.55 g, 90%): $R_f = 0.10$ (49:1:50 EtOAc:Et₃N:hexanes); ¹H NMR (500 MHz, CDCl₃) δ 7.27 (dd, $J = 13.3, 5.3$ Hz, 2H), 7.18 (dd, $J = 12.0, 7.6$ Hz, 3H), 5.80 (ddt, $J = 17.0, 10.2, 6.7$ Hz, 1H), 5.00 (dd, $J = 17.1, 1.5$ Hz, 1H), 4.95 (d, $J = 10.2$ Hz, 1H), 2.79–2.69 (m, 2H), 2.67–2.57 (m, 1H), 2.13–1.99 (m, 2H), 1.80–1.69 (m, 1H), 1.62–1.53 (m, 1H), 1.52–1.36 (m, 3H), 1.35–1.17 (m, 3H); ¹³C NMR (126 MHz, CDCl₃) δ 142.5, 138.8, 128.42, 128.41, 125.8, 114.6, 50.8, 40.0, 37.7, 33.9, 32.7, 25.5.



(E)-1-Phenyloct-6-en-3-amine (5.28c). Clear oil (1.06 g, 94%): $R_f = 0.11$ (49:1:50 EtOAc:Et₃N:hexanes); ¹H NMR (500 MHz, CDCl₃) δ 7.32–7.23 (m, 2H), 7.22–7.11 (m, 3H), 5.51–5.34 (m, 2H), 2.79–2.68 (m, 2H), 2.66–2.57 (m, 1H), 2.13–2.04 (m, 1H), 2.04–1.94 (m, 1H), 1.79–1.69 (m, 1H), 1.64 (d, $J = 4.7$ Hz, 3H), 1.61–1.47 (m, 2H), 1.39–1.32 (m, 1H), 1.30 (br s, 2H); ¹³C NMR (126 MHz, CDCl₃) δ 142.5, 131.1, 128.4 (2), 125.8, 125.1, 50.4, 39.9, 38.0, 32.6, 29.3, 18.0; IR (neat) 3364, 3025, 2918, 1582, 1453, 967; HRMS (ESI/MeOH) m/z calcd for C₁₄H₂₂N (M + H)⁺ 204.1752, found 204.1749.



6-Methyl-1-phenylhept-6-en-3-amine (5.28d). Clear oil (1.09 g, 98%): $R_f = 0.10$ (49:1:50 EtOAc:Et₃N:hexanes); ¹H NMR (500 MHz, CDCl₃) δ 7.31–7.24 (m, 2H), 7.22–7.16 (m, 3H), 4.72–4.70 (m, 1H), 4.70–4.68 (m, 1H), 2.80–2.71 (m, 2H), 2.68–2.59 (m, 1H), 2.17–2.08 (m, 1H), 2.08–1.99 (m, 1H), 1.81–1.74 (m, 1H), 1.73 (s, 3H), 1.66–1.54 (m, 2H), 1.48–1.38 (m, 1H), 1.29 (s, 2H); ¹³C NMR (126 MHz, CDCl₃) δ 145.9, 142.4, 128.4, 128.4, 125.8, 110.0, 50.7, 40.0, 36.1, 34.5, 32.7, 22.5; IR (neat) 3372, 3026, 2931, 1648, 1453, 886; HRMS (ESI/MeOH) m/z calcd for C₁₄H₂₂N (M + H)⁺ 204.1752, found 204.1747.

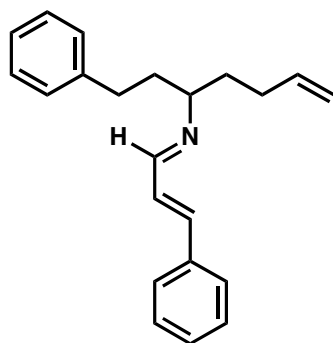


7-Methyl-1-phenyloct-6-en-3-amine (5.28e). Clear oil (0.29 g, 76%): $R_f = 0.09$ (49:1:50 EtOAc:Et₃N:hexanes); ¹H NMR (500 MHz, CDCl₃) δ 7.31–7.25 (m, 2H), 7.22–7.15 (m, 3H), 5.11 (dddd, $J = 8.5, 7.1, 2.6, 1.3$ Hz, 1H), 2.79–2.70 (m, 2H), 2.62 (ddd, $J = 13.7, 10.4, 6.0$ Hz, 1H), 2.15–1.96 (m, 2H), 1.75 (dddd, $J = 13.6, 10.7, 6.0, 4.8$ Hz, 1H), 1.69 (s, 3H), 1.61 (s, 3H), 1.60–1.55 (m, 1H), 1.54–1.46 (m, 1H), 1.33 (dddd, $J = 13.7, 9.2, 7.9, 6.0$ Hz, 1H), 1.19 (s, 2H); ¹³C NMR (126 MHz, CDCl₃) δ 142.6, 131.8, 128.5 (2), 125.9, 124.4, 50.7, 40.1, 38.3, 32.8, 25.9, 24.8, 17.8; IR (neat) 3374, 3026, 2916, 1603, 1453, 699; HRMS (ESI/MeOH) m/z calcd for C₁₅H₂₄N (M + H)⁺ 218.1909, found 218.1917.

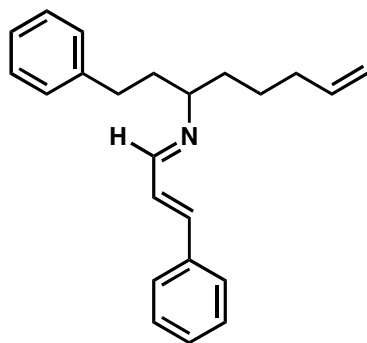
General procedure for imine formation:

A flamed dried Ar-flushed vial containing MgSO₄ (1.00 equiv) was charged with a solution of *trans*-cinnamaldehyde (1.00 equiv) in PhH (0.4 M), followed a solution of amine

(1.00 equiv) in PhH (0.4 M) and was allowed to stir at 25 °C for 12 h. The resultant hazy mixture was filtered through a plug of MgSO₄, rinsed with PhH (4 x 0.5 mL), and concentrated *in vacuo*. NMR analysis of the crude oil showed virtual consumption of the aldehyde and was carried on directly to the oxidation without further purification.

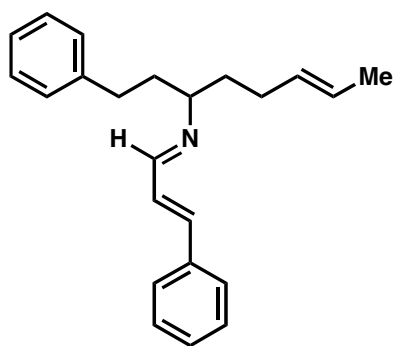


(E)-1-Phenyl-N-((E)-3-phenylallylidene)hept-6-en-3-amine (5.31a). Clear oil (18 mg, 82%): ¹H NMR (500 MHz, C₆D₆) δ 7.80 (d, *J* = 8.7 Hz, 1H), 7.27–7.17 (m, 4H), 7.14–6.97 (m, 7H), 6.65 (d, *J* = 16.1 Hz, 1H), 5.78 (ddt, *J* = 13.4, 10.0, 6.7 Hz, 1H), 5.04 (d, *J* = 17.2 Hz, 1H), 4.99 (d, *J* = 10.1 Hz, 1H), 2.97 (ddd, *J* = 12.3, 8.5, 3.4 Hz, 1H), 2.67 (ddd, *J* = 14.3, 10.5, 5.2 Hz, 1H), 2.49 (ddd, *J* = 13.7, 9.9, 6.7 Hz, 1H), 2.15–2.02 (m, 2H), 1.97 (ddd, *J* = 21.3, 14.1, 6.2 Hz, 1H), 1.90–1.77 (m, 2H), 1.67–1.58 (m, 1H).

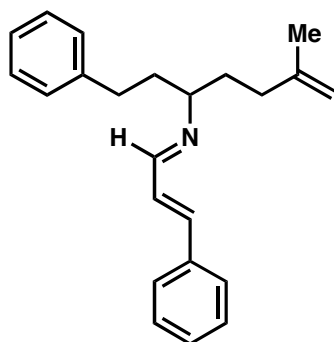


(E)-1-Phenyl-N-((E)-3-phenylallylidene)oct-7-en-3-amine (5.31b). Clear oil (24 mg, quant.): ¹H NMR (500 MHz, C₆D₆) δ 7.81 (d, *J* = 8.6 Hz, 1H), 7.26–7.17 (m, 4H), 7.15–6.97 (m, 7H), 6.65 (d, *J* = 16.1 Hz, 1H), 5.77 (ddt, *J* = 13.5, 9.9, 6.6 Hz, 1H), 5.04 (d, *J* = 17.9 Hz, 1H), 4.98

(d, $J = 10.2$ Hz, 1H), 2.93 (dt, $J = 12.2, 4.1$ Hz, 1H), 2.69 (ddd, $J = 14.5, 10.0, 5.0$ Hz, 1H), 2.51 (ddd, $J = 13.9, 9.9, 7.0$ Hz, 1H), 2.06 (ddd, $J = 13.6, 9.4, 4.9$ Hz, 1H), 2.02–1.93 (m, 2H), 1.88 (dddd, $J = 12.5, 9.4, 6.2, 3.5$ Hz, 1H), 1.71 (ddd, $J = 19.1, 13.2, 4.8$ Hz, 1H), 1.54 (ddd, $J = 13.3, 10.0, 4.2$ Hz, 1H), 1.42 (qd, $J = 12.5, 7.3$ Hz, 1H), 1.28 (qd, $J = 13.4, 6.5$ Hz, 1H).

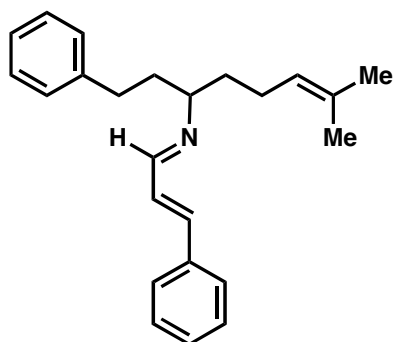


(6*E*,*NE*)-1-Phenyl-*N*-((*E*)-3-phenylallylidene)oct-6-en-3-amine (5.31c). Clear oil (26 mg, quant.): $^1\text{H NMR}$ (500 MHz, C_6D_6) δ 7.82 (d, $J = 8.7$ Hz, 1H), 7.25–7.17 (m, 4H), 7.15–6.97 (m, 7H), 6.65 (d, $J = 16.1$ Hz, 1H), 5.50–5.35 (m, 2H), 3.00 (dt, $J = 12.0, 4.1$ Hz, 1H), 2.69 (ddd, $J = 14.7, 10.5, 5.2$ Hz, 1H), 2.51 (ddd, $J = 13.8, 10.0, 6.7$ Hz, 1H), 2.15–2.02 (m, 2H), 2.01–1.93 (m, 1H), 1.93–1.79 (m, 2H), 1.69–1.63 (m, 1H), 1.61 (d, $J = 4.7$ Hz, 3H).



(*E*)-6-Methyl-1-phenyl-*N*-((*E*)-3-phenylallylidene)hept-6-en-3-amine (5.31d). Clear oil (23 mg, quant.): $^1\text{H NMR}$ (500 MHz, C_6D_6) δ 7.83 (d, $J = 8.7$ Hz, 1H), 7.26–7.17 (m, 4H), 7.15–6.97 (m, 7H), 6.66 (d, $J = 16.1$ Hz, 1H), 4.82 (s, 2H), 2.98 (td, $J = 8.4, 4.1$ Hz, 1H), 2.69 (ddd, $J =$

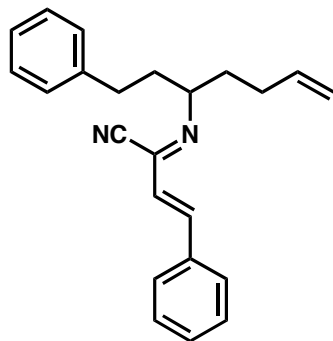
14.7, 10.3, 5.1 Hz, 1H), 2.51 (ddd, $J = 13.8, 10.0, 6.8$ Hz, 1H), 2.12–2.01 (m, 2H), 2.00–1.84 (m, 3H), 1.73 (ddd, $J = 12.8, 10.2, 5.4$ Hz, 1H), 1.65 (s, 3H).



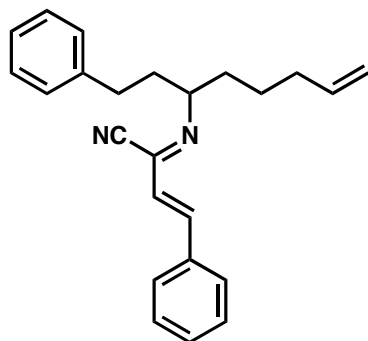
(E)-7-Methyl-1-phenyl-N-((E)-3-phenylallylidene)oct-6-en-3-amine (5.31e). Clear oil (24 mg, quant.): ^1H NMR (500 MHz, C_6D_6) δ 7.84 (d, $J = 8.7$ Hz, 1H), 7.26–7.17 (m, 4H), 7.15–6.97 (m, 7H), 6.65 (d, $J = 16.1$ Hz, 1H), 5.23 (t, $J = 7.0$ Hz, 1H), 3.03 (ddd, $J = 12.2, 8.5, 3.5$ Hz, 1H), 2.70 (ddd, $J = 14.3, 10.5, 5.1$ Hz, 1H), 2.52 (ddd, $J = 13.8, 10.1, 6.6$ Hz, 1H), 2.19–1.97 (m, 3H), 1.96–1.80 (m, 2H), 1.68 (s, 3H), 1.67–1.63 (m, 1H), 1.56 (s, 3H).

General procedure for oxidative cyanation:

A solution of the crude imine (1.00 equiv) in MeCN (0.35 M) was treated with a solution of TMSCN (1.10 equiv) in MeCN (0.80 M), followed by a solution of MeOH (1.10 equiv) in MeCN (0.80 M) and stirred at 25 °C for 1 h. The clear reaction mixture was then treated with tetrabutylammonium bromide (1.10 equiv) and 2-iodoxybenzoic acid (1.10 equiv) and stirred at 25 °C for 16 h. The cloudy mixture was filtered through a plug of Celite, concentrated *in vacuo*, and chromatographed using 6.0 g of silanized⁵¹ SiO_2 (0:100 – 1:99 EtOAc:Hexane).

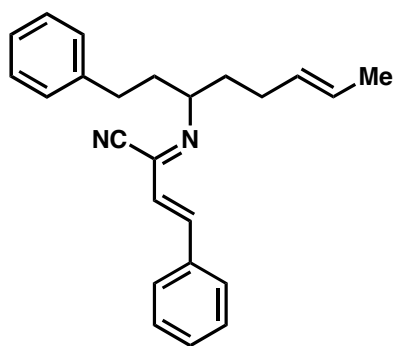


(Z)-N-(1-Phenylhept-6-en-3-yl)cinnamimidoyl cyanide (5.23a). Clear yellow oil (12 mg, 51%); $R_f = 0.32$ (10:90 EtOAc:hexanes); $^1\text{H NMR}$ (500 MHz, C_6D_6) δ 7.41 (d, $J = 16.4$ Hz, 1H), 7.10–7.04 (m, 4H), 7.03–6.94 (m, 6H), 6.91 (d, $J = 16.5$ Hz, 1H), 5.73 (ddt, $J = 16.8, 10.0, 6.6$ Hz, 1H), 5.07–4.96 (m, 2H), 3.94 (dt, $J = 8.5, 4.7$ Hz, 1H), 2.51 (t, $J = 8.3$ Hz, 2H), 2.01–1.89 (m, 3H), 1.81 (ddq, $J = 8.9, 3.9, 2.8$ Hz, 1H), 1.76–1.68 (m, 1H), 1.63–1.54 (m, 1H); $^{13}\text{C NMR}$ (126 MHz, C_6D_6) δ 142.3, 141.90, 141.88, 138.0, 134.9, 130.1, 129.0, 128.8, 128.7, 128.4, 126.4, 126.3, 115.3, 110.0, 68.5, 38.4, 35.8, 33.1, 30.9; IR (neat) 3027, 2941, 2220, 1628, 1583, 1450, 967; HRMS (ESI/MeOH) m/z calcd for $\text{C}_{23}\text{H}_{24}\text{N}_2\text{Na}$ ($\text{M} + \text{Na}$) $^+$ 351.1837, found 351.1835.

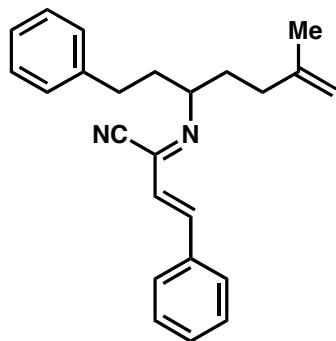


(Z)-N-(1-Phenyl-oct-7-en-3-yl)cinnamimidoyl cyanide (5.23b). Clear yellow oil (13 mg, 52%); $R_f = 0.33$ (10:90 EtOAc:hexanes); $^1\text{H NMR}$ (500 MHz, C_6D_6) δ 7.41 (d, $J = 16.3$ Hz, 1H), 7.11–7.05 (m, 4H), 7.02–6.94 (m, 6H), 6.92 (d, $J = 16.5$ Hz, 1H), 5.71 (ddt, $J = 14.0, 10.1, 6.8$ Hz, 1H), 5.09–5.00 (m, 1H), 4.97 (d, $J = 10.1$ Hz, 1H), 3.98–3.84 (m, 1H), 2.52 (t, $J = 9.1$ Hz, 2H), 1.95 (h, $J = 7.8, 7.2$ Hz, 3H), 1.88–1.79 (m, 1H), 1.64–1.57 (m, 1H), 1.55–1.45 (m, 1H), 1.35–

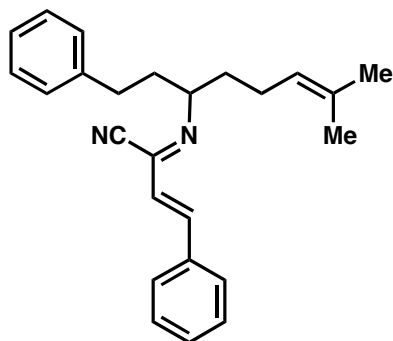
1.27 (m, 2H); ^{13}C NMR (126 MHz, C_6D_6) δ 142.2, 142.0, 141.6, 138.6, 134.9, 130.0, 129.0, 128.78, 128.76, 128.4, 126.4, 126.3, 115.1, 110.0, 69.0, 38.5, 36.1, 34.0, 33.2, 25.9; IR (neat) 3027, 2938, 2220, 1629, 1583, 1450, 967; HRMS (ESI/MeOH) m/z calcd for $\text{C}_{24}\text{H}_{26}\text{N}_2\text{Na}$ ($\text{M} + \text{Na}$) $^+$ 365.1994, found 365.1989.



(Z)-N-((E)-1-Phenyl-3-yl)cinnamimidoyl cyanide (5.23c). Clear yellow oil (19 mg, 76%); $R_f = 0.32$ (10:90 EtOAc:hexanes); ^1H NMR (500 MHz, C_6D_6) δ 7.42 (d, $J = 16.4$ Hz, 1H), 7.06 (d, $J = 7.6$ Hz, 3H), 7.04–6.89 (m, 8H), 5.46–5.35 (m, 2H), 3.98 (dt, $J = 8.6, 4.5$ Hz, 1H), 2.52 (t, $J = 8.4$ Hz, 2H), 2.03–1.91 (m, 3H), 1.84 (ddt, $J = 13.3, 9.2, 4.1$ Hz, 1H), 1.75 (dq, $J = 15.2, 7.7$ Hz, 1H), 1.63 (d, $J = 4.6$ Hz, 3H), 1.52 (dd, $J = 18.0, 6.1$ Hz, 1H); ^{13}C NMR (126 MHz, C_6D_6) δ 142.1, 142.0, 141.9, 135.0, 130.6, 130.0, 129.0, 128.87, 128.86 (2), 126.5, 126.3, 126.0, 110.0, 68.5, 38.6, 36.4, 33.2, 29.8, 18.2; IR (neat) 3027, 2918, 2220, 1629, 1583, 1450, 966; HRMS (ESI/MeOH) m/z calcd for $\text{C}_{24}\text{H}_{26}\text{N}_2\text{Na}$ ($\text{M} + \text{Na}$) $^+$ 365.1994, found 365.1990.



(Z)-N-(6-Methyl-1-phenylhept-6-en-3-yl)cinnamimidoyl cyanide (5.23d). Clear yellow oil (13 mg, 54%): $R_f = 0.30$ (10:90 EtOAc:hexanes); $^1\text{H NMR}$ (500 MHz, C_6D_6) δ 7.42 (d, $J = 16.4$ Hz, 1H), 7.08 (d, $J = 7.6$ Hz, 4H), 7.03–6.88 (m, 7H), 4.80 (d, $J = 9.1$ Hz, 2H), 3.95 (tt, $J = 8.5, 3.3$ Hz, 1H), 2.53 (t, $J = 8.3$ Hz, 2H), 1.97 (td, $J = 8.3, 4.4$ Hz, 3H), 1.83 (ddd, $J = 16.0, 10.4, 5.3$ Hz, 2H), 1.72 (dq, $J = 6.7, 3.2$ Hz, 1H), 1.62 (s, 3H); $^{13}\text{C NMR}$ (126 MHz, C_6D_6) δ 145.0, 142.3, 141.91, 141.88, 134.9, 130.1, 129.0, 128.78, 128.76, 126.4, 126.3, 110.8, 110.4, 110.0, 68.8, 38.5, 34.74, 34.66, 33.2, 22.6; IR (neat) 3027, 2941, 2220, 1628, 1583, 1450, 967; HRMS (ESI/MeOH) m/z calcd for $\text{C}_{24}\text{H}_{26}\text{N}_2\text{Na}$ ($\text{M} + \text{Na}$) $^+$ 365.1994, found 365.1993.

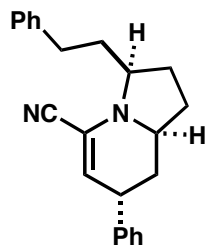


(Z)-N-(7-Methyl-1-phenyloct-6-en-3-yl)cinnamimidoyl cyanide (5.23e). Clear yellow oil (12 mg, 47%): $R_f = 0.31$ (10:90 EtOAc:hexanes); $^1\text{H NMR}$ (500 MHz, C_6D_6) δ 7.42 (d, $J = 16.4$ Hz, 1H), 7.11–7.04 (m, 4H), 7.03–6.92 (m, 7H), 5.18 (t, $J = 7.3$ Hz, 1H), 4.01 (tt, $J = 8.4, 4.0$ Hz, 1H), 2.54 (t, $J = 8.3$ Hz, 2H), 2.08–1.94 (m, 3H), 1.87 (dtd, $J = 12.9, 8.2, 3.7$ Hz, 1H), 1.82–1.73 (m, 1H), 1.71 (s, 3H), 1.65 (tq, $J = 8.8, 4.2$ Hz, 1H), 1.55 (s, 3H); $^{13}\text{C NMR}$ (126 MHz, C_6D_6) δ

142.1, 142.0, 141.9, 135.0, 132.2, 130.0, 129.0, 128.77, 128.75, 128.6, 126.5, 126.3, 124.2, 110.0, 68.7, 38.6, 36.6, 33.2, 25.9, 25.3, 17.9; IR (neat) 3025, 2928, 2219, 1628, 1582, 1450, 967; HRMS (ESI/MeOH) m/z calcd for $C_{25}H_{28}N_2Na$ ($M + Na$)⁺ 379.2150, found 379.2143.

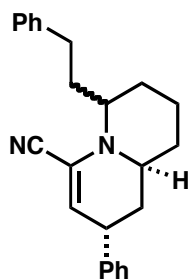
General procedure for the intramolecular Diels–Alder reaction:

An acid/base treated microwave vial was charged with a solution of the substrate (1.00 equiv) in PhCH₃ (0.05 M). The PhCH₃ was removed under vacuum to dry the sample to a yellow oil. The residue was then charged with PhCH₃ (0.04 M), degassed by sparging with Ar for 10 minutes, capped and heated thermally to 180 °C for 30 hours. The reaction was cooled to 25 °C, concentrated *in vacuo*, and chromatographed using 4.0 g of SiO₂ (0:100 – 10:90 EtOAc:hexanes).



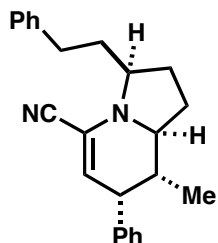
***rac*-(3*S*,7*S*,8*aS*)-3-Phenethyl-7-phenyl-1,2,3,7,8,8*a*-hexahydroindolizine-5-carbonitrile**

(5.32a). Clear yellow oil (5 mg, 38%): R_f = 0.25 (10:90 EtOAc:hexanes); ¹H NMR (500 MHz, C₆D₆) δ 7.13 (s, 5H), 7.11–7.03 (m, 2H), 7.00 (s, 1H), 6.96 (d, J = 7.5 Hz, 2H), 5.18 (d, J = 5.3 Hz, 1H), 3.65 (t, J = 8.9 Hz, 1H), 3.18 (t, J = 5.7 Hz, 1H), 2.88–2.78 (m, 1H), 2.50 (dtd, J = 12.2, 10.8, 5.9 Hz, 1H), 2.38 (dtd, J = 15.0, 13.1, 4.9 Hz, 1H), 2.07 (td, J = 13.3, 3.9 Hz, 1H), 1.60 (d, J = 12.7 Hz, 1H), 1.45–1.32 (m, 3H), 1.29–1.22 (m, 2H), 1.03 (td, J = 12.5, 5.9 Hz, 1H); ¹³C NMR (126 MHz, C₆D₆) δ 146.3, 141.9, 128.8, 128.7, 128.60, 128.58, 126.7, 126.3, 119.1, 116.4, 112.3, 60.2, 52.2, 39.2, 37.8, 37.0, 33.6, 29.8, 28.2; IR (neat) 3025, 2928, 2225, 1601, 1450, 700; HRMS (ESI/MeOH) m/z calcd for $C_{23}H_{24}N_2Na$ ($M + Na$)⁺ 351.1837, found 351.1833.



***rac*-(2*S*,9*aS*)-6-Phenethyl-2-phenyl-2,6,7,8,9,9*a*-hexahydro-1*H*-quinolizine-4-carbonitrile**

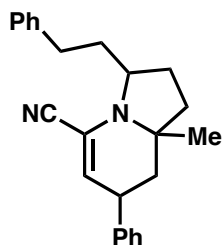
(5.32b). Clear yellow oil (4 mg, 33%): $R_f = 0.24$ (10:90 EtOAc:hexanes); ^1H NMR (500 MHz, C_6D_6) δ 7.24–7.18 (m, 5H), 7.12–7.04 (m, 3H), 7.02–6.97 (m, 2H), 5.28 (d, $J = 4.1$ Hz, 1H), 3.28–3.20 (m, 1H), 3.18–3.12 (m, 1H), 2.77–2.66 (m, 2H), 2.65–2.56 (m, 1H), 1.74–1.66 (m, 1H), 1.50–1.45 (m, 1H), 1.43–1.37 (m, 1H), 1.35–1.26 (m, 2H), 1.24–1.10 (m, 2H), 1.09–0.99 (m, 1H), 0.95–0.86 (m, 2H); ^{13}C NMR (126 MHz, C_6D_6) δ 145.7, 142.2, 128.93, 128.89, 128.8, 128.7, 127.4, 126.8, 121.8, 118.1, 117.2, 59.2, 52.3, 37.9, 37.8, 33.6, 27.2, 27.0, 19.8, 18.7; IR (neat) 3025, 2937, 2222, 1603, 1453, 700; HRMS (ESI/MeOH) m/z calcd for $\text{C}_{24}\text{H}_{26}\text{N}_2\text{Na}$ ($\text{M} + \text{Na}$) $^+$ 365.1994, found 365.1984.



***rac*-(3*S*,7*S*,8*R*,8*aS*)-8-Methyl-3-phenethyl-7-phenyl-1,2,3,7,8,8*a*-hexahydroindolizine-5-**

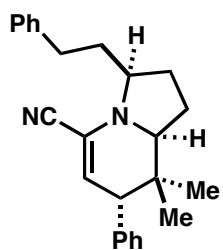
carbonitrile (5.32c). Clear yellow oil (7 mg, 37%): $R_f = 0.25$ (10:90 EtOAc:hexanes); ^1H NMR (500 MHz, C_6D_6) δ 7.24–7.16 (m, 3H), 7.16–7.04 (m, 5H), 6.92 (d, $J = 6.5$ Hz, 2H), 5.17 (d, $J = 5.4$ Hz, 1H), 3.74 (t, $J = 9.1$ Hz, 1H), 2.97 (t, $J = 5.5$ Hz, 1H), 2.82 (td, $J = 10.1, 6.3$ Hz, 1H), 2.55 (ddd, $J = 16.7, 11.0, 5.8$ Hz, 1H), 2.40 (td, $J = 12.9, 4.8$ Hz, 1H), 2.17–2.07 (m, 1H), 1.45 (td, $J = 12.9, 6.6$ Hz, 1H), 1.34 (ddt, $J = 19.9, 12.0, 6.4$ Hz, 3H), 1.13 (dq, $J = 11.4, 6.4$ Hz, 1H),

1.02 (ddd, $J = 21.1, 12.0, 8.0$ Hz, 1H), 0.37 (d, $J = 7.0$ Hz, 3H); ^{13}C NMR (126 MHz, C_6D_6) δ 141.9, 141.7, 130.4, 128.9, 128.7, 128.4, 126.9, 126.3, 118.1, 116.6, 113.8, 60.6, 57.7, 45.2, 37.9, 37.5, 33.8, 29.2, 28.3, 14.5; IR (neat) 3025, 2962, 2224, 1603, 1453, 700; HRMS (ESI/MeOH) m/z calcd for $\text{C}_{24}\text{H}_{26}\text{N}_2$ ($\text{M} + \text{Na}$) $^+$ 365.1994, found 365.1997.



8a-Methyl-3-phenethyl-7-phenyl-1,2,3,7,8,8a-hexahydroindolizine-5-carbonitrile (5.32d).

Clear yellow oil (3 mg, 21%): $R_f = 0.23$ (10:90 EtOAc:hexanes); ^1H NMR (500 MHz, C_6D_6) δ 7.27–6.95 (m, 10H), 5.20 (s, 1H), 3.43–3.36 (m, 1H), 3.19–3.13 (m, 1H), 2.60 (ddt, $J = 14.4, 10.3, 5.8$ Hz, 2H), 2.38–2.27 (m, 1H), 1.67–1.25 (m, 6H), 1.16–1.08 (m, 1H), 0.87 (s, 3H); ^{13}C NMR (126 MHz, C_6D_6) δ 144.1, 142.0, 128.9, 128.8, 128.8, 127.6, 127.0, 126.5, 126.3, 115.3, 110.4, 63.0, 60.5, 41.6, 39.3, 39.0, 38.3, 33.0, 28.6, 26.6; IR (neat) 3025, 2927, 2222, 1601, 1453, 698; HRMS (ESI/MeOH) m/z calcd for $\text{C}_{24}\text{H}_{26}\text{N}_2\text{Na}$ ($\text{M} + \text{Na}$) $^+$ 365.1994, found 365.1989.



***rac*-(3*S*,7*S*,8*aS*)-8,8-Dimethyl-3-phenethyl-7-phenyl-1,2,3,7,8,8a-hexahydroindolizine-5-carbonitrile (5.32e).** Clear yellow oil (2 mg, 19%): $R_f = 0.24$ (10:90 EtOAc:hexanes); ^1H NMR (500 MHz, C_6D_6) δ 7.23–7.18 (m, 4H), 7.14–7.07 (m, 4H), 7.00–6.95 (m, 2H), 5.00 (d, $J = 5.4$ Hz, 1H), 3.68 (t, $J = 8.7$ Hz, 1H), 2.99–2.92 (m, 1H), 2.72 (d, $J = 5.5$ Hz, 1H), 2.63–2.55 (m, 1H), 2.55–2.45 (m, 1H), 2.21–2.11 (m, 1H), 1.49–1.37 (m, 2H), 1.35–1.27 (m, 1H), 1.19–1.09

Table 5.2. Tabulated NMR data for **5.32c**.

Tabulated NMR Data for (3S,7S,8R,8aS)-8-methyl-3-phenethyl-7-phenyl-1,2,3,7,8,8a-hexahydroindolizine-5-carbonitrile (5.32c)

Label	Carbon	Type	Proton	Shift	Shift prime	Integration	COSY	NOESY
A	141.9	QUAT	—	—	—	—	—	—
B	141.7	QUAT	—	—	—	—	—	—
C	130.4	Ar-H	c	6.92	—	2	Ar-H	k, l, m, n, t
D	128.9	Ar-H	d	7.20	—	2	Ar-H	—
E	128.7	Ar-H	e	7.20	—	1	Ar-H	—
F	128.4	Ar-H	f	7.10	—	2	Ar-H	—
G	126.9	Ar-H	g	7.10	—	2	Ar-H	—
H	126.3	Ar-H	h	7.10	—	1	Ar-H	—
I	118.1	QUAT	—	—	—	—	—	—
J	116.6	QUAT	—	—	—	—	—	—
K	113.8	H	k	5.17	—	1	n	c, n
L	60.6	H	l	3.74	—	1	p, p', s, s'	c, q, q' + COSY
M	57.7	H	m	2.82	—	1	o, r, r'	c, t + COSY
N	45.2	CH	n	2.97	—	1	k, o	c, t + COSY
O	37.9	CH	o	1.13	—	1	m, n, t	COSY
P	37.5	CH ₂	p, p'	2.11	—	2	l, q, q'	COSY
					1.34	—	—	overlap
Q	33.8	CH ₂	q, q'	2.55	—	2	p, p'	l + COSY
					2.40	—	—	l + COSY
R	29.2	CH ₂	r, r'	1.40	—	2	m, s, s'	overlap
					1.02	—	—	s, s', t
S	28.3	CH ₂	s, s'	1.45	—	2	l, r, r'	l, m, s', r'
					1.35	—	—	overlap
T	14.5	CH ₃	t	0.37	—	3	o	c, m, n, o, r'
Total # of C =	20					Total # of H =	26	

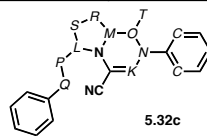
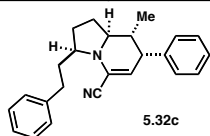
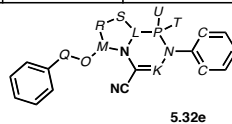
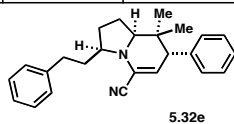


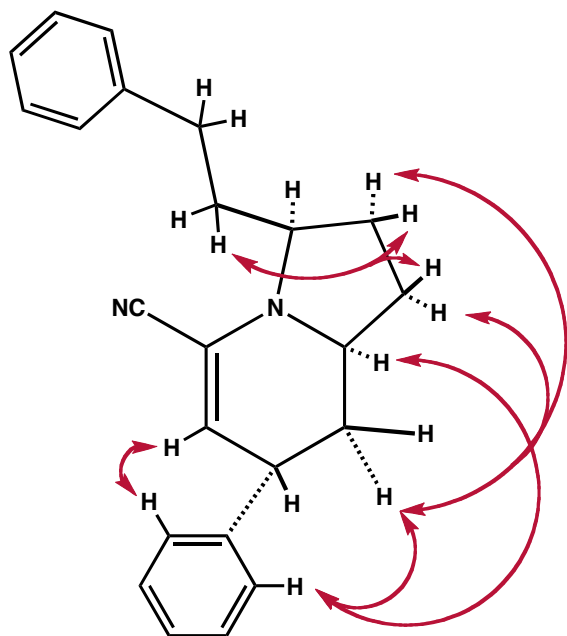
Table 5.3. Tabulated NMR data for **5.32e**.

Tabulated NMR Data for (3S,7S,8aS)-8,8-dimethyl-3-phenethyl-7-phenyl-1,2,3,7,8,8a-hexahydroindolizine-5-carbonitrile (5.32e)

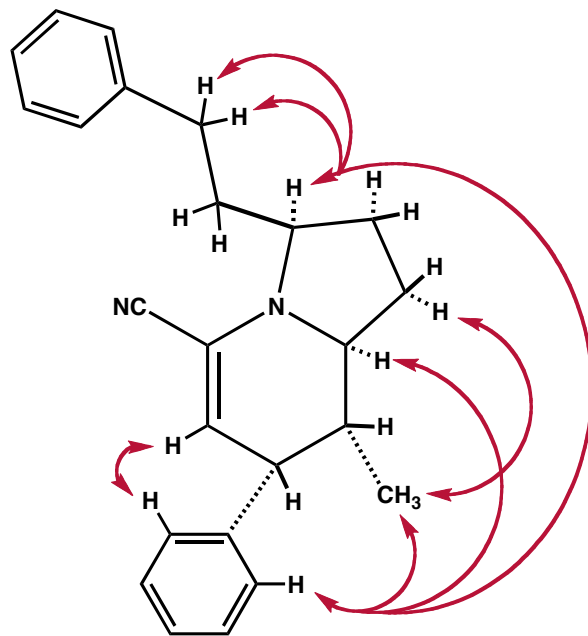
Label	Carbon	Type	Proton	Shift	Shift prime	Integration	COSY	NOESY
A	143.3	QUAT	—	—	—	—	—	—
B	141.9	QUAT	—	—	—	—	—	—
C	130.4	Ar-H	c	6.98	—	2	Ar-H	k, l, n, t
D	130.2	Ar-H	d	7.20	—	1	Ar-H	—
E	128.9	Ar-H	e	7.20	—	2	Ar-H	—
F	128.8	Ar-H	f	7.20	—	1	Ar-H	—
G	126.9	Ar-H	g	7.10	—	2	Ar-H	—
H	126.3	Ar-H	h	7.10	—	2	Ar-H	—
I	117.4	QUAT	—	—	—	—	—	—
J	116.2	QUAT	—	—	—	—	—	—
K	110.6	H	k	5.00	—	1	n	c, n, u
L	60.9	H	l	2.96	—	1	n, s, s'	m, r', s, s', t
M	59.8	H	m	3.68	—	1	o, o', r, r'	l + COSY
N	52.7	CH	n	2.72	—	1	k, l	u, t
O	39.0	CH ₂	o, o'	2.16	—	2	m, q, q'	COSY
					1.40	—	—	overlap
P	33.9	QUAT	—	—	—	—	—	—
Q	33.5	CH ₂	q, q'	2.60	—	2	o, o'	r', m + COSY
					2.50	—	—	r', m + COSY
R	28.7	CH ₂	r, r'	1.45	—	2	m, s, s'	overlap
					1.31	—	—	l, q, q', t + COSY
S	24.3	CH ₂	s, s'	1.14	—	2	l, r, r'	t, u + COSY
					1.04	—	—	t + COSY
T	23.9	CH ₃	t	0.34	—	3	—	c, l, n, r', s, s'
U	22.8	CH ₃	u	0.64	—	3	—	k, n, o, r, s
Total # of C =	21					Total # of H =	28	



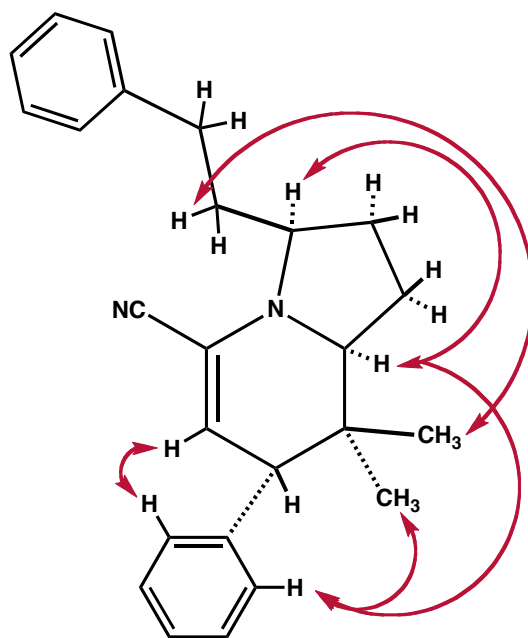
Key NOESY correlation diagrams for 5.32a, 5.32c, and 5.32e



5.32a



5.32c



5.32e

References

- ¹ Review of indolizidine and quinolizidine natural products: Michael, J. P. *Nat. Prod. Rep.* **2007**, *24*, 191–222.
- ² Review of indolizidine and quinolizidine natural products: Michael, J. P. *Nat. Prod. Rep.* **2008**, *25*, 139–165.
- ³ Review of saturated nitrogen heterocycles: Mitchinson, A.; Nadin, A. *J. Chem. Soc., Perkin Trans. 1* **2000**, 2862–2892.
- ⁴ Review of CNS activity of nitrogen heterocycles: Ahmed, A.; Molvi, K. I.; Nazim, S.; Baig, I.; Memon, T.; Rahil, M. *J. Chem. Pharm. Res.* **2012**, *4*, 872–880.
- ⁵ Review of Diels–Alder reactions of azadienes: Boger, D. L. *Tetrahedron* **1983**, *39*, 2869–2939.
- ⁶ Review of Diels–Alder reactions of heterocyclic azadienes: Boger, D. L. *Chem. Rev.* **1986**, *86*, 781–794.
- ⁷ Review of Diels–Alder reactions of 1-azadienes: Behforouz, M.; Ahmadian, M. *Tetrahedron* **2000**, *56*, 5259–5288.
- ⁸ Review of imino Diels–Alder reactions: Buonora, P.; Olsen, J.-C.; Oh, T. *Tetrahedron* **2001**, *57*, 6099–6138.
- ⁹ Review of imino Diels–Alder reactions: Memeo, M. G.; Quadrelli, P. *Chem. Eur. J.* **2012**, *18*, 12554–12582.
- ¹⁰ Review of electron-deficient azabutadienes: Monbaliu, J.-C. M.; Masschelein, K. G. R.; Stevens, C. V. *Chem. Soc. Rev.* **2011**, *40*, 4708–4739.
- ¹¹ Isolation of 261C: Kaneko, T.; Spande, T. F.; Garraffo, H. M.; Yeh, H. J. C.; Daly, J. W.; Andriamaharavo, N. R.; Andriantsiferana, M. *Heterocycles* **2003**, *59*, 745–757.

- ¹² Isolation of himeradine A: Morita, H.; Hirasawa, Y.; Kobayashi, J. *J. Org. Chem.* **2003**, *68*, 4563–4566.
- ¹³ Isolation of gephyrotoxin: Daly, J. W.; Witkop, B.; Tokuyama, T.; Nishikawa, T.; Karle, I. L. *Helv. Chim. Act.* **1977**, *60*, 1128–1140.
- ¹⁴ Structural elucidation of yohimbine: Swan, G. A. *J. Chem. Soc.* **1950**, 1534–1539.
- ¹⁵ Reductive decyanation review: Mattalia, J.-M.; Marchi-Delapierre, C.; Hazimeh, H.; Chanon, M. *ARKIVOC (Gainesville, FL, United States)* **2006**, 90–118.
- ¹⁶ For examples of reductive cyanation in the Rychnovsky group, see: Perry, M. A. Ph.D Dissertation, University of California, Irvine, 2013, pp. 1–221.
- ¹⁷ For examples of conjugate addition using cyanoenamines, see: Fleming, F. F.; Wang, Q. *Chem. Rev.* **2003**, *103*, 2035–2077 and references therein.
- ¹⁸ The first report of cyanoenamine conjugate addition: Ahlbrecht, H.; Pfaff, K. *Synthesis* **1978**, 897–899.
- ¹⁹ Reduction of cyanoenamines: Fang, J. M.; Chang, H. T. *J. Chem. Soc., Perkin Trans. 1* **1988**, 1945–1948.
- ²⁰ Radical cyclization of cyanoenamines: Fang, J. M.; Chang, H. T.; Lin, C. C. *J. Chem. Soc., Chem. Commun.* **1988**, 1385–1386.
- ²¹ Photochemical reactions of cyanoenamines: Drenkard, S.; Ferris, J.; Eschenmoser, A. *Helv. Chim. Act.* **1990**, *73*, 1373–1390.
- ²² Diels–Alder reaction of 1-azadienes: Teng, M.; Fowler, F. W. *Tetrahedron Lett.* **1989**, *30*, 2481–2484.
- ²³ Aniline-derived aza-IMDA reaction: Sisti, N. J.; Fowler, F. W.; Grierson, D. S. *Synlett* **1991**, 816–818.

- ²⁴ Alkyl-tethered aza-IMDA reaction: Sisti, N. J.; Zeller, E.; Grierson, D. S.; Fowler, F. W. *J. Org. Chem.* **1997**, *62*, 2093–2097.
- ²⁵ For oxazine-masked cyanoazadiene IMDA reactions, see: Motorina, I. A.; Fowler, F. W.; Grierson, D. S. *J. Org. Chem.* **1997**, *62*, 2098–2105.
- ²⁶ For *O*-vinyl aza-IMDA reactions, see: Motorina, I. A.; Grierson, D. S. *Tetrahedron Lett.* **1999**, *40*, 7211–7214.
- ²⁷ Lewis-acid activation of cyanoazadiene IMDA reactions: Motorina, I. A.; Grierson, D. S. *Tetrahedron Lett.* **1999**, *40*, 7215–7218.
- ²⁸ Cyanoazadiene IMDA reaction with electron-deficient dienophile: Tarver, J. E.; Terranova, K. M.; Joullie, M. M. *Tetrahedron* **2004**, *60*, 10277–10284.
- ²⁹ One-pot three-component synthesis of α -iminonitrile: Fontaine, P.; Chiaroni, A.; Masson, G.; Zhu, J. *Org. Lett.* **2008**, *10*, 1509–1512.
- ³⁰ Synthetic studies on 261C: Toyooka, N.; Kawasaki, M.; Nemoto, H.; Awale, S.; Tezuka, Y.; Kadota, S. *Synlett* **2005**, 3109–3110.
- ³¹ Organocatalytic asymmetric Mannich reaction: Notz, W.; Tanaka, F.; Watanabe, S.; Chowdari, N. S.; Turner, J. M.; Thayumanavan, R.; Barbas, C. F. *J. Org. Chem.* **2003**, *68*, 9624–9634.
- ³² Snyder, S. A.; Treitler, D. S.; Brucks, A. P.; Sattler, W. *J. Am. Chem. Soc.* **2011**, *133*, 15898–15901.
- ³³ Synthesis of phenethyl ketones: Harris, J. R.; Waetzig, S. R.; Woerpel, K. A. *Org. Lett.* **2009**, *11*, 3290–3293.
- ³⁴ *N*-Methoxy-*N*-methylamides as acylation agents: Nahm, S.; Weinreb, S. M. *Tetrahedron Lett.* **1981**, *22*, 3815–3818.

- ³⁵ Seminal publication of Johnson orthoester Claisen rearrangement: Johnson, W. S.; Werthemann, L.; Bartlett, W. R.; Brocksom, T. J.; Li, T.-T.; Faulkner, D. J.; Petersen, M. *R. J. Am. Chem. Soc.* **1970**, *92*, 741–743.
- ³⁶ Review of the Strecker reaction: Shibasaki, M.; Kanai, M.; Mita, T. In *Organic Reactions*; John Wiley & Sons, Inc.: Hoboken, NJ, 2008; Vol. 70, pp. 1–119.
- ³⁷ Adachi, Y.; Kamei, N.; Yokoshima, S.; Fukuyama, T. *Org. Lett.* **2011**, *13*, 4446–4449.
- ³⁸ Weyermann, P.; Keese, R. *Tetrahedron* **2011**, *67*, 3874–3880.
- ³⁹ Bruecher, O.; Bergstraesser, U.; Kelm, H.; Hartung, J.; Greb, M.; Svoboda, I.; Fuess, H. *Tetrahedron* **2012**, *68*, 6968–6980.
- ⁴⁰ Ansell, M. F.; Emmett, J. C.; Coombs, R. V *J. Chem. Soc.* **1968**, 217–225.
- ⁴¹ Blenderman, W. G.; Joullie, M. M.; Preti, G. *J. Org. Chem.* **1983**, *48*, 3206–3213.
- ⁴² Braddock, D. C.; Cansell, G.; Hermitage, S. A. *Chem. Commun.* **2006**, 2483–2485.
- ⁴³ Mori, K.; Sugai, T.; Maeda, Y.; Okazaki, T.; Noguchi, T.; Naito, H. *Tetrahedron* **1985**, *41*, 5307–5311.
- ⁴⁴ Menon, S.; Sinha-Mahapatra, D.; Herndon, J. W. *Tetrahedron* **2007**, *63*, 8788–8793.
- ⁴⁵ Goncalves-Martin, M. G.; Saxer, A.; Renaud, P. *Synlett* **2009**, 2801–2802.
- ⁴⁶ Ng, S. M.; Bader, S. J.; Snapper, M. L. *J. Am. Chem. Soc.* **2006**, *128*, 7315–7319.
- ⁴⁷ Cuellar, R. A. D. Ph.D Dissertation, University of North Carolina, Chapel Hill, 2008, pp. 1–136.
- ⁴⁸ Ramirez, A. P.; Thomas, A. M.; Woerpel, K. A. *Org. Lett.* **2009**, *11*, 507–510.
- ⁴⁹ Sugawara, M.; Yoshida, J. *Tetrahedron* **2000**, *56*, 4683–4689.
- ⁵⁰ Clive, D. L. J.; Pham, M. P. *J. Org. Chem.* **2009**, *74*, 1685–1690.
- ⁵¹ Silanized SiO₂ preparation: Panne, P.; Fox, J. *J. Am. Chem. Soc.* **2006**, *129*, 22–23.